Biotechnical engineering on alluvial riverbanks of southeastern Australia:

A quantified model of the earth-reinforcing properties of some native riparian trees

Benjamin Brougham Docker

A thesis submitted in fulfilment of the requirements
for the degree Doctor of Philosophy

School of Geosciences

The University of Sydney

2003

Abstract

It is generally accepted that tree roots can reinforce soil and improve the stability of vegetated slopes. Tree root reinforcement is also recognised in riverbanks although the contribution that the roots make to bank stability has rarely been assessed due to the reluctance of geomorphologists to examine riverbank stability by geomechanical methods that allow for the inclusion of quantified biotechnical parameters. This study investigates the interaction between alluvial soil and the roots of four southeastern Australian riparian trees. It quantifies the amount and distribution of root reinforcement present beneath typically vegetated riverbanks of the upper Nepean River, New south Wales, and examines the effect of the reinforcement on the stability of these banks.

The ability of a tree to reinforce the soil is limited by the spatial distribution of its root system and the strength that the roots impart to the soil during shear. These two parameters were determined for the following four species of native riparian tree: *Casuarina glauca*, *Eucalyptus amplifolia*, *Eucalyptus elata*, and *Acacia floribunda*. The four species all exhibit a progressive reduction in the quantity of root material both with increasing depth and with increasing lateral distance from the tree stem. In the vertical direction there are two distinct zones that can be described. The first occurs from between 0 and approximately 15 % of the maximum vertical depth and consists of approximately 80 % of the total root material quantity. In this zone the root system consists of both vertical and lateral roots, the size and density of which varies between species. The second zone occurs below approximately 15 % of the maximum vertical depth and consists primarily of vertical roots. The quantity of root material in this zone decreases exponentially with depth due to the taper of individual roots.

The earth reinforcement potential in terms of both geometric extent and the quantity of root material expressed as the Root Area Ratio (RAR) varies significantly from species to species. *E. elata* exhibited the highest values of RAR in soil zones beneath it while *E. amplifolia* reinforced a greater volume of soil than any of the other species examined.

The increased shear resistance (S_r) of alluvial soil containing roots was measured by direct in-situ shear tests on soil blocks beneath a plantation. For three of the species (*C. glauca*, *E. amplifolia*, *E. elata*) S_r increased with increasing RAR measured at the shear plane, in a similar linear relationship. The shear resistance provided by *A. floribunda* roots also increased with increasing RAR at the shear plane but at a much greater rate than for the other three species. This is attributable to *A. floribunda*'s greater root tensile strength and therefore pull-out resistance, as well as its smaller root diameters at comparative RARs which resulted in a greater proportion of roots reaching full tensile strength within the confines of the test.

Tree roots fail progressively in this system. Therefore determining the increased shear strength from the sum of the pull-out or tensile strengths of all individual roots and Waldon's (1977) and Wu's (1979) simple root model, would result in substantial over estimates of the overall strength of the soil-root system. The average difference between S_r calculated in this manner and that measured

from direct in-situ shear tests is 10.9 kPa for *C. glauca*, 19.0 kPa for *E. amplifolia*, 19.3 kPa for *E. elata*, and 8.8 kPa for *A. floribunda*.

A riverbank stability analysis incorporating the root reinforcement effect was conducted using a predictive model of the spatial distribution of root reinforcement beneath riparian trees within the study area. The model is based on measurements of juveniles and observations of the rooting habits of mature trees. It indicates that while the presence of vegetation on riverbank profiles has the potential to increase stability by up to 105 %, the relative increase depends heavily on the actual vegetation type, density, and location on the bank profile. Of the species examined in this study the greatest potential for improved riverbank stability is provided by *E. amplifolia*, followed by *E. elata*, *A. floribunda*, and *C. glauca*.

The presence of trees on banks of the Nepean River has the potential to raise the critical factor of safety (FoS) from a value that is very unstable (0.85) to significantly above 1.00 even when the banks are completely saturated and subject to rapid draw-down. It is likely then that the period of intense bank instability observed within this environment between 1947 and 1992 would not have taken place had the riparian vegetation not been cleared prior to the onset of wetter climatic conditions. Typical 'present-day' profiles are critically to marginally stable. The introduction of vegetation could improve stability by raising the FoS up to 1.68 however the selection of revegetation species is crucial. With the placement of a large growing Eucalypt at a suitable spacing (around 3-5 m) the choice of smaller understorey trees and shrubs is less important.

The effect of riparian vegetation on bank stability has important implications for channel morphological change. This study quantifies the mechanical earth reinforcing effect of some native riparian trees, thus allowing for improved deterministic assessment of historical channel change and an improved basis for future riverine management.

Biotechnical engineering on alluvial riverbanks of southeastern Australia: a quantified model of the earth-reinforcing properties of some native riparian trees

Table of Contents

Chapter One

Introduction

Chapter Two

Review of root reinforcement theory

Chapter Three

Root system architecture

Chapter Four

Individual root strength and pull-out resistance

Chapter Seven

The stability of root-reinforced riverbanks

Chapter Eight

Conclusions and implications of the research

APPENDIX A: Data supporting chapter Three

APPENDIX B: Data supporting chapter Four

APPENDIX C: Data supporting chapter Five

APPENDIX D: Data supporting chapter Six

APPENDIX E: Data supporting chapter Seven

List of figures

Chapter Four

Chapter Five

Chapter Six

Chapter Seven

List of tables

Chapter One

Chapter Two

Chapter Three

Chapter Four

Chapter Five

Chapter Six

Chapter Seven

Sample numbering

The numbering of samples involved characters that represent the soil or species being tested, the test type, and the number of the sample.

S :	Soil		A :	Architectural
CG :	*Casuarina glauca*		ST :	Shear tests
EA :	*Eucalyptus amplifolia*		PT :	Pull-out test
EE :	*Eucalyptus elata*		TT :	Tension Test
AF :	*Acacia floribunda*			

e.g. AFA3 is *Acacia floribunda* Architectural sample number 3.

Illustration Key

| *Casuarina glauca* | *Eucalyptus amplifolia* | *Eucalyptus elata* | *Acacia floribunda* |

Chapter One

Introduction and Overview

1.1   Overview and background to the research

1.1.1   General

This thesis examines the general problem of evaluating the contribution of riparian vegetation to alluvial riverbank stability. It does this by presenting the results of experiments designed to determine the increase in geomechanical strength provided to alluvial riverbank soils by the roots of four species of Australian riparian tree. Previous studies have demonstrated that the strengthening of riverbank soils can increase the resistance of the channel to morphological change both in terms of hydraulic geometry (Smith, 1976) and lateral stability (Hicken, 1984). By focussing on specific sites from the upper Nepean River this investigation extends and provides a sound quantitative basis for the pioneering work of Hubble (2001) who used simple and generalised geomechanical models to demonstrate that the removal of vegetative root reinforcement was a major contributor to the widespread bank collapse between 1947 and 1992.

The importance of channel boundary conditions for overall channel morphology has been recognised by many geomorphologists both regionally and internationally (e.g. Thorne, 1990; Huang & Nanson, 1997; Abernethy & Rutherfurd, 1998), although quantifying the effect of vegetation on the channel boundary properties has remained largely unstudied. In this country there exists only one other quantified assessment of the role of woody vegetation in riverbank stability, that of Abernethy (1999)(see also Abernethy & Rutherfurd, 2000a,b; 2001). Abernethy's work is pioneering not just from a local context but also through its application to riverbanks and their unique stability problems. Essentially this thesis addresses a similar problem to the one Abernethy (1999) dealt with: application of vegetative earth reinforcement in a riparian situation. This study approaches the problem from a somewhat different perspective focussing on the more process-orientated concerns of soil-root interaction and with particular emphasis on the effectiveness of different species. By the assessment of four representative riparian tree species it has been possible to model for the first time, the riverbank stability problem under a mixed as well as single species forest. Management issues such as tree spacing, location, and size are addressed, with discussion on the implications for overall riverine morphological change.

This is not the first attempt to incorporate the effects of vegetation into bank stability modelling on the Nepean River. However previous analyses (Hubble & Hull, 1996; Hubble, 2001; Docker & Hubble, 2001c) were dependent on conservative estimates of vegetative earth reinforcement inferred from studies mostly undertaken on exotic species growing in different environments, rather than on direct measurements of species extant within the study area. Given the large variation in earth reinforcement values measured between different environments (see Wu, 1995) there are clear concerns regarding the utility and accuracy of these previous stability analyses. This thesis directly addresses this problem and resolves it by the collection of data on the spatial distribution of earth reinforcement below riparian trees within the study area. Through examination of direct in-situ

shear tests, tension tests, and root pull-out tests a description of the root failure process within this environment is presented. From this process the strength of the soil-root system is determined and combined with the measured distributions of root material both with depth and lateral distance from the tree stem to present a model that estimates the increased shear strength of alluvial riverbank soils. Although concerned specifically with the study area it has more general application throughout southeastern Australia. The results have implications across environments both in terms of soil-root interaction and more general issues concerning vegetative effects on riparian morphological process. This thesis develops a biotechnical engineering approach to evaluate a geomorphological process of universal relevance and in so doing provides a basis for: a) an improved understanding of the response of vegetated banks to environmental change; and b) improved riverine management decision-making.

1.1.2   Riparian vegetation and morphological change

The presence of riparian vegetation has the potential to inhibit riverine morphological change through the alteration of bank material properties. The influence of bank properties on channel geometry is well documented (e.g. Hey & Thorne, 1986; Thorne & Osman, 1988b; Abernethy & Rutherfurd, 1998) such that the earth reinforcing effects of vegetation can increase bank stability and therefore prevent channel widening by mass collapse (Millar & Quick, 1993). Although Thorne (1990) aptly points out that it is not sufficient to consider banks as simply vegetated or un-vegetated. The role of vegetation is often both subtle and complex and factors such as type and density of vegetation, its age and health all influence the magnitude and type of effect that the vegetation will have on bank stability. While there are rare examples of vegetation having a negative effect on riverbank stability (e.g. Harvey & Watson, 1986), most case studies generally describe a positive influence.

Several studies have demonstrated that channels with vegetated banks are narrower and deeper than those that are un-vegetated (e.g. Schumm, 1960; Mosley, 1981; Millar & Quick, 1993; Huang & Nanson, 1997). This is a logical consequence of improved perimeter stability, whereby stronger bank material resists lateral expansion, concentrating floodwaters within the channel that increase riverbed scour. Numerous case studies demonstrate this phenomenon, often through observations of channel widening upon the removal of riparian vegetation (e.g. Montgomery, 1997; Trimble, 1997).

It has also been demonstrated that the type and distribution of riparian vegetation along a channel will affect the channel's ability to recuperate following periods of degradation (Wolman & Gerson, 1978) and that it is an indicator of the relative stage development of the bank and its resulting stability or instability (Simon & Hupp, 1986; 1990; 1992; Simon, 1989; Simon & Downs, 1995). Simon & Hupp's work indicates that riparian vegetation located high on the bank relative to the flow line indicates channel degradation while the re-emergence of vegetation closer to the flow line indicates and also aids, aggradation and restabilisation of the bank.

Clearly then there is considerable evidence that riparian vegetation is a crucial element in river morphology dynamics. There is a however a large body of literature in this country that argues that channel change is dominated by climatic factors, and which tends to discount the importance of channel boundary conditions (Erskine & Bell, 1982; Warner, 1983; 1987a,b; 1991; Erskine, 1986; Nanson, 1986; Erskine & Warner, 1988; Nanson & Erskine, 1988; Page, 1988; Riley, 1988; Simpson & Cane, 1993; and Simpson *et al.*, 1997). Others contend that climatic factors have a significant effect only because the removal of riparian vegetation reduces channel roughness and perimeter stability (Brooks & Brierley, 1997; Hubble, 2001). A review of this discourse as it relates to the study area is presented in the following section, but briefly, as Abernethy (1999) asserts, whether or not channel change is a response to catchment-wide human disturbance or to these factors in combination with climatic influence, the erodibility of a riverbank and thus the speed of channel change is limited or at least moderated by the condition of the riparian vegetation (see also Brooks & Brierley, 1997; 2000).

1.1.3   The study area: an overview

Location and geological setting

The study area (Fig. 1.1) encompasses the river banks and nearby floodplain of the two alluvial reaches of the Nepean River upstream of Wallacia Weir. The two reaches consist of The Camden Valley and The Wallacia Valley and total approximately 43 km in length. They are part of the Hawkesbury-Nepean River system which drains an area of 22 000 km² into the Tasman Sea north of Sydney.

Within the study area the Nepean River channel is entrenched in relatively broad, relict Tertiary and Quaternary river terraces comprised of sands and muddy sands set in bedrock valleys of Early to Middle Triassic age (Jones & Clark, 1991). The bedrock consists of two main lithologic substrates: the Hawkesbury Sandstone and the Wianamatta Group Shales. Within each substrate the morphology of incised gorge and alluvial flanked floodplain respectively dominate but are not necessarily exclusive. Soils of the Nepean River's banks and floodplains are fairly uniform throughout the study area and are dominated by Nepean Association Quaternary alluvium. They are comprised of deep, friable, weakly structured brown loams and sandy loams (Walker, 1960), classified by Stace *et al.* (1968) as Alluvial Soils or Minimal Prairie Soils.

The channel is highly regulated with a number of dams and weirs over its length. As a result flow is almost non-existent except during periods of heavy rainfall, and today the river resembles more a series of long, narrow lakes, rather than the original riffle and pool sequence of pre- and early-European settlement (Hubble, in press).

The morphology of the channel in the alluvial reaches is quite distinct from the surrounding gorge sections and as a result responds differently to changes in water and sediment discharges. Both types

of channel are limited in the extent to which they can change due to the restriction on channel migration imposed by the shale and sandstone basement. Climatic, eustatic, and tectonic events have caused this stream to be steeply incised (Hicken, 1967). In addition to these longer term events recent down-cutting appears to have lowered the existing channel in relation to the alluvial flats (Hicken, 1967). This control limits change in parameters such as meander wavelength, gradient, and sinuosity (Warner, 1983) and increases the height of the riverbanks. As it exists today the planform of the Hawkesbury-Nepean River is that of a low sinuosity stream. The valley geometry has been stable for a geologically significant period of time (in the order of 5 to 60 million years) and by all accounts is in a state of long-term stability (Bishop, 1982; Bishop, 1986; Hubble, 2001).
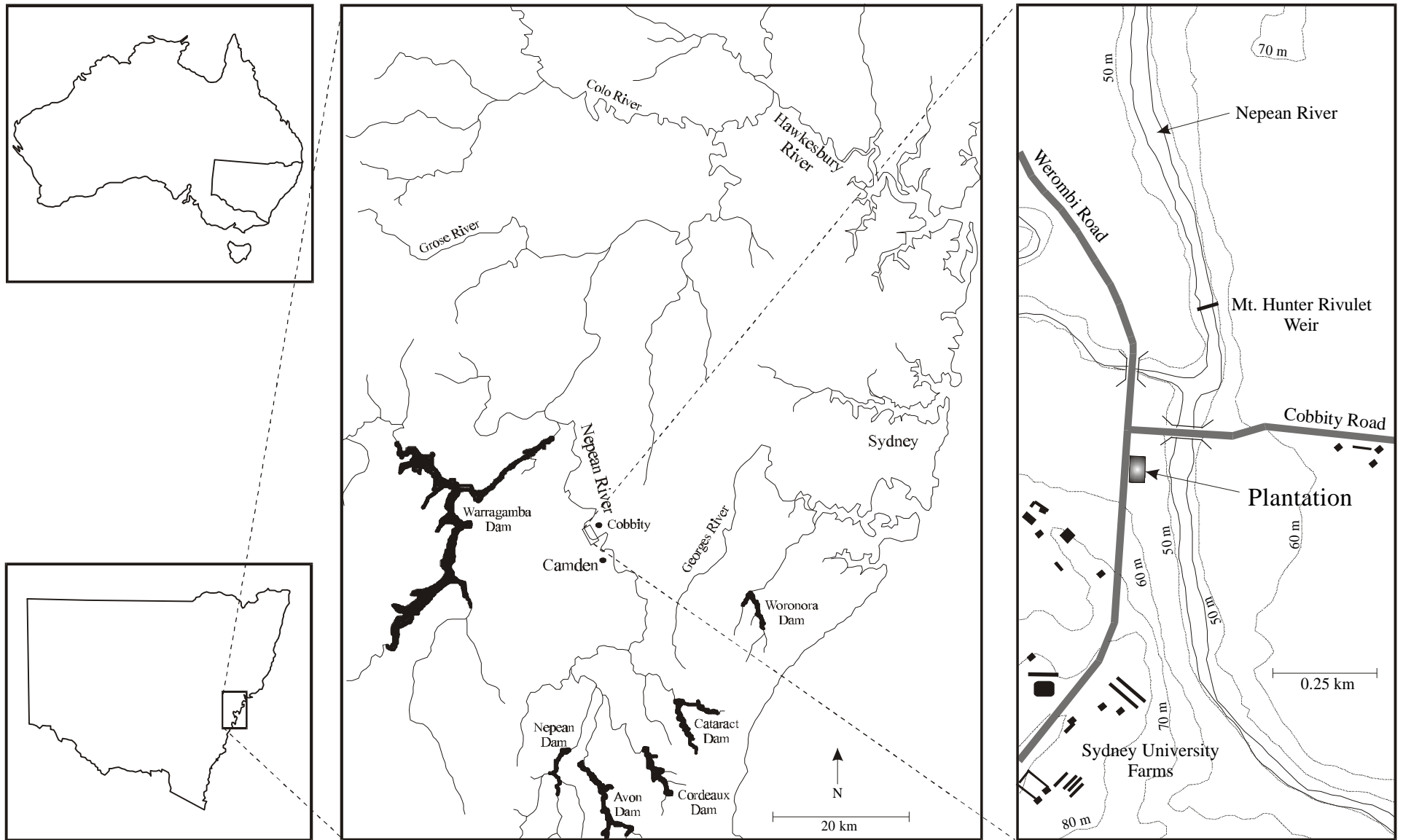
Figure 1.1: Location of the study area on the Hawkesbury-Nepean River system and the plantation near Cobbity Bridge where experimental work was undertaken.

Hydrology and flow regime

In the late 1940s there was a dramatic shift to a wetter climate in south-eastern New South Wales (Pittock, 1975; Cornish, 1977). Kraus (1955) also recognised that annual rainfall in New South Wales was much greater in the latter part of the 19th century than in the first half of the 20th century; prompting some quarters to propose the existence of alternating climatic regimes (Erskine & Bell, 1982; Warner, 1987a; Erskine & Warner, 1988) characterised by periods of generally wet or generally dry conditions several decades long. This apparent secular climate change has obvious repercussions for the hydrological regime of coastal river systems. Hall (1927) and Pickup (1976) recognised that the increase in mean annual rainfall since the late 1940s had resulted in an increase in the magnitude and frequency of floods in the Cumberland Basin west of Sydney (Fig. 1.2) however they did not show that the trends and inter-relationships were statistically significant. Bell & Erskine (1981) were the first to show that the post 1946 increase in rainfall produced statistically significant increases in annual runoff and flood frequencies. Conversely, Hall (1927) examined the magnitude and frequency of floods at Windsor and found that the latter part of last century was characterised by many floods and high rainfall in comparison to the early part of this century. A finding supported by Gentilli (1971) in his analysis of mean annual rainfall for coastal New South Wales.
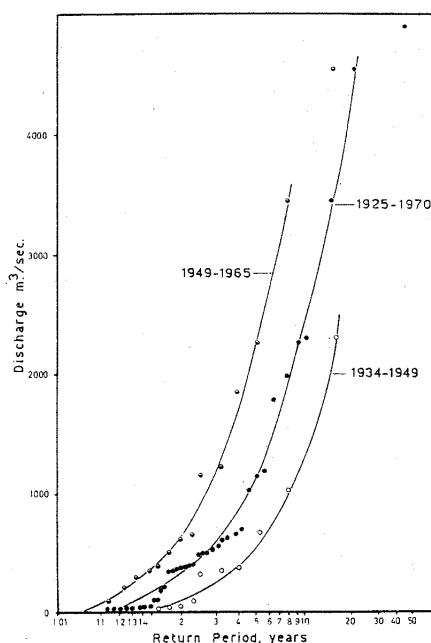
Figure 1.2: Flood frequency curves for the Nepean River at Wallacia demonstrating the significant increase in flood discharge on the Nepean River since the late 1940s. (From Pickup, 1976; *Source*: Records of the Metropolitan Water Sewerage and Drainage Board).

Warner (1987a; 1987b) described these periods of higher than average and lower than average rainfall and flooding, as flood- and drought-dominated regimes respectively, or FDR and DDR. These periods appear to last from 3 to 5 decades with DDR suggested to have occurred from 1821

to 1856 and again from 1901 to 1948; while FDR are suggested to have occurred from 1799 to 1820, from 1857 to 1900, and from 1949 to 1991. Erskine & Warner (1988) indicate that the change in flood regime involves a significant variation in the number of floods of a given height class and that this variation in flood frequency may also be accompanied by a significant variation in flood height.

Recent work (see Brooks & Brierley, 1997; Kirkup *et al.*, 1998) questions the validity of the FDR/DDR model and instead proposes that there is only enough reliable evidence to support a single, secular climatic change (i.e. the change to a wetter climate in the late 1940s). It suggest that the statistical procedures used by Erskine & Warner (1988) in the derivation of FDRs and DDRs may possess some limitations.

Documentation and interpretation of morphological change

Despite the constraints on morphological change imposed by the bedrock entrenchment of the channel, the adjustment of the Hawkesbury-Nepean since European settlement has been dramatic (Warner, 1983; 1987a,b; 1991; 1997; Roeson, 1995; Hubble, 1997; 2001). Hubble & Harris (1993) found that both bank failure and toe erosion are currently problems in most parts of the Hawkesbury-Nepean that are comprised of unlithified sediments. Hubble (1997) examined bank failures on the Nepean River between Theresa Park Weir and Menangle Weir and indicated that the significant morphological changes of bank steepening, channel widening, and toe retreat are extensive.

There is considerable debate as to the causes of this morphological change. Until fairly recently the literature was primarily focused on the apparent shift in climatic regime since the late 1940s as the main cause for change both within this study area and throughout southeastern Australia. However there is a growing body of work that indicates a combination of both human-induced and natural factors to be responsible (see Hubble & Hull, 1996; Erskine & White, 1996; Brooks & Brierley, 1997; 2000; Hubble, 2001).

Since the apparent shift in climatic regime in the late 1940s severe mass failure of the banks of the Nepean River can be observed throughout the aerial photographic record. Most large failures appear in the interval between 1947 and 1965 (Hubble, 1996; Docker, 1997; Hubble, 2001), corresponding with a period of repeated large floods (Pickup, 1976; Warner, 1987a,b). Verifying theory by Schumm (1971) which states that increasing both water and sediment discharge will cause width increases and depth decreases, Warner (1983) notes that since 1949 the width of the Nepean River has increased dramatically (see also Warner, 1987; Erskine & Warner, 1988). While the increased size and frequency of floods was undoubtedly the driving force in this process, recent investigations (Clarke & Geary, 1987; Hubble & Hull, 1996; Hubble, 1997 & 2001; Docker, 1997; Docker & Hubble, 2001c) note that bank failure was much more common on devegetated banks, and these studies generally conclude that the dramatic morphological change documented since 1949 would not have been as severe if human activity had not removed the riparian vegetation protecting the banks.

Other human activities listed by Hubble & Hull (1996), Erskine & Green (2000), and Hubble (2001) that influence morphological change on the Nepean River include the construction of dams and weirs within the catchment, and the extraction of sand and gravel from within the channel. Kirkup *et al.* (1998) suggest that the effect of climatic change on river geomorphology has been gravely over-emphasized considering the extensive anthropogenic alteration to the catchment and riparian vegetation that has occurred concurrently.

Previous research into morphological change within the study area has mostly employed a temporal coincidence approach based on comparison of the flood record with observational analysis of the aerial photographic record and measured channel widths. It is only recently that the situation has begun to be treated in terms of riverbank stability processes. Hubble & Hull (1996) used geomechanical models to describe bank collapse and toe retreat within the Camden Valley and to assess the relative contributions that the soil, vegetation density, and changes in bank geometry have in determining the long-term stability of these natural slopes. Modelling was undertaken for both plane failures (by the infinite slope method) and circular failures (by Bishop's circle method) and in both cases the investigators demonstrated that critically stable vegetated slopes become unstable if they are devegetated and saturated by flooding. Findings confirmed by Docker & Hubble (2001c) in the Wallacia Valley and Hubble (1998; 2001; in press) in the Camden Valley using similar methods. However the models used in these investigations used assumed rather than measured values of root strength that were based on minimum values of reinforcement obtained from studies of exotic tree species in different environments. The models also assumed a uniform root reinforcement over the bank profile and with depth, which is probably an oversimplification given the complex nature of root system morphology. No study has been identified that assesses root system morphology or root strength contributions to soil shear resistance along the Nepean River, and only one other study has been conducted within Australia; that of Abernethy (1999) on the Latrobe River, Victoria (see also Abernethy & Rutherfurd, 2000a; 2001), who characterised *Eucalyptus camaldulensis* (River Red Gum) and *Melaleuca ericifolia* (Swamp Paperbark).

1.2   Research aims and objectives

The ultimate aim of the research presented here is to model and assess the stability of alluvial riverbanks by quantifying the earth-reinforcing effects of the roots of four riparian tree species native to Australia. It is apparent from the literature review (chapter 2) that this requires information on: a) the spatial root distribution within the bank material below trees of each species; b) the amount of soil reinforcement provided by roots of each species; c) the mechanisms of root failure within this environment; and d) determination of the factors of safety for typical riverbanks within the study area that incorporate root reinforcement effects. To collect this information and therefore achieve the stated ultimate aim the following aims and objectives were undertaken by chapter:

1. To provide a review of the literature concerning tree root reinforcement and its effects on slope stability. {Chapter 2}

2. To determine and describe the root system architecture of the trees: *Casuarina glauca, Eucalyptus amplifolia, Eucalyptus elata*, and *Acacia floribunda* growing within the study area; and to present a model based on this architecture that allows an estimation of the spatial root distribution beneath a mature tree of typical dimensions. This is achieved by: (a) extracting and measuring the entire root systems of juvenile trees of the said species with respect to spatial variation in their total root cross-sectional area; and (b) documenting observations on the extent and form of the partially exposed root systems of some mature trees growing within the study area. {Chapter 3}

3. To assess the individual strength and pull-out resistance of tree roots of the above species by measuring the force required to pull individual tree roots from the soil and comparing it with their measured tensile strengths. {Chapter 4}

4. To determine the amount of root reinforcement across a shear surface provided by tree roots of the above species. This is achieved by: (a) measuring the direct shear resistance of soils containing tree roots of the above species and assessing the relationship of this parameter with root area quantity at the shear plane; (b) interpreting observations of the root failure process during direct in-situ shear tests to describe the mechanism of failure and its implications; and (c) comparing direct shear test measurements with individual root pull-out results to assess the utility of the simple root model of Waldron (1977) and Wu *et al.* (1979) in this particular environment. {Chapter 5}

5. To incorporate the root system architecture data and the root reinforcement data into an integrated model of earth-reinforcement beneath riparian trees of the above species, for use in riverbank stability assessments. {Chapter 6}

6. To assess the stability of typical 'pre-failure' and 'present-day' riverbank profiles within the study area under a variety of vegetated conditions by a determination of the effect of different tree species, tree size, spacing and location, on the factor of safety of the banks. {Chapter 7}

1.3   Overview of experimental methods

There were three main components to this research: root system architecture analysis, root strength determination, and riverbank stability modelling. These components were all undertaken on elements from within the study area described in section 1.1.2. The analysis and testing of roots was performed on small trees grown in a plantation near the Nepean River at Cobbity Bridge (Fig. 1.3). The riverbank stability modelling involved the application of a reinforced earth model, consisting of the amalgamated root strength and architectural data, to analyse typical riverbanks within the study area.

Figure 1.3: The Cobbity plantation where root strength and architectural assessment samples were taken. December 1999 immediately after the second planting. The tree plantation at the left of view marks the levee crest of the Nepean River channel.

The Cobbity tree plantation was located on the University of Sydney Farms and consisted of five sub-plantations. Four of these were single species (90 trees each) and used for root strength testing, while the fifth was planted with multiple species (6 trees of each species) and used for root architecture assessment. The area to be planted was prepared by spraying the existing vegetation with roundup and cultivating the soil to a depth of 0.2 m. This process was completed two days prior to planting. Seedlings of up to 8 months old were planted in two batches. The first planting occurred in February 1999 and the second in December 1999. Seedlings were grown in large diameter pots (20 cm) and planted just as the root system was making contact with the pot wall. Watering was conducted on a limited basis during periods of low rainfall and pests were kept to a minimum with an insecticide treatment. A layer of straw mulch was applied to the soil shortly after planting but no fertilisation or chemical soil improvement was conducted.

The fieldwork undertaken to determine the various root measurements was extremely laborious and required many thousands of field hours to obtain the necessary data. Although it would have been extremely beneficial to perform the measurements on mature trees and on all species common to the study area, time and resources restricted the analysis to small trees of four representative species found throughout large parts of southeastern Australia. Estimates of mature tree characteristics were based on observation and measurement of naturally exposed roots within the river channel. Accessing the roots of mature, living trees in an environmentally sensitive area is problematic at best and usually restricted to no more than a few specimens. Assessment of a larger number of small trees allowed a comparison both within and between species.

1.3.1   Plantation soil properties

The location of the plantation on the floodplain immediately adjacent to the river channel (Fig. 1.1) enabled tests to be conducted in alluvial soils similar to those that occur throughout the study area. In-situ shear tests were conducted at an average depth of 0.30 m where the soil is a clay sand. Table 1.1 describes the particle-size distribution and unified soil classification with depth to 1.75 m. Bulk unit weights for both dry and saturated samples are also given. The average specific gravity of the soil is 2.68.

Table 1.1: Particle-size distribution and classification for plantation soils. SC = clay sand, by the Unified Soil Classification System.

Depth (m)	% Sand	% Silt	% Clay	g_{dry} (kN/m³)	g_{wet} (kN/m³)	Classification
0.25	55.45	18.20	26.35	15.68	19.64	SC
0.75	57.67	11.76	30.57	18.44	21.56	SC
1.25	50.46	16.51	33.03	17.80	21.06	SC
1.75	53.00	14.10	32.90	17.79	21.28	SC

Undisturbed soil samples were taken from a depth of 0.30 m beneath the plantation at locations where no root material was found. They were transported to the laboratory for direct shear testing under five normal loads of 3.0 kPa, 19.3 kPa, 41.4 kPa, 85.2 kPa, and 173.3 kPa. Tests were conducted under saturated and submerged conditions and at a slow rate of strain to allow water to drain and pore pressures to dissipate at the failure surface. The Mohr-Coulomb failure envelope (Fig. 1.4) for peak soil strength gave the effective strength parameters c' = 8.3 kPa and f = 39.6º.
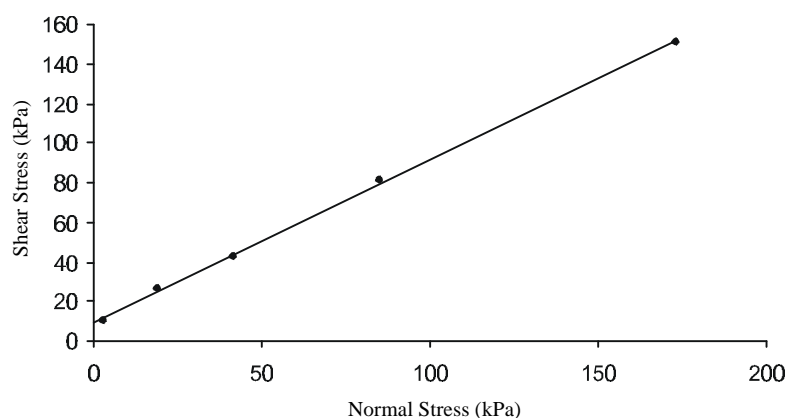
Figure 1.4: Mohr-Coulomb failure envelope for laboratory direct shear tests on undisturbed soil samples taken from beneath the plantation. $c' = 8.3$ kPa and $f' = 39.6°$. $R^2 = 1.00$.

1.3.2   Riparian tree species examined

The tree species selected for analysis in this study were: *Casuarina glauca*, *Eucalyptus amplifolia*, *Eucalyptus elata*, and *Acacia floribunda*. These species were chosen due to their commonality within the study area, their relatively fast growing constitution and the varying locations they occupy upon a riverbank profile. *C. glauca* is usually found at the permanent waterline and in swampy areas. *A. floribunda* is usually found on mid-bank regions while *E. amplifolia* and *E. elata* grow in the upper-bank and floodplain soils. The four species also represent a range of above ground sizes. Initially it was planned to study *Casuarina cunninghamiana* rather then *C. glauca* due to the former's dominance in the freshwater reaches of the study area. Unfortunately upon delivery of the seedlings from the nursery it was discovered that the wrong species had been grown and that to rectify the problem a further 6 to 8 months would be required for *C. cunninghamiana* to be seeded and grown to a size suitable for planting. It was important to have the trees grown specially from seed in order to be able to plant them with their root systems still relatively unaffected by the pots. Particularly since normal commercial practice is to grow the trees to a larger size in smaller pots before selling them. *C. cunninghamiana* trees were ordered at this time and later planted however it has not been possible within the time constraints of this project to grow them to a size suitable for testing. They will however be the subject of future experimental work due to their recognised function in bank stabilisation (see Midgley *et al*, 1983).

Casuarina glauca (Fig. 1.5a) is a medium sized tree that grows to 20 m in height. It is more common in brackish marshes and estuaries with waterlogged soils and a saline influence but is not restricted to them and is often found within the study area of the upper Nepean River. Generally *C. cunninghamiana* is more dominant in freshwater reaches but the two species hybridise naturally where their ranges meet (Howell, *et al.*, 1995) suggesting that any differences of morphology between them may be as much related to site conditions as inherent biology. *C. glauca* is a neat and pyramidal tree when young, but rapidly grows into a tall, scraggly tree with contorted, misshapen branches

(Robinson, 1991). When mature it displays a hard, furrowed bark, grey-green needle-like foliage with male and female flowers on separate trees (Howell, *et al.*, 1995). It is capable of root-suckering and often grows in dense stands. It has a range from Eden in southern New South Wales up to southern Queensland and its common name is 'Swamp She Oak'.
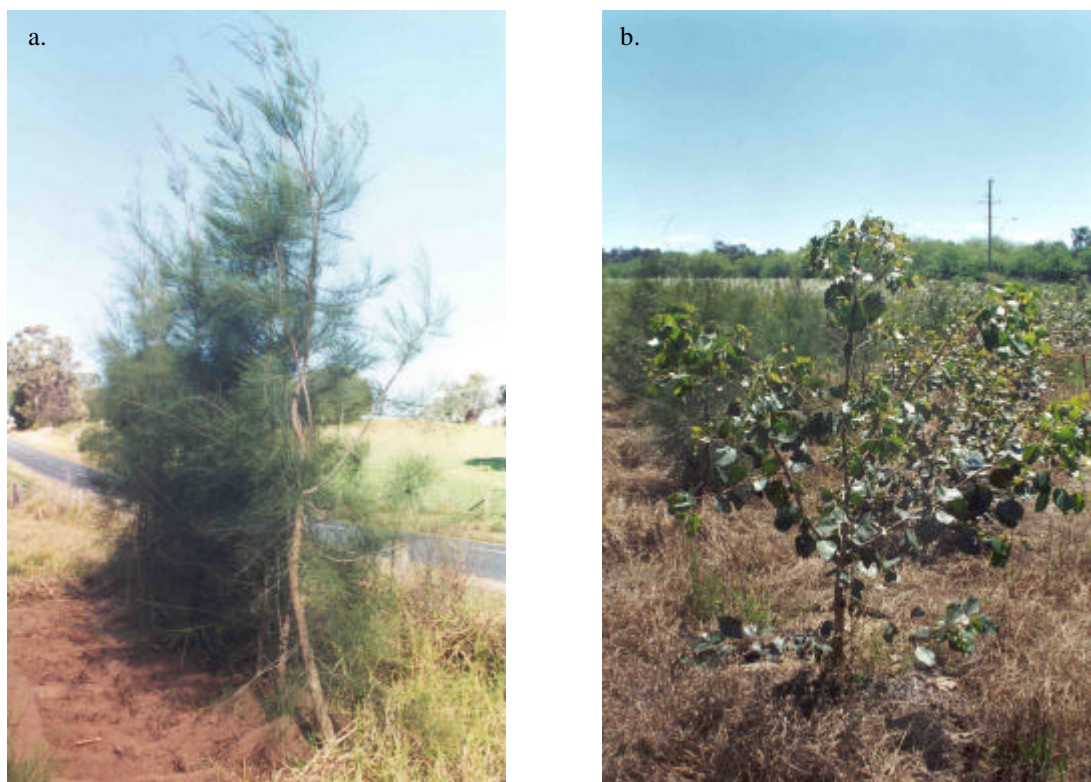
Figure 1.5: Tree species growing within the plantation: **a.** *Casuarina glauca* **b.** *Eucalyptus amplifolia.*

Eucalyptus amplifolia (Fig. 1.5b) grows on levee banks and wetland margins within the study area. It occurs more generally in coastal regions from Bega to Coffs Harbour and is known commonly as 'Cabbage Gum' due to a very broad leaf that is particularly large in the juvenile. It can survive periods of water-logging and grows particularly well in clayey, shale-derived soils. The species can live to a considerable age (up to 100 yrs) and when mature is a large tree up to 30 m tall with smooth, white and grey platy bark. Flowering occurs between December and January with seeds dispersed locally by wind (Howell, *et al.*, 1995).

Eucalyptus elata (Fig. 1.6a) is a large tree that grows on levee banks of both alluvial and gorge reaches of the study area. Although relatively short lived it is a quick growing species and can reach heights of up to 45 m when mature. It has a rough grey-black bark on its lower trunk and a smooth pale bark above. Propagating by wind-dispersed seed it is recognised by its sparse, slender bluish foliage and white flowers around September (Robinson, 1991). It is commonly known as 'River Peppermint'.

Acacia floribunda (Fig. 1.6b) is a small shrubby tree growing to 3-8 m in height in both alluvial and gorge reaches of the study area. It is a fast growing tree (growing 5 metres to maturity in 3-4 years)

and when mature displays an attractive drooping foliage with an abundant display of pale yellow flowers from July to September (Howell, *et al.*, 1995). Seeds are dispersed by fauna and propagate from heat treatment on levee banks and near the water's edge. It is known commonly as 'White Sallow Wattle' or 'White Sally' and occurs on the New South Wales coast and ranges as well as in Victoria and southern Queensland.

Figure 1.6: Tree species growing within the plantation: **a**. *Eucalyptus elata* **b**. *Acacia floribunda.*

1.3.3   Root system architectural assessment

The methodological process designed, allowed for a best estimate of root system architecture based on a reasonably attainable dataset consisting of multiple samples. The entire root systems of six specimens of each species were extracted from the soil for analysis by the classical method described in Böhm (1979) and employed by Riestenberg (1994). The extraction of entire root systems, although extremely laborious, allows direct observation and detailed measurement in a complete description of root distribution within the soil layer. This approach was used because it was suspected from the literature review presented in the following chapter that overall architecture may play a role in the manner in which different trees act to reinforce the soil. An alternative method for assessing root distribution within the soil is the 'profile wall' method (also of Böhm, 1979) as employed by Abernethy and Rutherfurd (2001). This method has obvious advantages in that if undertaken with mechanical excavation equipment it can reduce the labour costs considerably. It also allows the collection of root distribution data in both the vertical and lateral direction however it does not enable any observation of the root system in its totality and as such

may preclude an explanation of root reinforcement behaviour that cannot be provided by root quantity alone. The vertical orientation of the walls may also result in a significant portion of vertical roots not being measured as they either grow down parallel with the profile wall or are removed during excavation of the trench. Complete extraction was also preferred due to the possibility of observing the 3-dimensional growth pattern and therefore the radial distribution of roots around the tree stem.

1.3.4   Soil-root strength determination

The increased shear strength of soil containing roots was measured by direct in-situ shear tests on blocks of soil beneath the Cobbity plantation. In-situ shear tests replicate the failure process of Coulomb's shear-box method (see Lambe & Whitman, 1979; Craig, 1992), by applying different normal confining loads to produce a failure envelope on a plot of shear stress versus normal stress (e.g. Fig. 1.4). The different normal loads represent different confining stresses in the field that are representative of different depths within the soil layer. These tests allow a relationship between root quantity at the shear plane and increased shear resistance to be obtained.

Root pull-out and tensile strength tests were also conducted on excavated root segments to assist the explanation of in-situ tests and determine the likely root failure process. An assessment of the simple root reinforcement model is possible with this data and the implication of its use in this environment is discussed.

1.3.5   Analysis of reinforced riverbanks and their stability

The ability of roots of the trees examined in this study to reinforce the earth and thereby contribute to the increased stability of riverbanks within the study area was examined by the integration of the root strength and architectural data obtained, into a simple slope stability model based on Bishop's (1955) simplified method. Using the commercially available slope stability programme XSLOPE to model circular failures, the critical failure surface was found for a bare soil profile as well as the following vegetated conditions:

1. A single tree of each species located at different positions on the bank profile.
2. A single species forest at different tree spacings, for each species.
3. A single species forest with different tree sizes, for each species.
4. A multiple species forest with *C. glauca* located at the waterline, *A. floribunda* on the mid-bank, and *E. elata* and *E. amplifolia* at the bank crest.
5. A forest consisting of two species in alternating positions over the bank profile.

Typical riverbank profiles and material properties were modelled as both 'pre-failure' and 'present-day' geometries under conditions of complete saturation as well as a partly drained condition.

Chapter Two

Review of root reinforcement theory

2.1   Introduction

It has been illustrated in chapter one that riparian vegetation can affect the morphological development of a channel. The underlying processes involved however have not been the subject of much attention amongst fluvial geomorphologists although it is suspected that the direct mechanical reinforcement of soils is the primary vegetative influence. This chapter reviews the literature concerning the ability of tree roots to reinforce soil and therefore improve slope stability. It provides the context for this project and the methodological design presented in the previous chapter.

2.2   Tree roots and reinforced earth

Woody and herbaceous vegetation is commonly used to prevent surficial soil erosion (Coppin & Richards, 1990). Its influence on the processes of mass stability is less well appreciated although it is generally accepted that vegetation affects slope stability through six primary mechanisms (Gray & Leiser, 1982). These are:

1. Root reinforcement of the soil
2. Soil moisture modification
3. Buttressing and soil-arching
4. Surcharge weight of trees
5. Root wedging
6. Wind-throw

It is likely that the first four factors listed here generally aid in the stabilisation of a slope although the surcharge weight of a tree may have either a beneficial or adverse effect depending on such characteristics as its position on a slope, and the geometry and angle of the slope (see Styczen & Morgan, 1995). Both Abernethy & Rutherfurd (2000b) and Hubble (2001) modelled the effect of surcharge weight on riverbank stability and found that generally it had minimal effect. Root wedging and wind-throw will potentially have a negative effect on slope stability however their significance is largely unstudied and therefore unknown. Brown & Sheu (1975) developed a theoretical framework for assessing the effect of wind on trees and asserted that forces could be transmitted to the soil via the roots, thus increasing the likelihood of failure.

The factors listed above have been the subject of comprehensive reviews (Gray & Leiser, 1982; Greenway, 1987; Coppin & Richards, 1990; Styczen & Morgan, 1995; Wu, 1995) with a general consensus that the positive effects on slope stability far outweigh the negative. As root reinforcement and soil moisture modification directly impact upon soil strength it is suspected that they will have the greatest effect on slope stability. This research focuses only on root reinforcement

of the soil as it has not been possible to assess both mechanisms within the constraints of a research programme of this nature.

An understanding of the probable mechanisms of root reinforcement has been developed through a number of areas of research including: theories of reinforced earth (Vidal, 1969; Schlosser & Long, 1974), testing of soil reinforcement with low modulus fabrics and fibres (Broms, 1977; Tumay *et al.*, 1979; Collios *et al.*, 1980; Gray & Ohashi, 1983; Shewbridge & Sitar, 1989), theoretical models of fiber-root reinforcement (Waldron, 1977; Wu *et al.*, 1979; Luckman *et al.*, 1982; Wu *et al.*, 1988b), laboratory and field tests of root-reinforced soil (Kassif & Kopelovitz, 1968; Endo & Tsurata, 1969; O'Loughlin, 1974a,b; Waldron, 1977; Waldron & Dakessian, 1981; Ziemer, 1981; Terwilliger & Waldron, 1990; Abe & Ziemer, 1991; Zhou *et al.*, 1997; Wu & Watson, 1998; Ekanayake & Phillips, 1999; Abernethy & Rutherfurd, 2001), and studies of root interaction with landslide shear surfaces (Burroughs & Thomas, 1977; Riestenberg & Sovonick-Dunford, 1983; Terwilliger & Waldron, 1991; Riestenberg, 1994). These studies indicate that root reinforcement of soil is a significant consequence of soil-root interaction that has implications for vegetated slope stability across a range of environments. A background to these areas of research that have led to the development of knowledge in this field is presented in this section.

2.2.1 Earth reinforcement theory

Soil is strong in compression but weak in tension, and roots are weak in compression but strong in tension. Therefore when soil and roots are combined the resultant soil-root matrix produces a mass which is much stronger than either the soil or the roots on their own. The roots act by transferring the shear stresses developing in the soil to the tensile resistance in the roots, and also by distributing stresses through the soil, so avoiding local stress build-ups and progressive failures.

The theory of reinforced earth was first developed by Vidal (1969). As a vertical principal stress is applied to an unconfined element of soil the element will strain laterally as it compresses axially (Fig. 2.1). If reinforcement is added to the soil in the form of horizontal strips, the lateral movement induced in the soil generates a frictional force between the soil and the reinforcement. As a tensile force develops within the reinforcement a corresponding compressive lateral confining stress is generated within the soil. This lateral confining stress is analogous to an externally applied confining pressure and is proportional to the applied normal confining stress up to a limit defined as the 'critical confining stress' (Long *et al.*, 1972, in Ingold, 1982). The action of reinforcement in soil is therefore not one of carrying developed tensile stresses but of the anisotropic reduction or suppression of an applied normal strain rate. This suppressive mechanism led to the concept of anisotropic cohesion.
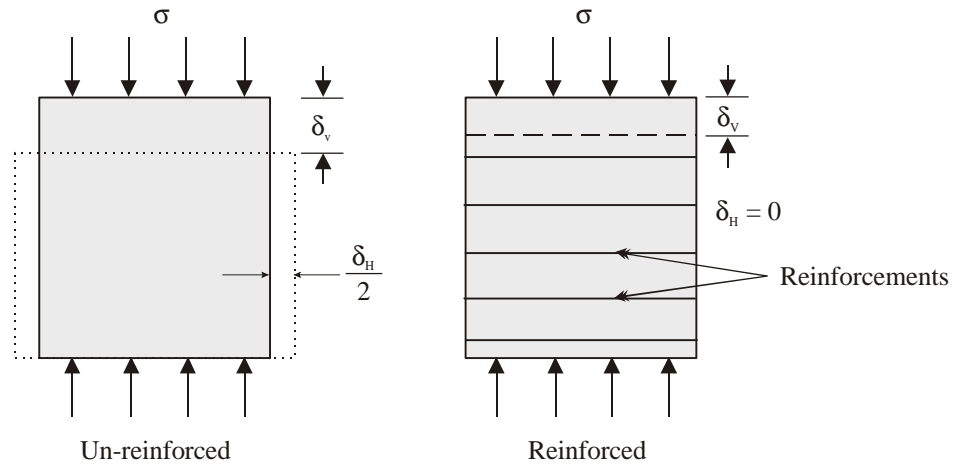
Figure 2.1: The action of reinforcements on a cohesionless soil element (after Gray & Leiser, 1982). The reinforced element resists lateral expansion through the mobilisation of a frictional force between the soil and the reinforcement.

Observations by Long *et al.* (1972) of the critical confining stress and failure modes of fibre reinforced sand samples indicated that above this critical stress value the reinforcement tended to fail in tension rather than slip or pull-out of the soil, as was the case below. It was also shown that above this point the 'equivalent confining stress' ceases to increase, but instead a constant increase in shear resistance occurs (provided the applied confining stress remains above this point). As a result the failure envelopes of both the reinforced and unreinforced sand are parallel (Fig. 2.2) for tensile reinforcement failure, indicating the same angle of internal shearing resistance. They therefore concluded then that the additional strength imparted by the reinforcement could be represented by an apparent anisotropic cohesion. Schlosser & Long (1973, cited in Ingold, 1982) supported these observations with an expression for the anisotropic cohesion obtained by theoretical analysis:

$$c' = \frac{T\sqrt{K_p}}{2h}$$

[2.1]

where c' is the anisotropic cohesion; T is the tensile strength of the reinforcement; h is the vertical reinforcement spacing; and K_p is the coefficient of passive earth pressure.

Below the critical confining stress failure occurs by disruption of the soil-reinforcement bond whereby the reinforcement slips or pulls-out of the soil. As stated above, for this kind of failure it is assumed that friction along the reinforcement is proportional to the normal confining stress. The resultant effect is for an increased friction angle of the earth reinforced sample (Fig. 2.2). The increased friction angle is determined by (Hausmann, 1976):

$$\sin\phi'_r = \frac{K_a - F - 1}{F - K_a - 1}$$

[2.2]

where ϕ'_r is the friction angle of the reinforced earth sample; K_a is the coefficient of active earth pressure; and F is the Tensile force developed by reinforcements and acting on the failure plane.
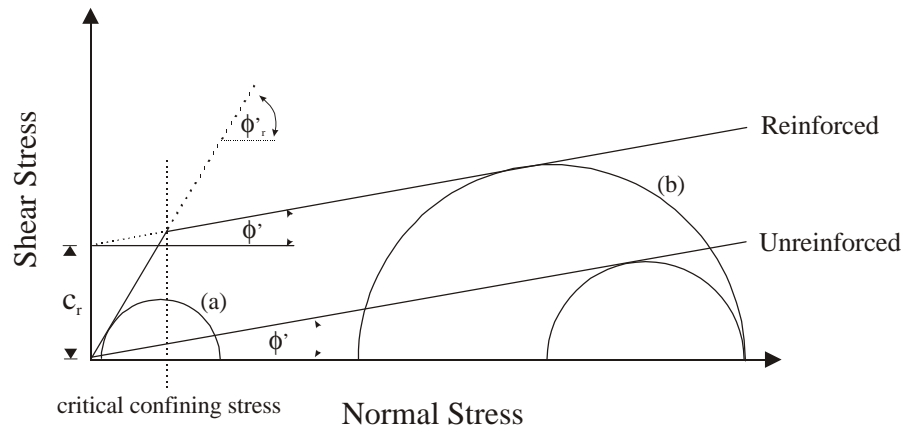
Figure 2.2: Mohr-Coulomb envelopes for reinforced and unreinforced soils with circles describing failure by (a) slippage and (b) reinforcement rupture (after Hausmann, 1976). The critical confining stress varies for different soil-fibre systems and is a function of such properties as tensile strength and modulus of the fibres, length/diameter ratio of the fibres, and frictional characteristics of the fibres and soil (Gray & Ohashi, 1983).

Investigators of root reinforcement in soil have generally found that roots have failed in tension and therefore posit that root systems have a negligible influence on the frictional component of soil strength (Endo & Tsurata, 1969; O'Loughlin, 1974a,b; Waldron, 1977; Gray & Megahan, 1981; Waldron & Dakessian, 1981; O'Loughlin *et al*, 1982; Riestenberg & Sovonick-Dunford, 1983; Abernethy & Rutherfurd, 2001). That is, the confining stresses within the soil are large enough to surpass the critical confining stress for a given root length, thereby allowing mobilisation of the required frictional bond between the soil and the root that prevents the root from pulling out of the soil intact. The shear zone must also be wide enough to allow roots crossing it to deflect, elongate, and develop their maximum tensile strength, rather than failing in shear, as would be the case with a thin shear zone (a few millimetres wide) where the roots are held rigidly by the soil on either side (Burroughs & Thomas, 1977). These observations have been used to demonstrate that root reinforcement of soil is best approximated by an increase in apparent soil cohesion that varies in proportion to the concentration of roots within the soil.

Some studies indicate that the increase in apparent soil cohesion is limited to roots up to about 2 cm in diameter (Coppin & Richards, 1990). Beyond this size the reinforcing effect is thought to be largely due to a root's ability to anchor a relatively weak layer of soil across a discontinuity, the shear surface, to an underlying stronger soil or bedrock. The justification for this limit is not completely clear as field studies often cited as supporting it (e.g. Burroughs & Thomas, 1977; O'Loughlin & Watson, 1979), although demonstrating the importance of small roots to increased soil shear strength, do not actually measure the effect of larger roots. Burroughs & Thomas (1977) measured roots up to 1 cm in diameter, and O'Loughlin & Watson (1979) up to 3 cm. An extensive literature search was unable to locate any study that assessed the reinforcing actions of roots of different sizes. There are also many examples of small roots (< 2 cm diam.) acting or suspected as acting like ground anchors by growing into discontinuities and fissures in the bedrock or more stable substrate (e.g. Swanston, 1970; Swanston & Dyrness, 1973; Riestenberg, 1994). Irrespective of any specific

size limit it is generally agreed that apart from an increase in apparent soil cohesion roots may also increase the shear strength of a soil by an anchoring mechanism.

2.2.2 Tree roots as anchors

The mechanism of root anchoring is similar to that of root reinforcement, except that it occurs on a larger scale (Greenway, 1987) and as with flexible cables or ground anchors (Hanna, 1982) the individual roots act to resist shear by mobilising their tensile strength upon displacement, and fail either by pull-out or by breaking in tension, rather than in shear. The magnitude of tensile resistance that a root can mobilise to prevent failure will be a measure of the overall tensile strength of the root as well as its individual morphology, which includes the length of the root embedded within the soil (Gray & Sotir, 1996) and its branching pattern (Riestenberg, 1994).

The ability of roots to resist failure as anchors can be measured by in-situ pull-out tests, where the pull-out resistance has often been found to be a function of the root diameter at the shear surface, although it is strongly dependent on the number and orientation of branch roots (Wu *et al.*, 1979; Riestenberg, 1994). The pull-out resistance of a highly branched system may be considerably less than the strength of the main root segment due to progressive failure of the branches. In cases where branching is minimal the difference between pull-out resistance and tensile strength of the main root segment has been found to be statistically insignificant (Abernethy & Rutherfurd, 2001). In general however the pull-out resistance will increase with increasing diameter of the root at the shear surface (Riestenberg, 1994).

An important difference between root anchorage and roots that act as part of a soil-root matrix is the ability of the root anchors to act independently and provide varying levels of shear resistance at different displacements. The effect is to provide a reduced increase in shear resistance for roots that pull-out of the soil as anchors compared to roots of the same size that fail simultaneously in a soil-root matrix (Waldron & Dakessian, 1981). Despite the apparent recognition of root anchorage as a significant contributor to increased soil strength and the widely reported progressive failure of root systems (Greenway, 1987), investigations into this effect on overall soil shear resistance are rare (for exception see Riestenberg, 1994). When discussing the effect of root anchoring, comprehensive reviews of mechanical root-soil interaction focus almost exclusively on the resultant buttressing effect that may result from a well anchored tree (Gray & Leiser, 1982; Greenway, 1987; Coppin & Richards, 1990; Styczen & Morgan, 1995), with little attention given to the role of individual anchors.

2.2.3 Tree buttressing and soil arching

If a tree is well anchored to a firm base through a large number of large diameter roots and it is assumed that failure of the anchors will not occur then a vertical root cylinder with a high magnitude root reinforcement directly below the tree stem may act to buttress the soil layer against movement in shear (Gray & Leiser, 1982)(Fig. 2.3). Based on theory developed by Wang & Yen

(1974) the force acting on the soil and root system under each tree is calculated using the expression:

$$P = \frac{K_0}{2} D_r \gamma\ z^2 + (K_0 \gamma z - pBz)$$

[2.3]

where K_0 is the coefficient of lateral earth pressure; D_r is the diameter of the vertical soil-root cylinder; γ is the unit weight of the soil; z is the thickness of the yielding soil layer; *p* is the average lateral pressure in the openings between soil-root cylinders; and B is the clear spacing between soil-root cylinders.
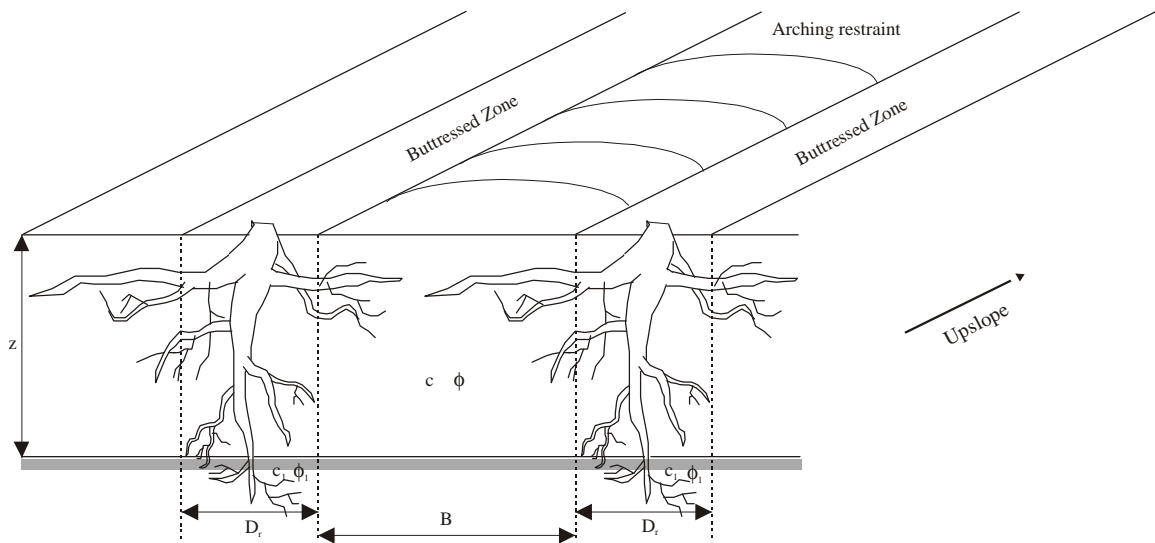
Figure 2.3: A schematic diagram of trees buttressing the soil in place on a slope with zones of arching restraint in between (after Gray, 1978).

In between vertical root cylinders on a slope, a zone of soil arching may occur (Gray & Leiser, 1982). The effect is to transfer stress to the adjacent root cylinders thus reducing the likelihood of slope failure. The magnitude of the arching effect is influenced by the spacing and diameter of soil-root cylinders, the thickness of the yielding soil, and the shear strength properties of the soil. Soil arching is no longer effective when the space between soil-root cylinders is greater than the critical value calculated by (Wang & Yen, 1974):

$$B_{crit} = \frac{zK_0(K_0 + 1)\tan\phi + \dfrac{2c}{\gamma}}{\cos\beta(\tan\beta - \tan\phi_1) - \dfrac{c_1}{\gamma\ z\ \cos\beta}}$$

[2.4]

where β is the slope angle; c_1 and ϕ_1 are the shear strength parameters on the underside of the potential sliding surface; c and ϕ are the shear strength parameters within the soil; and other parameters are as in equation [2.3].

As with root anchoring, buttressing and arching of the soil due to the presence of trees is not well studied. Riestenberg & Sovonick-Dunford (1983) and Thorne (1990) are two studies that indicate trees can buttress hill-slopes and riverbanks respectively, with significant effect. On the other hand Abernethy (1999) suggests that buttressing of riverbanks, although effective, is too localised and sporadic to provide a particularly significant effect. This is more likely to be the case on riverbanks that have been affected by devegetation, where tree density is not sufficient to enable arching restraint to occur. As described in the equations above, the buttressing effect is dependent on the values of root reinforcement within the soil-root cylinder at the potential sliding surface.

2.2.4   Theoretical models of fibre-root reinforcement

In its simplest form the shear strength of soil is described by the Mohr-Coulomb failure criterion (e.g. Terzaghi, 1943):

$$S = c + \sigma \tan f \hspace{4cm} [2.5]$$

where c is the cohesion of the soil; σ is the normal stress acting on the soil; and f is the angle of internal friction. In a root-permeated soil the increased shear strength provided by the roots (S_r) can be added:

$$S_{sr} = c + \sigma \tan f + S_r \hspace{4cm} [2.6]$$

In order to evaluate the contribution of tree roots to soil shear strength (i.e. to determine S_r) a simple model was developed independently by Waldron (1977) and Wu *et al.* (1979). The model was designed to simulate the idealised situation of a tree's vertical roots extending across a potential sliding surface in a slope. It consists of a flexible, elastic root extending vertically across a horizontal shear zone of thickness z (Fig. 2.4).
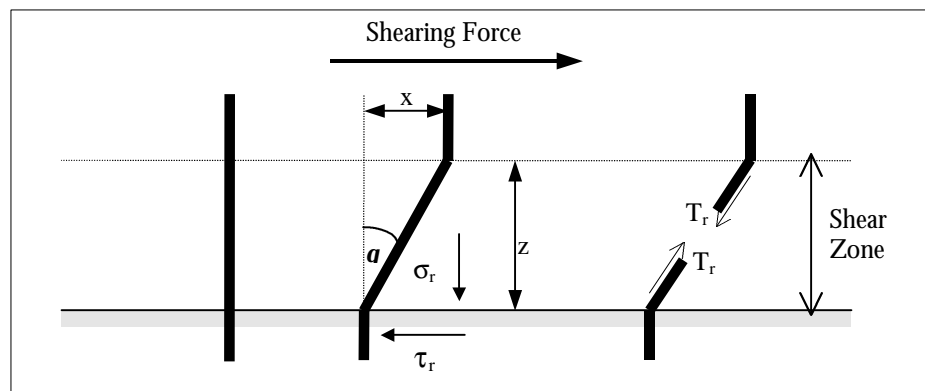
Figure 2.4: Model of a flexible, elastic root extending vertically across a horizontal shear zone.

As the soil is sheared a tensile force T_r develops in the roots. As shown in Figure 2.4 this force is resolved into a tangential component (τ_r) which resists shear and a normal component (σ_r) which increases the confining stress on the shear plane:

$$\tau_r = t_r \sin\theta \quad \text{and} \quad \sigma_r = t_r \cos\theta \qquad\qquad [2.7]$$

where τ_r and σ_r are the tangential and normal stresses applied to the soil by T_r; t_r is the average tensile strength of roots per unit area of soil; and θ is the angle of shear distortion of the root. The contribution of the root to shear strength is then given by:

$$S_r = \sigma_r \tan f + \tau_r = t_r (\cos\theta\tan f + \sin\theta) \qquad\qquad [2.8]$$

The average tensile strength of the roots per unit area of soil (t_r) is determined by multiplying the average tensile strength of the roots by the fraction of the shear surface cross section occupied by roots:

$$t_r = T_r (A_r/A) \qquad\qquad [2.9]$$

According to this model it is therefore feasible to determine the maximum possible root contribution to soil strength by measuring the tensile strength (T_r) of the roots and the fraction of soil cross-sectional area occupied by the roots (A_r/A) - assuming of course that the shear distortion (θ) is known or can at least be estimated. This method has been employed by numerous investigators over the years with some success (see Coppin & Richards, 1990; Wu, 1995), although it has limited applicability due to a number of simplifying assumptions that are imposed.

The model assumes that the tensile strength of the roots are fully mobilised during failure. It does not take into account roots that may slip or pull-out of the soil before failure and was therefore extended by Waldron & Dakessian (1981) to include a spectrum of root diameters and to account for the possibility that roots may not only stretch, but may slip through the soil as well as break. Thus the model accounts for a from of 'progressive' failure as roots slipping through the soil continue to contribute a reinforcing increment. The total root reinforcement is subsequently made up of contributions from slipping (equation [2.10]) and non-slipping but stretching (equation [2.11]) roots:

$$\Delta S_s = \{\pi\tau'\delta/2A_s\}\sum_{i=1}^{j} n_i L_i d_i \qquad\qquad [2.10]$$

$$\Delta S_{ns} = \{\pi (\tau'z)^{\frac{1}{2}} \gamma\delta/2A_s\}\sum_{i=1}^{m} E_i^{\frac{1}{2}} n_i d_i^{3/2} \qquad\qquad [2.11]$$

where τ' is the maximum tangential stress; z is the thickness of the shear zone; γ is $(\sec \theta)^{\frac{1}{2}}$; δ is $(\sin\theta + \cos\theta\tan f)$; A_s is the total cross-sectional area of the shear surface; j is the number of slipping root size classes; m is the number of non-slipping root size classes; n_i is the number of roots in each size class; d_i is the diameter of root in each size class; L_i is the root length in each size class; and E_i is the modulus of root in each size class.

It was suggested by Waldron & Dakessian (1981) that the strength of the soil-root bond was the most important unmeasured model parameter. Its value rather than root strength, limited root reinforcement in a saturated clay loam permeated with barley and pine roots, and led to the failure

of different roots at different displacements. As such, they went on to suggest that the assumption that all roots fail in tension simultaneously may lead to large overestimates of the increased shear strength of the soil-root system.

The above models assume that the roots are initially orientated perpendicular to the shear surface. In nature plant roots may be inclined at many different angles to a sliding or failure surface and so to take this effect into account Gray & Ohashi (1983) developed a model for a long elastic fibre orientated either perpendicular to the shear surface or at some arbitrary angle. It was found that the maximum values of increased shear-strength correspond to fibre inclinations close to $(45 + f/2)^o$, however for fibres inclined between 30 and 90 degrees to the shear plane, both the theory and experiment indicate little difference in reinforcement (Gray & Leiser, 1982). For investigators of root-reinforced soil the perpendicular root model provides a useful and the most widely applied interpretation of the situation.

As a shear zone develops and tree roots that pass through it displace with the soil, the increased shear resistance can be approximated through known solutions for the cable and pile (Wu *et al.*, 1988a; Wu, 1995; Wu & Watson, 1998). The solution used depending on the root orientation within the shear zone. When $\alpha < 90°$ the cable solution (Fig. 2.5a) is used. As the root is displaced towards the right, soil resistance is mobilised up to a maximum limit p_p (the passive pressure). The solution gives the tensile force in the Y and Z directions by:

$$T_Y = p_p DL \tag{2.12}$$

$$T_Z = \frac{p_p DL}{-u_s'} = \frac{p_p DL^2}{2u_s} \tag{2.13}$$

where D is the root diameter; L is the root length from the shear plane to a stationary point b; u is the root deflection from the point b, where the orientation of the root is vertical, or where the slope $u' = du/dz = 0$; $u = u_s$ at $z = z_s$; u'_s is the slope at $z = z_s$; and p_p is the passive resistance of the soil. z_s is the depth of the shear plane. When $\alpha > 90°$ the root will be subject to compression and so the pile solution (Fig. 2.5b) is used to measure the root resistance. The compression is calculated in the Y and axial directions (Poulis & Davis, 1980) by:

$$P_Y = \frac{30cD^2}{\sin\delta} \tag{2.14}$$

$$P_a = P_Y \cos\delta \tag{2.15}$$

where c is the cohesion of the soil; D is the root diameter; and $\delta = 180° - \alpha$, where α is the root orientation relative to the shear plane. Of course to use these solutions a knowledge of the positions of the roots is essential. This presents obvious difficulties, particularly if any application to slope stability analysis is required and will necessitate numerous simplifying estimates, either to determine the likely root orientations within the shear zone, or to estimate the root forces directly. Wu &

Watson (1998) give some simplified approximations for T_Y and T_Z and based on their test results suggest that they should give estimates on the conservative side.
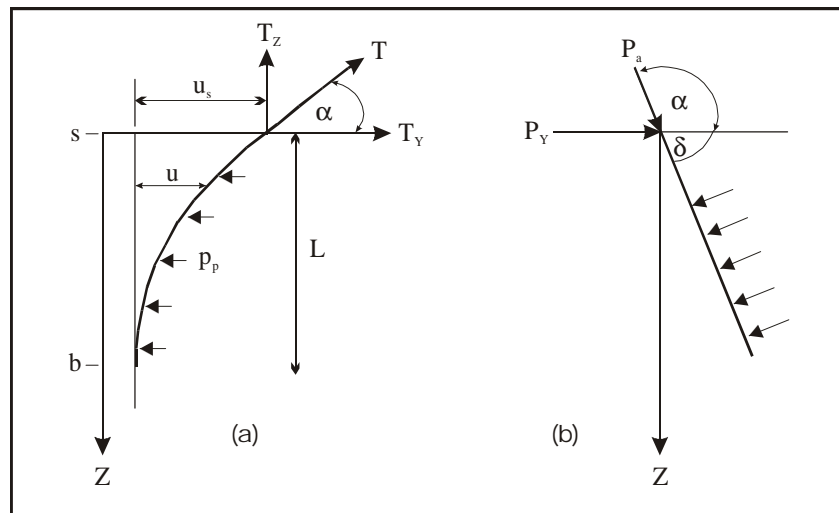
Figure 2.5: The root forces for (a) the cable solution, and (b) the pile solution; used in the approximation of shear resistance provided by roots not constrained within a thin shear zone. The solution used depends on the angle of inclination (α) of the root (after Wu & Watson, 1998).

The models presented in this section are used to explain the processes operating at the interface of soil and root. They allow a calculation of increased shear strength based on certain assumptions about the deflection of roots across a shear zone and their intrinsic characteristics (e.g. tensile strength, skin friction). These assumptions require the substantial simplification of a complex process and should be tested for the conditions and environment to be assessed. Waldron & Dakessian's (1981) example of the simple root model presented above, overestimating shear strength due to pull-out and progressive root failure is a case in point. Their experimental results showed that simulated values of S_r for Barley and Pine roots were only 56 % of those calculated for all roots mobilising full tensile strength at once.

2.2.5 Root reinforcement measurements

Studies that have measured the direct contribution of roots to soil shear strength include Endo & Tsurata (1969), O'Loughlin (1974a,b), Ziemer (1981), Wu *et al.* (1988a), Wu & Watson (1998), and Ekanayake & Phillips (1999) by *in situ* tests; and Waldron (1977), Waldron & Dakessian (1981), Waldron *et al.* (1983) and Terwilliger & Waldron (1991) by laboratory tests. It is generally accepted from these studies that the increase in soil strength is a measure of increased apparent cohesion and that this increases as root quantity across the shear zone increases. The actual values of additional strength vary considerably from study to study as environmental conditions, soils and tree characteristics differ (Table 2.1).

The relationship between increased shear resistance and root quantity has been found to be both exponential (Tengbeh, 1989, cited in Styczen & Morgan, 1995) and linear (Endo & Tsurata, 1969; Waldron, 1977; Ziemer, 1981; Ekanayake & Phillips, 1999). Therefore the exact nature of the relationship remains elusive. Jewell & Wroth (1987) and Shewbridge & Sitar (1989) also argue that the strength increase in reinforced soil may not be linear. All of these studies show however that even at low root densities, root reinforcement can have a significant effect on soil strength.

Table 2.1: Typical values of root shear strength obtained in previous investigations (modified after O'Loughlin & Ziemer, 1982; and Wu, 1995).

Investigators	Soil/Vegetation	Study Method	S_r/A_r or $[C_r]$ (kPa)
Endo & Tsurata (1969)	Loam/European Alder (Hokkaido)	*In-situ* Shear	$0.05\% \times 10^4$
Swanston (1970)	Till, Colluvium/Conifers (Alaska)	Slope Failure	[3.4-4.4]
O'Loughlin (1974b)	Till, Colluvium/Conifers (British Columbia)	Slope Failure	[1.0-3.0]
Waldron (1977)	Loam/Barley	Laboratory Shear	$3\% \times 10^4$
Burroughs & Thomas (1977)	Till/Conifers (West Oregon & Idaho)	Tensile Strengths	[3.0-17.5]
Wu *et al.* (1979)	Till, Colluvium/Conifers (Alaska)	Slope Failure	[5.9]
Ziemer (1981)	Sand/*Pinus Contorta* (California)	*In-situ* Shear	$0.1\% \times 10^4$
Gray & Megahan (1981)	Sandy Loam/Conifers (Idaho)	Excavation	[10.3]
Waldron & Dakessian (1981)	Clay Loam/Pine Seedlings	Laboratory Shear	[~5.0]
Riestenberg & Sovonick-Dunford (1983)	Colluvium, Silty Clay Loam/Sugar Maple (Cincinnati, Ohio)	Slope Failure/Tensile strengths	$2.8\% \times 10^4$
Wu (1984)	Till, Colluvium/Conifers (Alaska)	Slope Failure/Tensile strengths	$1.4\% \times 10^4$
Terwilliger & Waldron (1991)	Loams/Chaparral	Laboratory Shear	[0.4-0.8]
Wu & Watson (1998)	Silty Sand/*Pinus radiata* (New Zealand)	*In-situ* Shear	[2.5-4.5]
Abernethy & Rutherfurd (2001)	Silty Loam/River Red Gum/Swamp Paperbark (Latrobe Valley, Vic)	Pull-out tests	[10-120]
Schmidt *et al.* (2001)	Colluvium/Mixed forest species (Oregon)	Tensile strengths	[6.8-94.3]

Most studies report that it is extremely difficult to obtain consistent, easily interpreted data from field tests of soil containing roots. However the general results have been substantiated by laboratory studies (as mentioned above) and by application of the simplified soil-root models presented in the previous section. These applied studies generally calculate the increased soil strength by measuring the tensile strength of roots and the distribution of root density within the soil layer.

The tensile strength of roots varies enormously not only between species but also within species growing at different locations (Greenway, 1987). It generally reduces with increasing root diameter, leading to claims that the finest roots have the potential to contribute most to soil reinforcement (Burroughs & Thomas, 1977; O'Loughlin & Watson, 1979). This is also probably due to the fact that smaller roots are more likely to be located at the margins of a root system where instability is more likely to occur; and because they are the first to decay upon death of the tree, resulting in a bigger influence on slope stability after clear-cutting. The strength of small roots is much easier to measure than for larger roots, which is the most probable reason that no studies can be identified that measure the influence of large roots (> 4 cm) on soil shear resistance.

Larger roots however, require a greater load to pull them from the soil or to cause failure in tension (Riestenberg, 1994; Nilaweera & Nutalaya, 1999) and therefore the amount of increased shear strength they provide should be larger than that supplied by small roots. This is supported by the observation that roots larger than 2 cm are rarely found in landslip scarps (Wu *et al.*, 1979). When failure of a large root does occur it is most likely to be by breaking at a distance within the soil layer where its size has been reduced by taper or branching, and then pulling out.

While most root reinforcement investigations have focused on an increase in soil shear strength, Zhou *et al.* (1997) studied the traction effect of lateral roots of *Pinus yunnanensis* by direct *in-situ* test in the Hutiaoxia Gorge, Southwest China. In contrast to the effect of vertically-extending roots, the traction effect reinforces the soil not by increasing shear strength, but by enhancing the tensile strength of the rooted soil zone. It was found that the traction effect of the roots increased the tensile strength of the shallow rooted soil by 4.2~5.6 kPa. The results of this study indicate that together with the pine's vertical roots, which may potentially anchor the shallow rooted soil zone to a more stable substrate, the lateral roots through a traction effect, are able to mitigate against shallow instability in forested slopes.

Clearly then there are different models and interpretations of the mechanism of soil reinforcement by roots. All published models agree however that the presence of tree roots increases the resistance to shear of a mass of soil that forms a slope. The main difference between the resultant effect of each model, whether it be by increasing the apparent cohesion of the soil, anchoring the soil to a more stable substrate, or buttressing and arching, will be the magnitude of the increased shear resistance and the manner in which it is calculated. The magnitude of increased shear resistance will obviously have a big influence on the relative stability of a slope and so it is essential to realise a good understanding of the reinforcement and subsequent failure mechanism of the roots in the particular environment being assessed.

2.3   Root system architecture

In order to assess the contribution of a plant's roots to a particular slope's stability it is necessary to know the morphology of the root system present. Despite the well recognised importance of this fact (see Wu, 1995) the systemic morphology of tree roots is one of the least understood aspects of arboriculture (Helliwell, 1986). This is due mainly to observational difficulties and variation, not only from region to region, but to a lesser extent from tree to tree. Kozlowski (1971) observed that root structure as well as depth and rate of root growth is chiefly controlled by the rooting environment. Local soil and site conditions such as moisture availability, soil aeration, temperature, nutrient availability, and mechanical impedance, all affect the development of a plant's root system.

The major components of a tree's root system are illustrated in Figure 2.6. Comprehensive descriptions of root system morphology have been provided by Sutton (1969) and Kozlowski (1971). The lateral roots are mostly found close to the soil surface while tap roots and sinker roots are to a large extent located close to the zone directly below the tree stem. Trees tend to have most of their roots in the upper layers of soil where the mass of laterals are located in what is often referred to as the 'root mat'. Although the lateral root system may play a role in binding the soil into a single mass, the main resistance to shear failure in slopes is provided by vertical roots which are more likely to intercept potential failure planes (Gray & Leiser, 1982). The depth to which vertical roots extend is therefore important and varies considerably between: a) species and b) rooting environment. Many tree species have the inherent capability to develop deep and far-reaching roots in the absence of restrictive soil or substrate characteristics (Stone & Kalisz, 1991).
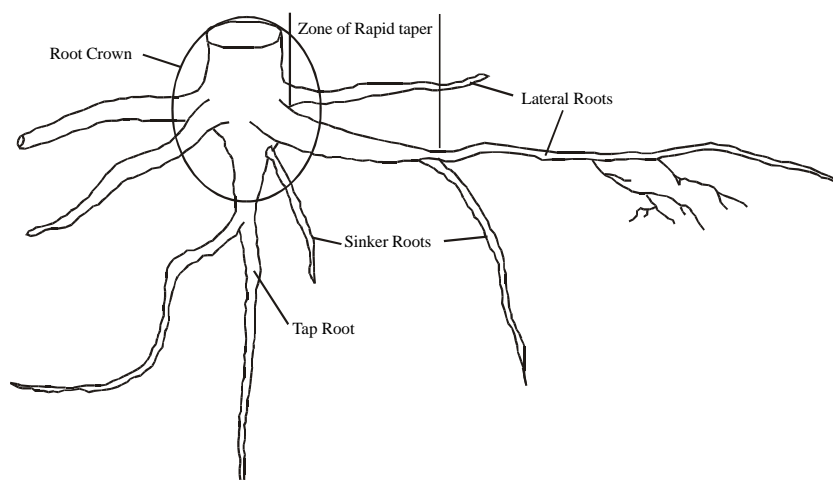
Figure 2.6: Representation of the main root system parts (From Wu, 1995).

2.3.1   Root system architectural investigations

Investigations of root system architecture include those undertaken on vegetative crops for growth analysis (Hewitt & Dexter, 1979; 1984; Tardieu, 1988), mathematical models of root structure form and geometry (Lungley, 1973; Henderson *et al.*, 1983; Rose, 1983; Diggle, 1988; Wu *et al.*, 1988b; Pages *et al.*, 1989; Clausnitzer & Hopmans, 1994), and general rooting habits as they relate to site conditions and processes (e.g. Zimmer & Grose, 1958; Ashton, 1975; Somerville, 1979; Watson & O'Loughlin, 1985; Dabral *et al.*, 1987; Riestenberg, 1994). Evidently there is an extremely wide range in root geometry from species to species (Fig. 2.7) and within species (Fig. 2.8) and so it is difficult to transfer data directly from one site to another because of the influence of local site conditions on root growth (Stone & Kalisz, 1991).

However some consistent relationships between soil conditions and root architecture have emerged. Zimmer & Grose (1958) studied the root systems of 14 Victorian Eucalyptus species and concluded that the species native to dry areas tend to develop a long tap-root with few weak laterals, while those on more favourable, moist sites usually develop a shallow, fibrous root system. Different root systems can be classified into different types (Kozlowski, 1971; Yen, 1984) based on their growth patterns (Fig. 2.9). The wide range in growth patterns means that different types will be more or less

(a) *Lathyrus sylvestris*

1 year   10 years

200 cm

(b) *Artemesia vulgaris*

1 year   2 years   3 years

100 cm

(c) *Acer saccharum*

56 cm

40 cm
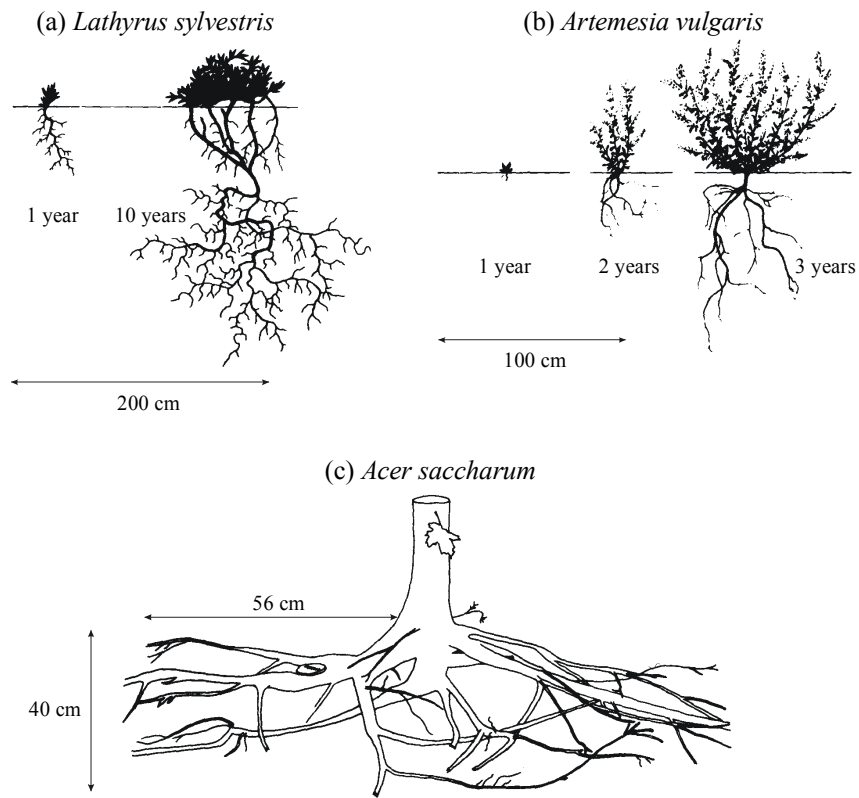
Figure 2.7: Some examples of the wide variety in root geometry of different species. (a) and (b) after Schiechtl (1980); (c) after Riestenberg (1987) (From Wu, 1995).

Well developed tap root with massive lateral roots and nodules in favourable soil & water table conditions under good *Casuarina* growth

Shallow root system under high water table condition having stunted growth

Long slender tap root in coarse sand with deep water table under very poor *Casuarina* growth
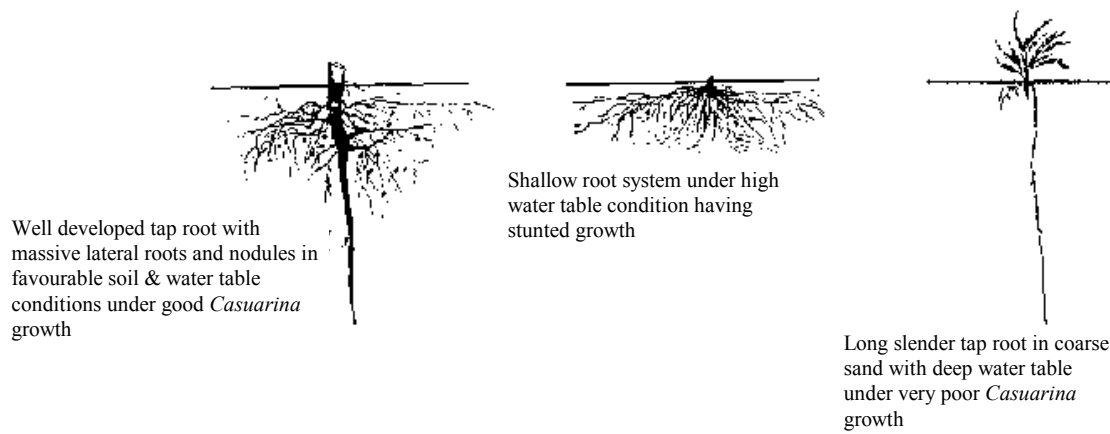
Figure 2.8: The root development of *Casuarina cunninghamiana* under different soil and water table conditions (From Yadav, 1983).
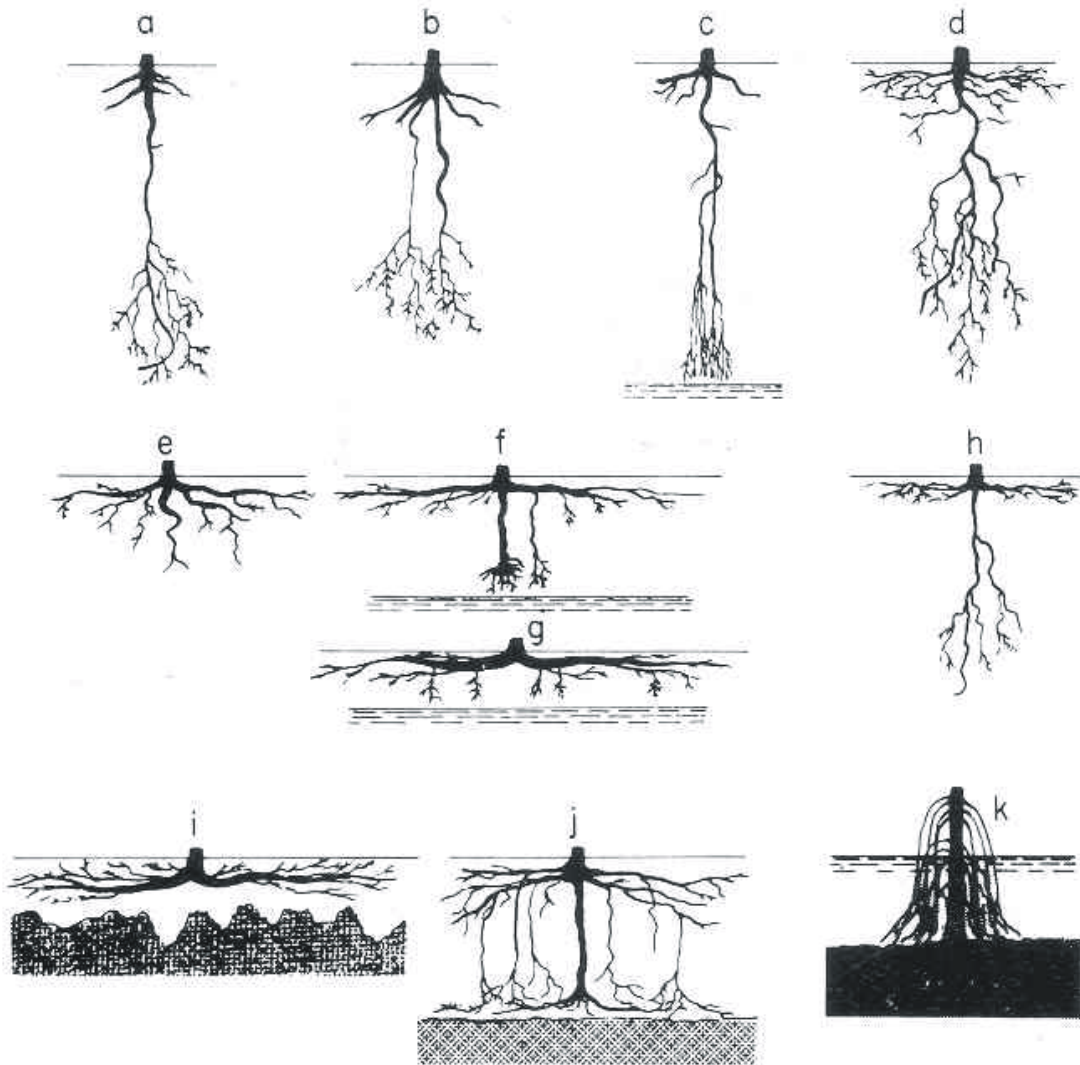
Figure 2.9: Different root system types as modified by growing site: Tap root system evident in a, b, c, d, and h. Heart root system evident in b and e. Plate root system evident in f, g, i, and j. Pneumatophores of a mangrove tree in k. (From Kozlowski, 1971, p.199).

2.3.2   Root system architecture and earth reinforcement

The architecture of a root system is a critical factor controlling the extent to which vegetation can reinforce the earth and stabilise a slope. The quantity and size of roots crossing a potential shear surface is of particular importance (equation [2.9]). The quantity of root material below a tree is generally found to decrease rapidly both with depth and with distance from the tree stem (see Watson & O'Loughlin, 1985; 1990; Shields & Gray, 1992; Riestenberg, 1994; Wu *et al.*, 1995; Abernethy & Rutherfurd, 2001). This appears to be the case for trees of all ages and it follows that the magnitude of potential earth reinforcement will exhibit a similar spatial pattern.

2.4   Vegetation and slope stability analysis

The link between vegetation and slope stability has been examined by a number of investigators, who have established a strong cause and effect relationship ascribing a decrease in slope stability with loss of root reinforcement due to clear-cutting and timber harvesting. Bishop & Stevens (1964) document a four to fivefold increase in the number and area of shallow landslides within ten years following clear-cutting. This accelerated slope failure occurrence was principally attributed to the destruction and gradual decay of the interconnected root system. A finding reiterated by Swanston (1970, 1974), O'Loughlin (1974b), Wu (1976), Ziemer & Swanston (1977), Burroughs & Thomas (1977), Wu *et al.* (1979), Wu & Swanston (1980), and Ziemer (1981) in similar studies undertaken in North America. Similar conclusions were also reached in Japan (Kawaguchi *et al.*, 1959; Kitamura & Namba, 1976; and Nakano, 1971) and in New Zealand (O'Loughlin & Pearce, 1976; Selby, 1981; O'Loughlin & Watson, 1979; and O'Loughlin *et al.*, 1982). The level of reinforcement attributed to tree roots depends however on the specific hydrologic, slope, soil-mantle, and plant conditions present at any given site.

To examine the effect of vegetation on slope stability various analytical methods have been modified to include vegetative factors. These factors include: a) the increased effective soil cohesion due to root reinforcement, b) soil suction resulting from evapotranspiration or a decrease in pore-water pressure, c) an increased surcharge due to the weight of vegetation, d) an increased disturbing force due to wind-throw, and e) an increased restoring force due to large diameter inclined roots acting as discrete tensile elements (Coppin & Richards, 1990). Not all factors contribute significantly in every analysis. This will depend on the prevailing conditions within a particular environment. The particular model chosen will also depend on actual on-site conditions. A brief review of general slope stability models that incorporate vegetative effects is presented in the following section.

2.4.1   Slope stability models

An analysis of stability may be used to evaluate an existing condition or to determine whether a proposed condition meets the requirement of safety. This procedure is commonly based on the limit equilibrium method whereby a mass of soil in place on a slope is considered to be on the verge of failure, and the shear strength of the soil is fully developed along a potential slip surface. The stability of the slope is generally expressed as a factor of safety, which is the ratio of Restoring to Disturbing forces present at incipient failure:

$$\text{FoS} = \frac{\text{Restoring Forces}}{\text{Disturbing Forces}}$$

[2.16]

A factor of safety ≥ 1.0 means the slope will resist failure, while a factor of safety < 1.0 will be calculated for an unstable slope and one that should fail in shear. In reality a factor of safety of 1.0

does not necessarily indicate that failure of a slope is imminent (De Mello, 1977) as the real factor of safety will be strongly influenced by minor geological details, stress-strain characteristics of the soil, actual pore-pressure distribution, initial stresses, progressive failure, and numerous other factors (Nash, 1987). The converse also applies and often necessitates the use of a safety margin above the factor of safety of 1.0 in order to be reasonably confident of stability.

The method of slices is a well established limit equilibrium approach for assessing the stability of slopes. In its most basic form the infinite slope method describes the condition where a single vertical slice is representative of the entire slope (Fig. 2.10). This method is only suitable for slopes that exhibit a large length to depth ratio but it is an effective and quick first approximation calculation that can be used to demonstrate the essential behaviour of a given slope (Mostyn & Small, 1987). It is expressed in the following form to include the effects of vegetation (after Wu *et al.*, 1979):

$$FoS = \frac{(c + S_r)l + [(W + S_w)\cos\beta - u]l\tan\phi}{(W + S_w)\sin\beta}$$

[2.17]

where c is the soil cohesion; S_r is increased shear strength due to roots; W is the weight of soil; S_w is the surcharge weight of vegetation; β is the slope angle; u is the pore water pressure which is $\gamma_w h_w \cos^2\alpha$; l is the length of shear surface; and f is the internal friction angle of the soil. For simplification the effects of wind-throw, soil suction, and root anchorage have been removed.
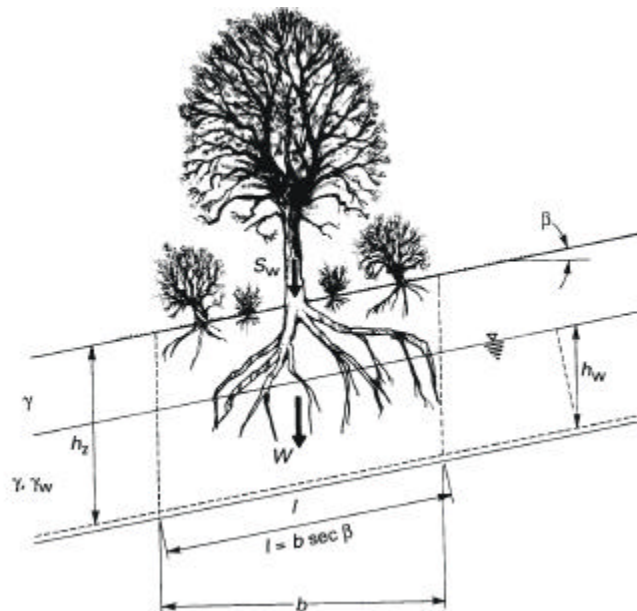
Figure 2.10: Diagrammatic representation of the infinite slope model with the addition of forces through the surcharge weight of vegetation. The soil mass is only partly saturated and under conditions of steady-state seepage (after Bache & MacAskill, 1984).

To model a finite slope composed of uniform soil the slip surface can be approximated by circular arcs (Fig. 2.11) and their stability investigated using methods by Fellenius (1936), Bishop (1955),

Morgenstern & Price (1965), and Spencer (1967). Differences between the models centre on different assumptions concerning the position, line of thrust, and inclination of inter-slice forces and the distribution of normal stress on the slip surface. Bishop's simplified method (1955) assumes that the inter-slice forces act horizontally and is calculated by summing the moments over all slices using equation [2.18] with the vegetative factors of increased shear strength and surcharge weight of vegetation added.

$$FoS = \frac{\Sigma[(c + S_r)l + (P - ul)\tan\phi]}{\Sigma(W + S_w)\sin\beta}$$

[2.18]

where

$$P = \frac{[W - \frac{1}{FoS}(c'l\sin\beta - ul\tan\phi'\sin\beta)]}{m_\beta} \quad \text{and} \quad m_\beta = \cos\beta\,(1 + \tan\beta\,\frac{\tan\phi'}{FoS})$$

and other parameters are as in equation [2.17]. As the FoS occurs on both sides of the equation it is initially calculated by the Fellenius (1936) method and then solved iteratively. Convergence usually occurs within a few iterations (Nash, 1987).

In cases where the non-uniformity of soil properties is pronounced, the slip surface may be irregularly shaped and quite different from a circular arc. Solutions based on Bishop's iterative technique or by Janbu (1954) are also applied to non-circular slip surfaces, with modifications (e.g. Bishop, 1955; Spencer, 1967).
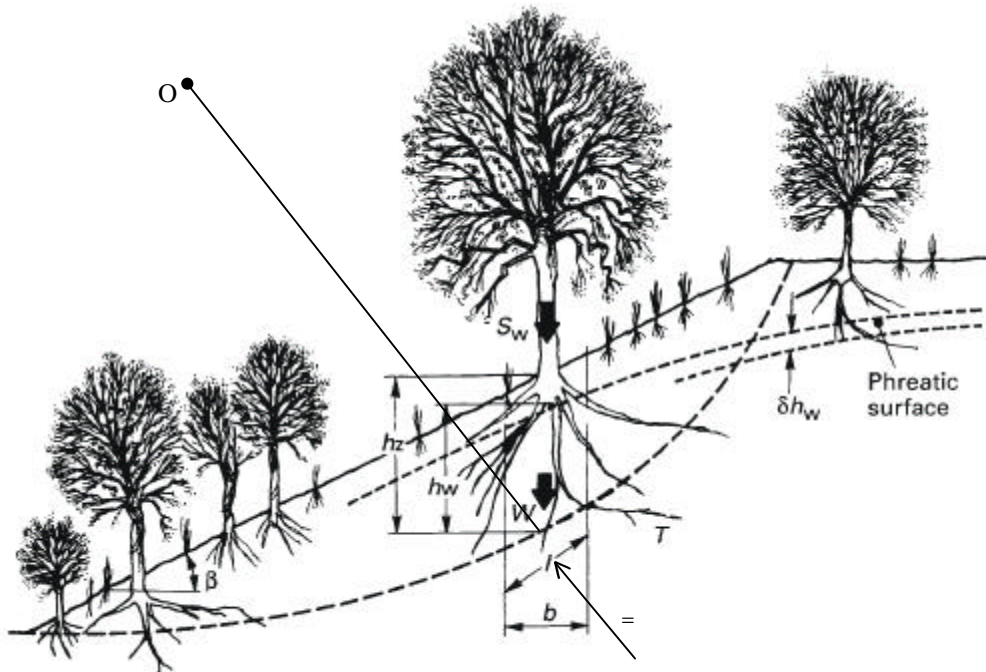
Figure 2.11: Circular slip surface showing the forces on individual slices including those due to vegetation (after Coppin & Richards, 1990).

An alternative to the limit equilibrium method for stability analysis of vegetated slopes has been proposed by Ekanayake & Phillips (1999). It concerns an assessment of the energy consumed in the shearing process as well as the ability of the soil-root system to withstand larger shear displacements and therefore larger shear strains than fallow soils. These authors suggest that the limit equilibrium method may underestimate the additional shear resistance of soils containing roots by only considering the increased peak shear resistance of the soil-root system and not the additional shear resistance provided during large displacements of the roots, prior to failure. Application of this method is limited at the present time to slopes that can be approximated by the simplified infinite slope model. There are also practical concerns about collecting sufficient data to deal with slopes exhibiting a variety of failure types and sizes (Ekanayake & Phillips, 1999).

2.4.2   Practical hill-slope analysis

An understanding of the earth reinforcing processes of tree roots has mostly been explored for the purpose of assessing their influence on slope stability. Initially this was based on a cause and effect relationship between clear-felling and observations of increased landslide activity, as the studies mentioned above attest. As general slope stability models were modified to include the effects of vegetation (see previous section), quantifiable stability analyses allowed more active assessment of tree root influence on slope stability problems.

Generally the increased shear resistance of tree roots is modelled as an increase in apparent cohesion that increases with increasing concentration of roots on a potential shear plane (see Gray, 1978; Greenway, 1987; Coppin & Richards, 1990; Styczen & Morgan, 1995). Clearly the distribution of root concentration in the soil beneath a tree will be a critically important parameter for input to the slope stability model. Analysis on hill-slopes with fairly uniform tree cover, often assume fairly uniform root concentrations at any given depth over the entire slope (see Greenway, 1987), which is a reasonable estimation for the average increased shear strength over a large area of a single species forest. Riestenberg (1994) for instance found that when modelled with a uniform distribution of root anchors, small white ash trees may be spaced as much as seven metres apart and still stabilise a 30 degree hill-slope with colluvium thickness of 43 cm. Variations in root distributions between multiple species however have led to measurements of large variation in increased shear strengths over relatively small areas (Terwilliger & Waldron, 1991; Schmidt *et al.*, 2001) resulting in adjacent zones of varying landslide susceptibility and potential scarp size.

The variability of increased shear resistance has been recognised not just between different vegetation types but also at different locations within the soil mass below a single tree (Shields & Gray, 1992; Abernethy & Rutherfurd, 2001). Accounting for these differences in slope stability modelling, results in different locations of the critical failure plane and different calculated factors of safety for different species and different tree locations on the hill-slope (Collison *et al.,* 1995), or riverbank (Abernethy & Rutherfurd, 2000a).

There is general agreement that a vegetation cover increases the stability of slopes across environments, although there are exceptions. Collison & Anderson (1996) point out that in humid tropical conditions where failure is mostly triggered by infiltration rather than a groundwater rise, large-scale vegetation covers may contribute to instability. Ellison & Coaldrake (1954), examining sub-tropical rainforest in southeastern Australia found that it was no better than sod in restraining mass soil movement. These exceptions as well as the considerable variation in the magnitude of positive slope stabilising reports mean that specific vegetative and environmental conditions need to be assessed on a site by site basis.

2.4.3   Stability analysis of riverbanks

Riverbanks are essentially a class of slope and so many of the principles of traditional slope stability analysis are applicable to them (see Thorne & Osman, 1988a). Riverbanks are however characterised by very different hydrological processes than hill-slopes and due to their mostly smaller length to height ratio and more varied profile, are influenced to a greater extent by the spatial variability of vegetative effects (Abernethy & Rutherfurd, 2000a). Therefore despite the general theoretical agreement concerning the stabilising influence of riparian vegetation on riverbanks (Thorne, 1990; Hubble & Hull, 1996; Abernethy & Rutherfurd, 1998; Abernethy & Rutherfurd, 2000a) the lack of knowledge concerning the variation in total volume and spatial distribution of tree roots within the bank material is a serious limitation on their assessment by geomechanical means.

Mass failure in riverbanks under worst-case hydrological conditions generally occurs when rapid drawdown of floodwaters leads to bank material that is heavily saturated with a positive pore-water pressure that weakens the riverbank. The weight of saturated material also leads to a greater down-slope force under gravity which clearly reduces the factor of safety of the bank. Failure of a riverbank can occur by a number of modes depending on the geotechnical properties of the bank material and the pre-failure geometry (Thorne, 1982; 1991). Hey *et al.* (1991) described eight different modes based on the shape of the failure surface. These are: (a) shallow failure, (b) planar failure, (c) slab failure, (d) rotational failure in homogenous material, (e) rotational failure with weak zone, (f) Massive rotational failure, (g) tensile cantilever failure, and (h) beam cantilever failure. The type of failure to be assessed and therefore the particular stability model used will depend on observations of the failure processes within the specific environment being investigated. It is common for many different failure modes to exist within relatively close proximity to each other (see Hubble & Hull, 1996; Abam, 1997; Hubble, 2001) due to variations in bank material properties and profile geometry along a channel. This may necessitate the assessment of multiple failure modes within the one system.

The incorporation of biotechnical factors in riverbank stability analysis has rarely been attempted and it has been uncommon even for a geotechnical approach (see Thorne & Osman, 1988a,b) to riverine morphological change to be pursued. Only three major studies of this type undertaken on Australian rivers have been identified (Hubble & Hull, 1996; Abernethy & Rutherfurd, 2000a;

Hubble, 2001). They focused on root reinforcement as the most important vegetative factor influencing riverbank stability. All three report significantly increased factors of safety under vegetated conditions, though only Abernethy & Rutherfurd (2001) measured the actual amount and distribution of increased shear strength within the riverbank.

2.5   Summary

Anthropological catchment disturbance, in particular within the riparian zone has been implicated in the substantial morphological response of alluvial river systems. The altering of channel boundary conditions by devegetation is considered to be a fundamental contributor to this response through increased riverbank instability and subsequent channel widening; effects that have been observed on the upper Nepean River and throughout southeastern Australia. It is contended that riparian vegetation enhances the bank properties through a mechanical root reinforcement of the soil although data is limited as to the exact magnitude and extent of this effect. Geomechanical analysis of hill-slopes have shown that it varies significantly with environment, root system morphology, and vegetation type and species. As such, studies undertaken in exotic locations using exotic plant species have limited applicability to local slope stability analyses in terms of an actual quantification of the effect. The general principles should however be transferable.

Tree roots generally act to reinforce soil through two main processes: 1. By transferring shear stresses developing within the soil to tensile stress within the roots leading to the development of anisotropic cohesion, and 2. By anchoring a relatively weak layer of soil across a discontinuity, the shear surface, to an underlying stronger soil or bedrock. Previous studies have therefore measured two main parameters when assessing root strength: the direct increased shear resistance of a soil-root matrix, and the pull-out resistance of individual roots. The increased shear resistance is generally measured by direct shear tests either *in-situ* or within the laboratory and is represented by the addition of a term S_r to the equation describing the Mohr-Coulomb failure envelope for the soil (equation [2.4]). Pull-out resistance is measured by root pull-out tests and describes the strength of the soil-root bond. Below the critical confining stress, this bond is the limiting factor determining the contribution of a root to the soil strength. There are many instances whereby a value for the increased shear strength of the soil is calculated using tensile strength measurements and a simplified model of soil-root interaction.

Models of soil-root interaction have been proposed to explain the relationship of the idealised circumstance of a root extending vertically across a shear zone. There are however variations about this idealised model to account for roots that extend across the shear zone at an angle other than vertical and to account for differences in shear-zone thickness. In all of these models it is considered that the increased soil strength is dependent on the root area ratio at the shear zone and in order to assess a plant's contribution to root reinforcement it is necessary to understand its root system architecture. Studies that have measured the direct contribution of roots to soil shear-strength have

found that strength increases with increasing root material quantity at the shear zone. Investigators of natural mass-failure conditions have confirmed that root system architecture is a limiting factor in explaining the resultant effects of vegetation on a mass of soil that forms a slope.

As a result of an increased soil strength due to root reinforcement, slope stability is improved and numerous studies have demonstrated the causal link between forest clearance and increased landslide activity. Devegetation has also been implicated in the instability of some alluvial riverbanks in New South Wales although previous research has been based on estimates of root reinforcing effects. Consequently these stability analyses, in terms of accounting for vegetative effects, are of somewhat limited utility. Only one previous investigation into the quantified effect of root reinforcement on riverbank stability has been conducted in this country. It demonstrated that root reinforcement of the bank substrate can provide a high level of protection against instability but the amount of protection varies spatially.

In order to assess the spatial variability of root reinforcement beneath trees common to the upper Nepean River and other southeastern Australian streams this study reports on a series of experimental investigations into root system geometry and strength. In chapter three the root system architectures of four species of tree are measured and some basic relationships describing the distribution of root material within the soil mass obtained. In chapter four the strength of the roots and the soil-root bond is measured through root tensile and pull-out tests. These results are compared with measurements from direct in-situ shear tests in chapter five, allowing for an understanding of the failure process of the soil-root system and an assessment of the simple root model described in section 2.2.4. The values of increased soil strength are combined with the root material distribution data in chapter six to model the predicted distribution of reinforced earth beneath trees of the four species examined. This model is used for a biotechnical assessment of riverbank stability in chapter seven.

Chapter Three

Root system architecture

3.1   Introduction and overview

Previous studies indicate (see Greenway, 1987; Coppin & Richards, 1990) that: a) the ability of a tree to reinforce soil is limited by the spatial distribution of its root system; and b) the spatial distribution of a root system varies enormously between different species and in response to environmental conditions. Tree root distribution varies in terms of its maximum extent in both the vertical and lateral directions, and the volume of root material within these limits. It is the combination of these factors that determine the magnitude of the reinforcement that a particular tree can provide to the soil. Currently there is a considerable lack of knowledge about these variables, which is mostly due to the inherent difficulties associated with root system measurement. No reliable general relationships have yet been determined for estimating the quantity of root material beneath a tree. Reliable determination of the root system architecture for a particular species must be assessed within the particular environment of interest, as extrapolation of results across species or environmental conditions is likely to introduce serious inaccuracies (Stone & Kalisz, 1991).

Previous investigators of root system architecture for the purposes of assessing its contribution to soil shear strength generally indicate that tree roots are dominantly located within the first one or two metres of the soil profile (see Shields & Gray, 1992; Riestenberg, 1994; Abernethy & Rutherfurd, 2001), so that in thick soil layers tree roots are thought to provide little or no protection against deep seated instability (Tsukamoto & Kusakabe, 1984). However, given favourable conditions it is also known that some tree species grow extensive roots that descend to great depths. For example, the roots of one species of Eucalyptus have been observed protruding into the roof of a cave some 60 m beneath ground (Stone & Kalisz, 1991; after Jennings, 1971). Similarly Coatsworth & Evans (1984) and Williams & Pidgeon (1983) report Eucalyptus roots at depths of 22 m and 27.5 m respectively. It is expected though that maximum depths of 1 to 3 m are typical for most trees and shrubs (Greenway, 1987; after Kozlowski, 1971).

It is generally believed that larger, mature trees with more robust and extensive root systems provide a greater earth-reinforcing potential than their younger relatives. Ashton (1975) and Wu *et al.* (1995) both describe an increasingly extensive root system and greater quantity of root material beneath trees of increasing size and age.

The spatial variation of root distribution is a key variable concerning the potential earth reinforcing effect of the root system. It is a variable that is not often reported in the literature, particularly variation in the lateral direction (Shields & Gray, 1992; Riestenberg, 1994; and Abernethy & Rutherfurd, 2001). In most cases root distribution values are presented as an average through the soil at a given depth across a slope under a particular type of vegetation cover (see Wu, 1995), and provide little insight into spatial variability. While these estimates provide consistent predictive results when used to model the stability of forested hill-slopes (e.g. Wu *et al*, 1979; Gray & Megahan, 1981), their applicability to modelling riverbanks where the scale of root systems are generally

comparable to the size of the failure blocks, is potentially suspect, and a more complete understanding of a root system's spatial variability both with depth and lateral distance from the tree stem is therefore important (see Abernethy & Rutherfurd, 2000a; 2001).

This chapter presents the results of root system architectural analyses for the four species under investigation in this study. The quantity of root material as it varies both with depth and lateral distance from the tree stem is determined in order to provide data necessary for the estimation of the potential magnitude of root reinforcement within the soil mass below, and at a distance from, a given tree. Assessments have been undertaken on juvenile trees and are compared to the geometries of the exposed root systems of mature trees. This data, when synthesized with the soil-root shear strength data presented in chapters four and five, forms the basis for quantifying the spatial distribution of increased soil shear resistance beneath riparian vegetation in this study.

3.2   Methodology

Architectural assessments were undertaken on juvenile trees grown in the plantation at Cobbity bridge. Whole root systems were extracted from the surrounding soil mass and transported to the laboratory for measurement. Excavation was carried out using hand tools (spade, fork, trowel, and a collection of small picks and brushes) by the classical method described in Böhm (1979). A trench was dug a suitable distance from the tree stem (about twice as far as the dripline) and the soil progressively removed from the trench towards the tree until all roots had been exposed. Notes were made as to the 3-dimensional location of structural roots and reconstruction of their spatial orientation, with the assistance of a series of photographs taken progressively during excavation, occurred in the laboratory. The excavated root system was reconstructed within a purpose-built cage that provided a frame of reference in both the vertical and horizontal plane. Root systems were then photographed and drawn, before measurements of the spatial distribution of root material were recorded.

Measurement of the root system involved the recording of root diameters for every root that crossed predetermined vertical and horizontal reference planes. In the vertical direction these planes were placed at 5 cm intervals with depth from the surface to the Maximum Vertical Depth (MVD) of the root system. In the horizontal direction measurement planes were placed at 12.5 %, 25 %, 50 %, 75 %, and 100 % of the Maximum Lateral Distance (MLD) of the root system. Planes in the horizontal direction were further divided into depth quartiles (i.e. 0-25 %, 25-50 %, 50-75 %, 75-100 % of MVD) (Fig. 3.1).

Six individual samples of each species were excavated from the plantation and assessed in this manner. The first three samples of each species were collected between April and October 2000 after 4 to 10 months of in-plantation growth. The second three samples of each species were collected between February and June 2001 after 14 to 18 months of in-plantation growth. The range

of tree sizes assessed in terms of above ground height was 1.19 m to 3.20 m for *C. glauca*, 1.10 m to 3.69 m for *E. amplifolia*, 1.70 m to 4.50 m for *E. elata*, and 1.51 m to 2.93 m for *A. floribunda*.

Inevitably roots were broken during excavation. In most cases this was limited to roots smaller than 1 mm in diameter. In any event every effort was made to recover broken roots so that they could be reassembled during reconstruction in the laboratory. When root systems were found to extend further than about 2 m below the ground surface the roots were broken off at this depth. Although clearly these roots would have extended to greater depths, safety considerations were given priority. As a result the MVD for some trees represents a conservative value.
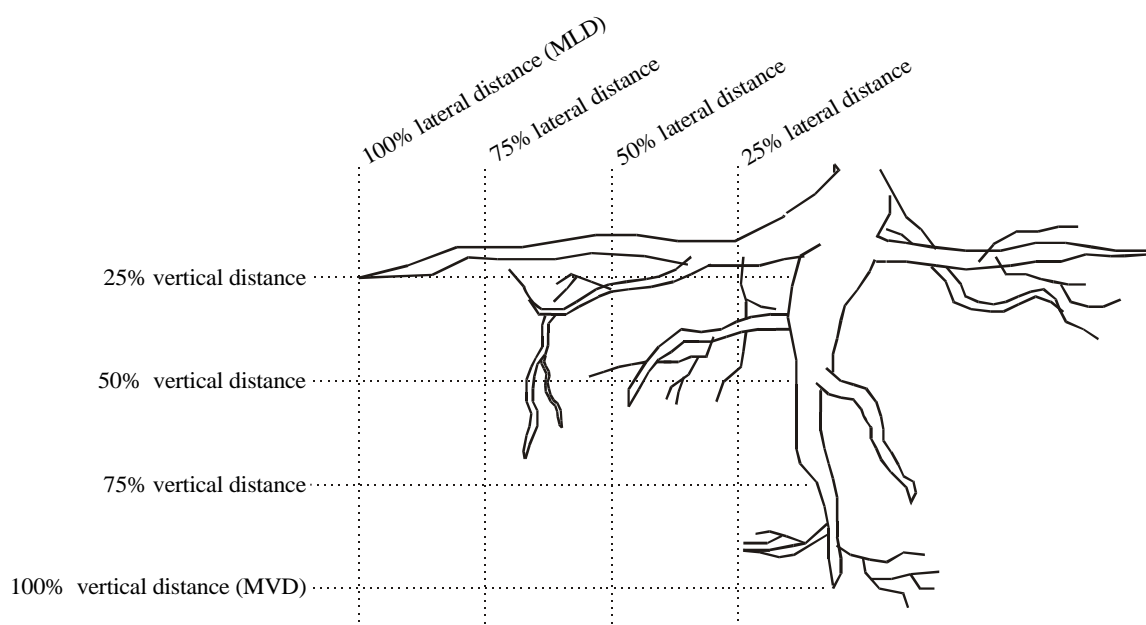
Figure 3.1 Root system measurement planes. Measurements were recorded in proportion to the total size of the root system, thereby allowing a comparison between trees of different sizes.

3.3 Root system extent and form

The maximum extent of a root system is a measure of the furthest possible influence that a tree can have for increasing the shear resistance of the soil, which makes it an important parameter to measure, but in itself does not provide knowledge of the magnitude of a potential reinforcement. This requires a measurement of the actual root quantity within these maximum limits. The maximum root extent of the samples excavated for this study are presented below (Table 3.1) both in terms of their actual values and as a proportion of the height of the above-ground portion of the tree. Although relationships between the diameter of a root mat below a tree and such above-ground properties as tree height, diameter of the crown, and stem diameter have been presented (see Wu, 1995, Table 7.2, p. 237), no attempt to suggest similar approximations for maximum rooting depth have yet been published.

Table 3.1: General measurements of above- and below- ground trees. CG: *Casuarina glauca*; EA: *Eucalyptus amplifolia*; EE: *Eucalyptus elata*; AF: *Acacia floribunda*.

Sample No.	Tree Height (m)	Surface Stem Diameter (mm)	Max. Root depth (m)	Max. lateral root extent (m)	Root Depth : Tree Height (%)	Lateral root extent : Tree Height (%)
CGA1	1.19	17.1	0.48	0.68	40	57
CGA2	2.02	25.2	0.74	1.00	37	50
CGA3	1.49	22.8	0.73	1.10	49	74
CGA4	2.45	46.7	1.16	2.19	47	89
CGA5	3.20	43.8	0.99	2.31	31	72
CGA6	2.36	49.0	1.55	2.91	66	123
Average	**2.12**	**34.1**	**0.94**	**1.70**	**44**	**78**
EAA1	1.28	25.4	1.70	0.95	133	74
EAA2	1.10	38.0	1.52	0.95	138	86
EAA3	1.35	29.3	1.00	1.00	74	74
EAA4	3.32	77.2	1.92	1.79	58	54
EAA5	3.23	58.6	1.65	1.42	51	44
EAA6	3.69	86.6	1.86	1.99	50	54
Average	**2.33**	**52.5**	**1.61**	**1.35**	**69**	**64**
EEA1	1.83	28.4	0.89	0.85	49	46
EEA2	1.70	25.7	0.67	0.70	39	41
EEA3	2.26	35.0	1.06	1.03	47	46
EEA4	4.46	64.7	1.58	1.40	35	31
EEA5	4.50	65.5	0.74	1.20	16	27
EEA6	4.24	68.1	0.90	2.02	21	48
Average	**3.17**	**47.9**	**0.97**	**1.20**	**35**	**40**
AFA1	1.51	28.0	0.53	0.85	35	56
AFA2	1.51	31.4	0.65	1.20	43	79
AFA3	1.75	31.8	0.87	1.50	50	86
AFA4	2.72	86.9	1.11	3.79	41	139
AFA5	2.55	94.4	1.25	1.39	49	55
AFA6	2.93	105.5	1.32	3.47	45	118
Average	**2.16**	**63.0**	**0.95**	**2.03**	**44**	**89**

Table 3.1 shows that *E. amplifolia* presents significantly greater maximum root depths than the other three species, averaging 1.61 m compared to around 0.95 m for *C. glauca*, *E. elata*, and *A. floribunda* for trees of similar height (av. 2.45 m for all species). *A. floribunda* presents the largest maximum lateral root extents with an average of 2.03 m, compared to the other three species which average 1.44 m from the tree stem.

Presented as a measure of the above ground height (H) the following approximate relationships were obtained for the small tree samples examined in this study:

      C. glauca   MVD = 0.4H   and   MLD = 0.8H

      E. amplifolia   MVD = 0.7H   and   MLD = 0.6H

| *E. elata* | MVD = 0.4H | and | MLD = 0.4H |
| *A. floribunda* | MVD = 0.4H | and | MLD = 0.9H |

These figures are similar to the approximate relationship $H < D_r < 2H$ reported for the lateral direction by Greenway (1987) and in Wu (1995), where D_r = the root mat diameter ($D_r = 2.MLD$). It should be noted that from this measure *E. elata* appears to exhibit a somewhat smaller root extent in both directions compared to the other species of this study, however it also grew faster above ground than the other species, recording greater tree heights (av. 3.17 m compared to 2.20 m) and therefore smaller ratios of root extent to tree height.

The root system data presented below provides an image of the sub-surface geometry of the trees studied. This root system form as viewed in total can give useful insights into the relative ability of a tree to reinforce soil, particularly in light of explaining the mode of both reinforcement and failure. For instance a shallow root system that consists entirely of fine (< 1 cm diam.) roots is expected to have limited capacity to anchor the soil to a more stable substrate. Conversely a deep root system with very few fine roots may have a capacity for anchorage but lack the ability to bind the soil into a single, more cohesive mass. Such differences may be crucial when selecting species for a particular stabilisation scheme and can be readily determined by knowledge of overall root form. The root form of each sample extracted for measurement is described below.

C. glauca

The root system of *C. glauca* (Fig. 3.2) consists of a dense network of fibres making up the main root ball with numerous lateral and sinker roots extending from it. The deepest sinker roots are present directly below the stem and there is a very even reduction in root depth with distance away from the stem-line such that in every sample the largest lateral root lengths are located in the upper depth quartile of MVD. This produces a shape similar to an inverted pyramid for spatial root extent – something like a flattened mirror image of the above ground tree. The species exhibits a fairly even radial spread with the roots not aligned in any particular direction. Root branching occurs to the 4th order.

The smaller samples (CGA1, CGA2, CGA3) showed some evidence of being planted from pots with obvious direction changes for many roots where the pot boundary existed. This tendency was only vaguely perceptible in the older trees (CGA4, CGA5, CGA6), which appear to have 'out grown' the constraining influence of the pot. With increasing tree size individual roots are larger in diameter and length although there does not appear to be any significant variation in root form. The smallest sample (CGA1) appears very similar to the largest (CGA6) in every sense other than scale, and perhaps root number. The form of the root system is probably best classified as a heart-root system (see Kozlowski, 1971).

CGA1

TH: 1.19 m
SD: 1.71 cm

CGA2

TH: 2.02 m
SD: 2.52 cm

CGA3

TH: 1.49 m
SD: 2.28 cm

CGA4

TH: 2.45 m
SD: 4.67 cm

CGA5

TH: 3.20 m
SD: 4.38 cm

CGA6

metres

0

0.5

1.0

1.5

2.0

TH: 2.36 m
SD: 4.90 cm
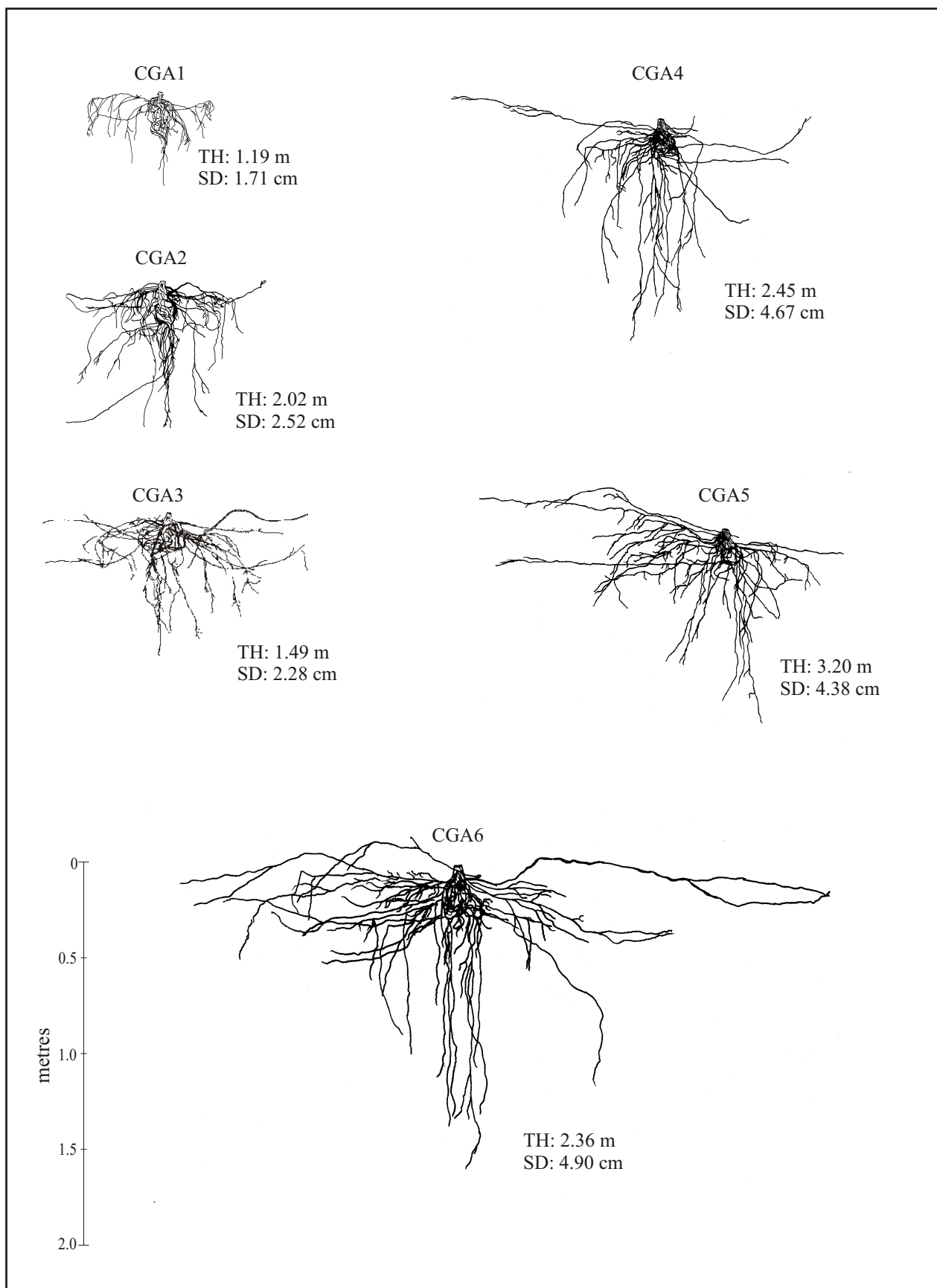
Figure 3.2: Root system drawings for excavated samples of *C. glauca*. The tree height (TH) and stem diameter (SD) at ground level is marked next to each sample. The vertical scale adjacent to CGA6 is the same for all samples. CGA2 from Docker & Hubble (2001a).

E. amplifolia

The root system of *E. amplifolia* (Fig. 3.3) consists of a small number of relatively large diameter, very long roots extending both vertically and laterally for large distances in comparison to the above ground size of the tree. A tap root which is branched at least once but more often multiple times (e.g. EAA6) is present in all samples close to the root stock. As a result there is usually a small number of dominant vertical roots directly below the root stem. These vertically oriented roots however are not necessarily present only beneath the tree stem. EAA3 and EAA5 both exhibit instances of deep vertical roots extending down from a distance away from the stem-line of the tree, although mostly they are smaller in diameter. Root branching occurs to the 4th order. There is no evidence of pot constraint in any sample although it is considered possible that some of the tap-root branching close to the root stock is a result of this earlier restriction (e.g. EAA4). As with *C. glauca* there appears to be very little difference in the root form of smaller trees in comparison to the larger samples. The form of the root system is best classified as a tap-root system (see Kozlowski, 1971).

E. elata

The root system of *E. elata* (Fig. 3.4) presents a fairly even distribution of fine roots with depth and with lateral distance from the stem that consists primarily of a mass of smallish roots extending in all directions from a large root stock of solid wood. No root dominates in the vertical direction although each sample has one or two larger, more extensive laterals. In general roots were evenly distributed around the stem although EEA2 and EEA3 present a slight concentration on one side. The root system is best classified as a heart-root system (see Kozlowski, 1971). Root branching occurs to the 4th order. The smaller samples (EEA1 and EEA2) show evidence of pot restriction although this is not observable in larger specimens. No significant differences between the root form of the smaller samples in comparison to the larger ones is observed.

A. floribunda

The root system of *A. floribunda* (Fig. 3.5) presents a mass of small diameter roots growing in all directions which forms a matted ball around the base of the tree stem. From this ball a small number of extensive lateral roots emerge and project large distances away from the root stem. The radial distribution of roots is fairly even around the base of the stem. Similarly, these specimens present a large number of extensive smaller diameter roots in the vertical direction. In the larger specimens (AFA5 and AFA6) a few larger diameter sinkers begin to dominate at depth. No root observed could be described as a tap-root and the root system form is best classified as a heart-root system (see Kozlowski, 1971). Root branching occurs to the 4th order. Evidence of pot restriction is observed in some smaller samples (e.g. AFA3) with sudden root directional change where this boundary previously existed. Again, roots of the larger samples appear to have 'out grown' this constraining influence.
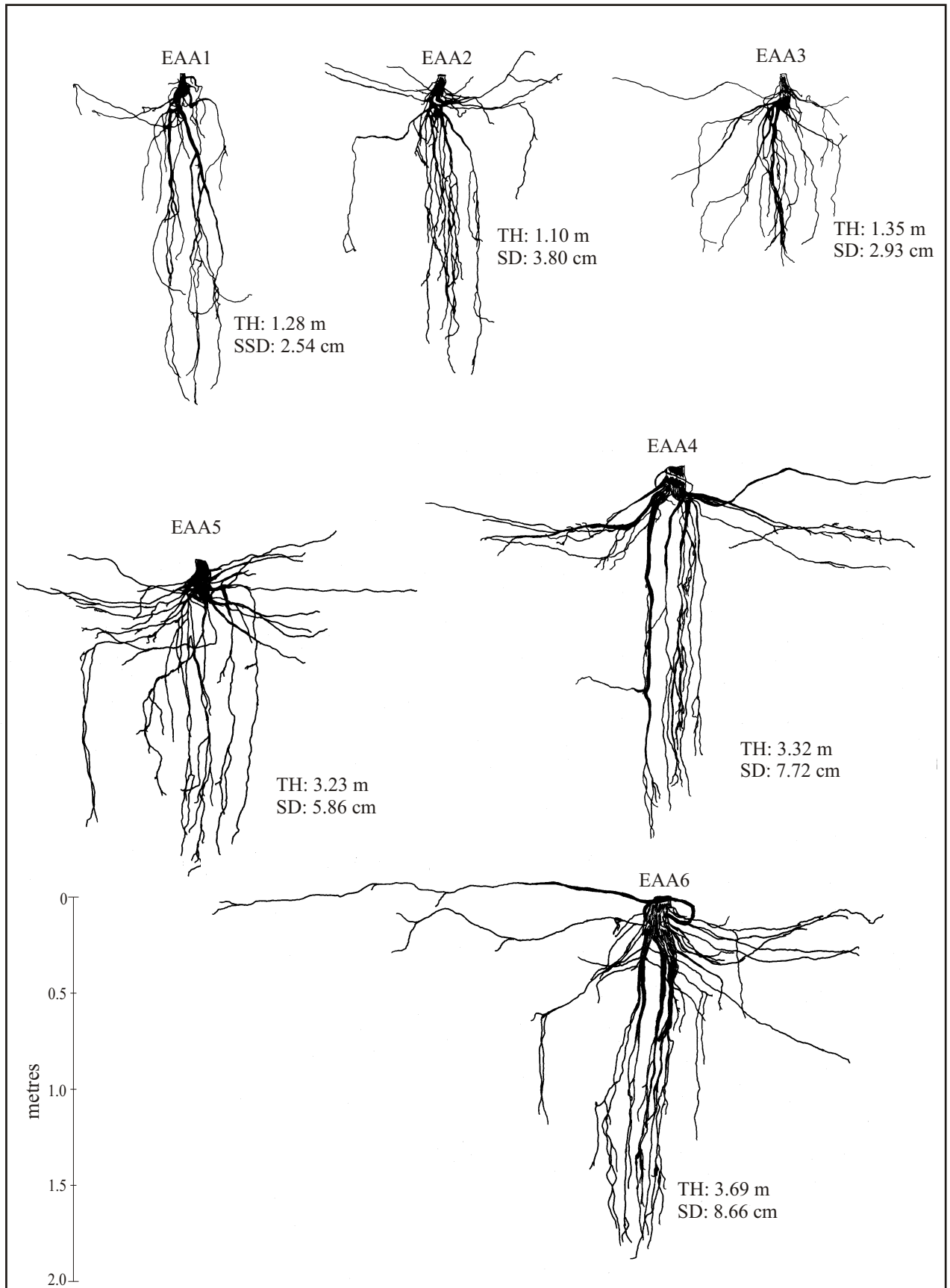
Figure 3.3: Root system drawings for excavated samples of *E. amplifolia*. The tree height (TH) and stem diameter (SD) at ground level is marked next to each sample. The vertical scale adjacent to EAA6 is the same for all samples. EAA1 from Docker & Hubble (2001a).
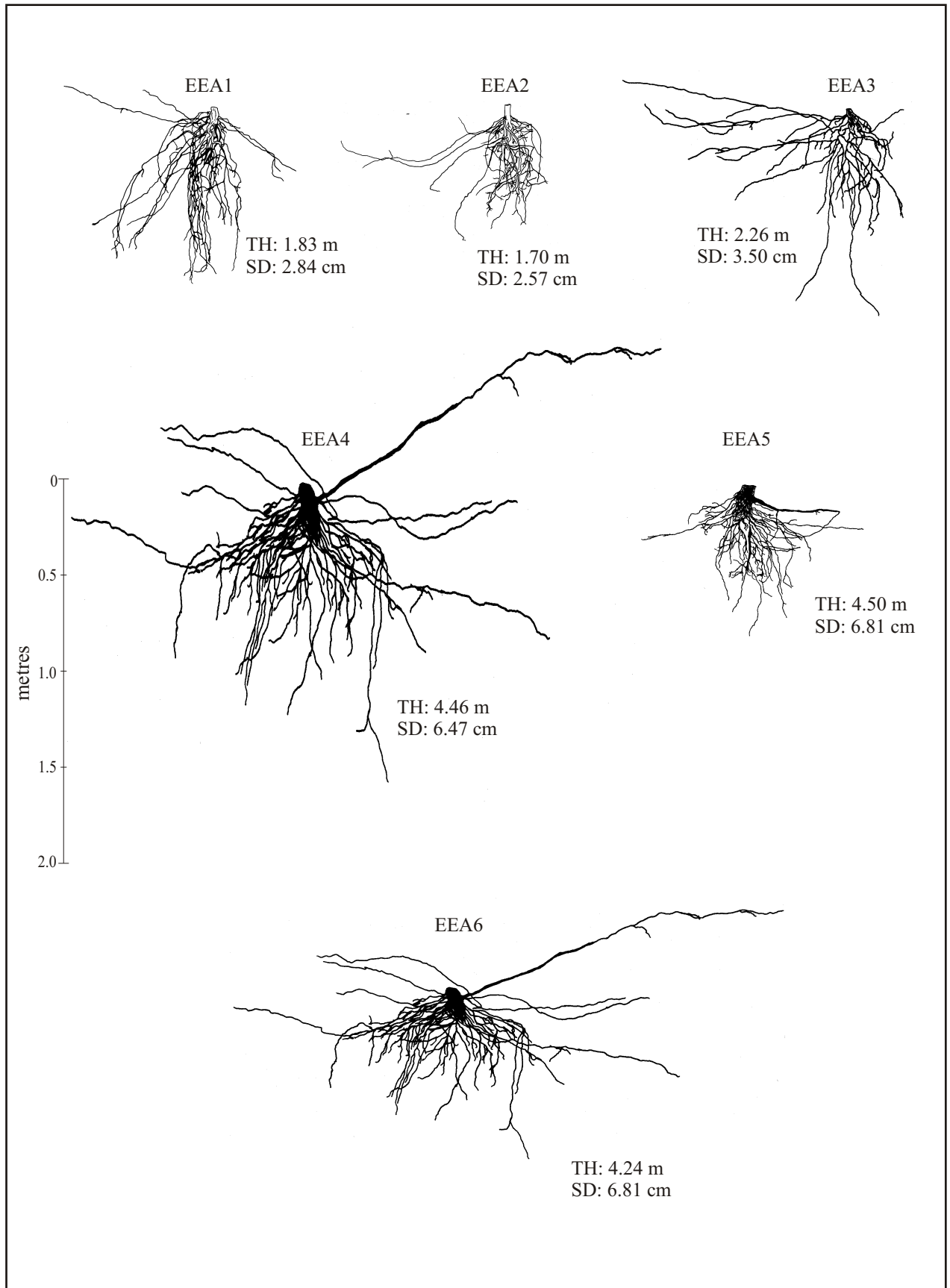
Figure 3.4: Root system drawings for excavated samples of *E. elata*. The tree height (TH) and stem diameter (SD) at ground level is marked next to each sample. The vertical scale adjacent to EEA4 is the same for all samples. EEA1 from Docker & Hubble (2001a).

AFA1
TH: 1.51 m
SD: 2.80 cm

AFA3
TH: 1.75 m
SD: 3.18 cm

AFA2
TH: 1.51 m
SD: 3.14 cm

AFA4
TH: 2.72 m
SD: 8.69 cm

AFA5
TH: 2.55 m
SD: 9.44

AFA6
TH: 2.93 m
SD: 10.55 cm

metres

0

0.5

1.0

1.5

2.0
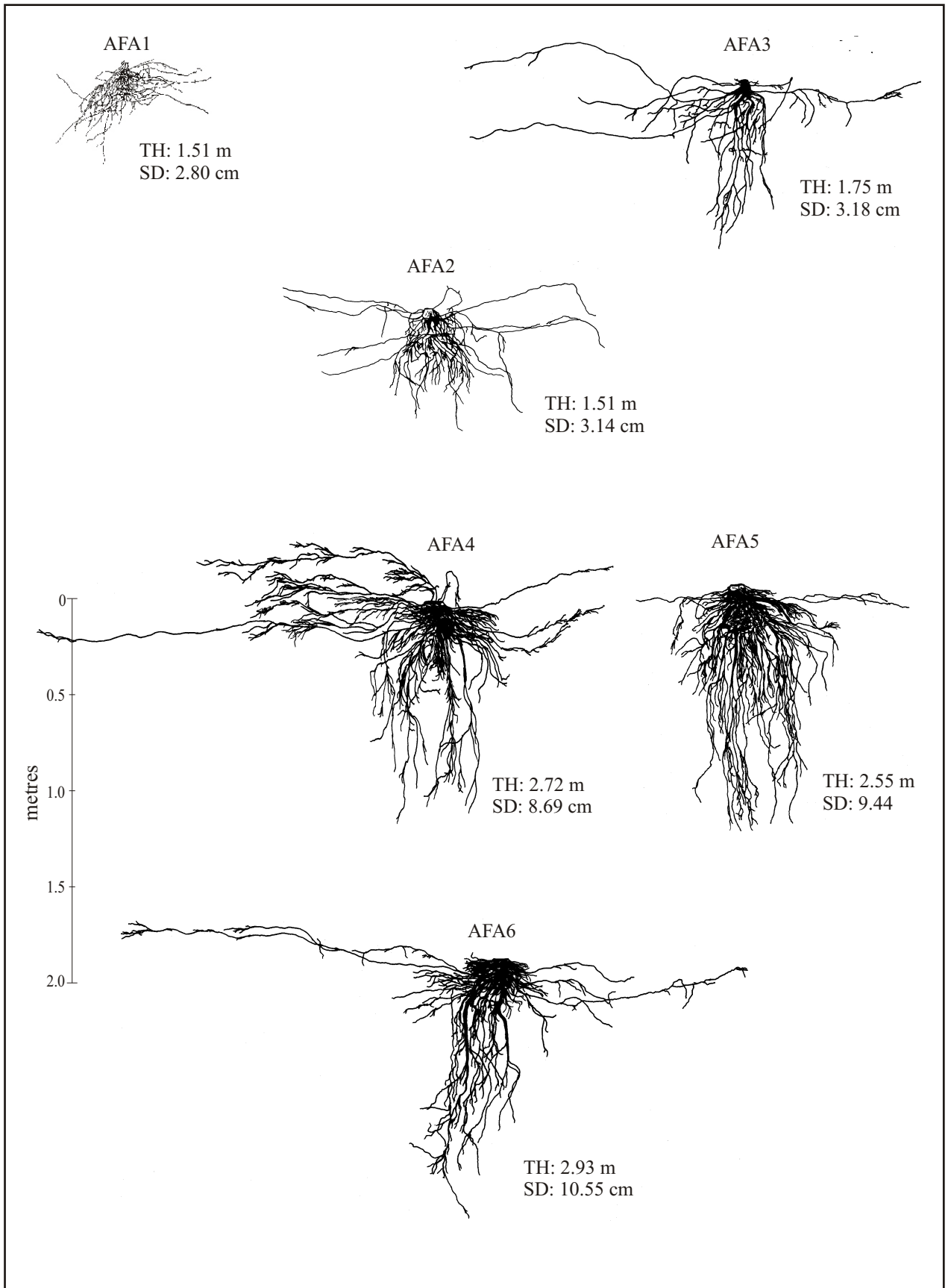
Figure 3.5: Root system drawings for excavated samples of *A. floribunda*. The tree height (TH) and stem diameter (SD) at ground level is marked next to each sample. The vertical scale adjacent to AFA4 is the same for all samples. AFA1 from Docker & Hubble (2001a).

Comparisons between species

There are some similarities of root form between species. In all species the deepest roots are mostly located directly below the stem and the lateral roots are mostly located close to the ground surface (< 20 cm depth). The shallower part of the root system tends to be composed of roots extending in all directions while the deeper parts tend to be dominated by vertical roots. These tendencies are more pronounced in the case of *E. amplifolia* than in the other three species. In general *E. amplifolia* consists almost exclusively of lateral roots in the soil immediately below the surface and vertical roots concentrated directly below the root stem (Fig. 3.3). There are very few if any obliquely oriented roots growing between the horizontal and vertical directions. As a general rule all species exhibit an even radial distribution about the tree stem, irrespective of overall morphology (e.g. Fig 3.6).
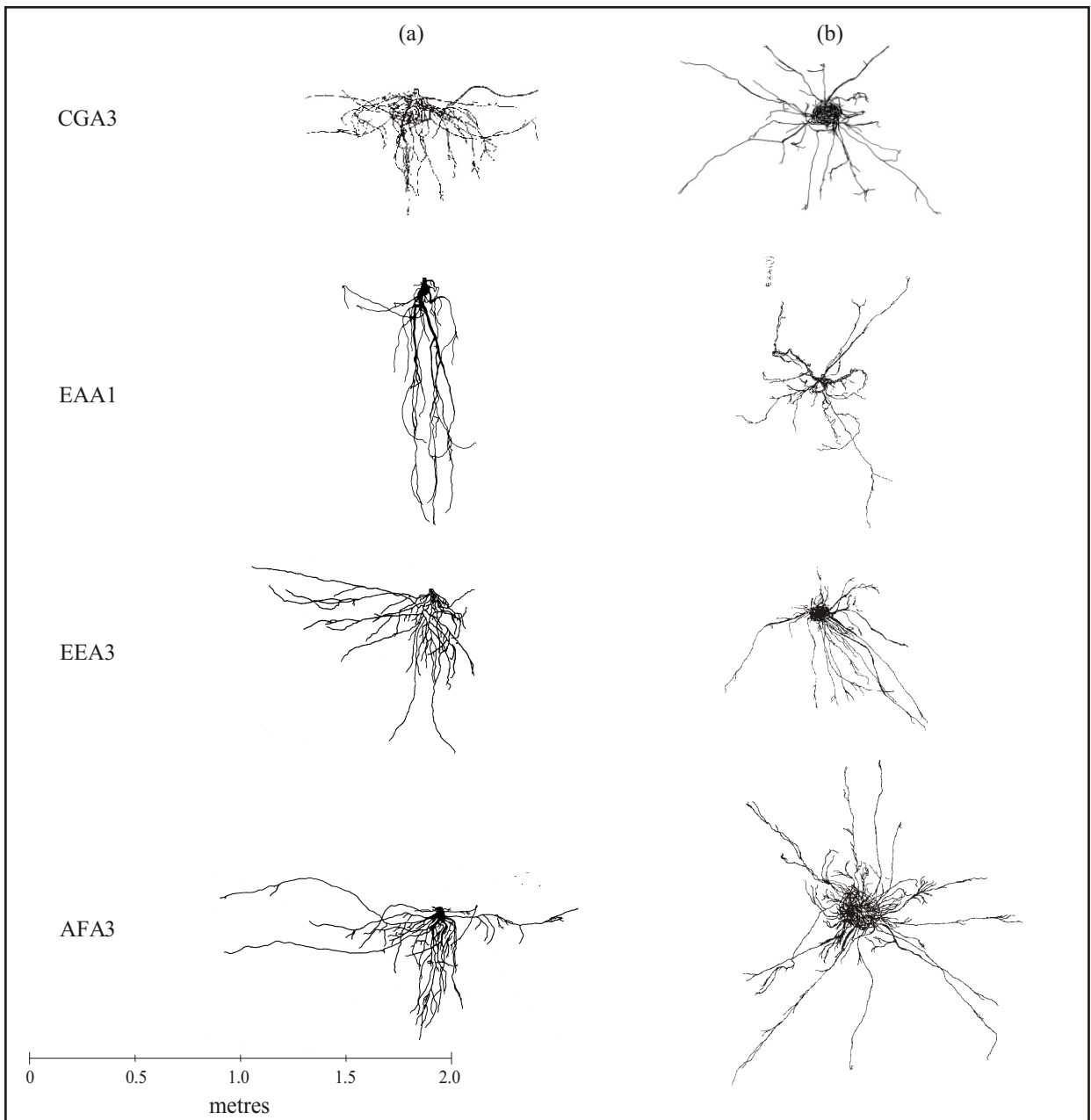
Figure 3.6: Comparisons between species in (a) Cross-sectional view; and (b) Plan view. Plan views are typical of each species, presenting a fairly even radial distribution of the root system. EEA3 is an exception with lateral root growth predominantly in one direction. Other samples shown here are samples EAA1, AFA3, and CGA3.

There are little if any observable differences between the smaller samples and the larger ones of each species (except for evidence of pot constriction) indicating that there is a continuity of form with tree size within the range of sizes examined. As mature trees have not been extracted it is not known it this continuity of form applies generally through the life of the tree, although observations of the partially exposed root systems of large trees (section 3.5) suggest that it is a reasonable first-approximation.

As expected there are also some differences of root form between species (Figs. 3.2-3.5). For instance the number and the size of roots varies significantly, with the greatest contrast between *E. amplifolia* and *A. floribunda*. The former presenting roots fewer in number but much larger in size, while the latter is made up almost entirely of large numbers of very fine roots. *C. glauca* and *E. elata* figure between the two extremes. This has implications for the mode of root reinforcement given the often repeated assertion that roots smaller than about 2 cm in diameter tend to contribute to soil strength through an increased apparent cohesion, while roots larger than about 2 cm in diameter tend to contribute to soil strength through an anchoring process (Coppin & Richards, 1990). If this assertion is correct then roots of the species *E. amplifolia* are more likely to provide reinforcement through an anchoring process at a younger age than the other species, while the mass of fine roots exhibited by *A. floribunda* will tend to provide a greater increase in the apparent cohesion of a shallow soil layer.

3.4   Spatial distribution of root area quantity

3.4.1   Root distribution with depth below the ground surface

The aggregate cross-sectional area of root material decreases rapidly with increasing soil depth for every sample measured (Appendix A-I). A rapid decrease occurs within the upper soil layer with a more gradual decrease at greater depths. Plots of root quantity expressed as a percentage of the stem area at the ground surface demonstrate this phenomenon (Fig. 3.7) such that the zone of greatest reduction is evident between approximately 5 and 20 % of the MVD. The data has been plotted in terms of a percentage of the Maximum Vertical Depth (MVD) on the y-axis and a percentage of the stem cross-sectional area at the ground surface on the x-axis, in order to allow a comparison between trees of different stem sizes and with different total root system depths. The raw values are presented for all samples in Appendix A-I.
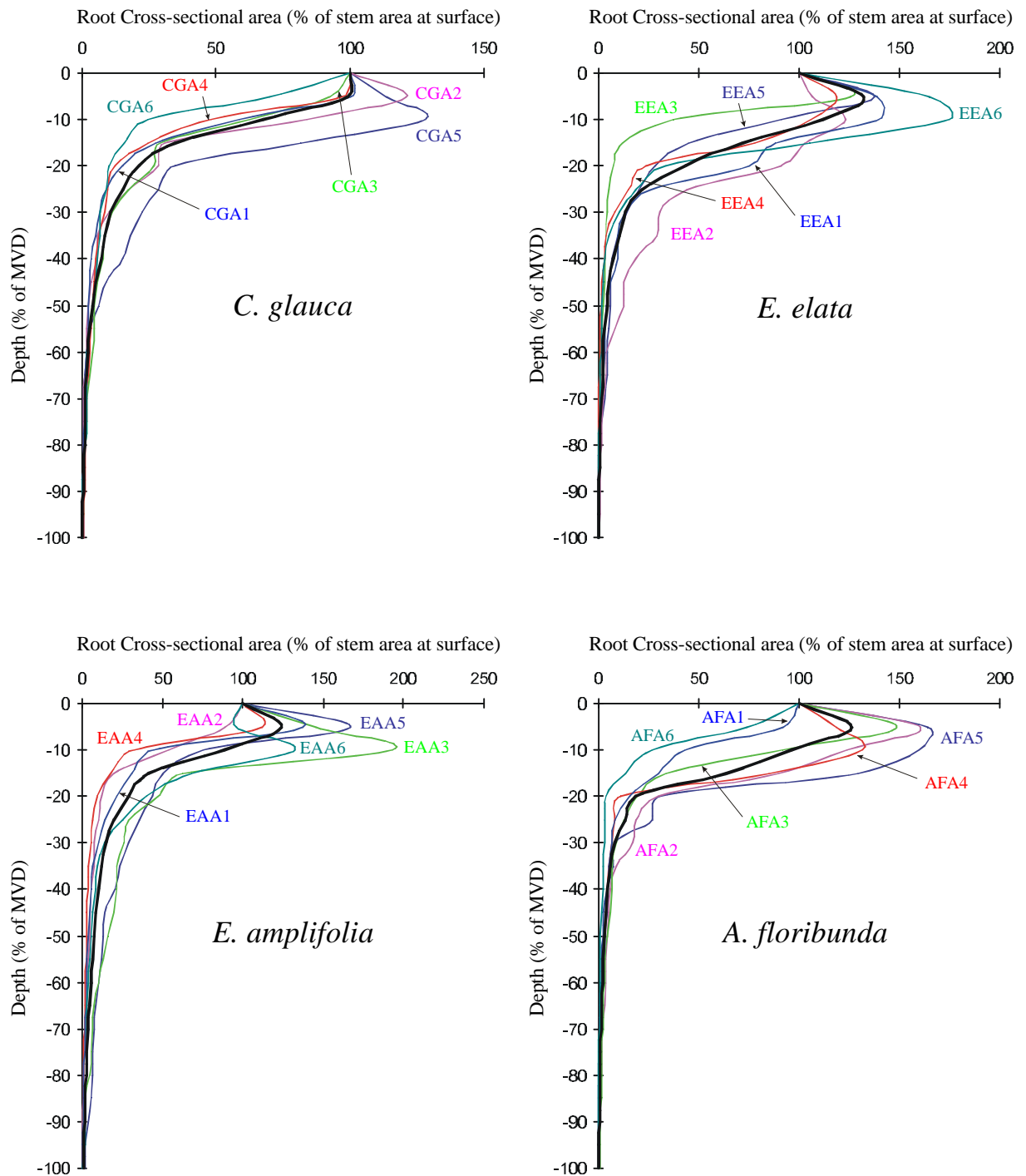
Figure 3.7: The variation in root quantity with depth for each species. Depth on the y-axis is set to the MVD at 100 % and root quantity on the x-axis is presented as a percentage of the cross-sectional area of the stem at ground level. The thick black line represents the average of the six samples in each species.

All species exhibit this rapid reduction in root area quantity with depth over approximately the first 15 % of root extent below the surface. So that in effect there are two zones of root area quantity beneath the tree. The first, in the shallow soil layer between 0 and 15 % of the MVD, and the second in deeper soil from 15 to 100 % of the MVD. The first, or upper zone is characterised by a small increase followed by a large decrease in root area quantity with approximately 80 % of the

total root area quantity contained within it. The second, or lower zone describes a continual reduction in root area quantity that slows with increasing depth. In the upper zone *E. elata* has on average the greatest root area quantity while in the lower zone *E. amplifolia* has a greater average quantity from about 25 % of MVD (Fig. 3.8). *C. glauca* has by far the least root area quantity in the upper zone but in the lower zone the difference reduces significantly such that *A. floribunda* has the least root material from approximately 20 % of MVD.
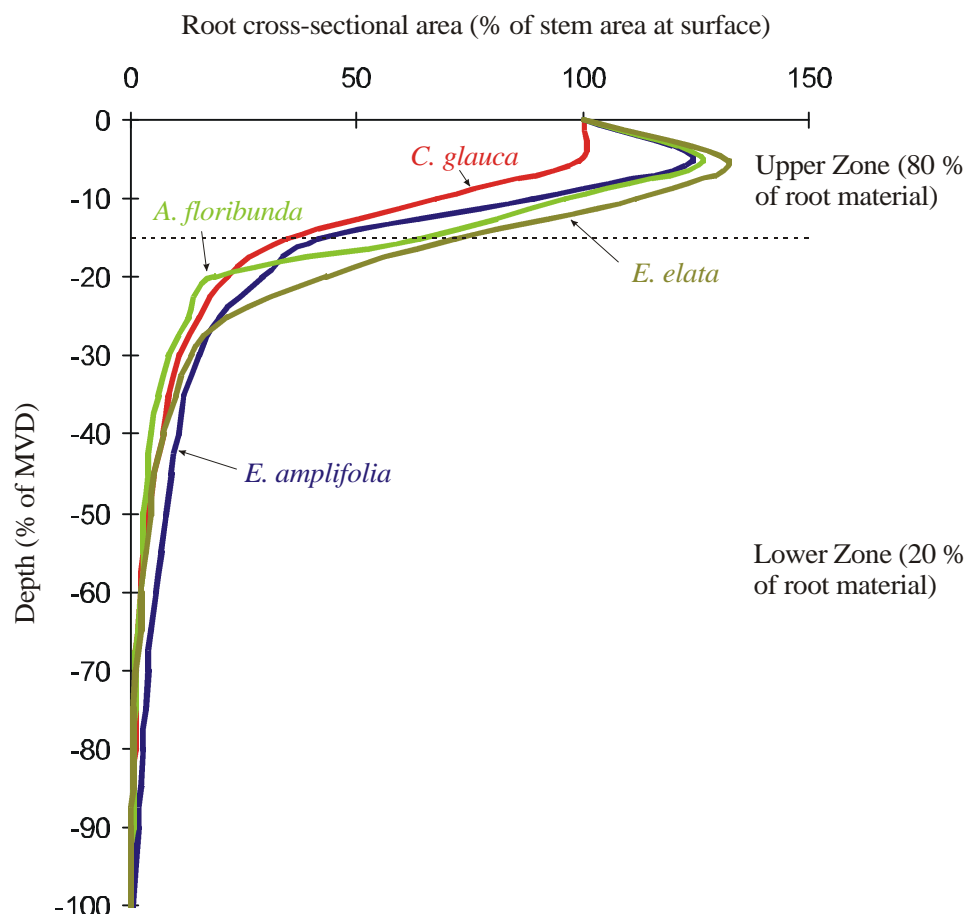
Figure 3.8: Average root area quantity with depth curves for the four species. In effect there are two zones of root area quantity beneath the trees. The dashed line represents the approximate division between the two (15 % of MVD).

The change in root area quantity with depth can be described using equations from the lines of best fit through the data points at each 10 % increment of depth (Fig. 3.9). For the upper zone this curve is best represented by a 2nd order polynomial while for the lower zone this curve is best represented by a negative exponential. The average for each species can be accurately described by these functions to determine an estimate of the average root area quantity at any given depth. The equations are presented below.
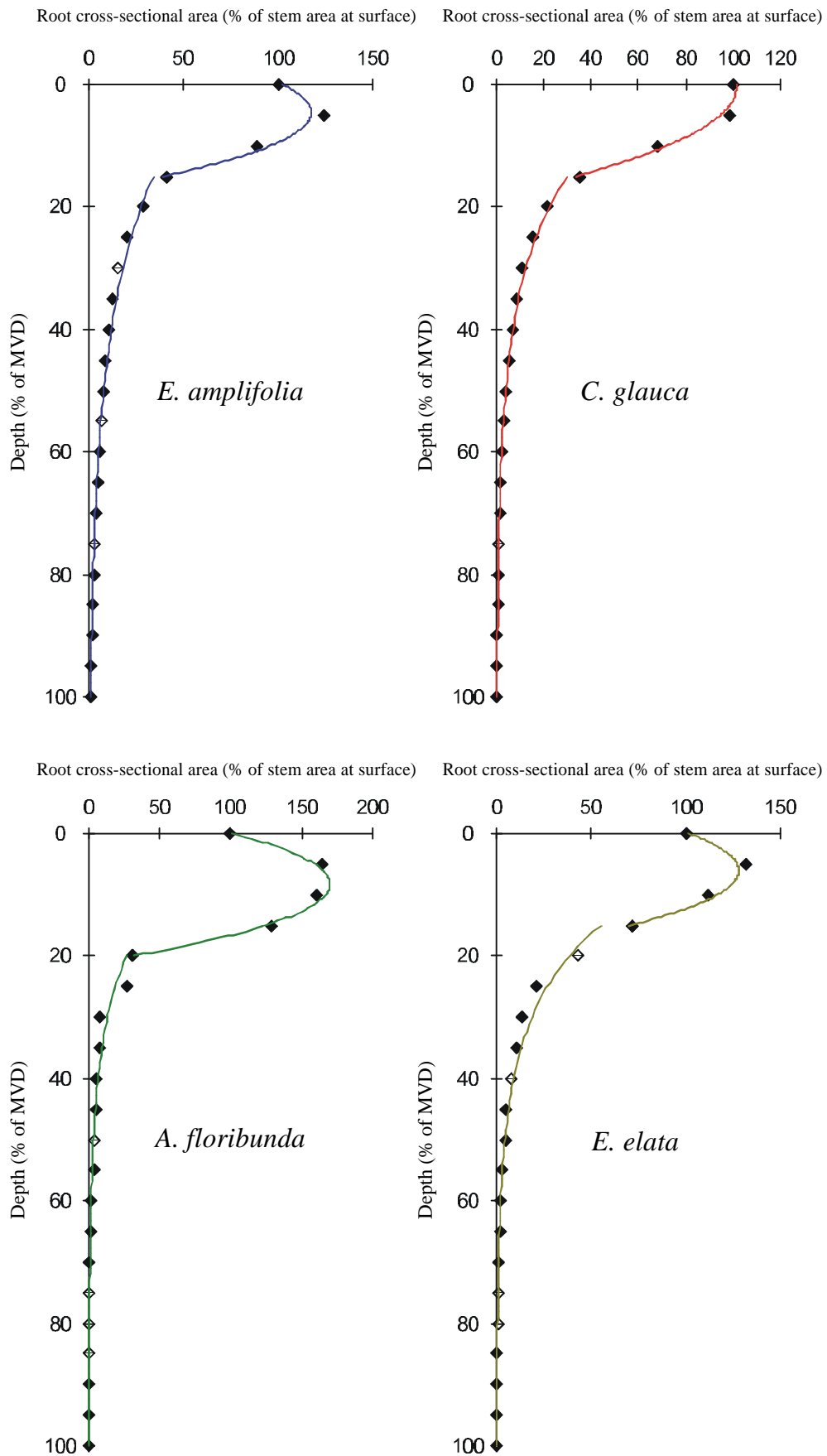
Figure 3.9: Best fit curves for root quantity determination with depth. From 0 to 15 % of the maximum vertical depth (MVD) the curve is a 2nd order polynomial and from 15 to 100 % of the maximum vertical depth the curve is a negative exponential function. The two different functions represent two distinct zones of root quantity. Approximately 80 % of all root material is located in the upper zone between 0 % and 15 % of MVD.

Upper zone relationships between depth (D) and root area quantity (Q; as a % of the stem cross-sectional area at ground level) for each species are:

C. glauca	$Q = -0.3182.D^2 + 0.2438.D + 101.41$	$R^2 = 0.99$	[3.1]
E. amplifolia	$Q = -0.7201.D^2 + 6.571.D + 102.41$	$R^2 = 0.97$	[3.2]
E. elata	$Q = -0.7216.D^2 + 8.7309.D + 101.57$	$R^2 = 0.97$	[3.3]
A. floribunda	$Q = -1.005.D^2 + 16.623.D + 101.22$	$R^2 = 0.99$	[3.4]

Lower zone relationships between depth (D) and root area quantity (Q; as a % of the stem cross-sectional area at ground level) for each species are:

C. glauca	$Q = 69.093.e^{-0.0582.D}$	$R^2 = 0.99$	[3.5]
E. amplifolia	$Q = 64.153.e^{-0.0423.D}$	$R^2 = 0.98$	[3.6]
E. elata	$Q = 165.86.e^{-0.073.D}$	$R^2 = 0.98$	[3.7]
A. floribunda	$Q = 110.24.e^{-0.0711.D}$	$R^2 = 0.98$	[3.8]

From these relationships it is possible to calculate the average root area quantity at any specified depth using the cross-sectional area of the stem at the ground surface. These equations however only give the total root cross-sectional area present at the specified depth and do not indicate the lateral distribution within the soil layer. This aspect is assessed in the following section.

3.4.2 Root distribution with lateral distance from the tree stem

To determine the distribution of root area quantity in the lateral direction it was first necessary to measure the maximum lateral root extent. That is, the furthest reach of the root system from the tree stem. This was measured for each depth quartile for each specimen (Appendix A-II). For each species the average maximum lateral extent is at a maximum in the first depth quartile and therefore reduces with increasing depth (Fig. 3.10). This result is expected given observations of root form (section 3.3) that account for most extensive lateral roots in the upper soil layers and the deeper vertical roots predominantly below the tree stem.

The rate of reduction in maximum lateral extent with depth varies slightly for each species and is represented by the lines of best fit in Fig. 3.10. *E. elata* exhibits a more even reduction than the other three species. The relationships between depth (D) and Maximum Lateral Extent (MLE) are presented in the equations that follow.
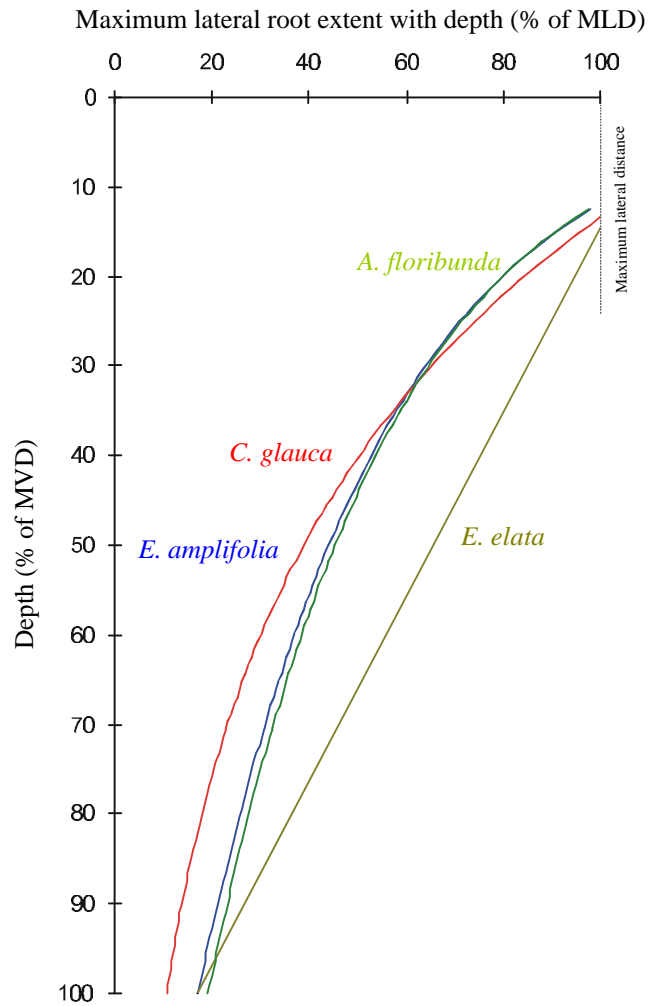
Figure 3.10: The variation in maximum lateral root extent with depth for each species. The maximum lateral root extent is recorded as a percentage of the MLD, which is 100 % in the first (upper) depth quartile for all species. All species exhibit a reduction with increasing depth although this is more regular for *E. elata* than the other three.

C. glauca	MLE = -44.63ln(D) + 214.51	$R^2 = 0.99$	[3.9]
E. amplifolia	MLE = -38.94ln(D) + 196.4	$R^2 = 0.99$	[3.10]
E. elata	MLE = -0.971.D + 114.12	$R^2 = 0.99$	[3.11]
A. floribunda	MLE = -37.728ln(D) + 192.93	$R^2 = 0.97$	[3.12]

The distribution of roots within this maximum lateral extent was recorded within each depth quartile as the root cross-sectional area that crossed a specified vertical plane. In all species the quantity of root cross-sectional area decreases markedly with increasing distance from the tree stem. For the average of each species within each depth quartile it can be approximated by a negative exponential relationship (Figs. 3.11 and 3.12). The equations obtained for each of these relationships are presented in Appendix A-III. These relationships represent the trend in reduced root cross-sectional area with distance away from the tree stem and are therefore expected to be proportionally representative of the change in root material quantity present in the lateral direction across a potential shear plane at a specified depth. As such they can be used to determine the quantity of

root material within a specified lateral distance from the tree stem. This is done by a determination of the area beneath the curve for a certain lateral distance, as a ratio of the total area beneath the curve (equation [3.13]).

$$RQ = \frac{\int_0^b F(x).dx}{\int_0^{b(MLE)} F(x).dx} \times 100$$

[3.13]

where RQ is the root quantity present within the lateral distance b from the tree stem as a percentage of the total root area quantity at that depth, which is determined by the root distribution with depth relationship presented in the previous section; $b^{(MLE)}$ is the maximum lateral root extent at that depth (100 % in the first depth quartile); and F(x) is the lateral root distribution curve for the species and depth in question as illustrated in Figs. 3.11 and 3.12 and presented in Appendix A-III.
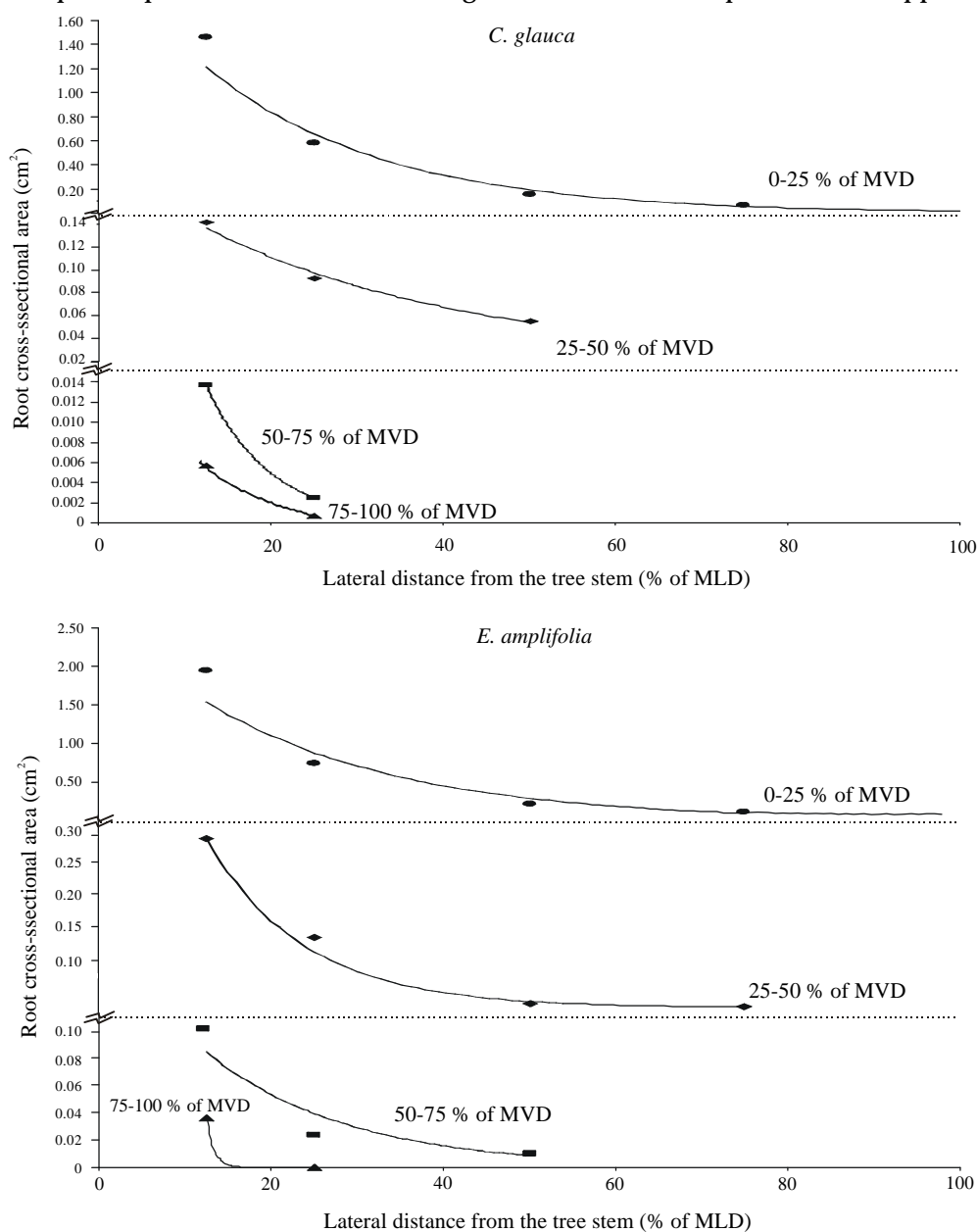
Figure 3.11: The reduction in root area quantity with increasing lateral distance from the tree stem at all depths for *C. glauca* and *E. amplifolia*. The reduction is approximated by a negative exponential relationship for each depth quartile. Note the broken scale on the y-axis.
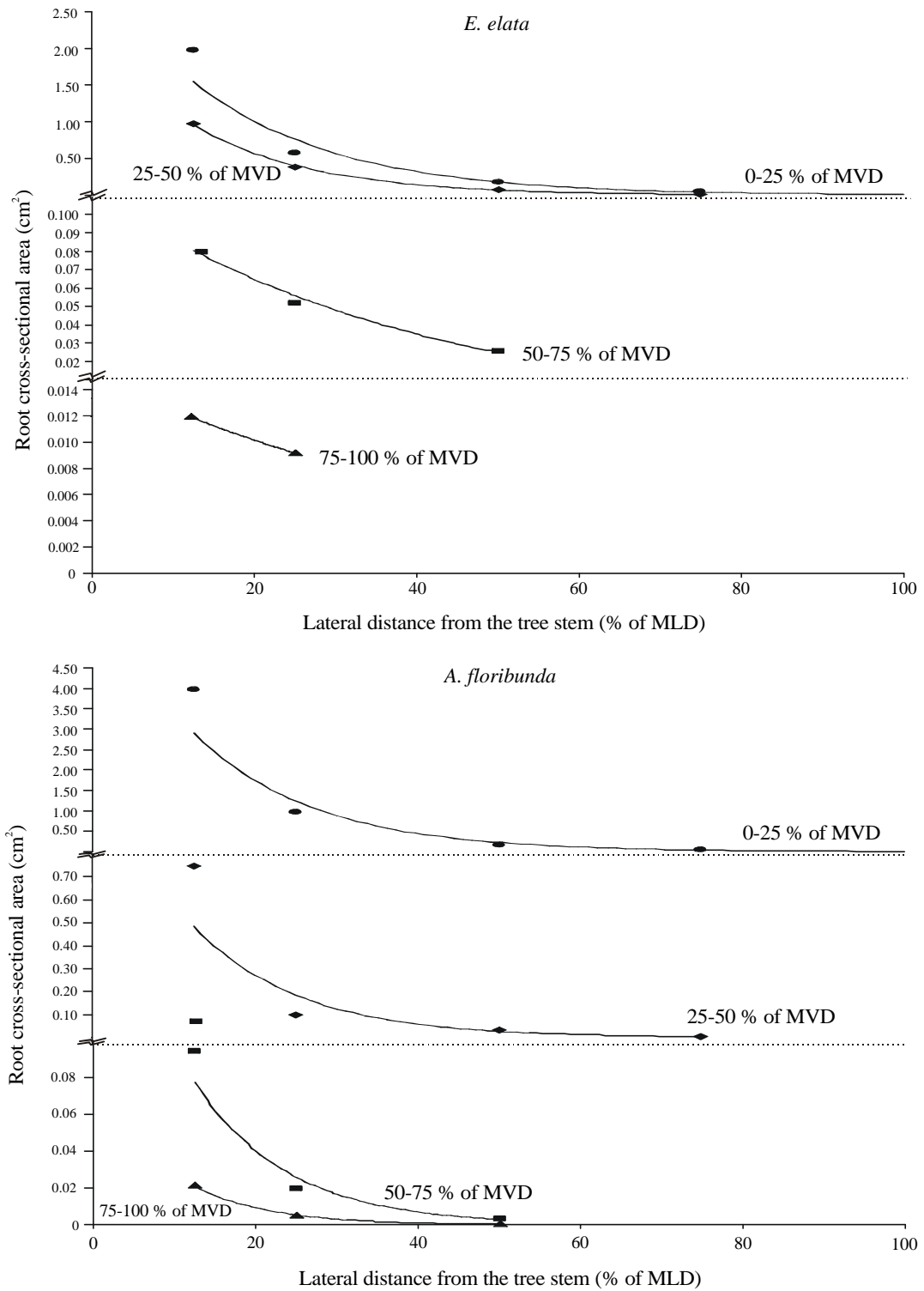
Figure 3.12: The reduction in root area quantity with increasing lateral distance from the tree stem at all depths for *E. elata* and *A. floribunda*. The reduction is approximated by a negative exponential relationship for each depth quartile. Note the broken scale on the y-axis.

3.5   Field observations on the root systems of mature trees

As the magnitude of increased soil shear strength has been shown to be related to the quantity and size of roots present within the soil layer (e.g. Greenway, 1987), it follows that larger, mature trees will have a greater capacity to reinforce the soil than will smaller individuals of the same species. It is therefore necessary to estimate the spatial root distribution underneath large trees within the study area. This is achieved by integrating the results for the extracted juveniles with observations of the naturally exposed root systems of mature trees growing along the river channel.

The average maximum root depth as a percentage of tree height for the small trees excavated, is 44 % for *C. glauca*, 69 % for *E. amplifolia*, 35 % for *E. elata*, and 44 % for *A. floribunda* (Table 3.1). If this same relationship were applied to large, mature trees then a 30 m tall *E. amplifolia* would have roots extending to a depth of around 20 m below the ground surface. Although roots to this depth have been observed beneath Eucalyptus trees elsewhere (see Stone & Kalisz, 1991) this is considerably greater than any depth used in previous investigations of increased soil strength due to mechanical vegetative effects, where maximum depths of less than 2 m are commonly applied (see Wu, 1995). However observations of the partially exposed root systems of mature trees growing within the study area suggest that a maximum rooting depth of 2 m is a significant underestimate for the species studied in this environment. It is likely that the relatively sandy soils and high banks of the upper Nepean River and other Australian coastal streams, as well as prolonged periods of drought, encourage extensive root growth down to at least the level of the permanent water table (see Hubble, 1996).

For example the mature Eucalyptus tree (around 35 m in height) growing on the crest of the river bank in Fig. 3.13 has exposed roots protruding from a failure scarp at a depth of approximately 4 metres below the ground surface. At this point many of the roots measuring up to 15 cm in diameter re-enter the bank material and descend. It is possible that the largest of these roots and their branches extend to the level of the permanent watertable, a further 8 m below, at the permanent low-flow level in the channel. The 15 m tall Eucalyptus in Fig. 3.14 has large roots exposed at a depth of 3 m below the ground surface, where they also re-enter the bank material and descend.

The 20 m tall Casuarina tree growing on bedrock in Fig. 3.15 has an extensive root system to 1.7 m below the position of the original ground level. Despite the presence of the bedrock, the roots descend into the riverbank and would likely do so with even greater penetration if deeper alluvial bank materials were present. The 10 m tall Casuarina growing on the bank edge and exposed after the collapse of some sediments in Fig. 3.16 exhibits large roots (up to 10 cm in diameter) re-entering the bank material at a depth of 1.6 m below the ground surface. The 5 m tall Acacia tree growing in Fig. 3.17 exhibits an exposed root system to a depth of 1.3 m below the ground surface where, as with the other examples presented, the roots re-enter the bank material and continue to grow in the vertical direction.

Figure 3.13: A mature Eucalyptus tree growing within the study area. Note the exposed root system in the failure scarp where it is possible to observe large roots re-entering the bank material directly below the tree stem at a depth of approximately 4 m below the ground surface.

Figure 3.14: A mature Eucalyptus tree growing within the study area. Part of the root system is exposed to a depth of approximately 3 m below the ground surface.

Figure 3.15: A mature Casuarina tree growing within the study area. Despite the presence of bedrock and washing away of the bank sediments, many of the comparatively large roots re-enter the bank face at a depth of around 1.7 m below the original ground surface.

Figure 3.16: A 10 m tall Casuarina tree growing within the study area. Substantial roots are visible growing into the bank material at a depth of 1.6 m below the ground surface.

Figure 3.17: A mature Acacia tree growing within the study area. Part of the root system of this 5 m tall tree is exposed to a depth of 1.3 m below the ground surface.

The above examples and many more similar observations in the field suggest that root growth of Australian riparian species in alluvial bank sediments, when unimpeded by bedrock can be considerably greater than the maximum depths described in previous investigations of this nature. Although it is impossible to determine if depths of between 35 and 69 % of the above-ground height are actually reached by mature trees in the field, evidence of maximum rooting depths considerably in excess of 2 m are illustrated in the above examples not only by the exposed portions of some of the trees but also by the large size of many of the roots re-entering the bank material below the tree. Furthermore, a number of the juveniles extracted from the Cobbity plantation had already reached depths of close to 2 m after only 18 months of growth (Table 3.1).

For the purposes of assessing vegetative effects on riverbank stability it is necessary to develop a measure of root extent that could be described as typical for a mature tree of the species and the environment of interest. This value cannot apply to every individual due to the natural variation inherent in biological systems and because soil conditions over the length of a riparian study area are not homogenous. The value should however be representative of the species, based on the best available data, and for the purposes of riverbank stability modelling, it also needs to be a conservative estimate. A 1 to 1 relationship between the maximum root depth of juveniles and mature trees although possible is probably not conservative, resulting in maximum root depths of between 10 and 20 m for a mature 30 m tall tree. A 4 to 1 relationship, giving maximum root depths of between 2.7 m and 5.3 m seems to be overly conservative based on observations of the root system form of partially exposed individuals in the study area. It seems likely then that the maximum

rooting depth of mature trees modelled at half of the maximum depth measured for juvenile trees (2:1) gives realistic measurements based on field observations of what might be described as typical or representative within the study area (Fig. 3.18). That is, 35 % of the above ground tree height for *E. amplifolia*, 22 % for *C. glauca* and *A. floribunda*, and 18 % for *E. elata*. Therefore a 30 m tall *E. elata* tree will for example present with a maximum root depth of 5.4 m. As a conservative estimate this fits with observations from the study area as described above and illustrated in Figure 3.18.
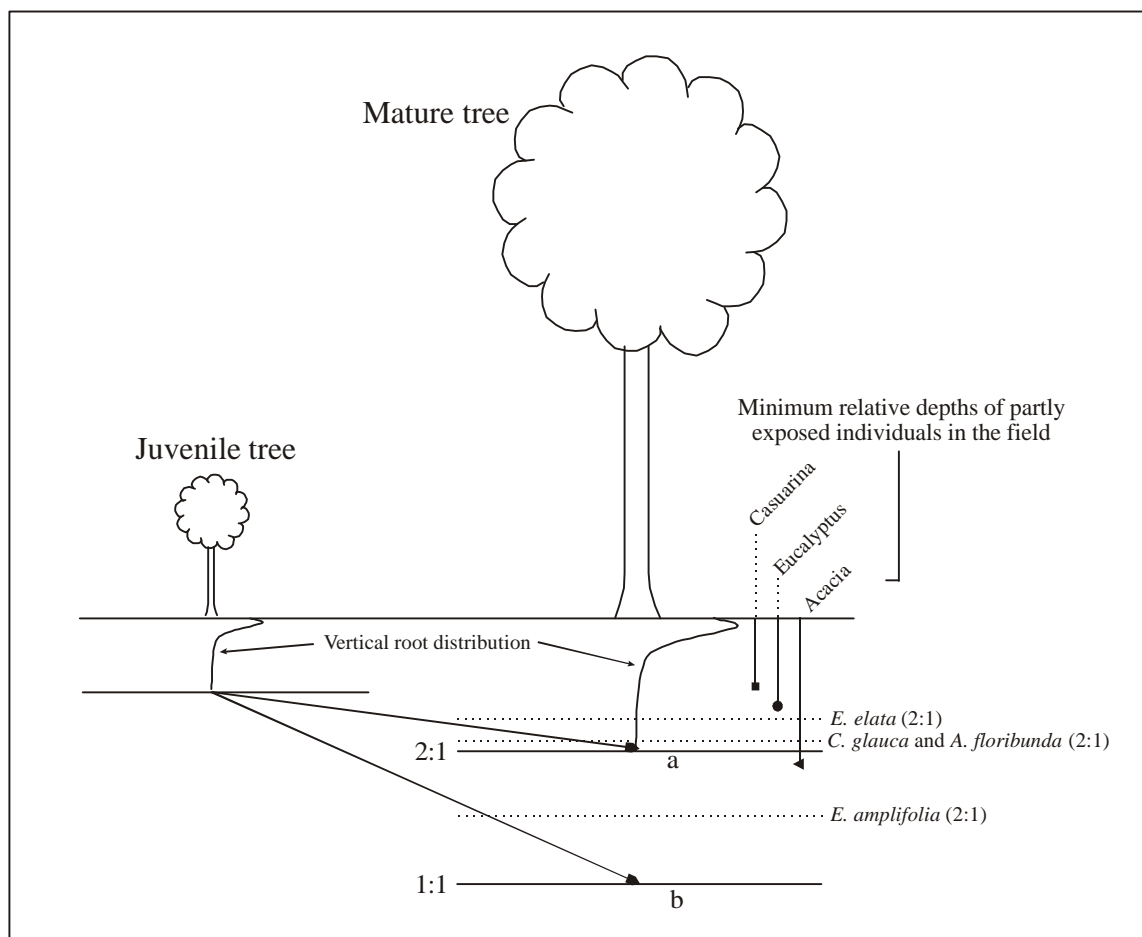
Figure 3.18: Diagrammatic representation of the vertical root system determination for mature trees. Using a 1:1 relationship (av. line b) for the MVD of juvenile trees probably overestimates the maximum depth for mature trees. A 2:1 relationship (av. line a) gives values closer to minimum typical depths observed in the field and therefore represents a likely conservative estimate for the purposes of stability modelling. The form and distribution of root material within this depth is expected to occur in a similar relationship for mature trees as for juveniles, with 80 % of the root material within the first 20 % of the depth of the root system.

The maximum depth for all species except *C. glauca* is limited by the depth of the permanent watertable, which is estimated to be at the level within the bank of the no-flow state in the channel. This does not apply to *C. glauca* as observations suggest that it is extremely comfortable with roots growing in saturated soil, and there are numerous sites along the Nepean River where exposed Casuarina roots grow directly into the weir-lake and to the bottom of the channel (Fig. 3.19). This behaviour is probably a consequence of the species' tendency to a waterline existence and is

presumably a response to achieve anchorage that improves its survival during flood events. It has not been observed in the other three species investigated.

Figure 3.19: Casuarina roots grow vigorously in saturated bank sediments and indeed directly into open water as evident by this individual. This phenomenon has not been observed in the other species or even genus' investigated in this study. Also note the bedrock located at the waterline, a common feature of this incised stream.

The measurements of juvenile trees in the previous section demonstrate that for every sample of every species there is a rapid reduction in root quantity in the upper soil layer which slows to a more gradual reduction as depth below the ground surface increases. Such a condition is evident in most other studies (see for example Riestenberg, 1994; Abernethy & Rutherfurd, 2001) and is consistently exhibited by trees of different sizes and ages (e.g. Wu *et al.*, 1995). The examples of mature trees growing within the study area also conform to this general behaviour, where the quantity of root material decreases rapidly with distance away from the tree stem in both the vertical and lateral directions. The mature trees also appear to conform to the overall root system form of the measured juveniles. That is, the deepest roots are located directly beneath the tree stem and the majority of lateral roots occur in the shallowest soils. For the purposes of modelling riverbank stability in this study the general root distribution form and relationships for small trees are assumed to apply to mature trees of the same species. Only excavation and measurement of the roots from a number of individual mature trees could demonstrate the validity of this assumption but such fieldwork is well beyond the resources of this study.

3.6   Spatial root distribution and earth reinforcement

The spatial distribution of a tree's roots will determine the magnitude of increased shear resistance at different locations within the bank material. Therefore it is necessary to produce an estimate, at a given depth and distance from the tree stem, of the likely quantity of root material present. An Excel spreadsheet based programme ROOTQ has been designed to provide this data for any given tree size, depth below the ground surface, and lateral distance from the tree stem. It uses both the juvenile relationships obtained by experimental procedure and the scaling relationship described in the previous section to estimate the quantity of root cross-sectional area at a specified location in the soil mass. A two-dimensional soil profile can then be built underneath a tree or group of trees that incorporates the variation in root area ratios through a given number of soil zones. In this study 12 soil zones have been selected for representation beneath a single tree due to limitations on the number of soil layers allowed by the slope stability programme (XSLOPE) which will be used for the riverbank stability analysis (chapter seven). The ROOTQ programme takes the following steps to arrive at a value (Fig. 3.20):

1. The maximum vertical depth (MVD) and the maximum lateral distance (MLD) of a tree's root system is obtained as a proportion of the tree's above ground height. As described in the previous section, for MVD this is the experimental value for a small juvenile (Table 3.1) and half this value for a mature tree; and for MLD is in the same proportions relative to the MVD for a mature tree as occurs in the small juveniles.

2. At four depths corresponding to the mid-point of the depth quartiles for each species, that is 12.5 %, 37.5 %, 62.5 %, and 87.5 % of the MVD from step 1, the quantity of root material as the total cross-sectional area, a_r, is calculated. This is undertaken using the appropriate experimentally derived relationships: equations [3.1]-[3.4] for the first point (12.5 %) and equations [3.5]-[3.8] for the other three depths (located in the lower root zone as described in section 3.4); whereby the total cross-sectional area of roots at a given depth, D, is determined as a percentage of the cross-sectional area of the stem at ground level.

3. The distribution of a_r as obtained in step 2 is then calculated in the lateral direction as the quantity of root material within a given lateral distance from the tree stem, a_{rl}. Three lateral distances have been chosen for simplification, 25 %, 50 %, and 100 % of the maximum lateral extent (MLE) for each depth quartile. The MLE is determined using the appropriate experimentally derived relationships: equations [3.9]-[3.12]. For each lateral distance the quantity of root material contained between the stem-line and this distance is calculated using equation [3.13] where F(x) is the relevant function given by the curves in Figures 3.11 and 3.12 and the respective experimentally derived relationships given in Appendix A-III. The result here is a proportion of the total root cross-sectional area calculated in step 2 for a given depth (a_{rl} = %.a_r) and within the specified lateral distance.

4. The root area ratio (RAR) is then calculated as the proportion of the root cross-sectional area obtained in step 3 over the potential shear area within that soil zone, i.e. a_{rl}/A_s.
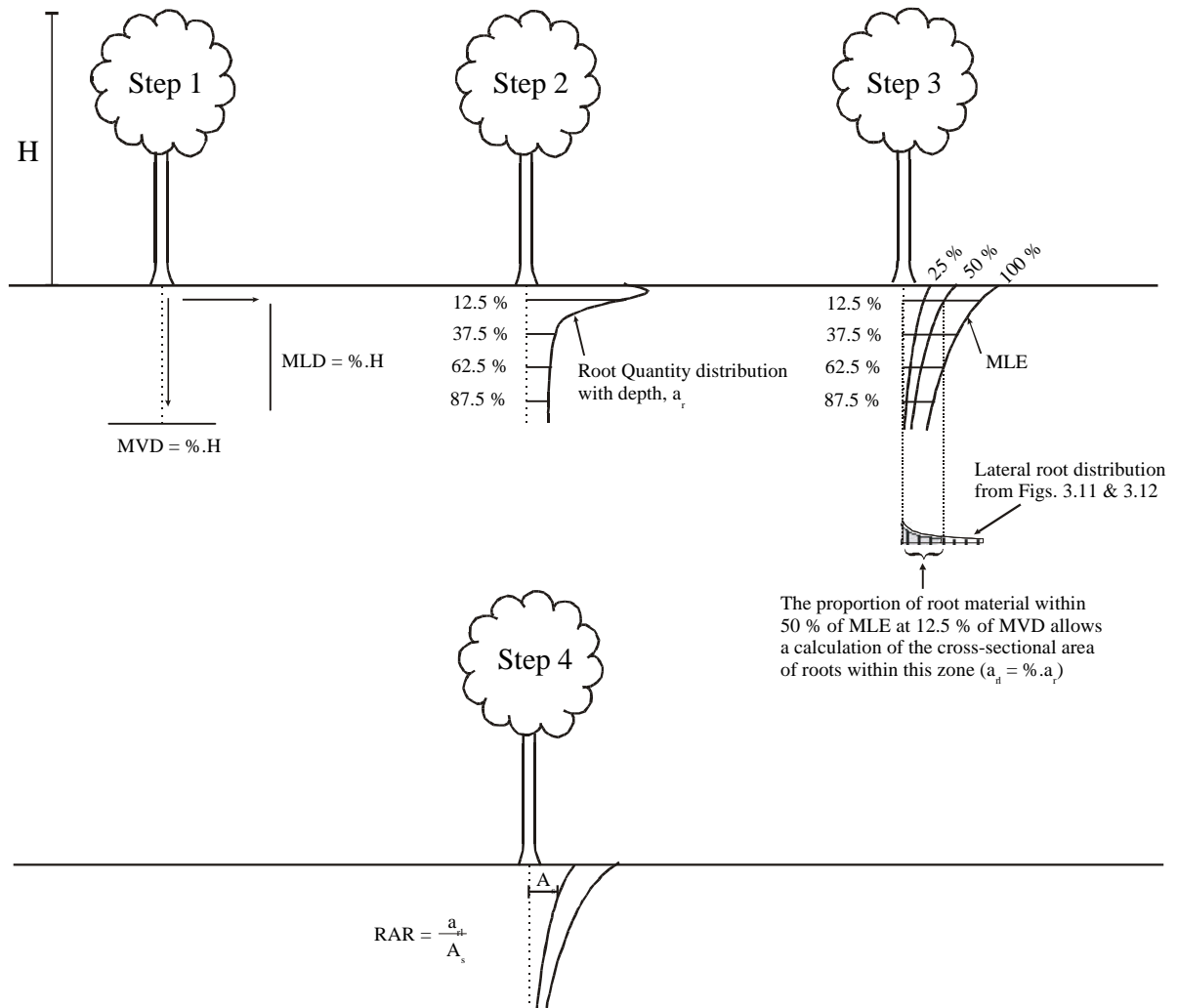
Figure 3.20: Diagrammatic representation of steps taken by ROOTQ to calculate the distribution of Root Area Ratio (RAR) in the soil mass beneath a tree. Step 1 calculates the MVD and MLD from the height of the tree. Step 2 calculates the cross-sectional area of root material at the specified depth. Step 3 calculates the cross-sectional area of root material within the specified lateral distance from the tree stem. Step 4 calculates the RAR within the relevant soil zone.

The result of this process is a series of soil zones that are characterised by different root area ratios. Illustrations of the result for a mature tree of each species are given below (Figs. 3.21-3.24). The tree dimensions selected were 20 m in height and 32 cm in stem diameter for *C. glauca*, 30 m and 70 cm for *E. amplifolia*, 30 m and 90 cm for *E. elata*, and 8 m and 24 cm for *A. floribunda*; based on typically representative values of trees growing within the study area and on descriptions of their growth habits (Benson & Howell, 1993; Howell *et al*, 1995). An analysis of sensitivity for the riverbank stability analysis results presented in chapter seven reveals that the final factor of safety value is quite insensitive over a range of representative tree heights and stem diameters within the same species, suggesting that for the purposes of modelling riverbank stability the values chosen give a good account of typical vegetated conditions.

Consideration of the differences between species in terms of overall root extent and the quantity of root material within different soil zones is instructive. In particular the massive volume of reinforced

soil beneath *E. amplifolia* compared to the other three species and also the large root area ratios of both Eucalypts directly below the tree stem, compared to *C. glauca* and *A. floribunda*. *A. floribunda* also has a very high root area ratio in the first soil zone directly below the stem however this dissipates rapidly with distance both laterally and with depth. It has the most restricted root system of the four species, which is probably a consequence of it being a smaller shrub-like tree. *C glauca* exhibits the smallest root area ratios throughout each soil zone. Values of root area ratio do not necessarily decrease with depth (e.g. *E. elata* between 50 and 100 % of the maximum lateral extent; soil zones 3, 6, 9, and 12: Fig. 3.24). This occurs because although the quantity of root material decreases, so too does the area of a potential shear plane over which roots are present, *i.e.* the maximum lateral root extent decreases with depth.
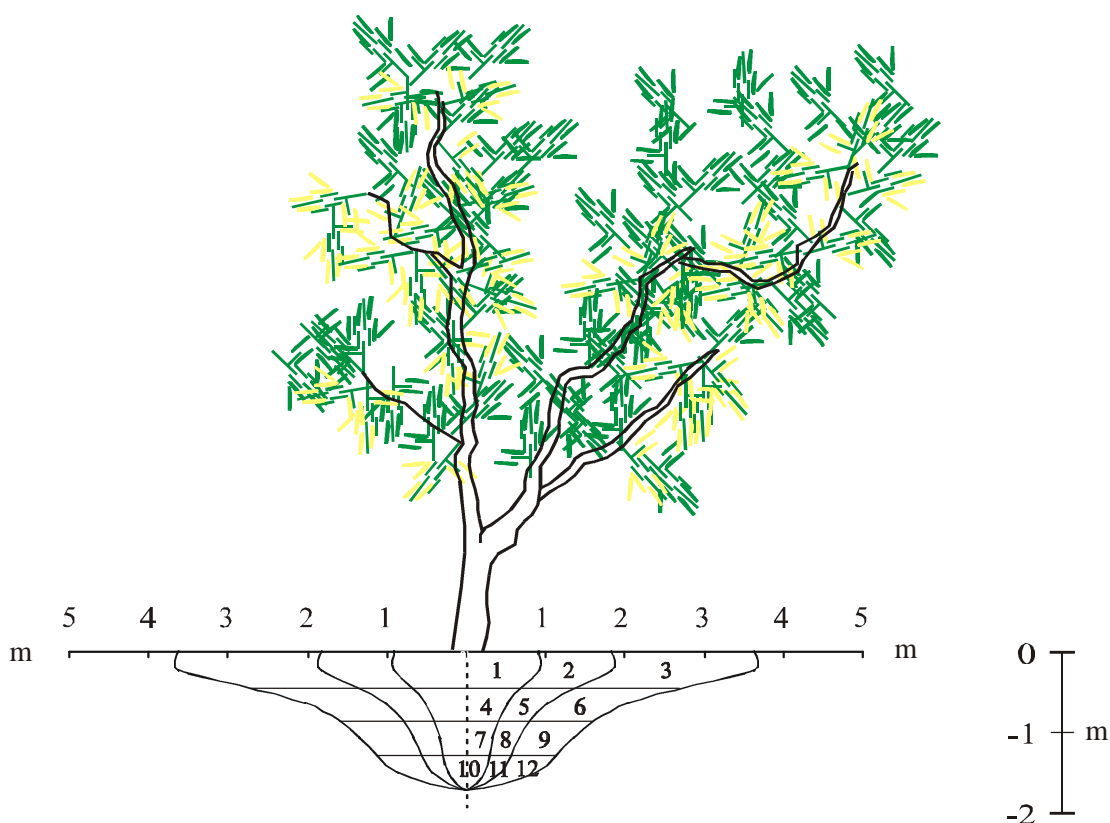
Figure 3.21: The spatial root distribution by soil zone beneath a mature *A. floribunda* tree. Soil zones are numbered with the RAR within each zone presented in the table below. Above-ground illustration is for scale (8 m tall tree).

Table 3.2: Values of RAR for each soil zone below a mature *A. floribunda* tree as represented in Figure 3.21.

	RAR (%)		*RAR (%)*
Zone 1	0.628	**Zone 7**	0.086
Zone 2	0.042	**Zone 8**	0.015
Zone 3	0.002	**Zone 9**	0.003
Zone 4	0.268	**Zone 10**	0.039
Zone 5	0.036	**Zone 11**	0.006
Zone 6	0.004	**Zone 12**	0.001
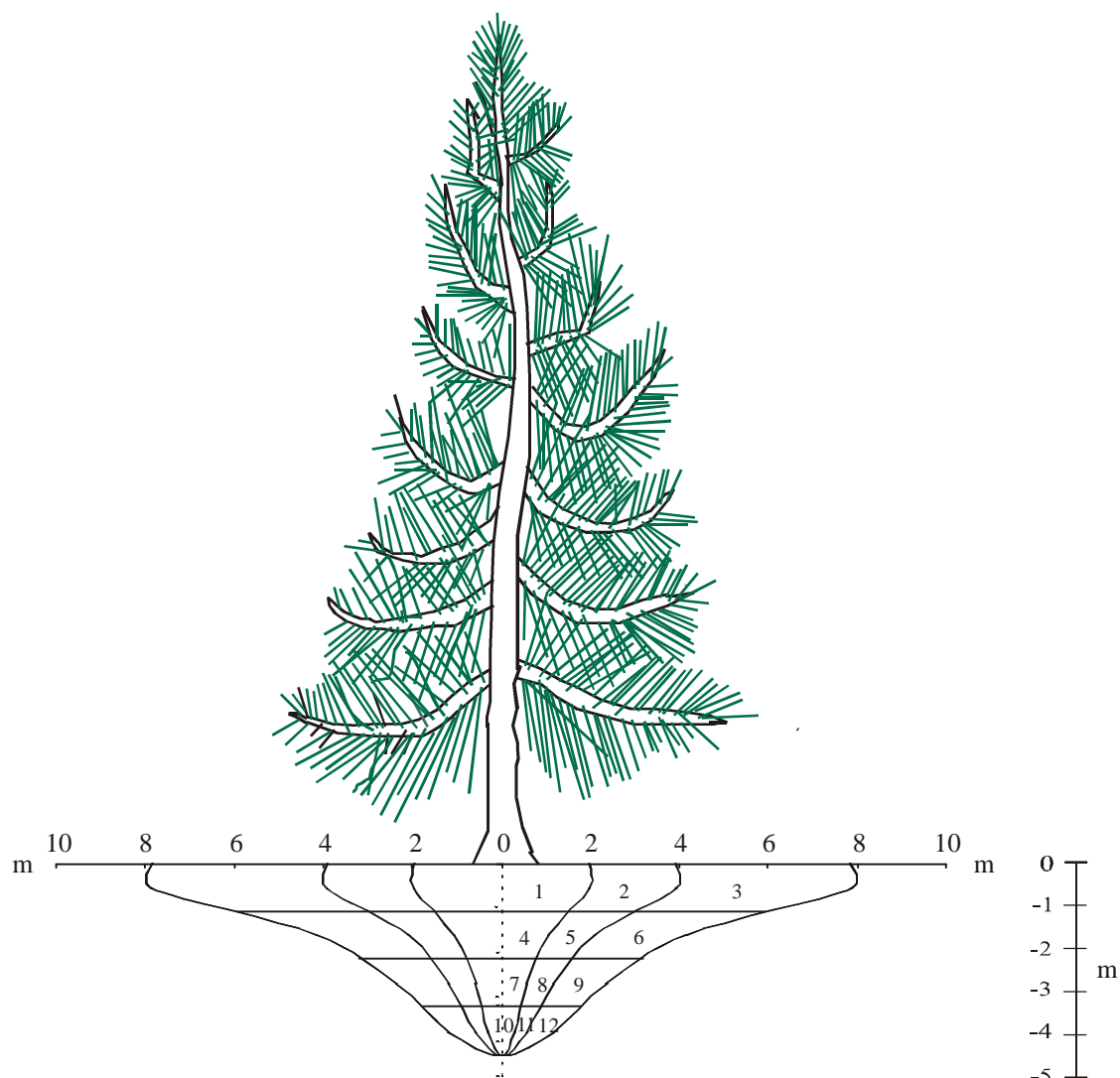
Figure 3.22: The spatial root distribution by soil zone beneath a mature *C. glauca* tree. Soil zones are numbered with the values of RAR within each zone presented in the table below. Above-ground illustration is for scale (20 m tall tree).

Table 3.3: Values of RAR for each soil zone below a mature *C. glauca* tree as represented in Figure 3.22.

	RAR (%)		*RAR (%)*
Zone 1	0.152	**Zone 7**	0.076
Zone 2	0.016	**Zone 8**	0.011
Zone 3	0.002	**Zone 9**	0.002
Zone 4	0.079	**Zone 10**	0.043
Zone 5	0.017	**Zone 11**	0.011
Zone 6	0.004	**Zone 12**	0.004
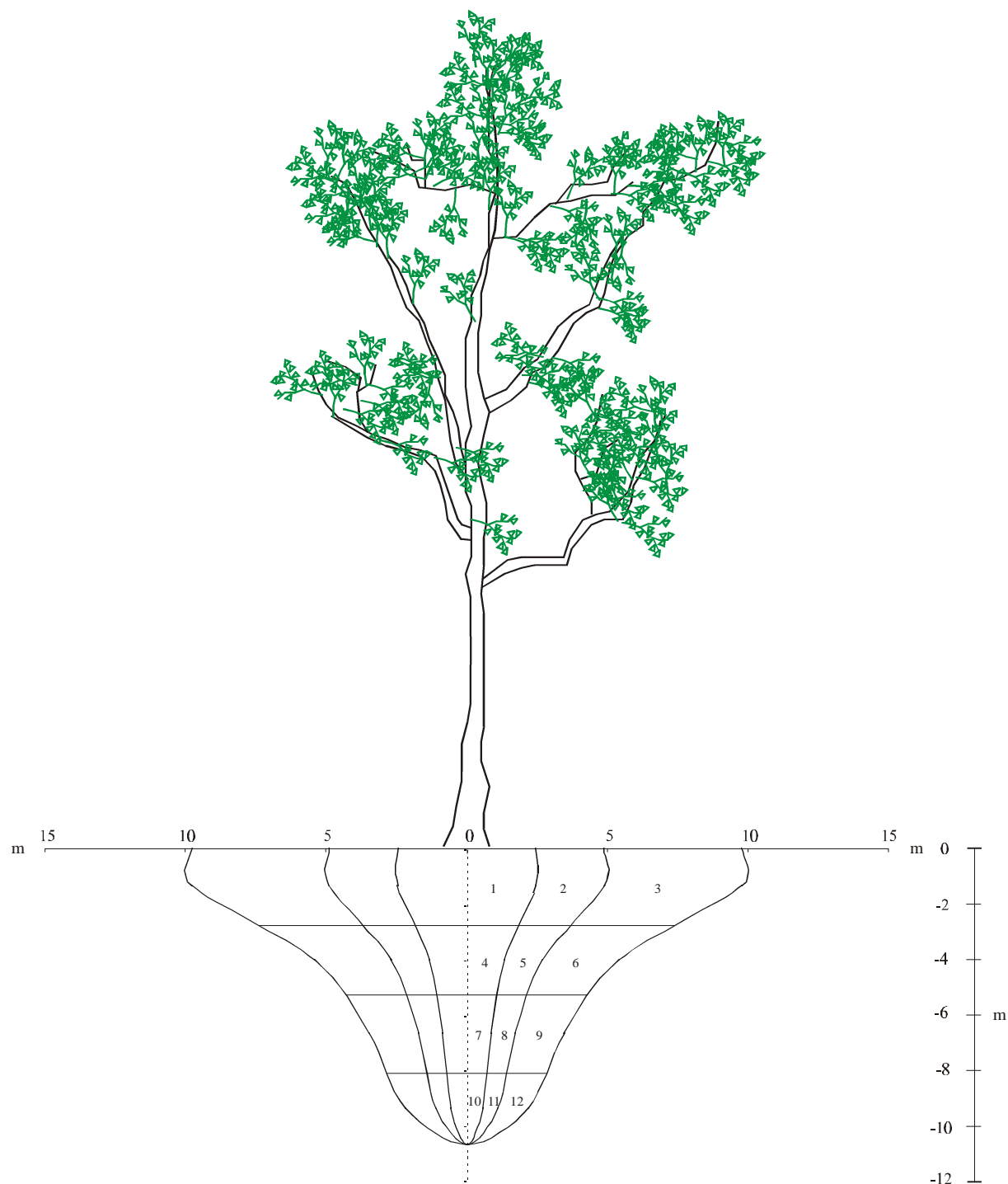
Figure 3.23: The spatial root distribution by soil zone beneath a mature *E. amplifolia* tree. Soil zones are numbered with the value of RAR within each zone presented in the table below. Above-ground illustration is for scale (30 m tall tree).

Table 3.4: Values of RAR for each soil zone below a mature *E. amplifolia* tree as represented in Figure 3.23.

	RAR (%)		*RAR (%)*
Zone 1	0.989	**Zone 7**	0.340
Zone 2	0.116	**Zone 8**	0.071
Zone 3	0.013	**Zone 9**	0.017
Zone 4	0.638	**Zone 10**	0.166
Zone 5	0.062	**Zone 11**	0.055
Zone 6	0.005	**Zone 12**	0.028
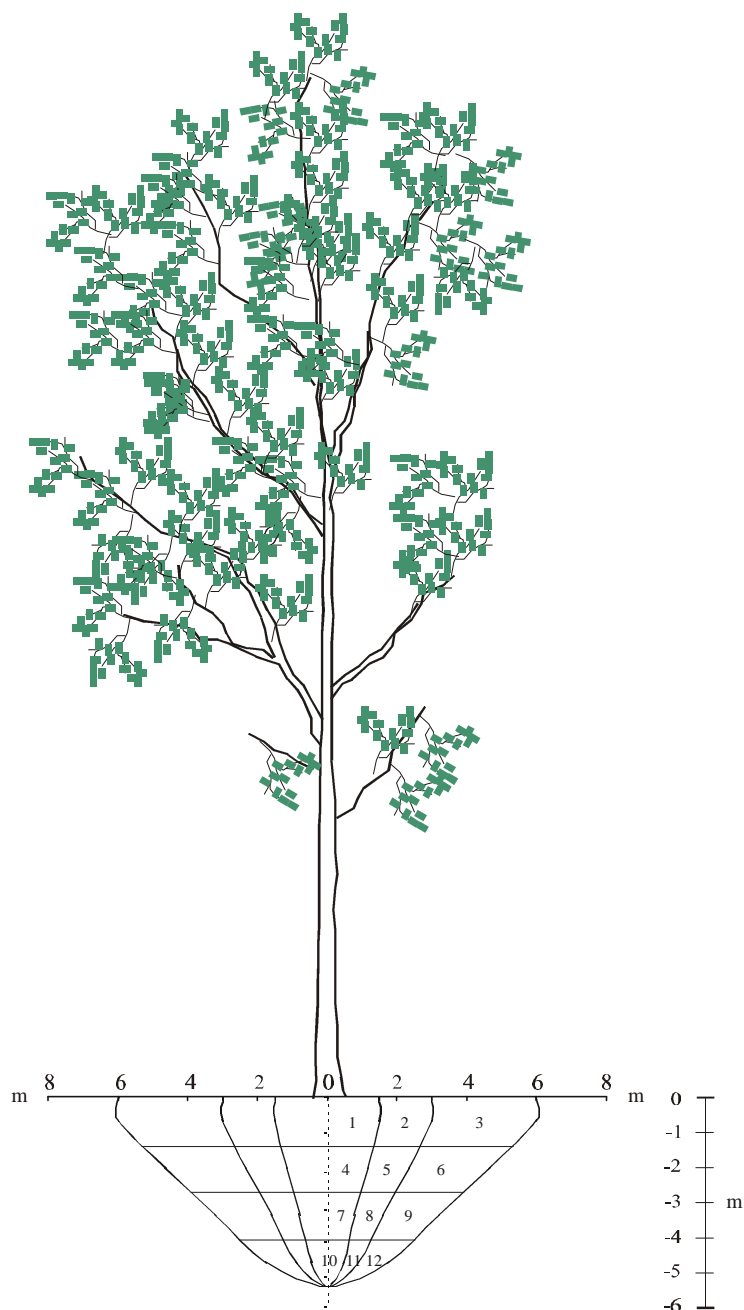
Figure 3.24: The spatial root distribution by soil zone beneath a mature *E. elata* tree. Soil zones are numbered with the value of RAR within each zone presented in the table below. Above-ground illustration is for scale (30 m tall tree).

Table 3.5: Values of RAR for each soil zone below a mature *E. elata* tree as represented in Figure 3.24.

	RAR (%)		RAR (%)
Zone 1	4.464	Zone 7	0.203
Zone 2	0.388	Zone 8	0.051
Zone 3	0.029	Zone 9	0.016
Zone 4	1.192	Zone 10	0.088
Zone 5	0.106	Zone 11	0.026
Zone 6	0.008	Zone 12	0.011

3.7   Conclusions

The entire root systems of 24 juvenile trees of the four species under investigation were removed from the soil and their root system architecture examined. Relationships were obtained from root area measurements to estimate the quantity of root material both with depth below the ground surface and with lateral distance from the tree stem. These relationships were incorporated with observations of the naturally exposed root systems of mature trees within the study area to construct a model of root distribution in the soil beneath different sized trees of each of the four species. The model can be used to estimate root area ratios within the alluvial soils of vegetated riverbanks. The following conclusions are drawn from this chapter:

1. Of the species investigated in this study *E. amplifolia* has the most distinctive root morphology. Its root system consists of a small number of very large roots that grow either laterally in the upper soil or vertically in a concentration directly below the tree stem.
2. A rapid reduction in root material both with depth below the soil surface and with lateral distance from the tree stem was observed in all species. This reduction can be approximated by the mathematical relationships described by equations [3.1]-[3.8] for the vertical direction and the equations in Appendix A-III for the lateral direction.
3. The vertical root distribution of each species studied can be divided into two zones:
    a)   An upper zone from between approximately 0 % to 15 % of the maximum vertical root depth that consists of approximately 80 % of the total quantity of root material and is characterised by numerous intermingled roots that grow in all directions; and
    b)   A lower zone from 15 % to 100 % of the maximum vertical root depth with roots that grow predominantly in the vertical direction and are concentrated directly below the tree stem.
4. Each species exhibited a reduction in lateral root extent with depth. This is expected as it is observed that the deepest roots of each species are located close to a vertical line projected directly beneath the tree stem. The reduction with depth can be estimated using the relationships described by equations [3.9]-[3.12].
5. Observations of the partially exposed root systems of mature trees within the study area suggest that the overall architecture is similar to the excavated juveniles. Maximum root system depths are considerably greater in this environment than have been reported for other studies investigating the root reinforcement of soil and it is expected that around half of the tree-height to root-system-depth ratio measured for juveniles is a conservative estimate for mature trees in this environment.
6. The earth reinforcement potential in terms of both geometric extent and the quantity of root material expressed as the Root Area Ratio varies significantly from species to species. *E. elata* exhibits the greatest values of Root Area Ratio in soil zones beneath it while *E. amplifolia* reinforces a greater volume of soil than any of the other species examined.

Chapter Four

Individual root strength and pull-out resistance

4.1   Introduction and overview

The ability of a tree to reinforce soil relies not only on its overall root structure but also on the strength of its individual root fibres. This is usually measured as the root tensile strength, T_r, and is a major component of the simple model of soil-root interaction first proposed by Waldron (1977) and Wu *et al.* (1979). The increased soil shear strength is accounted for by determining T_r and the root area ratio on a potential shear surface (equations [2.8] & [2.9]). Application of this approach with different tree species in a wide range of environments has yielded results that correspond quite well to field observations (Riestenberg & Sovonick-Dunford, 1983; Greenway, 1987; Shields & Gray, 1992).

The Wu/Waldron model assumes that each root across a shear plane will fail in tension at the same time (i.e. at some given displacement of the sliding soil mass). In many cases this scenario does not eventuate (Greenway, 1987), particularly in a thick soil layer where root deformation occurs in a wide shear zone (Wu & Watson, 1998). Indeed Riestenberg (1994) re-examined her earlier work in light of more recent observations and concluded that root pull-out resistance is mobilised gradually and that roots fail in tension at different amounts of displacement, depending on their individual morphology. She also found, as suggested by Waldron & Dakessian (1981), that the root pull-out resistance and therefore the strength of the soil-root bond was a more important measure of the strength of soil-root interaction than the tensile strength of the root itself. Abernethy & Rutherfurd (2001) however, found no statistical difference between values of root pull-out resistance and the force required to induce tensile failure in roots of the same diameter. Hence it can be inferred that the behaviour varies and needs to be assessed for the specific environment and tree species under investigation. This chapter investigates the tensile strength and pull-out resistance of individual roots from four riparian tree species common to the study area and the banks of other southeastern Australia streams: *Casuarina glauca*, *Eucalyptus amplifolia*, *Eucalyptus elata*, and *Acacia floribunda*.

4.2   Apparatus and method

Root pull-out and tensile strength tests were conducted on individual roots growing beneath the plantation within the study area (Fig. 1.3). Forty-five pull-out and thirty tensile strength tests were conducted on roots of each of the four species investigated in this study. Tests were conducted in June and July 2001.

4.2.1   Individual root pull-out resistance

The pull-out resistance of individual roots of the four species was measured by the process illustrated in Figure 4.1. First it was necessary to expose the ends of broken roots at a trench face. To do this the above-ground portion of the tree was removed and a trench dug around the base of

the stem. The main part of the root ball and the soil surrounding it were then removed to leave a small rectangular pit with free root ends protruding from both its floor and sides. The pit was repeatedly filled with water over a period of days preceding the tests in order to saturate as much as possible the surrounding soil, thereby simulating conditions of natural riverbank failure. When the free head of water had disappeared the pull-out apparatus was lowered into place over the test pit.

1. Trees grown in plantation for up to 27 months

2. Above ground portion of tree removed and trench cut around root ball

3. Root ball and surrounding soil removed to create pit with free root ends protruding

4. Pit filled with water over a period of days preceding the tests in order to saturate the surrounding soil mass

5. Apparatus placed in position with free root end clamped and attached to apparatus by a metal chain

6. Hydraulic pressure applied by hand pump to lift roots from the soil. Resistance is measured by load cells and transmitted to data logger

Figure 4.1: Methodological steps undertaken to measure the pull-out resistance of individual roots present beneath the plantation in the study area.

The pull-out apparatus was the same as used for direct in-situ shear tests (chapter five) with some slight modifications. The entire mechanism was turned on its end so that the reaction plate was lying flat with its ends on the level ground at each side of the pit (Fig. 4.2a). A metal hook was bolted to the plywood of the pushing plate and a chain attached at one end. The chain was connected at its opposite end to a nylon cable puller by a series of U-bolts. And the nylon cable puller in turn

connected to the free end of a root exposed within the pit. Appropriately sized cable pullers were attached to different sized roots although for larger roots it was often necessary to use two, one inside the other. The bias weave of the cable puller allowed for tight holding with little damage to the root although in most cases it was necessary to reinforce the grip with a series of U-bolts around the root end (Fig. 4.2b).

(a)

(b)
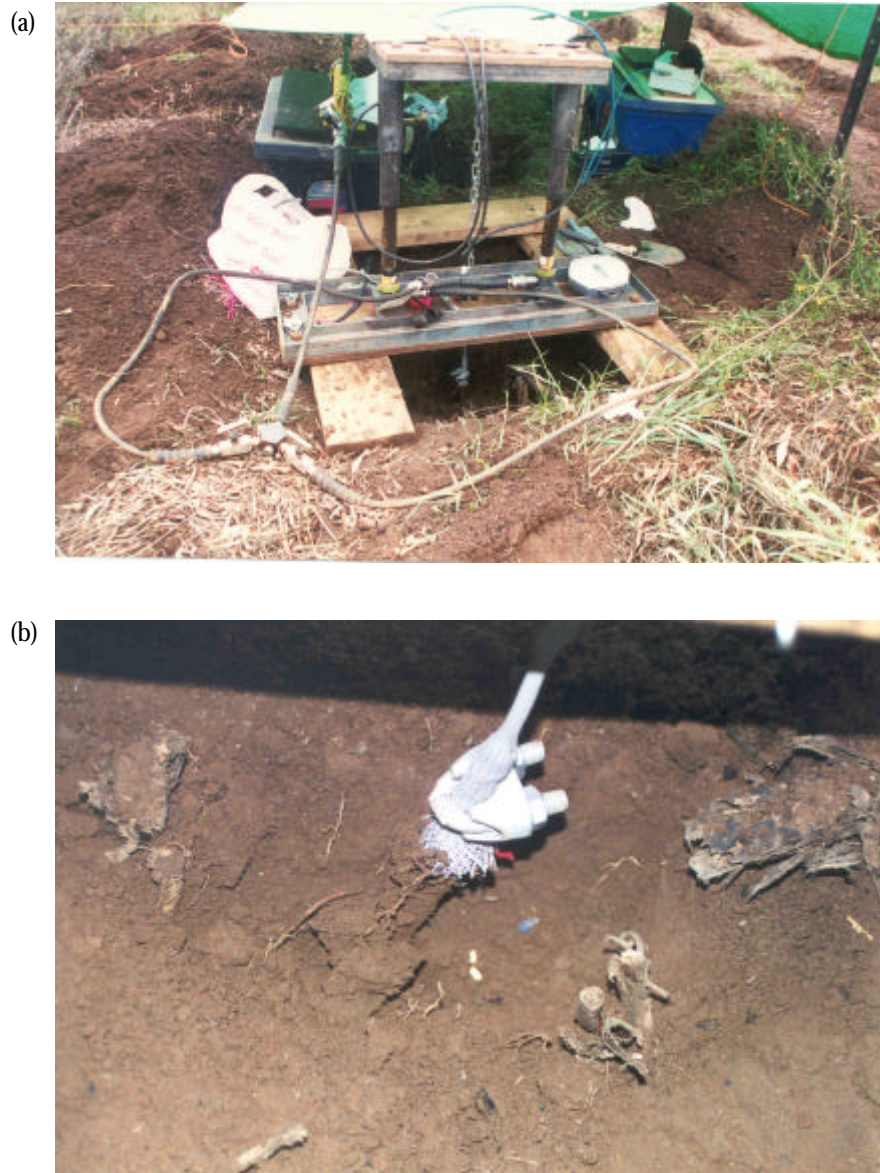
Figure 4.2: (a) Pull-out apparatus in place over a test pit ready for testing as in step 5 from Figure 4.1. (b) Nylon cable puller with U-bolt attached to the free end of a root inside a test pit.

The chain was connected from the pushing plate to the root end through an opening cut in the centre of the reaction plate so that force was applied in the vertical direction. Force was applied by pumping hydraulic fluid into the cylinders fitted between the two plywood plates of the apparatus. The root resisted this force through its tensile strength and the frictional bond with the soil, and the resistance was measured by two load cells positioned between the hydraulic cylinders and the pushing plate.

Tests were run at a constant rate of approximately 2 mm/min until the root failed and was pulled from the surrounding soil. Upon removal its diameter at ground level, its length, and the diameters of all broken ends were recorded. Sketches of root morphology were also conducted at this time. The modification of the direct in-situ shear apparatus was found to be very effective at pulling small roots (< 15 mm in diameter) from the soil and recording the force required to do so. For roots larger than about 15 mm in diameter it was difficult to grip the root-end effectively and slippage of the cable pullers often occurred. This is known to be a common problem in experiments of this nature (see Greenway, 1987; Nilaweera & Nutalaya, 1999), which therefore only allow the testing of small diameter roots.

4.2.2   Individual root tensile strengths

The tensile strengths of individual roots were determined using the same apparatus used for pull-out tests with some minor modifications. In this case the two free ends of an excavated root were clamped using nylon cable pullers and U-bolts that were attached to both plates of the apparatus by a small chain and hook. The application of a tensile force through the hydraulic cylinders caused an axial strain in the root until failure occurred, usually in a sudden and violent manner.

Roots to be tested were collected by carefully excavating them from the soil beneath particular trees. They were then sealed in air-lock plastic bags to keep them fresh and transported to the laboratory for testing. The roots collected were generally straight segments of between 15 and 20 cm in length and the maximum root diameter that could be tested was approximately 10 mm. This is less than the 15 mm achievable in field pull-out tests as a result of two clamps being used rather than one and therefore two points of weakness. Various techniques, including the introduction of an epoxy resin between the clamp and the root were tested in an attempt to measure the tensile strength of larger roots, however none were successful due to the smooth root surface of the root without its bark. The tensile strength of a root, T_r, is calculated as a measure of the force, F, required to induce failure of the root divided by its cross-sectional area, a_r: $T_r = F/a_r$.

4.3   Individual root strength results

In-situ root pull-out tests presented fairly consistent behaviour both within and between species. Initially there was a rapid increase in the tensile resistance with minimal displacement of the root, followed by a more gradual increase as the root started to distort and move. After reaching a peak resistance there was usually a sudden drop in the force being measured and then a more gradual reduction as the root pulled free from the soil. In some cases there were a series of peaks corresponding to different root branches breaking and so the overall shape of the load-displacement plots was very much influenced by the individual morphology of the root being pulled. Roots with a high branching nature, such as those of *C. glauca* and *A. floribunda* exhibited plots with multiple

peaks as different branches failed at different displacements (Fig. 4.3a) while the relatively low branching roots of *E. amplifolia* and *E. elata* were more likely to exhibit plots with fewer peaks (Fig. 4.3b). Similar observations have been reported by Riestenberg (1994) on *Acer saccharum* (Sugar Maple) and *Fraxinus americana* (White ash) roots, and Abernethy & Rutherfurd (2001) on *Eucalyptus camaldulensis* (River Red Gum) and *Melaleuca ericifolia* (Swamp Paperbark) roots.
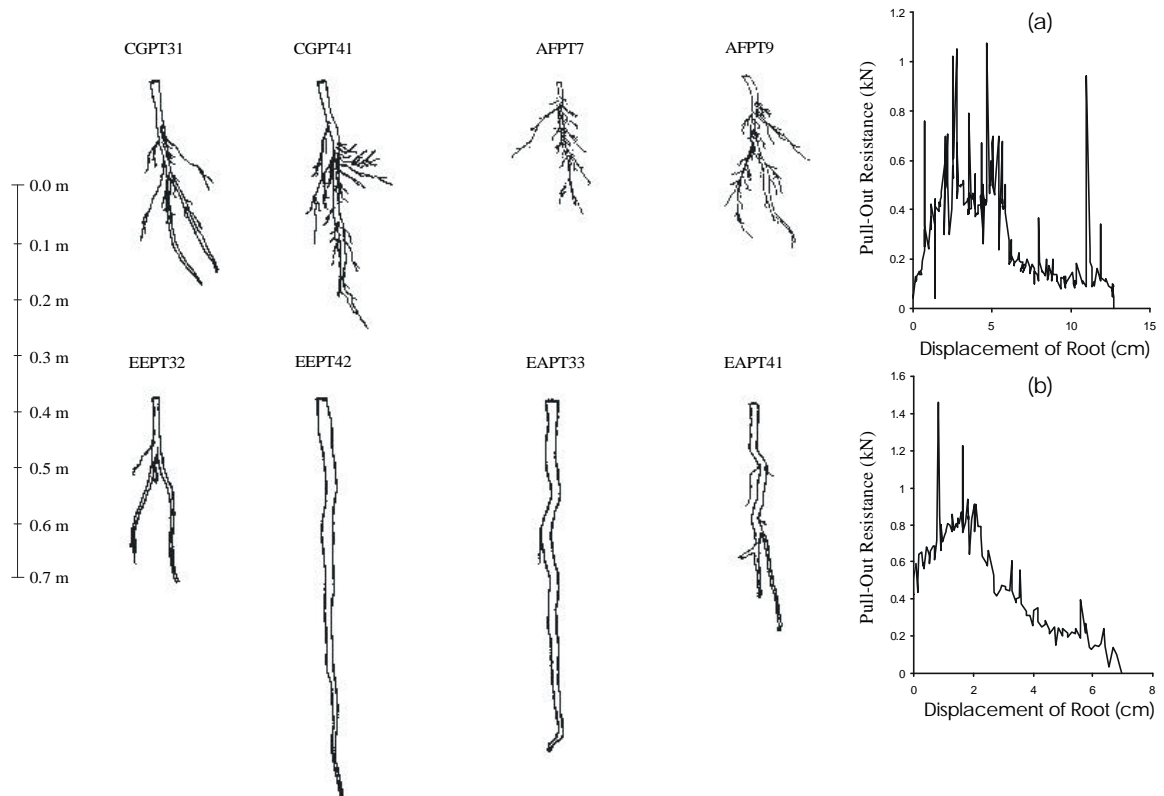
Figure 4.3: Differences in individual root morphologies for each species and typical load versus displacement plots. The highly branched and fine root natures of *C. glauca* and *A. floribunda* are in contrast to the large roots of *E. amplifolia* and *E. elata* that exhibit few branches. The multiple peaks shown in the load-displacement plot (a) correspond to the multiple root failures required to pull the AFPT9 root from the soil. In (b) the EAPT41 root has fewer peaks due to the fewer root failure points necessary to pull the root from the soil

Test results are presented as plots of root diameter versus peak resistance in figure 4.4. The results of root pull-out tests are plotted with the root diameter at both the ground surface and at the broken end of the root, while the results of tension tests are plotted with the root diameter at the point of rupture. In both test types, tension and pull-out, there is an increasing peak resistance with increasing root diameter for all species.
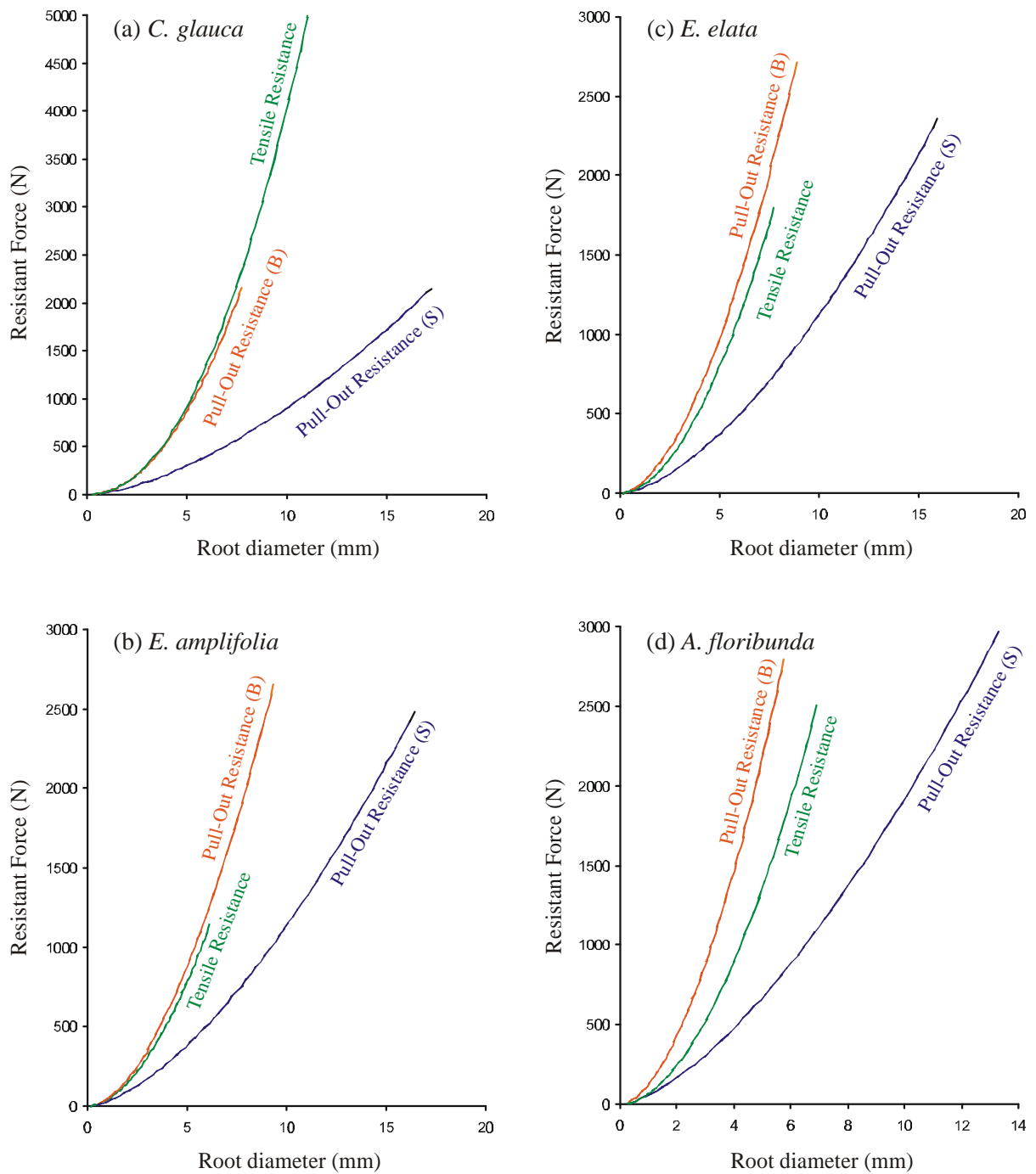
Figure 4.4: Tensile resistance versus root diameter curves for both pull-out tests and tensile tests of each tree species. The pull-out resistance is determined as a function of both the root diameter at the surface (S) and of the root diameter at the broken end (B). As expected the root diameter at the broken end is considerably smaller that at the ground surface for all species. (a) *C. glauca*; (b) *E. amplifolia*; (c) *E. elata*; (d) *A. floribunda*. Individual data points are presented in Appendices B-I and B-II.

In pull-out tests the diameters of the roots at the broken end were significantly smaller than the diameters at the ground surface. This was because tensile failure occurred at a depth below the ground surface where the root diameter had been reduced by taper and branching. The larger the root the larger this difference. The effect is visible in Figure 4.4 where for equivalent diameters at the ground surface and at the broken end the plotted relationships give markedly different values of

peak pull-out resistance for all species. The relationship between pull-out resistance as determined by the diameter at the broken end of the root is much closer to the relationship for tension tests where the diameter is also measured at the point of rupture. It is expected that the difference between these two relationships results from the effect of the soil-root bond however an analysis of variance suggests that it is insignificant for three of the species: P = 0.22, 0.29, and 0.14 for *C. glauca*, *E. amplifolia*, and *E. elata* respectively. For *A. floribunda* P < 0.001, suggesting that the difference due to test method between tension tests and pull-out tests where resistance is measured as a function of the diameter at the broken end of the root, is highly significant. Therefore the bond between the root and the soil is greater for *A. floribunda* than for the other three species.

A comparison of root pull-out tests between species indicates that *A. floribunda* requires the greatest force to induce failure, followed by *E. amplifolia* and *E. elata*, and then *C. glauca* (Fig. 4.5). The magnitude of this difference increases with increasing root diameter due to the positive power curves that describe the relationship between root diameter at the ground surface and pull-out resistance for each species.
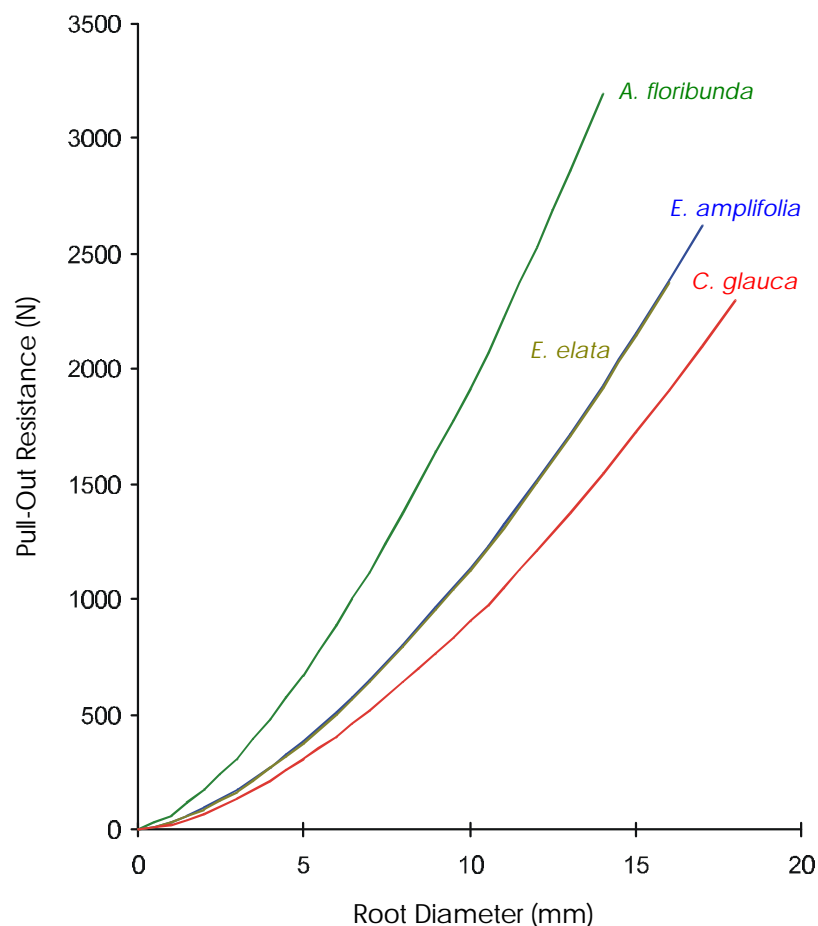
Figure 4.5: A comparison of root pull-out resistance between the four tree species. The root diameter plotted is that measured at the ground surface.

The pull-out resistance, F_{po}, as a measure of the root diameter at the ground surface, d_s, can be estimated using the following relationships (obtained from Fig. 4.5):

C. glauca	$F_{po} = 23.31.d_s^{1.589}$	$R^2 = 0.90$	[4.1]
E. amplifolia	$F_{po} = 30.59.d_s^{1.5705}$	$R^2 = 0.92$	[4.2]
E. elata	$F_{po} = 29.03.d_s^{1.5883}$	$R^2 = 0.93$	[4.3]
A. floribunda	$F_{po} = 58.40.d_s^{1.5169}$	$R^2 = 0.86$	[4.4]

Using these relationship for the range of root sizes tested, *E. amplifolia* and *E. elata* require on average a load 26 % greater than *C. glauca* to induce tensile failure, while *A. floribunda* requires a load 78 % greater than the two Eucalypt species. These differences in pull-out resistance result from a combination of root tensile strength, skin friction between the root and the soil, and individual root morphology. Ultimately these factors determine the amount of shear resistance that individual roots can provide to the soil.

The tensile resistance as determined by tension tests also describes a positive power relationship when plotted against root diameter (Fig. 4.6). As with pull-out tests, *A. floribunda* requires the greatest force to induce tensile failure, followed by *E. elata*, *E. amplifolia*, and *C. glauca*.
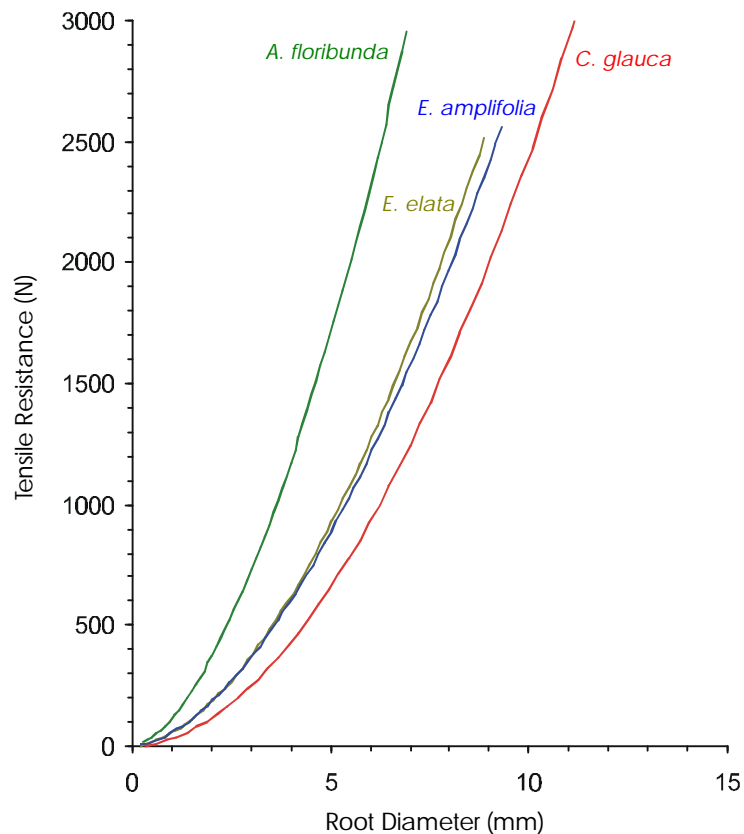
Figure 4.6: A comparison of root tensile resistance between the four tree species. The root diameter plotted is that measured at the point of rupture.

The tensile resistance, F_t, as a measure of the root diameter at the point of rupture, d_b, can be estimated using the following relationships (obtained from Fig. 4.6):

C. glauca	$F_t = 30.02.d_b^{2.128}$	$R^2 = 0.94$	[4.5]
E. amplifolia	$F_t = 41.35.d_b^{1.829}$	$R^2 = 0.85$	[4.6]
E. elata	$F_t = 39.83.d_b^{1.8624}$	$R^2 = 0.88$	[4.7]
A. floribunda	$F_t = 67.03.d_b^{1.8709}$	$R^2 = 0.93$	[4.8]

Plotting the depth of root failure against the root diameter at the ground surface and regressing the relationship between these two parameters (Fig. 4.7) indicates that the greater the force required to induce tensile failure in the roots the greater the soil depth at which roots will most likely fail during pull-out tests. Therefore *A. floribunda* roots will fail at generally greater depths than *E. amplifolia* and *E. elata* roots, which in turn will fail at greater depths than *C. glauca* roots (Fig. 4.7). This is because a greater pull-out resistance forces the point of tensile rupture deeper into the soil where the diameter of the root and therefore tensile resistance is less (equations 4.5-4.8). This is also the reason why larger roots of the same species, as measured by their diameter at the ground surface generally fail at greater depths below the soil surface (Fig. 4.7). The greater force required to pull them from the surrounding soil results in the point of tensile rupture being forced deeper below the surface.
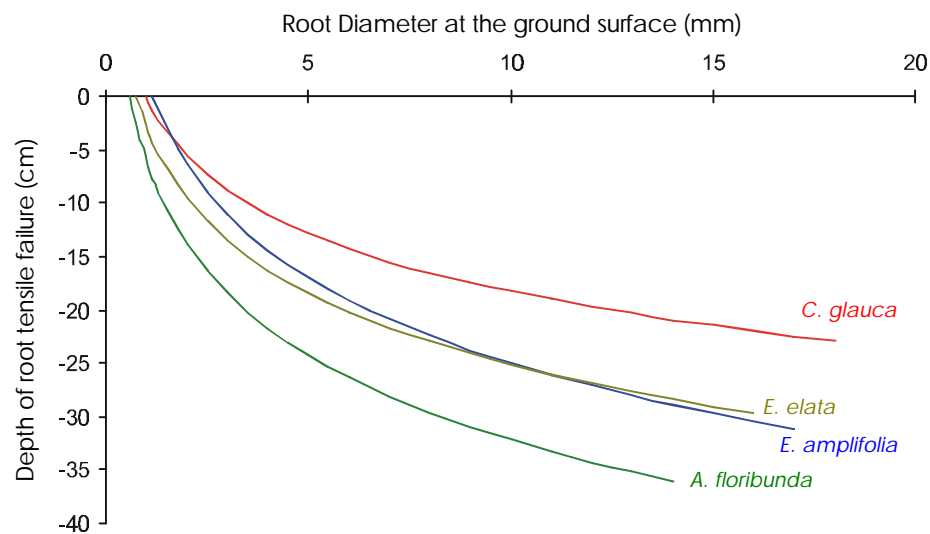
Figure 4.7: Relationship between root diameter at the surface and the depth of likely tensile failure of the root. Individual data points are presented in Appendix B-III.

The tensile strength of a root is a measure of the force required to induce tensile failure divided by the cross-sectional area of the root. This calculation was made for both pull-out tests and tension tests and is summarised for each species in Table 4.1. The mean root tensile strength calculated from tension tests is significantly greater than that calculated from pull-out tests. This is expected given the above results where the force required to induce failure in pull-out tests is significantly less than that required to induce tensile failure in laboratory tension tests. Table 4.1 also indicates the differences in root strength between different species. *A. floribunda* clearly exhibits the greatest root tensile strengths followed by *E. elata, E. amplifolia*, and then *C. glauca. A. floribunda* roots are close to twice as strong as *C. glauca* roots by both test measurements.

Table 4.1: Summary of results from individual root strength tests. The full data set appears in Appendices B-IV to BIX.

Species	Test	Root Diameter[1] (mm)			Root Strength[2] (MPa)		
		Min	Max	Mean	Min	Max	Mean
C. glauca	Pull-Out	0.56	17.23	4.49	3.34	81.68	22.43
	Tension	0.36	10.52	3.74	16.78	136.79	49.59
E. amplifolia	Pull-Out	0.45	16.43	5.00	8.88	130.65	27.33
	Tension	0.23	6.15	2.56	11.79	118.03	55.39
E. elata	Pull-Out	0.21	15.93	4.85	8.57	198.06	31.49
	Tension	0.21	7.73	2.95	15.69	198.06	56.74
A. floribunda	Pull-Out	0.31	13.33	4.09	11.19	217.89	58.09
	Tension	0.29	6.93	3.04	29.88	190.15	85.14

[1] Root diameter is measured at the ground surface for pull-out tests and at the point of rupture for tension tests.

[2] Root strength is calculated as the force required to induce root failure divided by the cross-sectional area of the root.

It is also apparent from these results that the tensile strength of a root is dependent on its diameter. An analysis of correlation between root diameter at the surface and the $\log_{10}$ transformed root strength data obtained from pull-out tests gave correlation coefficients: r = -0.56 for *C. glauca*, -0.69 for *E. amplifolia*, -0.60 for *E. elata*, and -0.75 for *A. floribunda*, indicating that root tensile strength determined from pull-out tests decreases with increasing root diameter. This finding is consistent with Nilaweera & Nutalaya (1999) who tested several tropical hardwood species, and Abernethy & Rutherfurd (2001) who tested two species of Australian riparian tree. Regressing the root tensile strength obtained from field pull-out tests, T_r, with root diameter at the ground surface, d_s, yields:

$$C.\ glauca \qquad T_r = 29.67.d_s^{-0.411} \qquad R^2 = 0.31 \qquad [4.9]$$

$$E.\ amplifolia \qquad T_r = 38.95.d_s^{-0.430} \qquad R^2 = 0.45 \qquad [4.10]$$

$$E.\ elata \qquad T_r = 36.96.d_s^{-0.412} \qquad R^2 = 0.47 \qquad [4.11]$$

$$A.\ floribunda \qquad T_r = 74.36.d_s^{-0.483} \qquad R^2 = 0.38 \qquad [4.12]$$

Previous investigations (Nilaweera & Nutalaya, 1999; Abernethy & Rutherfurd, 2001) describe similar relationships between T_r and d, and when plotted with the results of this study (Fig. 4.8) give values within the same order of magnitude for the range of root diameters tested. *A. floribunda* is at the upper limit. It should be pointed out however that Nilaweera & Nutalaya's (1999) data was obtained using laboratory tension tests while Abernethy & Rutherfurd's (2001) data was obtained using both field pull-out and laboratory tension tests. In contrast to this study Abernethy & Rutherfurd (2001) found no statistical difference between the results of the two test methods.
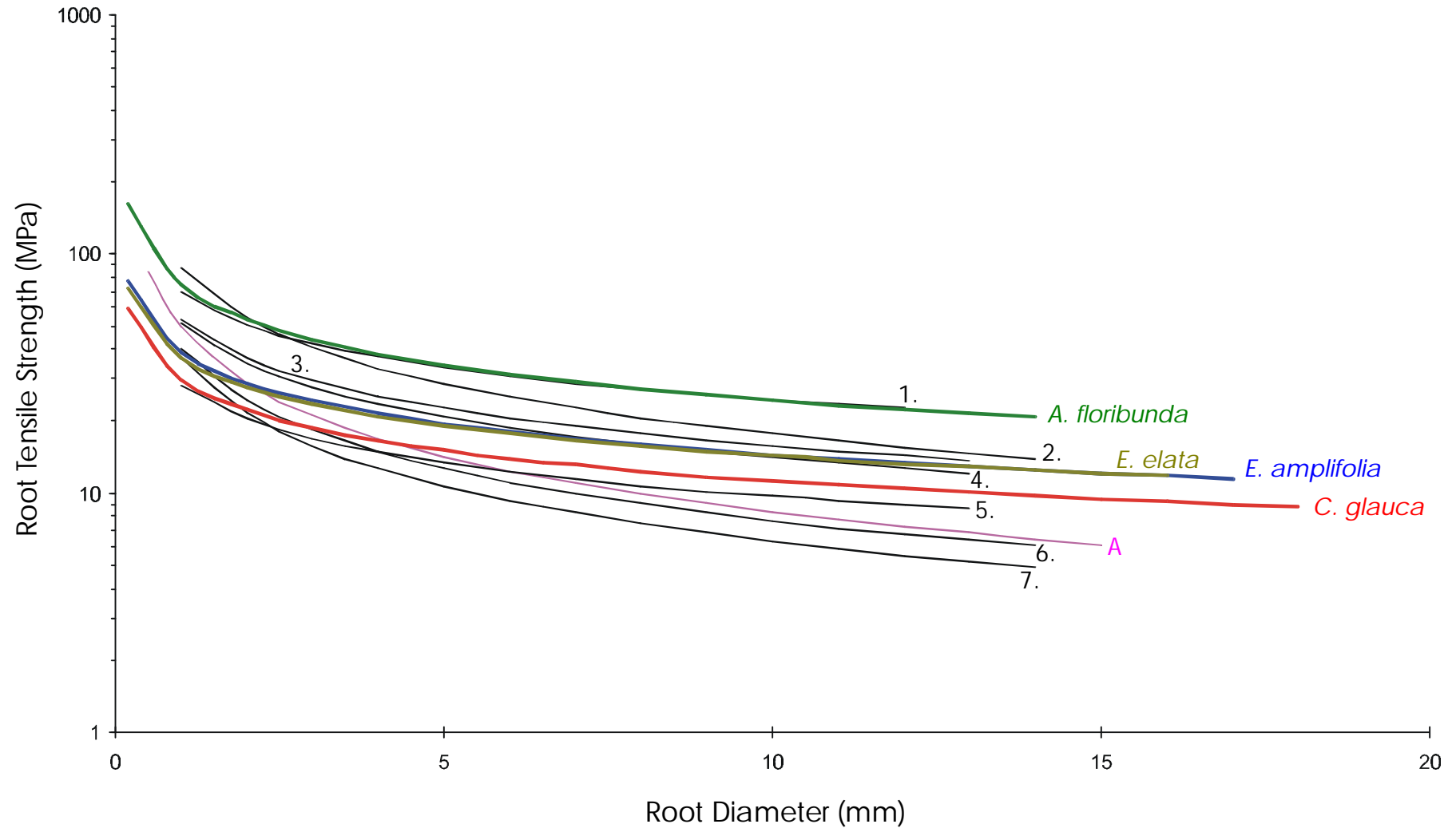
Figure 4.8: Root tensile strength curves plotted against root diameter. For the four species examined in this study the values have been obtained using the root pull-out resistance divided by the cross-sectional area of the root at the ground surface. Relationships obtained for previous studies are based on the root tensile strengths obtained during laboratory tension tests. Line A is from Abernethy & Rutherfurd (2001): *Eucalyptus camaldulensis* and *Melaleuca ericifolia*; No. 1-6 from Nilaweera & Nutalaya (1999): 1 = *Dipterocarpus alatus*; 2 = *Hopea odorata*; 3 = *Alangium kurzil*; 4 = *Hibiscus macrophyluus*; 5 = *Alsonia macrophylla*; 6 = *Ficus benjamina*; 7 = *Hevea brasiliensis*.

4.4   Discussion

The strength of a tree's roots is a critical factor in determining that tree's contribution to soil strength and therefore slope stability. As this strength has been found to be a function of root diameter both in this study and elsewhere, it is possible to determine the increased shear resistance from the size and number of roots that cross a potential shear plane. This is the basis of Waldron's (1977) and Wu *et al.*'s (1979) simple root model. However the model assumes that the full tensile strength of the root is mobilised during failure. Clearly this assertion depends on the point along the root at which the full tensile strength is determined, because the diameter of an individual root often decreases rapidly with increasing depth (Kozlowski, 1971). It has been observed in this study that tensile failure during field pull-out tests occurs at a depth below the ground surface where the root diameter is smaller and requires a smaller force to induce rupture than that required to break a root of the diameter present at the surface (Fig. 4.9).
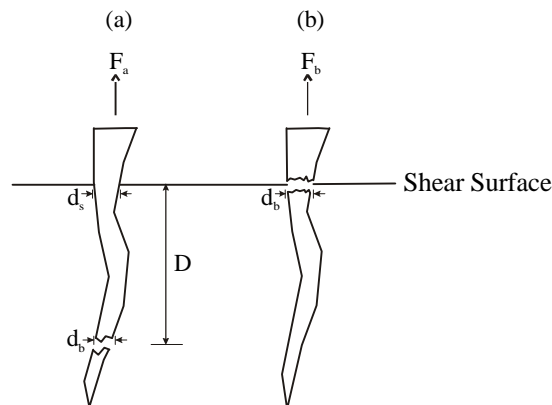
Figure 4.9: Failure of individual roots in a thick soil layer. With application of sufficient force F, tensile failure of the root in (a) occurs at a distance D below the shear plane. Tensile failure of the root in (b) occurs at the shear plane. Although both roots measure the same diameter at the shear plane, the tensile resistance of the root in (a) is significantly less than the root in (b) due to the smaller diameter at which it fails. That is, taper or branching of the root leads to $d_b < d_s$. Due to this discrepancy a knowledge of the likely failure point is essential for the determination of tensile resistance using tensile strength and root area ratio calculations.

Riestenberg (1994) also observed in her investigations that many roots pulled out of the materials underlying the shear surface and therefore failed at less than their full tensile strength. This is not to say that the entire root pulled from the soil intact. As with the roots in this study, tensile failure did occur, but at a displacement below the ground surface where the root diameter and therefore force required to induce failure was significantly lower than at the surface. In these circumstances a calculation of additional soil shear resistance based on the diameters of roots present at the shear plane, and their tensile strength, will potentially overestimate the root reinforcement at that point within the soil. For example a 10 mm root of the species *C. glauca* will require a load of approximately 900 N to pull it from the soil however the measured tensile resistance of a root of this size in tension tests is more than four times this value at approximately 4 kN (Fig. 4.4).

When measured by the root diameter at the broken end the pull-out resistance is very similar to that obtained in tension tests for three of the species tested (Fig. 4.4). Therefore if the diameter of the root at the point of tensile failure could be predicted, using the tensile strength obtained in tension tests to calculate the increased soil shear strength should give a reasonable estimate. This diameter however is expected to be very much dependent on the individual root morphology beyond the shear plane and to predict it would require detailed knowledge of this morphology for every root that crossed a potential shear plane. It is much simpler to determine the strength of the soil-root interaction in this environment from the root diameter at the shear plane. As demonstrated, the relationship between pull-out resistance and this diameter is obtained from field pull-out tests.

Different species exhibit different soil-root strengths that are largely influenced by the tensile strength of the root itself. Therefore *A. floribunda*, with the greatest mean tensile strength (Table 4.1) also has the greatest pull-out strength. In the case of *A. floribunda* the soil-root bond is also perhaps important, as a greater tensile strength and more branched morphology (Fig. 4.3) causes the likely root failure point to be forced deeper within the soil (Fig. 4.7), thereby increasing the overall friction between the root and the soil. *C. glauca* also has quite a highly branched morphology (Fig. 4.3) however its relatively small tensile strength (Table 4.1) results in root failure closer to the surface (Fig. 4.7) and therefore a smaller pull-out resistance and overall soil-root strength.

4.5   Conclusions

Root pull-out and tension tests were conducted on individual roots of four riparian species native to Australia. The strength of soil-root interaction for roots of the four species is determined from these experiments. In combination with root architectural studies and the use of the simple root model of Waldron (1977) and Wu *et al.* (1979) this is the most common method of assessment of the earth reinforcing potential of trees. The following conclusions are drawn from this chapter:

1.   Root strength is a function of root diameter. The force required to induce tensile failure in a root increases with increasing root diameter.
2.   Tree roots generally fail in tension at a distance below the ground surface and then pull-out of the soil. This occurs because the diameter of the root decreases with depth into the soil, resulting in a decreased tensile resistance. The assumption that roots break in tension as a measure of the full tensile strength at the shear plane is not applicable to roots growing in this environment therefore the pull-out resistance of a given root is best estimated from the root diameter at the shear surface and the results of field pull-out tests using the equations [4.1] to [4.4] for each species.
3.   Inter-species differences in root pull-out resistance are most likely the result of different individual root morphologies in combination with the tensile strength of the roots themselves.

4.   Inter-species differences in the depth below the shear plane at which root failure occurs are the result of differences in root tensile strength and the soil-root bond. For the depths observed in this study the soil root bond was insignificant for all species except *A. floribunda*. The depth at which a root fails in tension is also a function of root diameter at the shear surface.

5.   The tensile strengths of the soil-root interaction obtained for different species in this study are within the range of the previous investigations reported. Tensile strength describes a negative power relationship with increasing diameter and can be estimated using the equations [4.9]-[4.12] for each species. Of the species examined in this study *A. floribunda* roots exhibit the greatest root tensile strengths, followed by *E. elata* and *E. amplifolia*, and then *C. glauca*.

Chapter Five

Shear resistance of root-reinforced soil

5.1   Introduction

The theory of reinforced earth allows for inclusive fibres to enhance the shear strength of a soil mass through an increase in the apparent cohesion of the soil (chapter 2). Measurement of the shear strength of root-reinforced soils is commonly undertaken using direct in-situ shear tests. This method induces a failure plane to form at a pre-determined location and through the simulation of the actual failure process gives a realistic assessment of the increased shear resistance generated beneath and by trees. Results for the soil-root matrix are compared to soil-only tests to determine the proportion of soil resistance provided by the roots.

In-situ shear tests provide an opportunity to measure and observe the shear resistance of a number of roots under natural growth conditions. This chapter examines the failure of root-reinforced soil using the results of direct in-situ shear tests conducted for four different riparian tree species. Measured values of increased shear resistance are also compared to shear resistance values calculated using the root pull-out data from the previous chapter and Waldron's (1977) and Wu *et al.*'s (1979) simple root model.

5.2   Apparatus and method

The additional soil shear strength provided by the roots of four riparian tree species was determined using direct in-situ shear tests. These tests, which replicate Coulomb's shear-box method (see Lambe & Whitman, 1979) were undertaken on blocks of soil containing the roots of juvenile trees (Fig. 5.1). The trees had been growing on site for a period of between 16 and 27 months and ranged in height from 1.41 m to 5.34 m. Before testing the above ground portion of the tree was removed and a block of soil directly below the base of the tree stem was cut from the surrounding soil mass using flat-bladed spades. The dimensions of the soil blocks ranged in size from 0.4 m by 0.4 m to 0.5 m by 0.5 m at the base and 0.21 m to 0.44 m in height and contained either one, two or three trees.

Soil and soil-root blocks were saturated for 24 hours prior to testing by placing a purpose built marine-plywood box around the soil block and repeatedly filling it with water. To reduce lateral leakage the base of the box was dammed with a soil barrier, however the block was allowed to drain just prior to and during testing and was therefore in a partially saturated state at the time of shear. A metal form guide was strapped tightly around the block and sets of weights ranging between 0 kg and 470 kg were loaded onto the top of the block in order to generate a normal confining stress.

A shear apparatus was placed in the trench between the soil block and the greater soil mass (Fig. 5.1). The apparatus (Fig. 5.2) consisted of two reinforced plywood plates, one a pushing plate (0.3 m

x 0.5 m) and the other a reaction plate (0.3 m x 1.0 m). Attached to the reaction plate were two hydraulic cylinders of 5 ton capacity that fit neatly into the metal sleeves of the pushing plate to provide the shearing force. The pushing plate was strapped adjacent to the soil block and the block was induced to move by the application of hydraulic pressure to the cylinders using a hand pump at a constant rate. The pressure in the main hydraulic line was recorded against displacement of the block. Measurement of the block's resistance to shear was also recorded via two 5 kN load cells that were fitted inside the metal sleeves of the pushing plate in between the plate and the hydraulic cylinders. The output of these load cells was transmitted to a data logger that also recorded displacement with a string-pot distance-measuring device clamped to the reaction plate and with the string extended out to the pushing plate.

1. Trees grown in plantation for between 16 and 27 months

2. Above-ground tree removed and soil blocks cut from greater soil mass

3. Soil block saturated up to 24 hours prior to testing

4. Hydraulic apparatus lowered into trench and normal load applied to the block

5. Hydraulic pressure applied by hand pump to push soil block along pre-determined failure plane

6. At the completion of testing soil is removed from around the roots and the diameters of all roots crossing the shear plane are recorded

Figure 5.1: In-situ shear test methodology.

Figure 5.2: In-situ shear test apparatus in a trench between a soil block ready for testing and the greater soil mass. The pushing plate is strapped adjacent to the metal form guide that contains the soil block and normal load.

The shear force was applied at a constant rate of approximately 1.5 mm/min for around two hours. The length of time per test varied according to how far the block could be pushed without breaking up or tipping over. Displacements of between 100 mm and 200 mm were generally achieved. Upon completion of the test the soil block was broken up to reveal the roots present at the shear surface. The diameters of all roots crossing this plane were measured using callipers.

The results of a number of tests were discarded. The reasons for this were: 1) the block was found to be non-uniformly saturated at the conclusion of the test and blocks that contain dry patches are prone to generate large soil suctions and inconsistent shear resistance values; 2) the front of the block had not moved despite a large displacement at the rear, therefore soil movement was primarily in the normal direction causing destabilisation of the load; and 3) distortion of the soil block during testing, which resulted in misalignment of the shear apparatus. Experiments were conducted until data from twenty-five problem-free tests were collected for each species. For the total of 100 problem-free tests to be completed, 130 tests were conducted.

The purpose of in-situ shear testing is to determine the increase in soil shear strength attributable to the roots of each species. To this end the increase was determined by measuring the difference between the peak shear stress for each root-enhanced test and the peak shear stress for soil-only tests at the comparative normal stress. Therefore:

$$S_r = \tau_r - \tau_s \qquad\qquad [5.1]$$
$$S_r = t_r - [\sigma_r.\tan f_s + c_s]$$

Ph.D Thesis: Benjamin Docker

where S_r is the increased shear stress due to tree roots; τ_r is the measured peak shear stress for the test block containing tree roots; τ_s is the measured peak shear stress for the test block without roots; σ_r is the normal load on the test block containing tree roots; f_s is the internal friction angle of the soil; and c_s is the cohesion of the soil. Soil values c_s and f_s are those obtained from the total stress envelope of the direct in-situ shear tests undertaken on soil blocks without roots.

5.3   Shear resistance of soil without roots: the control experiment

The control experiment for in-situ shear testing consisted of exactly the same procedure as outlined in section 5.2 except that blocks of soil were root-free. This was achieved by cutting the blocks from the surrounding soil at locations well away from any tree growth. The absence of tree roots was confirmed at the conclusion of each test when the soil block was broken up to reveal the shear plane. Seven soil-only tests were conducted. The conditions and results of each test (the peak and final shear stresses) are presented in Appendix C-I and Table 5.1.

Seven different normal loads were applied within the range of 0 kg to 469.5 kg on blocks that varied in shear area from 0.2 m² to 0.25 m². The average shear depth was 0.33 m and the average moisture content during testing was 18.1 %, or 72 % saturation. During testing all samples behaved in a similar fashion (Appendix C-II). Initially there was a rapid increase in shear stress to a peak level, followed by a rapid reduction to a level that was near to the final or residual shear stress. On average this peak stress occurred at a displacement of 16 mm. Tests were continued to displacements of between 80 mm and 125 mm by which time there was usually little change in the shear resistance and samples were at or close to their residual strength values.

Table 5.1: Summary of experimental results for direct in-situ shear tests on soil-only blocks.

Sample No.	Shear Depth (m)	Shear Area (m²)	Peak/Final test displacement (mm)	Total Normal Stress (kPa)	Peak Shear Stress (kPa)	Final Shear Stress (kPa)
1	0.33	0.2500	11.5/100	14.18	16.90	14.88
2	0.44	0.2250	8/100	11.07	16.16	11.68
3	0.42	0.2500	18/101	13.37	15.89	14.54
4	0.30	0.2025	8/80	27.44	26.67	18.37
5	0.20	0.2500	14/81.5	20.17	24.96	18.58
6	0.30	0.2000	45.5/100	28.59	24.90	21.75
7	0.30	0.2209	10/125	5.56	13.04	8.28

The Mohr-Coulomb failure envelope plotted for the soil-only blocks yields soil strength values of c = 9.30 kPa and f = 31.4° for peak shear resistance and c = 6.74 kPa and f = 27.0° for residual shear resistance (Fig. 5.3). In comparison to the undisturbed laboratory tests on saturated, drained samples (Fig. 1.4) the peak failure envelope for in-situ tests exhibits a slightly larger apparent cohesion but a lower angle of internal friction. This is expected given that in-situ tests were undertaken rapidly on

partially saturated soils thus representing the total stress condition, while the laboratory tests allowed for the effective stress parameters to be obtained (see Lowe, 1967).
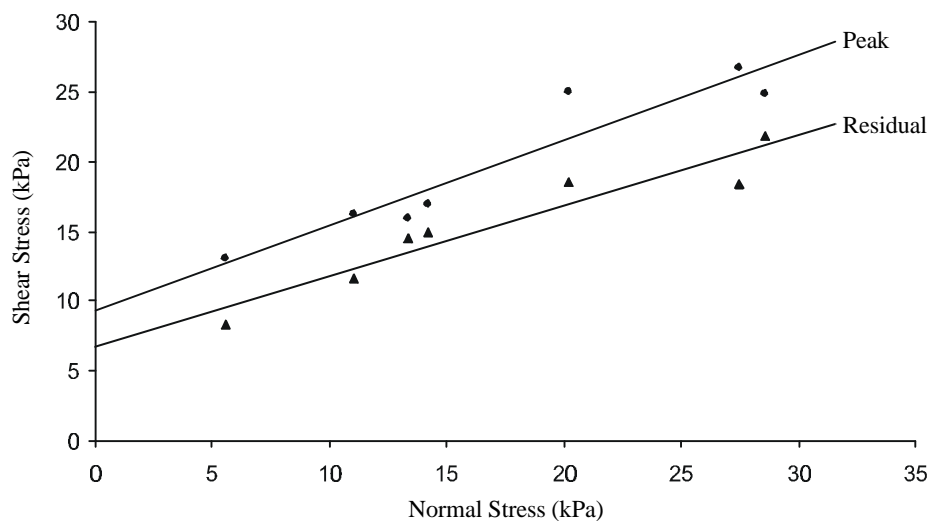
Figure 5.3: Mohr-Coulomb failure envelopes for peak and residual soil-only shear stresses as obtained through direct in-situ shear tests. The strength parameters described by these envelopes are for the total stress condition and they are used as the control values for the shear testing of soil containing roots, reported in the following section. Regression coefficients are 0.90 for the peak and 0.90 for the residual.

5.4   Shear resistance of soil containing roots

In-situ shear tests were conducted on blocks of soil containing roots of the four riparian tree species under investigation. Each species was tested twenty-five times under a range of normal loads. Plots of shear stress versus displacement were obtained for each sample (Appendix CIII-CVI). In all samples there was an immediate and rapid increase in the shear stress upon commencement of the test. As the test progressed this rate of increase invariably declined until a maximum shear stress for the sample was reached. Beyond this point incremental drops in shear stress occurred incidentally at various displacements until a fairly constant value of resistance was achieved. In many cases these incremental drops in shear stress were accompanied by audible root breakage. The displacements at which each of these events occurred varied considerably from sample to sample. In some tests a peak shear resistance may not necessarily have been reached.

Samples with higher applied normal loads generally demonstrated a larger peak shear resistance and a reduced loss of shear resistance after peak stress was achieved. In some cases there was no loss at all. At the conclusion of testing many samples exhibited roots across the shear plane that were found to be unbroken. As a general observation these samples were less likely to exhibit a reduction in shear resistance, such that the final constant shear stress was very often the peak stress recorded.

5.4.1   *Casuarina glauca*

In-situ shear tests on soil containing roots of *C. glauca* were undertaken between May and November 2000. The conditions for each test are presented in Appendix C-VII and the results in table 5.2. Normal loads were applied to *C. glauca* tests in the range of 0 kg to 465.4 kg over shear areas of between 0.15 m² and 0.25 m². The average depth to the shear plane was 0.30 m and the average moisture content of the soil at the completion of testing was 17.6 % or 69 % saturation.

Test displacements varied between 90 mm and 265 mm and on average the maximum shear stress was reached at a displacement of 70 mm. This compares with an average of 16 mm to develop the maximum shear stress during soil-only tests. Soils containing *C. glauca* roots take a significantly greater shear displacement to reach their maximum shear resistance than un-reinforced soils. Soil-only tests are at or close to their residual strength values at displacements of 70 mm.

Table 5.2: Summary of experimental results for direct in-situ shear tests on soil blocks containing *C. glauca* roots.

Sample No. (Prefix CGST)	No. Roots	Root Area Ratio (%)	Shear Depth (m)	Shear Area (m²)	Peak/Final test displacement (mm)	Total Normal Stress (kPa)	Peak Shear Stress (kPa)	Final Shear Stress (kPa)
1	15	0.025	0.30	0.2500	59/75	16.66	19.08	19.08
2	32	0.067	0.35	0.2500	93/117	20.55	21.26	20.76
3	33	0.040	0.35	0.2500	17/100	14.51	14.54	13.20
4	62	0.135	0.25	0.2025	66/100	21.63	27.70	27.70
5	38	0.146	0.25	0.2025	73/100	14.55	26.67	26.25
6	45	0.117	0.28	0.2025	113/132	15.81	26.67	23.76
7	50	0.110	0.28	0.2025	18/132	15.81	22.52	22.10
8	44	0.057	0.30	0.2025	10/100	9.04	17.54	8.00
9	43	0.179	0.23	0.2025	89/104	24.46	32.06	29.98
10	36	0.306	0.30	0.2025	167/177	26.49	39.11	37.04
11	38	0.218	0.30	0.2025	88/100	18.42	27.70	27.70
12	5	0.018	0.35	0.200	18/92	29.20	24.90	24.48
13	41	0.129	0.28	0.2025	58/180	5.16	17.12	10.07
14	46	0.113	0.30	0.2025	51/200	5.53	18.37	12.15
15	29	0.111	0.30	0.2025	50/102	26.85	27.08	26.67
16	28	0.276	0.30	0.1500	82/243	20.56	38.80	33.20
17	17	0.055	0.30	0.1750	66/264	5.53	15.02	8.30
18	43	0.181	0.25	0.1580	97/204	11.43	26.28	20.95
19	32	0.312	0.28	0.1800	39/134	5.16	26.73	16.00
20	37	0.201	0.30	0.2025	135/169	5.53	26.67	17.33
21	51	0.250	0.30	0.1800	87/184	12.91	31.40	27.67
22	43	0.212	0.30	0.2025	199/220	18.82	34.96	34.96
23	73	0.163	0.28	0.2250	70/160	7.71	26.99	21.20
24	30	0.077	0.30	0.1720	5/150	5.53	19.18	13.81
25	28	0.081	0.42	0.1845	4/160	11.25	21.57	13.33

In many *C. glauca* tests only a small, sometimes negligible, reduction in shear stress was recorded after the peak was reached. This is most likely due to the fact that some roots had not yet failed in

tension and were probably providing continued shear resistance through their distortion in a wide shear zone (see Wu & Watson, 1998). The in-situ tests conducted in this study were unable to produce shear displacements large enough for tensile failure of all roots to occur in every test. There were however thirty audible root failures over the twenty five tests, more than any other species (Appendix C-III).

The maximum shear resistance was greater for blocks containing *C. glauca* roots than for comparable soil-only blocks in all but four tests (Fig. 5.4a). A clear indication of the earth-reinforcing capability of root-reinforced soil. The relative increase in shear stress for each test is calculated by determining the difference between the maximum shear stress for the *C. glauca* test and the Mohr-Coulomb failure envelope for the soil at the same normal stress (equation [5.1]). The resulting shear stress increase for each sample is recorded in Appendix C-XI and plotted against the quantity of root material (expressed as the root area ratio) recorded at the shear surface (Fig. 5.4b). The mean increase was 6.90 kPa over the range of normal stresses tested with a clear linear relationship between the increased shear stress (S_r) and RAR. A greater root reinforcement present at the shear plane results in a greater increased shear resistance of the soil (Fig. 5.4b).

Figure 5.4: (a) Shear stress versus normal stress plot for twenty five *C. glauca* in-situ shear tests. All but four tests had a greater maximum shear stress than the soil-only tests, as indicated by the positions of the *C. glauca* results relative to the Mohr-Coulomb failure envelope for the soil-only tests. (b) The increase in shear stress for *C. glauca* tests over soil-only tests plotted against the quantity of root material measured at the shear surface (expressed as a RAR percentage).

Regressing the increase in shear stress, S_r (kPa), against root area ratio, RAR (%) yields:

$$S_r = 60.61 \text{ x RAR} - 1.78 \qquad\qquad R^2 = 0.80 \qquad\qquad [5.2]$$

and so a calculation of the strength of a soil containing roots of the tree species *Casuarina glauca* may take the form of equation [2.6] with S_r determined by equation [5.2]. This calculation is shown to be accurate for small normal loads and up to a RAR of 0.35 %.

The four tests that presented shear resistance values below the failure envelope for the soil-only (CGST1,2,3,12) resulted in the line of best fit plotted in Figure 5.5b to cross the y-axis below zero. This is most likely to be due to the tendency for continuous natural parameters and experimental errors to be normally distributed about a mean (Berthouex & Brown, 1994) and it has not been interpreted that a small RAR reduces the shear strength of the soil. The discrepancy of 1.78 kPa is well within the standard deviation for the population (5.29).

5.4.2   *Eucalyptus amplifolia*

In-situ shear tests on soil containing roots of *E. amplifolia* were undertaken between November 2000 and April 2001. The conditions for each test are presented in Appendix C-VIII and the results in table 5.3. Normal loads were applied to *E. amplifolia* tests in the range of 0 kg to 406.5 kg on shear areas of between 0.20 m² and 0.25 m². The average depth to the shear plane was 0.30 m and the average moisture content of the soil at the completion of testing was 17.4 % or 69 % saturation.

Test displacements varied between 100 mm and 200 mm and on average the maximum shear stress was reached at a displacement of 73 mm. This is significantly greater than the soil-only tests and similar to the *C. glauca* tests. Upon completion of testing and examination of the shear zone it was found that very few roots had failed in tension due to their large size and flexibility within this wide zone. Only twelve audible root failures were recorded for all twenty-five tests (Appendix C-IV).

Every block containing *E. amplifolia* roots produced a maximum shear stress that was greater than that obtained for soil-only blocks (Fig. 5.5a). Using equation [5.1] the relative increase in shear stress was calculated for each test (Appendix C-XI) and plotted against the quantity of root material (expressed as the root area ratio) recorded at the shear surface (Fig. 5.5b). The mean increase was 8.90 kPa over the range of normal stresses tested and as with the *C. glauca* tests there is a clear linear relationship between the increased shear stress (S_r) and RAR. A greater root reinforcement present at the shear plane results in a greater increased shear resistance of the soil (Fig. 5.5b).

Table 5.3: Summary of experimental results for direct in-situ shear tests on soil blocks containing *E. amplifolia* roots.

Sample No. (Prefix EAST)	No. Roots	Root Area Ratio (%)	Shear Depth (m)	Shear Area (m²)	Peak/Final test displacement (mm)	Total Normal Stress (kPa)	Peak Shear Stress (kPa)	Final Shear Stress (kPa)
1	20	0.069	0.30	0.2250	11/158	7.92	20.27	12.80
2	13	0.103	0.30	0.2000	18/162	10.92	21.54	14.40
3	13	0.050	0.40	0.2000	73/154	15.46	20.70	19.02
4	14	0.100	0.35	0.2000	12/204	6.45	19.02	14.40
5	16	0.084	0.35	0.2025	119/183	11.95	24.59	22.52
6	13	0.072	0.33	0.2025	35/185	17.44	25.63	22.10
7	23	0.122	0.27	0.2000	113/173	4.97	14.40	12.30
8	31	0.104	0.25	0.2250	98/163	9.40	17.65	16.53
9	21	0.197	0.28	0.2250	106/161	12.35	24.37	24.37
10	27	0.189	0.28	0.2500	18/150	13.36	24.12	19.92
11	18	0.313	0.33	0.2250	148/148	14.71	29.60	29.56
12	11	0.337	0.30	0.2250	84/149	16.38	37.07	24.00
13	35	0.134	0.33	0.2500	17/164	6.08	15.22	14.88
14	18	0.257	0.27	0.2500	9/150	4.97	18.24	10.51
15	35	0.245	0.27	0.2500	104/123	20.92	36.72	35.04
16	18	0.221	0.30	0.2250	70/132	13.35	25.87	22.13
17	30	0.301	0.30	0.2500	28/164	19.61	33.69	27.31
18	19	0.223	0.35	0.2000	64/162	21.36	33.30	31.20
19	19	0.327	0.35	0.2000	90/168	17.58	37.50	35.40
20	32	0.284	0.30	0.2000	75/150	9.30	27.00	25.74
21	38	0.285	0.25	0.2112	96/155	13.10	27.56	23.98
22	35	0.206	0.28	0.2304	142/198	5.16	17.97	12.50
23	21	0.286	0.26	0.2400	165/165	15.41	31.25	31.25
24	31	0.381	0.28	0.2250	81/98	20.33	38.56	38.00
25	31	0.390	0.27	0.2250	60/132	4.97	24.37	24.00

Regressing the increase in shear stress, S_r (kPa), against root area ratio, RAR (%), yields:

$$S_r = 38.12 \times RAR + 0.85 \qquad\qquad R^2 = 0.69 \qquad\qquad [5.3]$$

and so a calculation of the strength of a soil containing roots of the tree species *Eucalyptus amplifolia* will take the form of equation [2.6] with S_r determined by equation [5.3]. This calculation is found to be accurate for small normal loads and up to a RAR of 0.40 %.

As with *C. glauca* tests the line of best fit plotted in Fig. 5.5b does not extend through the origin as might be expected. The discrepancy of 0.85 is however within the standard deviation of the population (5.53) and so is not considered significant.

Figure 5.5: (a) Shear stress versus normal stress plot for twenty five *E. amplifolia* in-situ shear tests. Every test had a greater maximum shear stress than the soil-only tests, as indicated by the positions of the *E. amplifolia* results relative to the Mohr-Coulomb failure envelope for the soil only. (b) The increase in shear stress for *E. amplifolia* tests over soil-only tests plotted against the quantity of root material measured at the shear surface (expressed as a RAR percentage).

5.4.3 *Eucalyptus elata*

In-situ shear tests on soil containing roots of *E. elata* were undertaken between February and June 2001. The conditions for each test are presented in Appendix C-IX and the results in table 5.4. Normal loads were applied to *E. elata* tests in the range of 0 kg to 337 kg on shear areas of between 0.15 m² and 0.26 m². The average depth to the shear plane was 0.27 m and the average moisture content of the soil at the completion of testing was 20.7 % or 82 % saturation.

Test displacements varied between 100 mm and 210 mm and on average the maximum shear stress was reached at a displacement of 63 mm. This is significantly greater than the soil-only tests and similar to the *C. glauca* tests and *E. amplifolia* tests. As with *E. amplifolia* there were also many blocks that revealed a number of large roots at the shear surface. Upon completion of testing and examination of the shear zone it was found that very few roots had failed in tension, most probably due to their large size and flexibility in this wide zone. Only fifteen audible root failures were recorded for all twenty five tests (Appendix C-V).

Table 5.4: Summary of experimental results for direct in-situ shear tests on soil blocks containing *E. elata* roots.

Sample No. (Prefix EEST)	No. Roots	Root Area Ratio (%)	Shear Depth (m)	Shear Area (m²)	Peak/Final test displacement (mm)	Total Normal Stress (kPa)	Peak Shear Stress (kPa)	Final Shear Stress (kPa)
1	16	0.020	0.28	0.2025	6/150	5.30	11.32	8.41
2	19	0.173	0.28	0.2250	19/182	5.30	20.70	14.40
3	19	0.085	0.25	0.1800	18/198	7.73	23.00	13.67
4	18	0.113	0.25	0.2250	16/172	7.13	16.91	12.80
5	28	0.077	0.25	0.2000	102/170	10.13	22.38	18.60
6	20	0.053	0.28	0.2025	15/172	10.63	18.37	14.22
7	11	0.021	0.28	0.2250	20/185	12.50	22.13	15.60
8	43	0.230	0.25	0.2025	100/155	4.74	18.37	14.22
9	19	0.029	0.23	0.1485	14/182	7.99	18.83	14.30
10	33	0.417	0.27	0.2250	74/122	12.94	26.61	26.24
11	20	0.159	0.23	0.2080	95/180	7.99	17.48	17.48
12	37	0.227	0.28	0.2250	106/106	19.99	26.24	26.24
13	25	0.076	0.30	0.2250	63/100	13.51	26.61	25.87
14	37	0.070	0.29	0.2600	18/180	5.49	16.57	11.88
15	46	0.271	0.28	0.2350	91/148	12.34	26.59	26.19
16	35	0.187	0.26	0.2150	85/128	4.93	25.12	25.12
17	62	0.195	0.30	0.2500	65/95	18.04	31.68	31.68
18	18	0.043	0.27	0.2350	5/124	8.33	17.62	17.62
19	19	0.218	0.26	0.2350	18/150	18.99	23.34	21.91
20	50	0.374	0.22	0.2350	89/140	8.76	25.84	24.76
21	45	0.586	0.30	0.2400	144/144	14.06	51.90	51.90
22	40	0.436	0.28	0.2016	41/160	10.12	46.58	22.62
23	40	0.455	0.30	0.2160	170/210	8.18	38.61	36.27
24	48	0.726	0.23	0.1845	75/165	9.62	52.03	40.65
25	22	0.296	0.22	0.2000	130/164	7.94	26.16	24.48

Every block containing *E. elata* roots except for one produced a maximum shear stress that was greater than that obtained for soil-only blocks (Fig. 5.6a). Using equation [5.1] the relative increase in shear stress was calculated for each test (Appendix C-XI) and plotted against the quantity of root material (expressed as the root area ratio) recorded at the shear surface (Fig. 5.6b). The mean increase was 10.58 kPa over the range of normal stresses tested and as with the *C. glauca* and *E. amplifolia* tests there is a clear linear relationship between the increased shear stress (S_r) and RAR. A greater root reinforcement present at the shear plane results in a greater increased shear resistance of the soil (Fig. 5.6b).
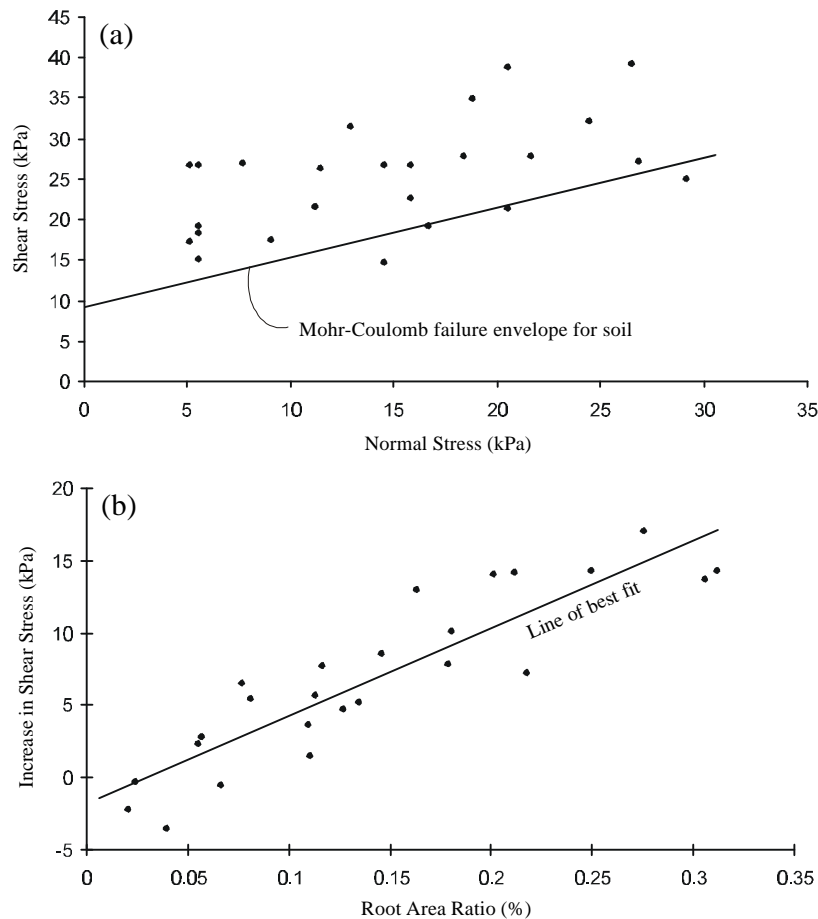
Regressing the increase in shear stress, S_r (kPa), against root area ratio, RAR (%), yields:

$$S_r = 47.44 \times RAR + 0.07 \qquad R^2 = 0.76 \qquad [5.4]$$

and so a calculation of the strength of a soil containing roots of the tree species *Eucalyptus elata* will take the form of equation [2.6] with S_r determined by equation 5.4. This calculation is found to be accurate for small normal loads and up to a RAR of 0.75 %.
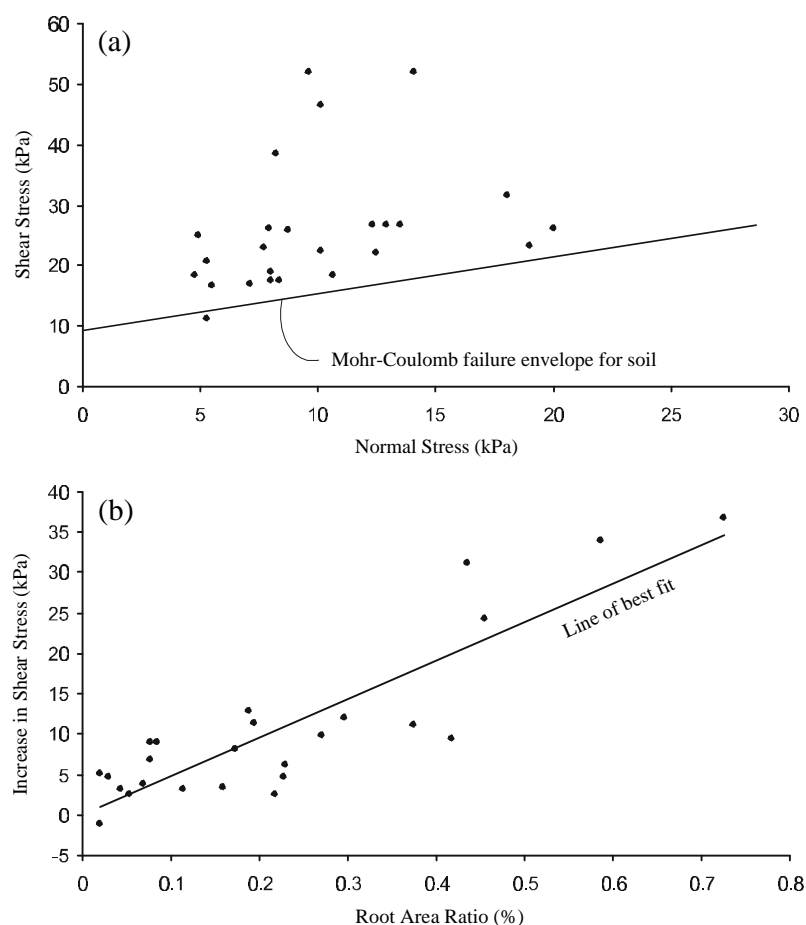
Figure 5.6: (a) Shear stress versus normal stress plot for twenty five *E. elata* in-situ shear tests. Every test except for one had a greater maximum shear stress than the soil-only tests, as indicated by the positions of the *E. elata* results relative to the Mohr-Coulomb failure envelope for the soil only. (b) The increase in shear stress for *E. elata* tests over soil-only tests plotted against the quantity of root material measured at the shear surface (expressed as a RAR percentage).

5.4.4   *Acacia floribunda*

In-situ shear tests on soil containing roots of *A. floribunda* were undertaken between February and June 2001. The conditions for each test are presented in Appendix C-X and the results in table 5.5. Normal loads were applied to *A. floribunda* tests in the range of 0 kg to 176 kg on shear areas of between 0.17 m² and 0.25 m². The average depth to the shear plane was 0.27 m and the average moisture content of the soil at the completion of testing was 19.8 % or 78 % saturation. The normal loads applied to *A. floribunda* tests were considerably lower than for the other three species. The reason for this was an increased tendency of the blocks to deform in comparison to those of the other three species; thus destabilising the weights placed on them. No useful shear displacement was possible under these conditions and so tests were undertaken at lower normal stresses. Some tests were also conducted on blocks of a height considerably less than the other species. This was to ensure a reasonable spread in the root area ratio that would not have been possibly at depths of greater than 0.27 m due to the shallow root system morphology of this species. The final test displacements varied between 110 mm and 180 mm and on average the maximum shear stress was

reached at a displacement of 57 mm. This is lower than the other three tree species but once again considerably greater than for soil-only tests. Upon completion of testing it was found that very few roots had failed in tension. Only six audible root failures were detected for all twenty five tests (Appendix C-VI).

Table 5.5: Summary of experimental results for direct in-situ shear tests on soil blocks containing *A. floribunda* roots.

Sample No. (Prefix AFST)	No. Roots	Root Area Ratio (%)	Shear Depth (m)	Shear Area (m²)	Peak/Final test displacement (mm)	Total Normal Stress (kPa)	Peak Shear Stress (kPa)	Final Shear Stress (kPa)
1	40	0.053	0.22	0.2500	33/140	4.13	27.65	24.96
2	42	0.039	0.26	0.2400	26/104	4.88	25.12	22.50
3	25	0.036	0.30	0.2250	27/140	8.03	24.93	19.52
4	20	0.023	0.35	0.2304	19/152	11.26	29.27	17.97
5	37	0.041	0.35	0.2250	36/117	11.37	33.33	31.47
6	31	0.034	0.30	0.2250	73/156	10.43	31.47	30.72
7	25	0.131	0.30	0.2250	140/140	11.39	38.93	38.93
8	1	0.005	0.26	0.2040	13/170	8.59	17.00	12.88
9	21	0.071	0.25	0.2025	24/155	7.36	25.84	23.35
10	17	0.063	0.25	0.2160	30/170	7.19	22.08	18.19
11	29	0.060	0.28	0.2025	21/165	10.59	22.93	19.61
12	37	0.078	0.27	0.1800	42/109	9.27	44.00	37.00
13	28	0.140	0.30	0.1800	175/180	7.43	34.67	34.66
14	33	0.106	0.30	0.1680	20/180	5.64	25.14	19.64
15	24	0.032	0.23	0.2400	35/175	6.57	29.50	14.80
16	23	0.074	0.22	0.2500	36/170	10.61	36.72	23.95
17	42	0.085	0.25	0.2160	65/158	6.69	34.72	28.50
18	36	0.159	0.21	0.1764	110/171	5.17	30.61	29.18
19	61	0.228	0.20	0.1890	88/115	8.89	53.46	53.01
20	91	0.108	0.26	0.2115	71/139	4.88	25.93	25.53
21	42	0.058	0.22	0.2064	110/134	12.50	34.71	30.64
22	44	0.124	0.30	0.2209	80/167	10.52	44.41	37.75
23	44	0.110	0.25	0.2025	80/150	4.70	22.93	20.44
24	36	0.048	0.27	0.1935	22/180	5.07	31.38	12.71
25	70	0.144	0.30	0.2550	57/112	6.90	52.47	30.07

Every block containing *A. floribunda* roots produced a maximum shear stress that was greater than that obtained for soil-only blocks (Fig. 5.7a). Using equation [5.1] the relative increase in shear stress was calculated for each test (Appendix C-XI) and plotted against the quantity of root material (expressed as root area ratio) recorded at the shear surface (Fig. 5.7b).

The mean increase in shear stress was 17.79 kPa over the range of normal stresses tested however unlike the other three species the relationship between increased shear stress (S_r) and RAR regresses more accurately to that of a power relationship. The reason for this difference between *A. floribunda* and the other three species is unclear although previous investigations have indicated that the relationship between increased shear strength and root quantity at the shear plane is not necessarily a linear one (e.g. Tengbah, 1989, cited in Styczen & Morgan, 1995).
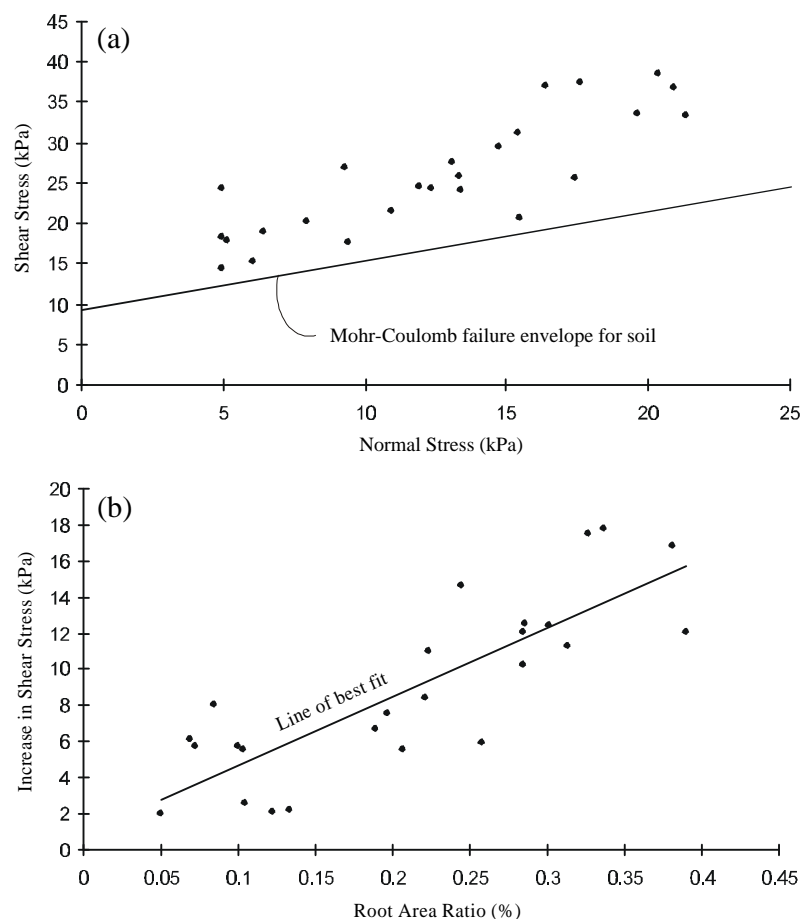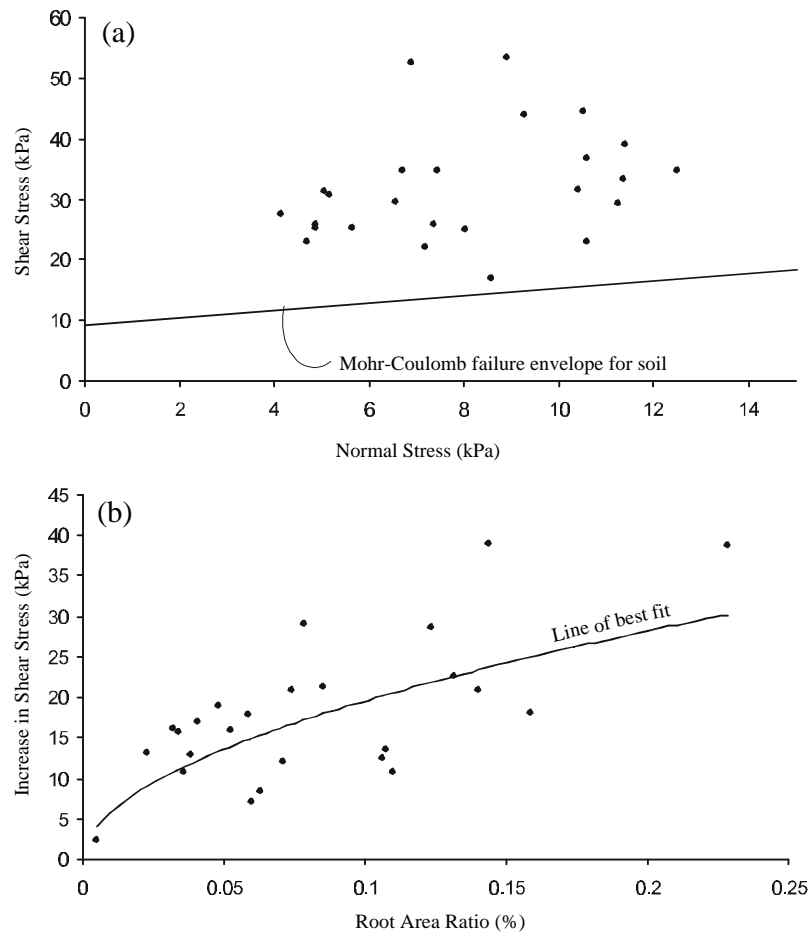
Figure 5.7: (a) Shear stress versus normal stress plot for twenty five *A. floribunda* in-situ shear tests. Every test had a greater maximum shear stress than the soil-only tests, as indicated by the positions of the *A. floribunda* results relative to the Mohr-Coulomb failure envelope for the soil only. (b) The increase in shear stress for *A. floribunda* tests over soil-only tests plotted against the quantity of root material measured at the shear surface (expressed as a RAR percentage).

Regressing the increase in shear stress, S_r (kPa), against root area ratio, RAR (%), yields:

$$S_r = 65.677 \text{ x } RAR^{0.5256} \qquad\qquad R^2 = 0.53 \qquad\qquad [5.5]$$

and so a calculation of the strength of a soil containing roots of the tree species *Acacia floribunda* will take the form of equation [2.6] with S_r determined by equation [5.5]. This calculation is found to be accurate for small normal loads and up to a RAR of 0.25 %.

The plots of Increased shear resistance versus root area ratio for all species illustrate some variability about the line of best fit plotted. This is expected given that other factors not measured here may influence the magnitude of shear resistance recorded. These other factors include the initial orientation of the roots, their morphology beyond the shear plane, their position within the apparatus, as well as the natural variability inherent in such systems. The line of best fit plotted here, be it linear or otherwise, allows for a best estimate of the relationship between increased shear resistance and root area ratio given the data extractable from direct in-situ shear tests.

5.5   Evaluation of soil-root shear resistance

5.5.1   Comparisons between species

The behaviour of the in-situ shear tests described above were very similar for three of the species. Blocks containing roots of *C. glauca*, *E. amplifolia*, and *E. elata* were generally fairly smooth with a definite shear plane gradually forming across the base of the block as the test proceeded. By the conclusion of testing the whole block was moving relative to the ground below. In general there was a difference in the amount of displacement of the front of the block compared to the amount of displacement of the back of the block. The back of the block was adjacent to the pushing plate of the shearing device and tended to move further than the front with corresponding compression of the soil block occurring in the early stages of testing. In the case of *A. floribunda* this process was of greater significance as the compression resulted in the tipping of applied normal loads. The shear plane at the base of the *A. floribunda* blocks was less obvious as the blocks presented a more unified soil-root matrix that was accordingly more difficult to shear. An illustration of this phenomenon is presented (Fig. 5.8) and was most likely due to a combination of the large number of very small *A. floribunda* roots present at the shear plane and the higher tensile strength of the roots of this species (chapter four), which bound the block to the underlying soil more effectively than the roots of the other species. *C. glauca* presented a similar number of fine roots at the conclusion of in-situ shear testing (Appendix C-XII) but their much lower tensile strength allowed formation of the shear plane and failure to progress more readily.
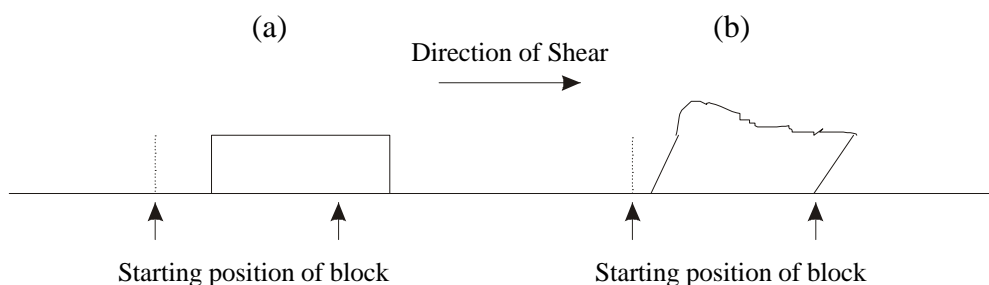
Figure 5.8: An illustration of the movement of soil blocks. (a) *C. glauca*, *E. amplifolia*, and *E. elata* blocks move quite freely relative to the soil below with the development of a definite shear plane. (b) *A. floribunda* blocks do not move as freely relative to the soil below and tend to stick across the developing shear plane as a more unified soil-root matrix. Compression of the soil leads to deformation in the normal direction.

The results presented in the previous section allow a comparison of the relative shear resistances obtained for each species. Plots of average shear stress versus displacement for each species are presented below (Fig. 5.9). They show that the greatest shear resistance is provided by *A. floribunda*, followed by *E. elata*, *E. amplifolia*, and then *C. glauca* although there is very little discernable difference between these latter three species. The average for *E. elata* must be strongly influenced by the much higher RAR's (0.02-0.73 %) recorded for this species, however the result for *A. floribunda* is in spite of the lowest recorded range (0.01-0.23 %). Once again the most likely explanation is the

much higher tensile strengths recorded for *A. floribunda* roots in comparison to the other three species (chapter four).
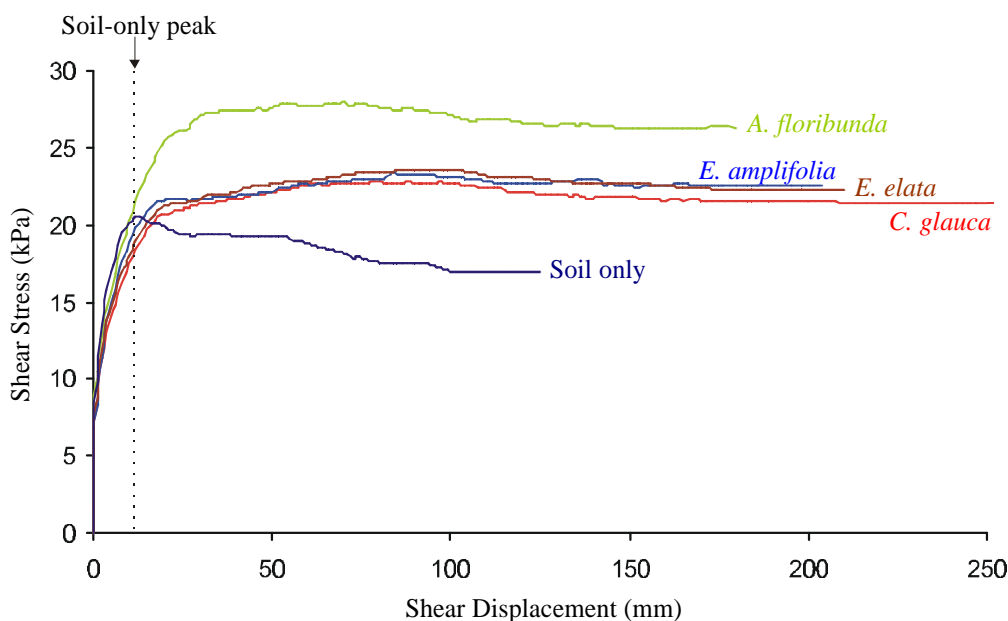
Figure 5.9: Average shear stress versus displacement plots for the four tree species and the soil-only tests. At the dashed vertical line when the soil reaches a peak strength, resistance of root-reinforced soil plots is still increasing. When the root-reinforced soil plots reach peak strength the soil-only resistance is at or close to its residual strength. All species demonstrate reinforcement of the soil although *A. floribunda* by a significantly greater amount than the other three.

All species recorded significantly higher shear resistance than the soil blocks containing no roots and for all species the average maximum shear stress was reached at a significantly larger displacement than for the soil only tests. In fact at the displacement at which root-enhanced soil reaches a maximum shear resistance the soil-only tests are at or very close to residual strength values. Therefore tree roots provide their greatest contribution to soil strength when the soil on its own would only be providing residual strength. The average maximum increase at this point is 54 % for *A. floribunda*, 36 % for *E. elata*, 32 % for *E. amplifolia*, and 29 % for *C. glauca*.

Figure 5.9 indicates that on average there is a reduction in shear resistance following a peak however many samples did not behave in this manner and as such there are generally two distinct types of test behaviour (Fig. 5.10). Type 1 tests are those that reached a maximum shear resistance before the conclusion of testing and exhibited a definite decrease in resistance as displacement increased. Type 2 tests are those that either reached a maximum resistance and recorded no reduction from that level, or blocks where the shear resistance continued to increase for the duration of the test. Both types of test behaviour are evident for all species (Fig. 5.11) although *A. floribunda* had the greatest number of Type 1 tests with 16, compared to 13 for *E. elata*, 12 for *C. glauca*, and 8 for *E. amplifolia*.
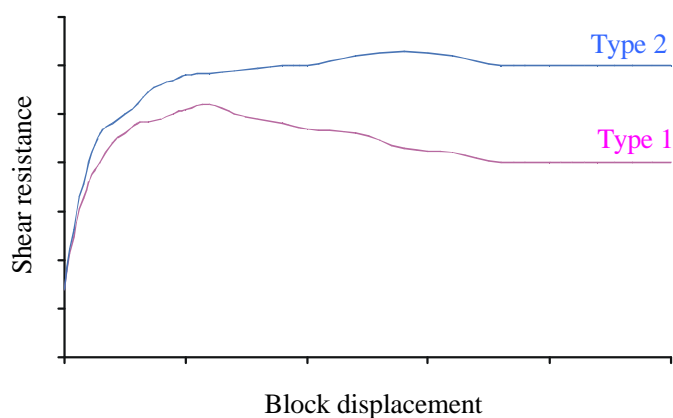
Figure 5.10: Diagrammatic representation of two generally distinct test behaviours. Type 1 exhibit a reduction in shear resistance after a peak in a similar fashion to soil-only tests except that they reach a greater peak resistance and at a greater shear displacement. Type 2 exhibit little or no reduction in shear resistance over the course of the test so that the final shear resistance is very often the peak.

The recording of both types of behaviour amongst all four species suggests a universality to the phenomenon, however investigation into the likely causes of the differing behaviours revealed no obvious explanation. It should be noted however that for three of the species (*E. amplifolia*, *E. elata*, and *A. floribunda*) Type 1 tests recorded lower average RARs due to lower root numbers than Type 2 tests. On the other hand *C. glauca* recorded essentially the same average RAR for both types. Of the 49 Type 1 tests there were 39 audible root breakages (a.r.b), compared to 22 a.r.b. for 51 Type 2 tests. This suggests that more roots have failed in tension in Type 1 tests leading to a reduction in shear resistance with displacement. This also suggests that in cases where a smaller number of roots cross the potential failure plane, as in Type 1 tests, there is a greater likelihood of soil-root system failure at a small displacement. A greater reinforcement concentration (as in Type 2 tests) perhaps leads to a wider shear zone (see Shewbridge & Sitar, 1996) allowing for greater deformation of the roots before their full tensile strength can be mobilised.

Type 1 test results demonstrate a consistently higher shear resistance than Type 2 tests for the same RARs in all species except for *E. amplifolia* (Fig. 5.12). It is expected that this is the result of some Type 2 tests having not reached their maximum shear resistance within the final displacement of the test. Generally the difference in measured shear resistance is small but consistent, with an average of: 0.95 kPa for *C. glauca*, 1.62 kPa for *E. elata*, and 1.06 kPa for *A. floribunda*. The scatter-plot of *E. amplifolia* Type 1 results on Type 2 results shows no significant difference in the increased shear resistance between the two test types (Fig. 5.12b).
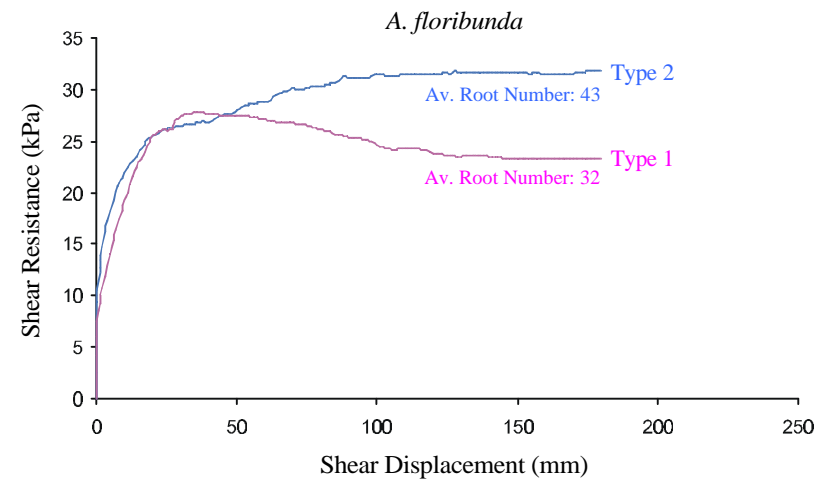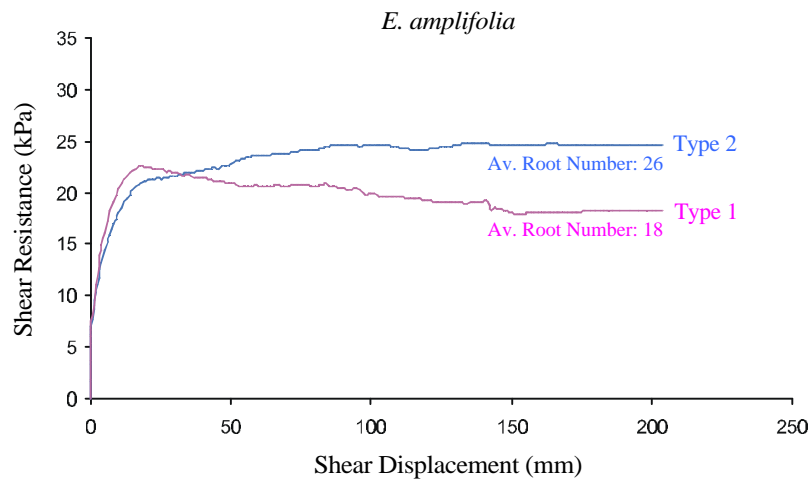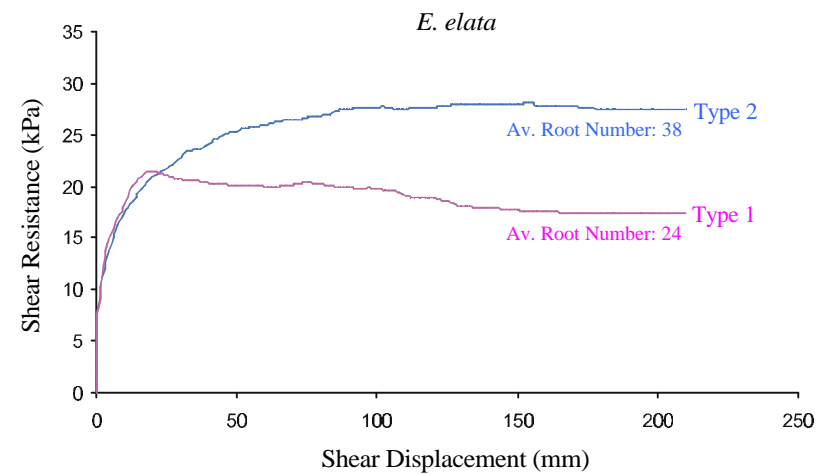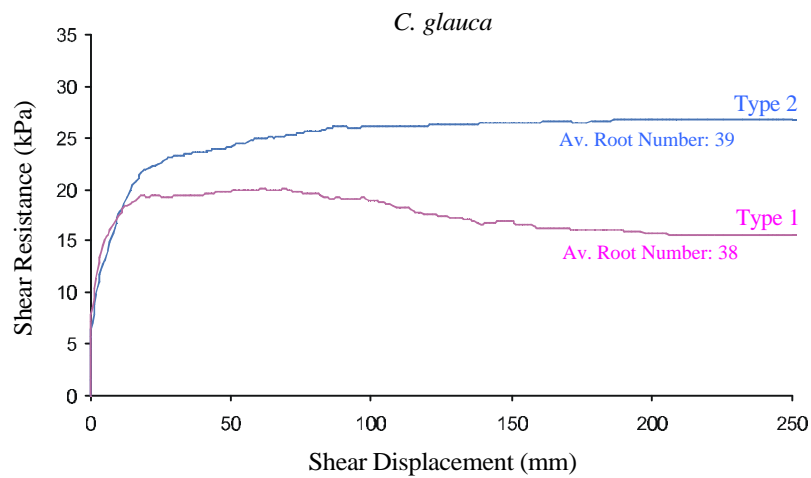
Figure 5.11: Average shear resistance versus shear displacement plots divided into two types. Type 1 tests exhibit a suspected peak shear resistance at a smaller displacement (~22 mm) of the block followed by a reduction in resistance as displacement increases. Type 2 tests exhibit a continually increasing shear resistance or a shear resistance that doesn't decrease as block displacement increases, therefore failure of the soil-root system as a whole is not believed to have taken place. Many roots have not yet failed in tension. This may potentially be due to the greater number of roots present in type 2 tests. For three of the species (*E. amplifolia*, *E. elata*, and *A. floribunda*) there are on average fewer roots recorded on the shear plane for type 1 tests although the difference is insignificant for *C. glauca*.
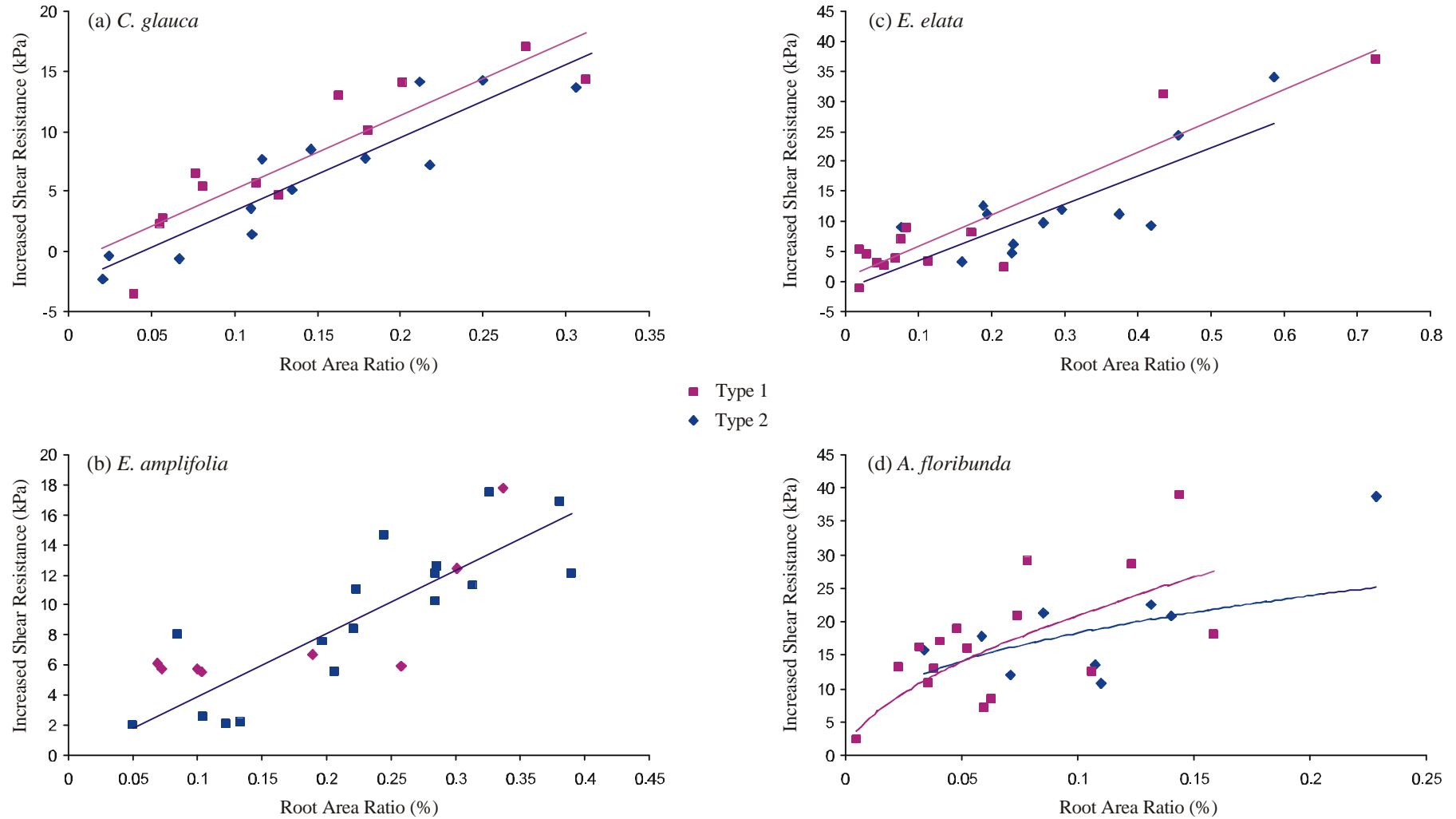
Figure 5.12: The relationship between RAR and increased shear strength according to test type. Type 1 tests (pink) demonstrate consistently higher increased shear strengths than type 2 tests (blue) over the range of RARs tested for all species except *E. amplifolia*. It seems likely that the relationships for type 1 tests are a more accurate representation of increased shear resistance provided by roots of three of the four tree species under investigation in this study. This is due to the increased likelihood that peak shear resistance has been measured in type 1 tests. (a) *C. glauca*, (b) *E. amplifolia*, (c) *E. elata*, (d) *A. floribunda*. Note the different scales for different species.

The difference between the maximum shear resistance measured for Type 1 and Type 2 tests with *E. amplifolia* roots, unlike the other three species, was negligible. The reason for this is most probably due to *E. amplifolia*'s different root system morphology (chapter three), which exhibits a small number of very large vertical roots concentrated directly below the tree stem and extending deep within the soil layer (Fig. 3.3). Their small number and location within the centre of the block (Fig. 5.13) meant that in many instances failure of the block occurred by deformation around the root mass and without tension failure (only 2 a.r.b. in 8 Type 1 tests), or even significant deformation, of many of the roots. This probably prevented the maximum shear resistance being recorded even in Type 1 tests for *E. amplifolia* and explains why they demonstrate no discernable difference in increased shear resistance compared to Type 2 tests at equivalent RARs (Fig. 5.12).
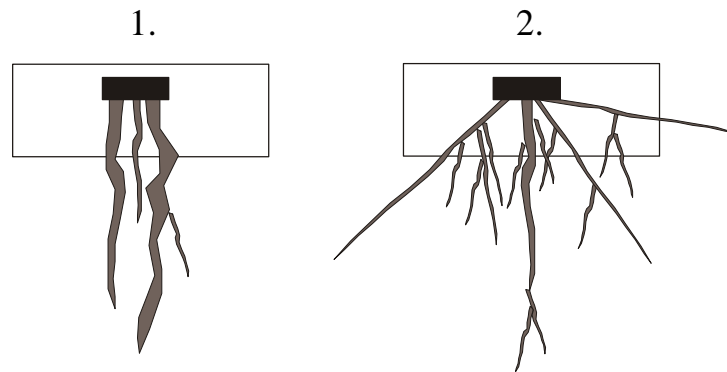
Figure 5.13: The distinct root morphology through an in-situ shear test-block of *E. amplifolia* (1) compared to the other three species (2). *E. amplifolia* roots are few in number and concentrated directly below the stem and subsequently the middle of the test block, while the other species exhibit a more even spread and therefore greater likelihood of more roots failing in tension as progressive failure of the block occurs.

Tests on blocks containing the roots of *C. glauca*, *A. floribunda*, and *E. elata*, which have roots spread over the entire surface of the failure plane (Fig. 5.13), most likely result in sufficient root failures close to the pushing plate of the test apparatus to overcome the maximum shear resistance within the displacement of Type 1 tests. Therefore the peak in Type 1 tests for these species represents the probable maximum shear resistance, with the peak in Type 2 tests for these species representing a small underestimate of the maximum shear resistance. In essence Type 1 tests represent a more advanced stage of the soil-root failure process than Type 2 tests because of the greater likelihood that a sufficient quantity of roots have failed in tension and therefore passed the maximum shear resistance at a displacement achievable within the limitations of the in-situ shear methodology (Fig. 5.14). It is expected then that the relationships between S_r and RAR obtained for Type 1 tests are a more accurate representation of root reinforcement in this investigation.

The uncertainty over whether or not the peak shear stress recorded in Type 2 tests is also the maximum, means that when all tests are grouped and analysed together the relationships obtained (Figs. 5.4b, 5.5b, 5.6b, 5.7b) may underestimate the potential root reinforcement. Such a result may partly explain Wu's (1995) suggestion that direct in-situ shear tests may provide an underestimate of the amount of root reinforcement.
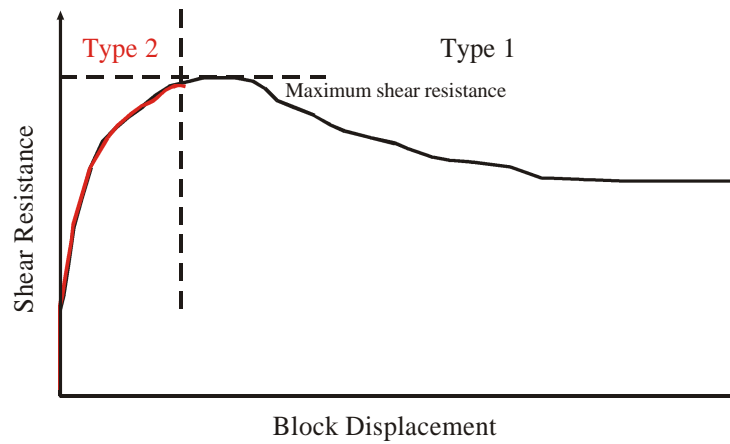
Figure 5.14: The soil-root failure process with respect to in-situ shear test behaviour. Type 1 tests represent a more advanced state having passed the maximum shear resistance, while Type 2 tests have still to reach the maximum due to the greater quantity of roots and therefore greater shear displacement required for a sufficient quantity of these roots to fail in tension.

In order to estimate the maximum increased shear resistance from the root are ratio present on the shear plane the relationships obtained from Type 1 tests in the case of *C. glauca*, *E. elata*, and *A. floribunda*; and all tests in the case of *E. amplifolia*, are expected to give the most appropriate values for use in this study. These relationships are:

C. glauca:	$S_r = 61.16 \times RAR - 0.91$	$R^2 = 0.80$	[5.6]
E. amplifolia:	$S_r = 38.12 \times RAR + 0.85$	$R^2 = 0.69$	[5.3]
E. elata:	$S_r = 52.09 \times RAR + 0.66$	$R^2 = 0.86$	[5.7]
A. floribunda:	$S_r = 81.13 \times RAR^{0.5866}$	$R^2 = 0.58$	[5.8]

The coefficients of determination (R^2) for the above linear relationships (equations [5.3],[5.6],[5.7]) are accurate to the 1% significance level for populations of this size (Hahn, 1973).

5.5.2   Comparisons with previous investigations

The increase in shear resistance due to root reinforcement reported in this study is comparable to the work of previous investigators (Fig. 5.15). All published studies based on multiple tests demonstrate broadly similar results to this study. That is, an increase in increased shear strength with increasing root area ratio at the shear plane. However all species in this study were found to provide a greater increase in shear strength at comparative root area ratios than the species tested in previous in-situ shear tests (see Endo & Tsurata, 1969; Ziemer, 1981; Wu *et al.*, 1988a; and Wu & Watson, 1998). Wu *et al.* (1988a) state that one should expect the value measured to be influenced by the test apparatus. The test apparatus that was most similar to the one used in this study was that of Wu &

Watson (1998), who's results were also closest to the results presented in this chapter, falling within one standard deviation for three of the four species tested. However given the multiple variables (e.g. soil type, tree species) it has not been possible to determine what effect the choice of test apparatus has had on producing the results presented. The differences between studies are therefore assumed to result from inter-species differences in root strength and morphology as well as the specific site conditions present. This result demonstrates the importance of specific study area evaluations if the relationships obtained are to be used for an accurate assessment of slope stability.
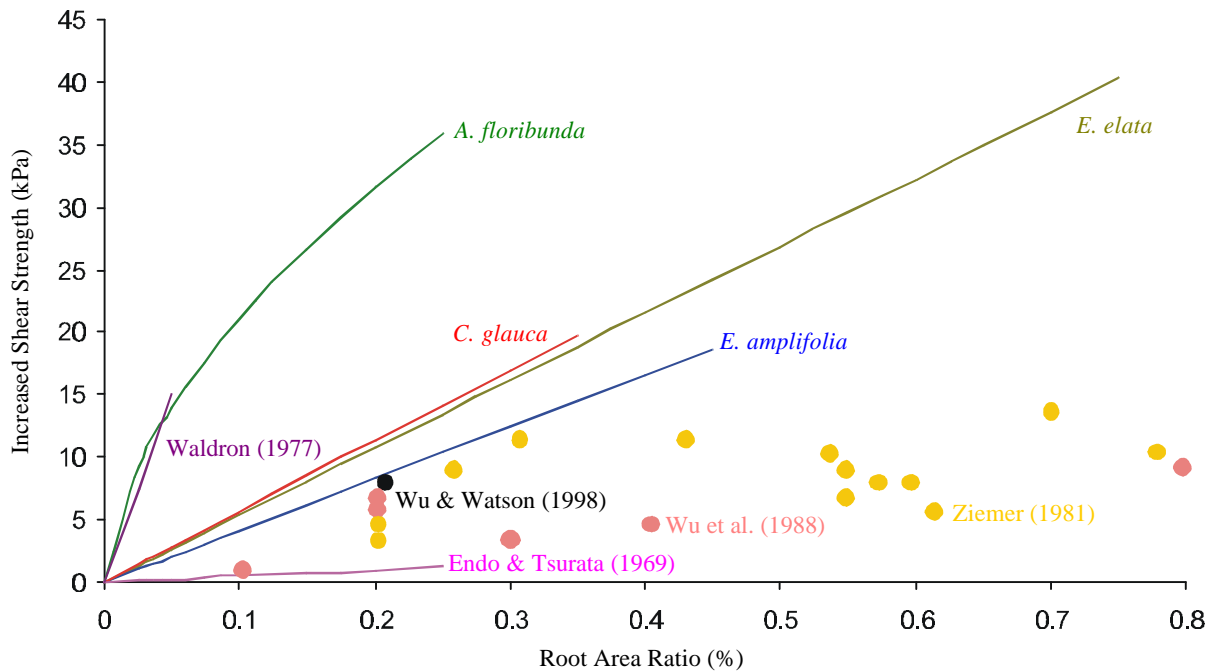
Figure 5.15: Increased shear strengths for direct shear tests conducted on soil containing roots. Plots for this study have been fitted through the origin if not already passing through. Direct in-situ tests were conducted by all researchers except for Waldron (1977) who's data originates from laboratory shear tests on barley roots. Wu & Watson (1988) examined *Pinus radiata*, Endo & Tsurata (1969) *Betula japonica* and *Alnus japonica*, Ziemer (1981) *Pinus contorta*, and Wu *et al.* (1988a) Western hemlock.

5.6   The root failure process

The analysis of the data and specific observations made during testing allow a few inferences to be made about the progression of failure in these direct in-situ tests. First, it has been observed that roots provide resistance to shear at displacements beyond that at which soil-only tests reach peak shear strength. In many cases this increase in shear resistance applies at relatively large displacements when a shear plane is well developed across the entire width of the soil block. In some tests many of the roots did not fail and therefore provided shear resistance through the mobilisation of soil resistance against the lateral displacement of the root. This process was identified by Wu & Watson (1998) for roots that occur in a thick shear zone.

Second, if the roots are constrained in their original position at some point along their length then tensile failure must occur before the entire system can be said to have failed. It is expected that most of the roots examined in this study were constrained by the confining pressure of the soil beneath the failure plane, given the depth to which they extend (chapter three) and the observation of in-situ pull-out tests breaking the root at a point below the ground surface.

Third, root failure occurs progressively across the test block. That is, the roots closest to the pushing plate, at the back of the block fail first, followed by roots in the middle and then roots at the front. Therefore it may not be appropriate to estimate the total reinforcement provided by roots by summing the reinforcement calculated for each individual root. The tests demonstrate that different roots provide reinforcement across the shear plane at different displacements depending on such factors as their location on the shear plane, their size and possibly their orientation relative to the shear plane. Progressive failure has been reported in previous investigations (cf. Greenway, 1987; Riestenberg, 1994; Wu & Watson, 1998). Riestenberg (1994) concluded that root pull-out resistance is mobilised gradually and that roots fail at different amounts of displacement, depending on their individual morphology. Consequently the measured shear resistance is a combination of the resistance provided by individual roots at different stages of strength mobilisation. Nevertheless it is still directly related to the total root area ratio present on the shear plane.

It seems therefore, that in this investigation shear failure in root reinforced soil does not progress according to the simple root model of Waldron (1977) and Wu *et al.* (1979). A more realistic model based on the results of this study is given in Figure 5.16. It consists of three stages:

1. Initially the roots are at rest.
2. An applied shear force causes deflection of the roots. Most roots provide a resistance to shear through a tensile force (T) that develops due to soil pressure (P) acting against the root. In some instances the tensile force will reach the full tensile strength (T_u) of the root and the root will break. At this stage the total shear resistance is still increasing as a sufficient quantity of root failures to cause a reduction in shear resistance has not occurred.
3. The full tensile strength is reached and therefore root breakage occurs, in a sufficient quantity of roots to cause a reduction in the measured shear resistance.

The equations given in Figure 5.16 represent an idealised case of three identical roots crossing the failure plane and are not applicable for assessment of any realistic condition. This is because in realistic conditions the value of T will vary significantly between different roots of different morphologies and locations on the shear plane, and at different displacements of the soil. These equations do however illustrate the different reinforcement potentials at different stages of in-situ shear tests. To calculate the maximum shear resistance that can be measured for a given soil-root system it is necessary to know the value of T for every root in the system at the appropriate displacement, and the value of T_u for the root that breaks at this point. It is not possible to determine these values and therefore present a definitive solution from the results in this

investigation and so the maximum shear stress is determined from the tests that are believed to have reached stage 3 and therefore passed the point at which the maximum shear resistance is recorded.
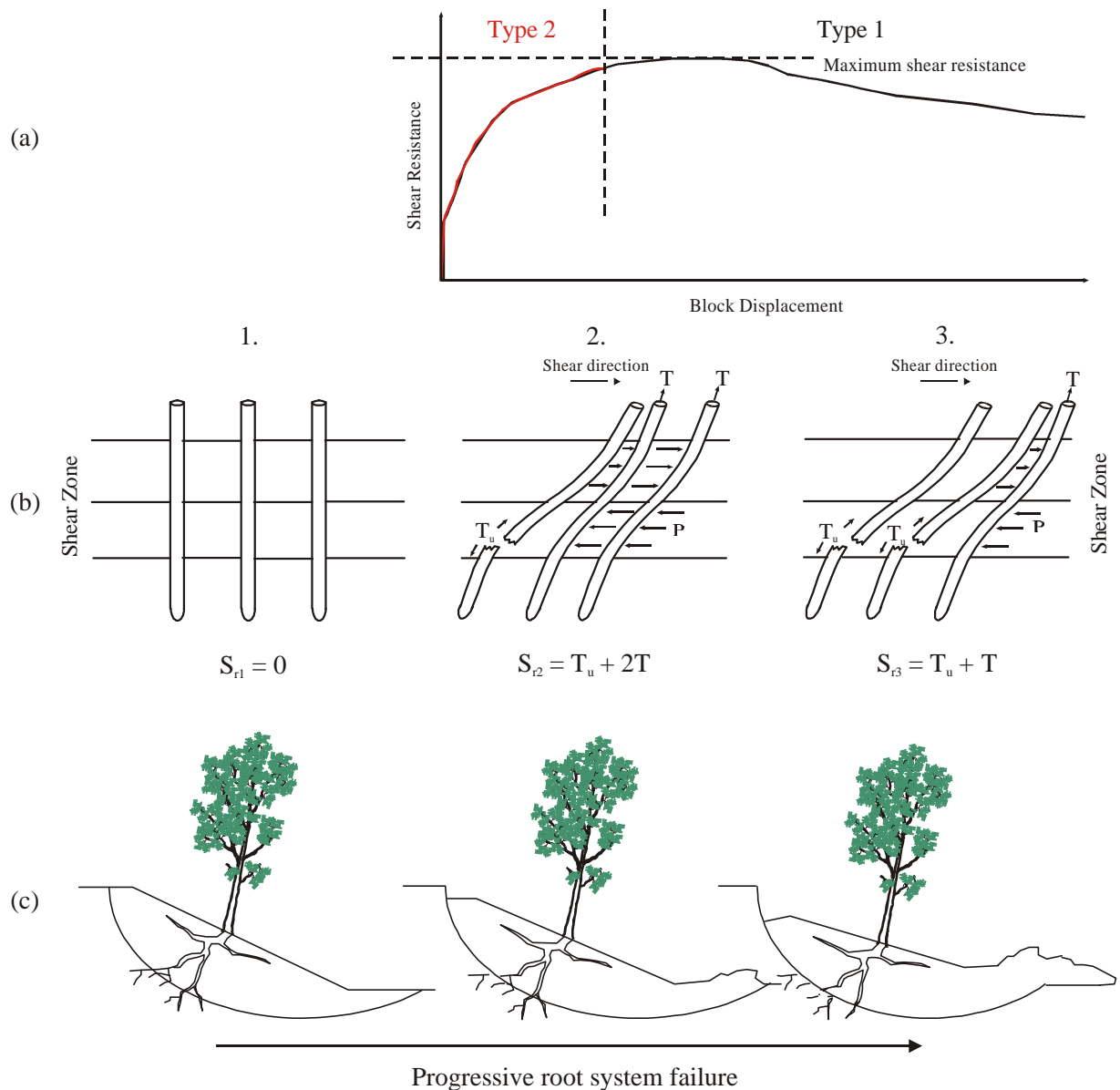
Figure 5.16: Three stages of root reinforcement for three idealised and identical roots as estimated from the results of direct in-situ shear tests conducted in this investigation. <u>Stage 1</u>: Prior to application of an applied shear force the roots are at rest across the potential shear plane. In the simplest model they are assumed to extend perpendicular to this plane. <u>Stage 2</u>: An applied shear force causes deflection of the roots in a wide shear zone. At this stage the majority of roots provide resistance through a tensile force (T) that is mobilised as soil pressure (P) acts against the root. <u>Stage 3</u>: Sufficient displacement of the block has mobilised the full tensile strength (T_u) in a sufficient quantity of roots to cause a reduction in measured shear resistance ($S_{r2} > S_{r3}$). **(a)** The three stages of root reinforcement and their representation on the shear resistance versus block displacement plots from direct in-situ shear tests. Stage 2 is characterised by Type 2 test behaviour and stage 3 is characterised by Type 1 test behaviour. **(b)** The three stages of root reinforcement for three idealised and identical roots. S_{r1}, S_{r2}, and S_{r3} are the shear resistance provided by the soil-root system at stages 1, 2, and 3 respectively. Note that the root furthest to the left in stage 3 does not contribute significantly to shear resistance, having previously failed at stage 2. **(c)** The progressive root failure as illustrated in a natural slope failure condition.

The two distinct types of shear test result described in the previous section indicate different stages within the failure process. A Type 1 test result indicates that a sufficient quantity of roots have ruptured in order for the peak shear resistance to have been measured (stage 3), while a Type 2 test result indicates that a sufficient quantity of roots are yet to mobilise their full tensile strength in order for the peak shear resistance to have been measured (stage 2). Therefore Type 2 tests, and probably the majority of all direct in-situ shear tests, underestimate the potential increased shear resistance. The difference between the measured shear resistance of Type 1 tests and that of Type 2 tests reported in this study was found to be very small however it may not be in every situation. Different root system morphologies, the number and size of the roots present at the shear plane, and the shear displacement achievable with the apparatus will all be factors to consider. It is likely that greater test displacements will allow more roots to rupture and the test to reach stage 3 of the failure process proposed above, such that the maximum shear resistance can be measured.

The value which is presumed to represent the shear strength of the soil with roots, that is, the peak stress on the shear stress – displacement plot has been questioned in recent work concerning its usefulness for slope stability analysis. Ekanayake & Phillips (1999) argue that because soil with roots have the ability to resist larger shear displacements than fallow soil, the improved stability of a hill-slope is a measure both of the increased peak shear resistance and the increased shear displacement. They suggest a method of analysis of the results of in-situ shear tests based on the energy consumed in the shearing process and conclude that the more traditional limit equilibrium method may underestimate the ability of soil with roots to resist large shear strains. However the limit equilibrium method has been shown by many investigators to be a useful analytical approach to root reinforced stability assessments (cf. Greenway, 1987; Coppin & Richards, 1990; Wu, 1995). The relationships between S_r and RAR obtained from Type 1 tests, for the reasons discussed above, are expected to give the most reliable values of root-reinforcement for use in limit-equilibrium slope stability modelling. A comparison of these values with those calculated using root pull-out data from chapter four and the simple root model of Waldron (1977) and Wu *et al.* (1979) is presented in the following section. It illustrates the effect that progressive root failure has on the overall shear strength of the soil-root system.

5.7   Increased shear resistance calculated from root tensile strengths

The previous section indicates that progressive rather than instantaneous root failure occurs in this study. This section investigates the effect of progressive failure on the measured values of root reinforcement by calculating the increased shear resistance that would result from simultaneous tensile failure of all roots that crossed the failure plane in the direct in-situ shear tests, and comparing it with the actual measured values.

5.7.1   Method of analysis

The calculation of increased shear resistance is based on the simple model of fibre-reinforced soil subject to direct shear (Waldron, 1977; Wu *et al.*, 1979) that is commonly used to determine shear resistance from root tensile strength data (see Riestenberg & Sovonick-Dunford, 1983; Greenway, 1987; Shields & Gray, 1992; Abernethy & Rutherfurd, 2001). That is

$$S_r = T_r.RAR.(\cos\theta.\tan f + \sin\theta) \qquad\qquad [5.9]$$

where T_r is the tensile strength of the roots as determined by equations [4.9]-[4.12] for each species, the RAR is the root area ratio as measured from in-situ shear tests, and $\grave{e}$ is the angle of shear distortion ($\tan\theta = x/z$, where x is the shear displacement at failure and z is the thickness of the shear zone; Fig. 5.17). It is not possible to determine from the data available, the exact size of the shear distortion for each root present at the shear plane. Estimates are therefore made based on previous investigations and some observations of the in-situ test behaviour presented in the previous sections of this chapter.
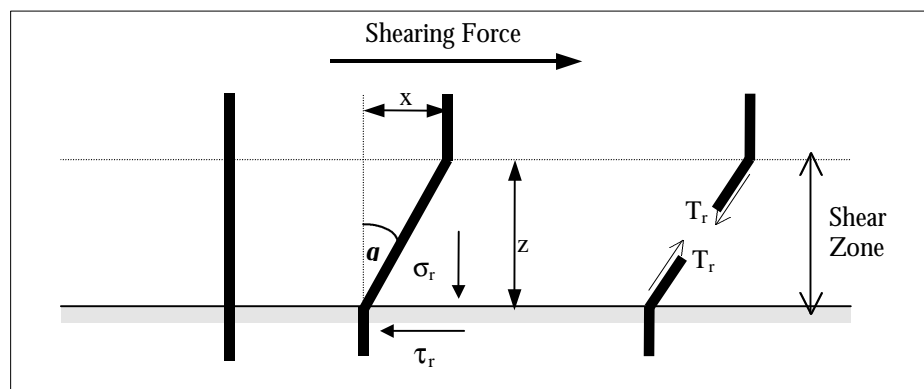
Figure 5.17: Model of a flexible, elastic root extending vertically across a horizontal shear zone.

In order to calculate the shear distortion, θ, it is necessary to estimate: 1) the shear displacement at failure, x; and 2) the thickness of the shear zone, z. First, as the model describes, all roots are assumed to be perpendicular to the shear plane in their initial position. While this situation is extremely unlikely, Gray & Ohashi (1983) report that such an assumption provides a reliable estimate of all possible root orientations. If all roots fail simultaneously then failure of the soil-root

system has effectively occurred when the peak shear resistance has been passed. Therefore the displacement of peak shear resistance, as determined from the direct in-situ shear test results, is the shear displacement at failure, x, for use in equation [5.9].

Second, it is necessary to estimate the likely thickness, z, of the shear zone. Wu & Watson (1998) investigating the root failure process when not constrained to a thin shear zone, estimated that shear zones were in the order of 42 cm thick. As the roots in this study are of a similar size to those measured by Wu & Watson (1998) and the shear zone is also not constrained to a thin zone, it is expected that the thickness of the shear zone will be of a similar size. Observations of the in-situ shear tests recorded in this chapter support this approximation. For instance if the shear plane, which occurs at the base of the block, exists at approximately the midpoint of shear zone thickness (i.e. 21 cm), in many tests reported in this chapter the shear zone will extend to the top of the block (block heights ranged between 21 cm and 42 cm). This is particularly so in *A. floribunda* tests, where the blocks were cut slightly shallower in order to access a range of root area ratios, and may help explain the shearing process in many of the *A. floribunda* tests where a tipping of the applied normal load often occurred (Fig. 5.8). When blocks were cut at depths greater than around 0.3 m the failure process in *A. floribunda* was relatively smooth, as it was for the other three species. This observation supports the estimation that the limit of shear zone thickness is around 20 to 25 cm above the failure plane. Assuming an equivalent limit below the failure plane suggest that Wu & Watson's (1998) estimations are a good approximation for use in this study.

As x = the displacement of the block at peak shear resistance for each test and z = 420 mm, as described in the previous two paragraphs, θ can then be calculated ($\tan\theta = x/z$), which enables the calculation of the term ($\cos\theta.\tan f + \sin\theta$) for use in equation [5.9]. The resulting shear distortion angles (θ), and values of ($\cos\theta.\tan f + \sin\theta$) range between 1 and 25 degrees, and 0.62 and 0.98 respectively (Table 5.6). The average angle is 35 degrees and the average value of ($\cos\theta.\tan f + \sin\theta$) is 0.75.

To calculate T_r and RAR for each in-situ shear test the roots crossing the shear plane were divided into five size classes based on diameter. The size classes used were 0-1 mm, 1-2 mm, 2-5 mm, 5-10 mm, and > 10 mm. The midpoint of each size class was the diameter used with the tensile strength relationships reported in chapter four to obtain T_{ri}, the tensile strength of roots in the size class i, which was then multiplied by n_i, the number of roots in size class i, to obtain T_r for roots of that size. The sum of T_r for each size class gives the total value of T_r. The RAR was also calculated using the midpoint diameter and the number of roots within each size class. With the other parameters determined as outlined above, equation [5.9] can then be used to calculate S_r, assuming simultaneous tensile failure of all roots present at the shear plane of in-situ shear tests.

Table 5.6: Shear distortion angles and values of (cosθ.tan$f$ + sinθ) = ✖, for use in equation [5.9]

Sample	C. glauca		E. amplifolia		E. elata		A. floribunda	
	θ°	✖	θ°	✖	θ°	✖	θ°	✖
1	8	0.74	2	0.64	1	0.62	4	0.69
2	12	0.81	2	0.65	3	0.65	4	0.67
3	2	0.65	10	0.77	2	0.65	4	0.67
4	9	0.76	2	0.64	2	0.65	3	0.65
5	10	0.77	16	0.86	14	0.83	5	0.69
6	15	0.85	5	0.69	2	0.65	10	0.77
7	2	0.65	15	0.85	3	0.66	18	0.89
8	1	0.63	13	0.82	13	0.83	2	0.64
9	12	0.80	14	0.84	2	0.64	3	0.67
10	22	0.94	2	0.65	10	0.77	4	0.68
11	12	0.80	19	0.91	13	0.82	3	0.66
12	2	0.65	11	0.79	14	0.84	6	0.71
13	8	0.74	2	0.65	9	0.75	23	0.95
14	7	0.73	1	0.63	2	0.65	3	0.66
15	7	0.72	14	0.83	12	0.81	5	0.69
16	11	0.79	9	0.77	11	0.80	5	0.69
17	9	0.76	4	0.68	9	0.76	9	0.76
18	13	0.82	9	0.75	1	0.62	15	0.84
19	5	0.70	12	0.81	2	0.65	12	0.80
20	18	0.89	10	0.78	12	0.80	10	0.77
21	12	0.80	13	0.82	19	0.90	15	0.84
22	25	0.98	19	0.90	6	0.70	11	0.79
23	9	0.77	21	0.93	22	0.94	11	0.79
24	1	0.62	11	0.78	10	0.78	3	0.66
25	1	0.62	8	0.75	17	0.88	8	0.74
Average:	**9**	**0.76**	**10**	**0.77**	**8**	**0.75**	**8**	**0.73**

5.7.2 Results and discussion

The root numbers, and increased shear resistance results are presented in Appendices C-XIII to C-XVI. Plots of increased shear resistance versus root area ratio gave positive power relationships (Fig. 5.18) approximated by the equations:

C. glauca	$S_r = 124.17 \times RAR^{0.9663}$	$R^2 = 0.92$	[5.10]
E. amplifolia	$S_r = 96.92 \times RAR^{0.7982}$	$R^2 = 0.90$	[5.11]
E. elata	$S_r = 116.34 \times RAR^{0.864}$	$R^2 = 0.94$	[5.12]
A. floribunda	$S_r = 287.27 \times RAR^{0.932}$	$R^2 = 0.91$	[5.13]

These relationships are much higher than the relationships measured from direct in-situ shear tests (Fig. 5.18). At the average RAR the calculated values are higher than the measured values by 10.9 kPa in *C. glauca*, 19.0 kPa in *E. amplifolia*, 19.3 kPa in *E. elata*, and 8.8 kPa in *A. floribunda*. This

magnitude of difference between calculated and measured values indicates clearly that a determination of increased shear resistance assuming simultaneous failure of all roots crossing the shear plane, is not appropriate for the conditions present in this study. Such an assumption would seriously over-estimate the potential earth-reinforcing ability of the roots and generate misleading indications of stability (i.e. an overestimate of the FoS for a slope).

Measured in-situ shear resistance values over the range of RARs assessed in this study, are on average only 32 % of the calculated shear strength values in the case of *C. glauca*, 27 % in the case of *E. amplifolia*, 32 % for *E. elata*, and 60 % for *A. floribunda*. The much higher values obtained for *A. floribunda* suggests that more roots are mobilising shear resistance at the same displacement. Just why this is the case in *A. floribunda* and not in the other three species is difficult to explain although it probably results from a greater proportion of total root area comprising smaller roots in *A. floribunda* tests (Appendix C-XII), and the likelihood that small roots reach their full tensile resistance at smaller shear displacements.
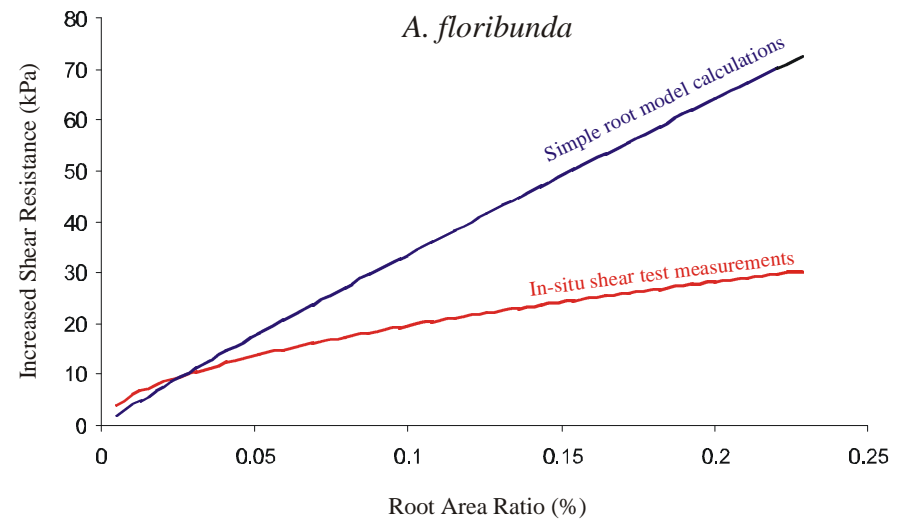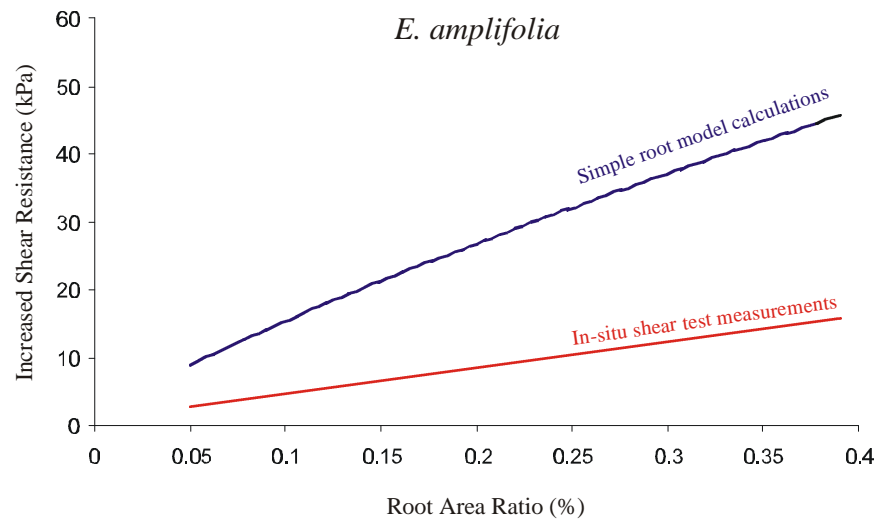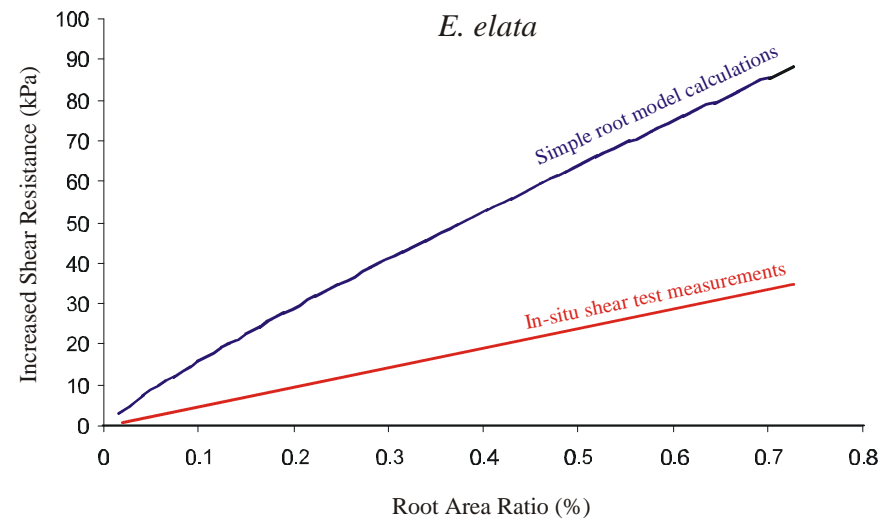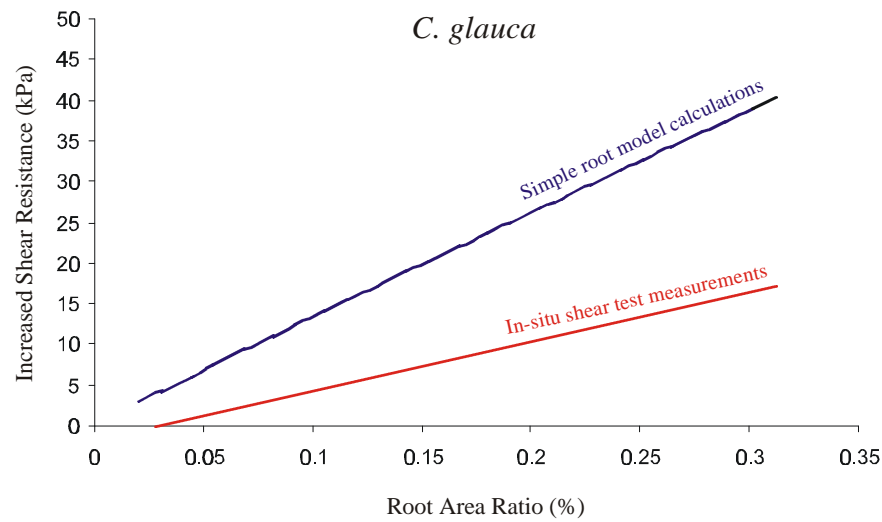
Figure 5.18: A comparison of increased shear strength between measured in-situ results (Red line) and calculated values (Blue line) using Waldron's (1977) and Wu *et al.*'s (1979) model, assuming that all roots fail simultaneously at the shear plane. For all RARs and all species the measured values are significantly lower than the calculated values that assume simultaneous tension failure of all roots at the shear plane.

5.8 Conclusions

Direct in-situ shear tests were conducted on blocks of soil containing roots of four species of native riparian tree. Variations in shear resistance with displacement were investigated within the context of the number and size of roots present on the shear plane. Relationships between RAR and increased shear resistance were obtained for each species. The results have also been interpreted in the context of the test methodology and soil-root interaction where the shear zone is not constrained to a thin zone. The following conclusions have been drawn from the results and interpretations presented:

1. There are significant differences in increased shear resistance between species tested by direct in-situ shear test at the same location. However all species demonstrate a predictable relationship between root quantity as expressed as RAR at the shear plane, and the increase in shear resistance relative to the soil-only tests. Root reinforcement of the soil increases with increasing RAR according to the relationships:

    $$S_r = 61.16 \text{ x RAR} - 0.91 \text{ for } \textit{Casuarina glauca}$$
    $$S_r = 38.12 \text{ x RAR} + 0.85 \text{ for } \textit{Eucalyptus amplifolia}$$
    $$S_r = 52.09 \text{ x RAR} + 0.66 \text{ for } \textit{Eucalyptus elata}$$
    $$S_r = 81.13 \text{ x RAR}^{0.5866} \text{ for } \textit{Acacia floribunda}$$

2. In order of greatest soil strength enhancement for equivalent RAR as measured by direct in-situ shear tests are: *A. floribunda*, *C. glauca*, *E. elata*, and *E. amplifolia*.

3. The direct shear tests demonstrate that roots do not break all at once as is often assumed in investigations of root enhanced shear resistance. Progressive failure of the soil and the deformation of roots in a large shear zone enable different roots to break at different displacements.

4. There are generally two distinct types of in-situ shear test behaviour which correspond to different stages of soil-root system failure. Type 1 tests are characterised by a definitive peak and then reduction in shear resistance and resemble an over-consolidated soil test. They result from a sufficient quantity of roots having failed in tension to enable the maximum shear resistance value for that sample to be achieved. Type 2 tests are characterised by no reduction in shear resistance and resemble a normally consolidated soil test. They result from a number of roots that have not failed within the displacement achievable in the test and therefore uncertainty over whether or not the maximum shear resistance has been measured. Type 1 tests are therefore considered a more accurate reflection of increased shear strength provided by tree roots during natural failures. The difference in S_r between the two test types, although fairly consistent for all species other than *E. amplifolia*, is small.

5. A three stage process of soil-root failure during shear is proposed based on some observations made in this study and the work of Wu & Watson (1998). Illustrated in Figure 5.16 the process consists of multiple roots that fail in tension at different amounts of shear

displacement. The stage at which the soil-root system is at depends on whether or not a sufficient quantity of roots have failed in tension for the maximum shear resistance to have been achieved. Prior to the maximum shear resistance being reached the soil-root system is at stage 2 and characterised as a Type 2 in-situ shear test behaviour. After the maximum shear resistance has been reached the soil-root system is at stage 3 and characterised as a Type 1 in-situ shear test behaviour.

6. Determining the increased shear strength of soil containing roots based on root tensile strength data and Waldron's (1977) and Wu *et al.*'s (1979) simple root model will lead to a significant overestimate of the actual root reinforcement potential in this environment. The average difference between S_r calculated in this manner and that measured from direct in-situ shear test is 10.9 kPa for *C. glauca*, 19.0 kPa for *E. amplifolia*, 19.3 kPa for *E. elata*, and 8.8 kPa for *A. floribunda*.

Chapter Six

Modelling earth reinforcement beneath riparian trees

6.1   Introduction and overview

This chapter presents the integration of the root system architectural assessment of chapter three with the root strength experimental results of chapters four and five, to generate models of reinforced earth for use in the riverbank stability assessment presented in chapter seven. A realistic estimation of the spatial distribution of reinforcement is required to enable an evaluation of the stability of the slopes that the roots reinforce. In order to do this a model of reinforced earth must be devised that allows for inclusion of root reinforcement data into slope stability computations. In a forested hill-slope analysis where root reinforcement is generally considered to display minor lateral variability and an infinite slope model is sufficient for analysis, this is achieved by the addition of S_r to the Mohr-Coulomb soil strength equation for the particular depth concerned (cf. Wu *et al.*, 1979). However in situations where lateral variability is recognised, and where the slopes are subject to rotational failures, a more complex analytical characterisation of the root reinforcement within the slope is required. Terwilliger and Waldron (1991) used a three-dimensional infinite slope analysis to model differences in soil-slip size beneath differing root reinforcement distributions. They did not however use different root reinforcement values on the same slide surface, and so their analysis was based on using a uniform distribution for each individual test. Abernethy & Rutherfurd (2000a) modelled root reinforcement in a conventional slope stability program by incorporating discrete values of C_r that defined root reinforcement at any given co-ordinate pair consisting of depth below the profile surface and lateral distance from the tree stem. The soil cohesion within the modelled riverbank therefore varied with respect to the location of a single tree (for River Red Gum) or a stand of trees (for Swamp Paperbark) present on the slope.

The approach undertaken to assess riverbank stability in this study, follows that of Abernethy & Rutherfurd (2000a), and involves the alteration of soil properties within a conventional slope stability program to incorporate the spatial distribution of root reinforcement with respect to both distance from the tree stem and depth within the soil layer. In contrast to Abernethy & Rutherfurd's (2000a) model which used discrete points for each value of cohesion, the model presented in this chapter describes soil zones of increased shear resistance (similar to Collison *et al.*, 1995). The model is based on a system of soil layers with different strength properties, that vary in both areal extent and magnitude of S_r for each of the four different tree species examined. The model is altered to incorporate the different soil strength properties extant beneath either a single tree, or multiple trees of the same species, and multiple species that replicate a simplified riparian forest.

6.2 The spatial distribution of increased shear resistance

It is well established that increased soil shear strength is dependent on the quantity of root material that crosses a potential shear plane. Hence the distribution of this reinforcement within the soil mass of a riverbank will be directly related to the spatial distribution of root material which can be quantified as the Root Area Ratio. The distribution of root material below an individual tree decreases exponentially and relatively smoothly both with depth and with distance away from the tree stem (chapter three). However in order to be able to incorporate the data into the slope stability program 'XSLOPE' (see chapter seven) it has been necessary to divide the soil mass into a series of zones with distinct limits. These limits were set at 25 %, 50 % and 100 % of the maximum lateral root extent and depths of 25 %, 50 %, 75 % and 100 % of the maximum vertical root extent. The RAR and therefore the value of S_r within each soil zone is that calculated at the midpoint of the zone's limits and is conservatively applied to the whole zone in a similar manner to the procedure used by Hubble & Hull (1996) and Hubble (2001).

S_r was determined from the experimental relationships in chapter five and is added to the Mohr-Coulomb soil shear strength failure criterion such that the soil shear strength, S is calculated by:

$$S = S_r + c' + (\sigma - u) \tan f \qquad [6.1]$$

where c' and f are the effective stress parameters for cohesion and internal friction angle respectively, and $(\sigma - u)$ is the effective normal stress with u, the pore pressure. As discussed in chapter one the value S_r is often considered as an additional apparent cohesion (Waldron, 1977; Wu *et al.*, 1979; O'Loughlin & Ziemer, 1982) as small roots are seen to behave as part of a soil-root matrix rather than as individual elements. While this has been shown to be an imperfect model of real behaviour in this study (chapter 5), the resultant reinforcing effect is effectively the same regardless of whether it is modelled as additional apparent cohesion or as an additional shear strength provided by distinct tensile elements within the soil mass.

The calculation of S_r to be used in equation [6.1] was undertaken using relationships that were obtained with RARs up to a maximum of 0.7 %. However the distributions of root material within the soil, that were determined in chapter three, include RARs much greater than this (up to 4.5 %). It is not known with certainty if the relationships used to calculate S_r continue beyond the range of RAR values measured in the tests. Therefore values of RAR used to calculate S_r were capped at a maximum of 1.0 %.

The resultant distribution of increased shear resistance, S_r, beneath each tree species is illustrated below (Figs. 6.1-6.4).
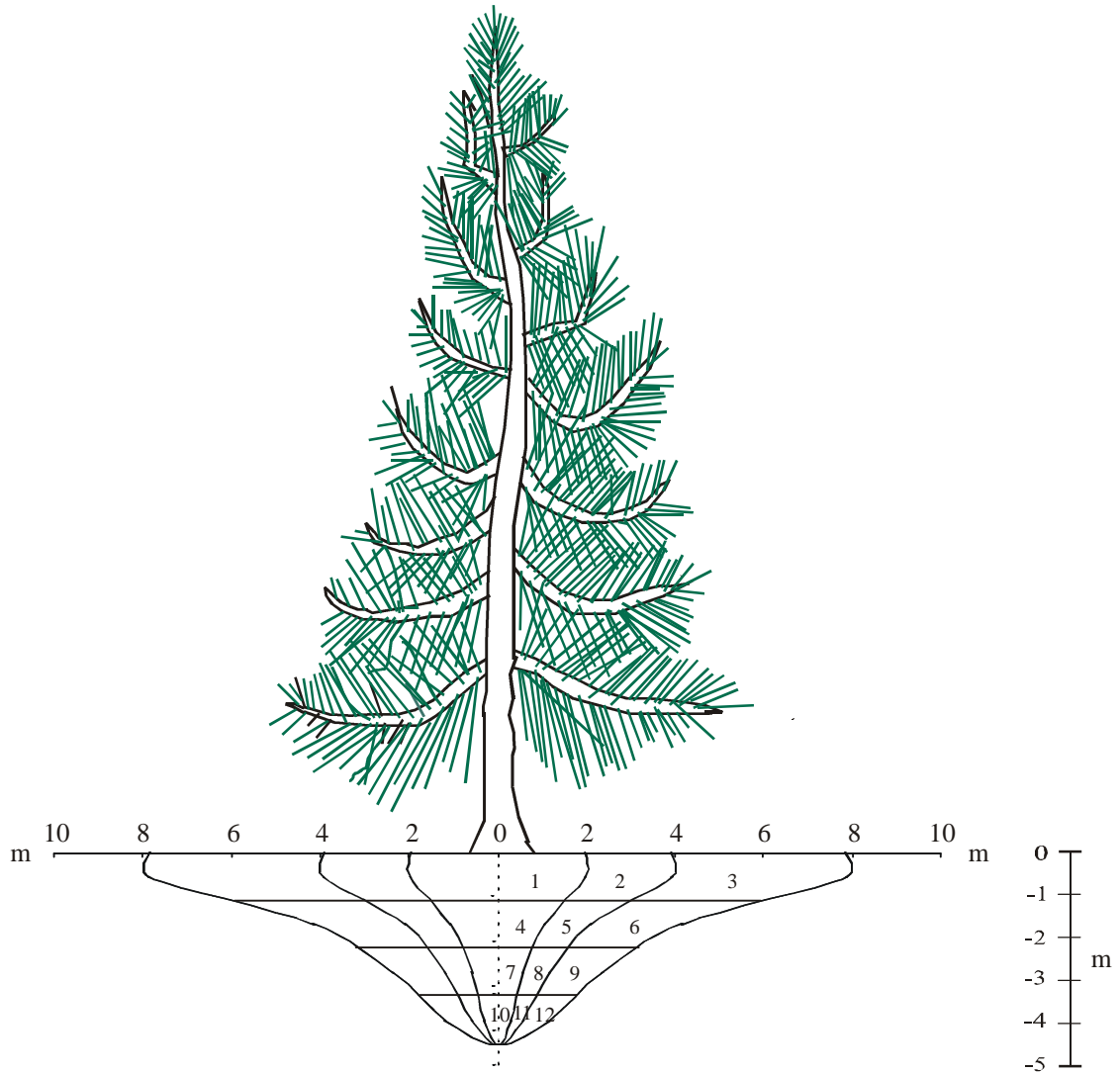
Figure 6.1: The distribution of increased shear resistance below a mature *C. glauca* tree. Reinforcement zones are numbered as soil layers with the value of S_r for each layer given in the table below. Vertical and lateral distances are in metres.

Table 6.1: Values of S_r for each soil layer below a mature *C. glauca* tree as represented in Figure 6.1.

	S_r (kPa)		S_r (kPa)
Layer 1	8.49	**Layer 7**	3.74
Layer 2	0.07	**Layer 8**	0.00
Layer 3	0.00	**Layer 9**	0.00
Layer 4	3.92	**Layer 10**	1.72
Layer 5	0.13	**Layer 11**	0.00
Layer 6	0.00	**Layer 12**	0.00
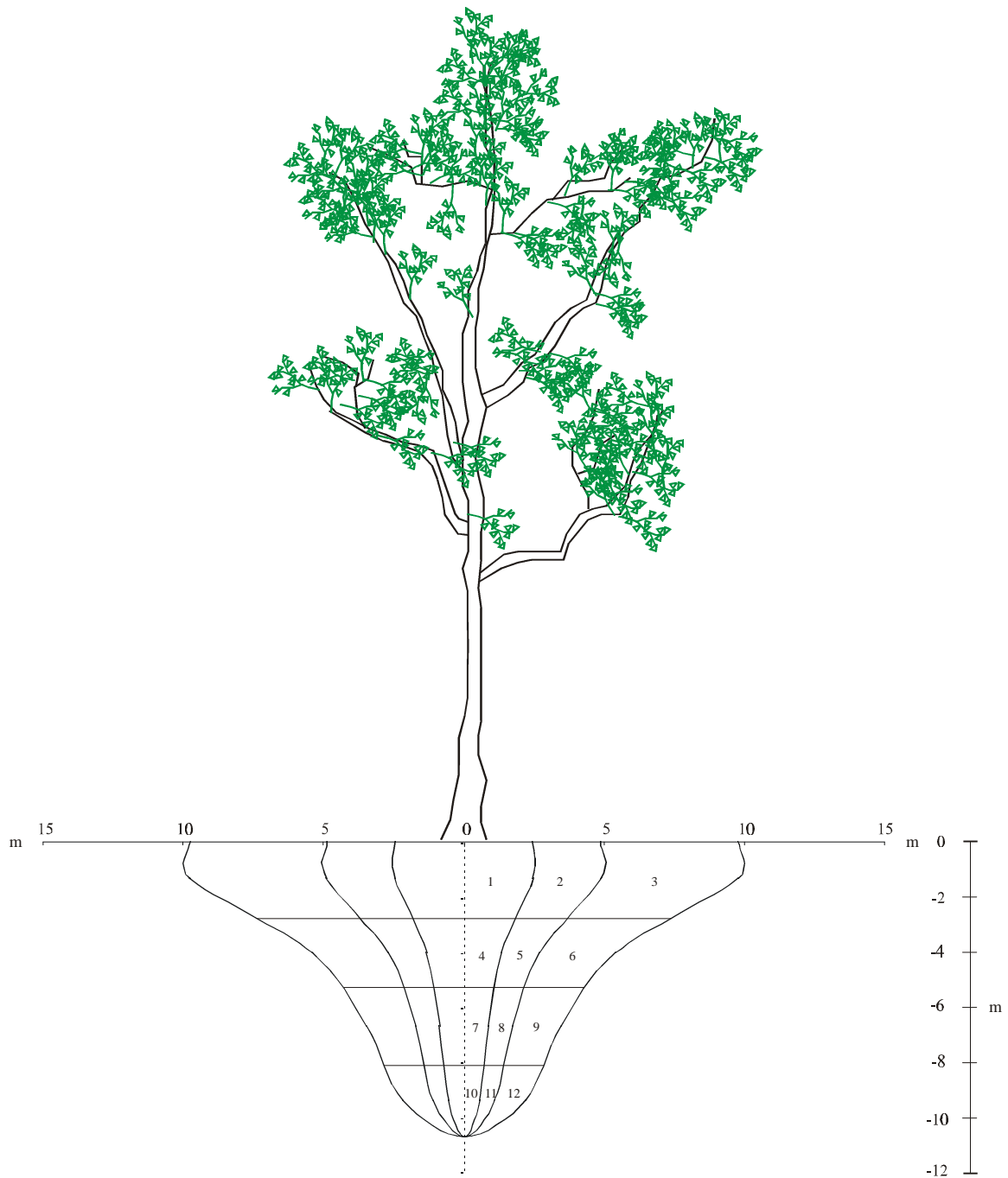
Figure 6.2: The distribution of increased shear resistance below a mature *E. amplifolia* tree. Reinforcement zones are numbered as soil layers with the value of S_r for each layer given in the table below. Vertical and lateral distances are in metres.

Table 6.2: Values of S_r for each soil layer below a mature *E. amplifolia* tree as represented in Figure 6.2.

	S_r (kPa)		S_r (kPa)
Layer 1	38.55	**Layer 7**	13.81
Layer 2	5.27	**Layer 8**	3.56
Layer 3	1.35	**Layer 9**	1.50
Layer 4	25.17	**Layer 10**	7.18
Layer 5	3.21	**Layer 11**	2.95
Layer 6	1.04	**Layer 12**	1.92
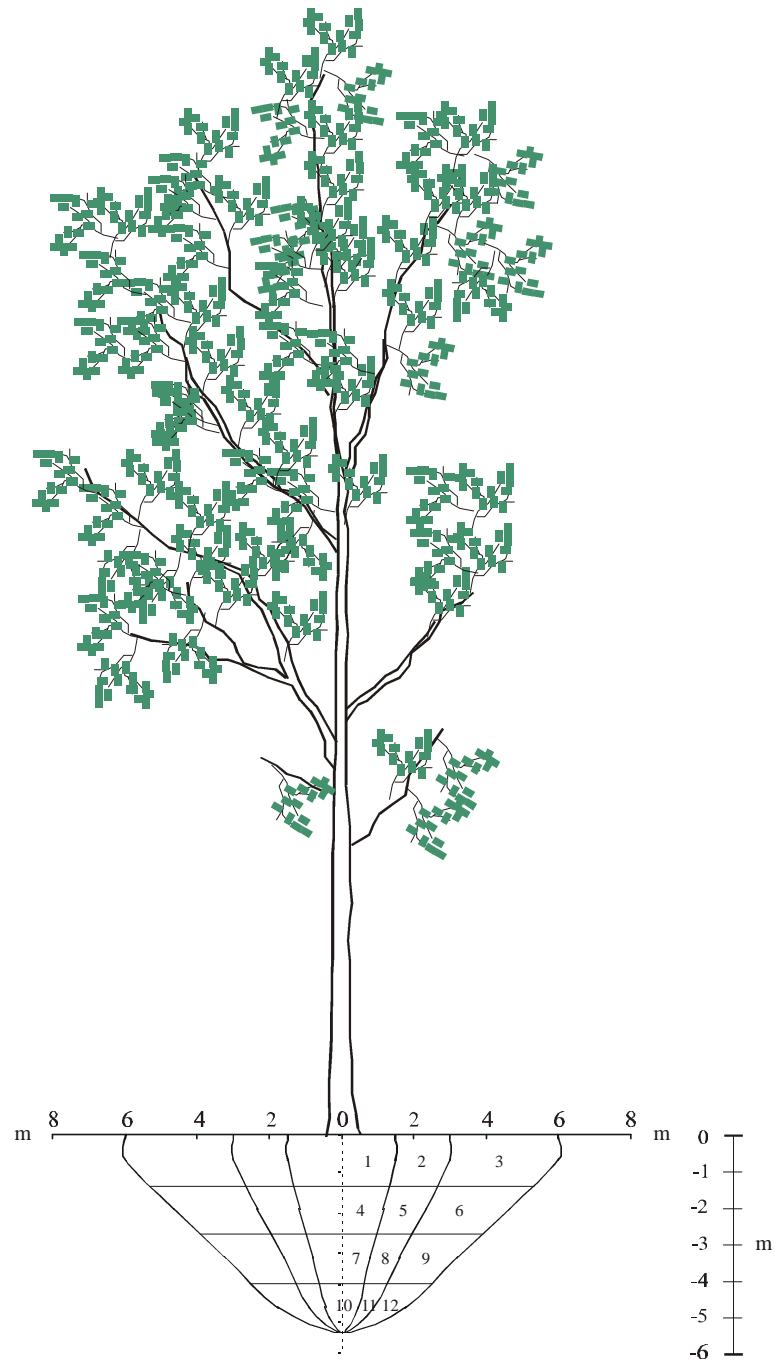
Figure 6.3: The distribution of increased shear resistance below a mature *E. elata* tree. Reinforcement zones are numbered as soil layers with the value of S_r for each layer given in the table below. Vertical and lateral distances are in metres.

Table 6.3: Values of S_r for each soil layer below a mature *E. elata* tree as represented in Figure 6.3.

	S_r (kPa)		S_r (kPa)
Layer 1	52.75	**Layer 7**	11.23
Layer 2	20.87	**Layer 8**	3.32
Layer 3	2.17	**Layer 9**	1.49
Layer 4	52.75	**Layer 10**	5.24
Layer 5	6.18	**Layer 11**	2.01
Layer 6	1.08	**Layer 12**	1.23
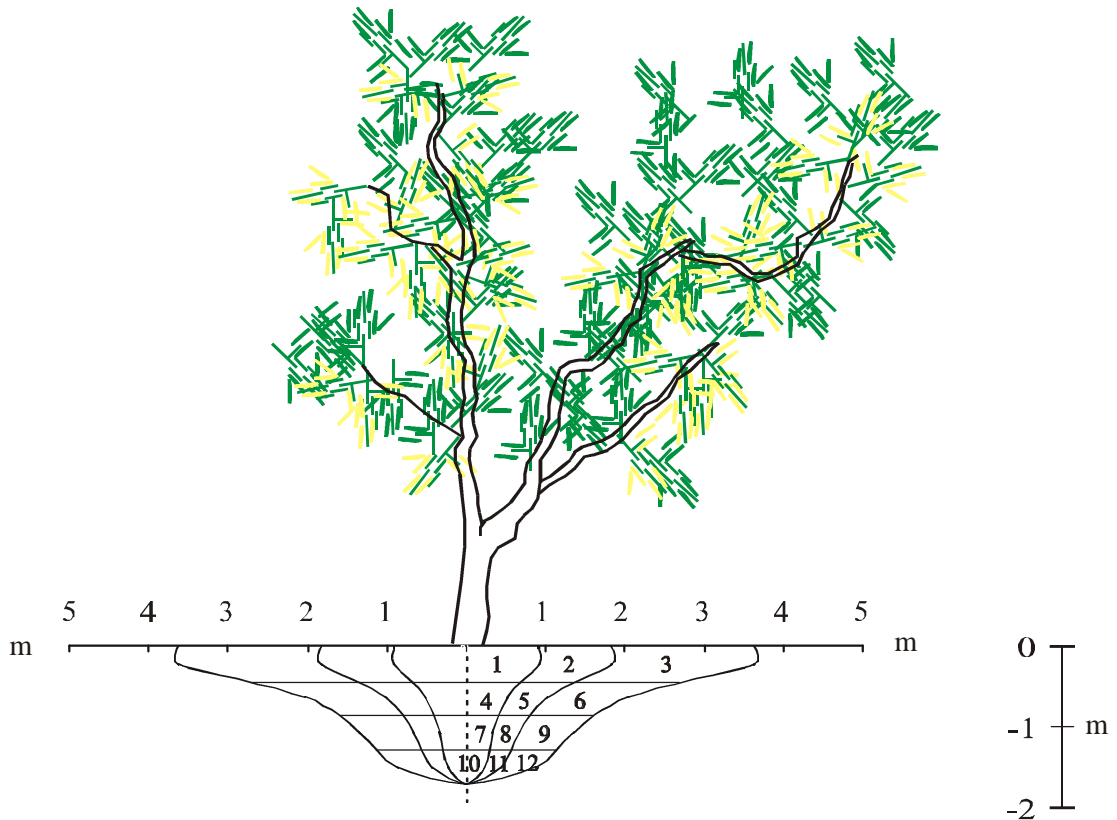
Figure 6.4: The distribution of increased shear resistance below a mature *A. floribunda* tree. Reinforcement zones are numbered as soil layers with the value of S_r for each layer given in the table below. Vertical and lateral distances are in metres.

Table 6.4: Values of S_r for each soil layer below a mature *A. floribunda* tree as represented in Figure 6.4.

	S_r (kPa)		S_r (kPa)
Layer 1	61.75	**Layer 7**	19.24
Layer 2	12.64	**Layer 8**	6.91
Layer 3	2.12	**Layer 9**	2.69
Layer 4	37.47	**Layer 10**	12.10
Layer 5	11.54	**Layer 11**	4.04
Layer 6	3.18	**Layer 12**	1.41

The distribution of S_r is clearly different between species both in terms of its amount and spatial extent. *A. floribunda* has the highest values of root reinforcement however the volume of soil over which it acts is smaller than any other species. *C. glauca* on the other hand reinforces a relatively large volume of soil however the actual quantity of root material within this zone is small (see chapter three) and so the amount of reinforcement is small. So much so that for all intents and purposes it is zero in the outer lateral zones: Layers 3, 6, 8, 9, 11, and 12.

All species clearly exhibit dramatic differences in root reinforcement values from one zone to the next. This is consistent with the exponential reduction in root quantity both with depth and lateral distance from the tree stem. Therefore all species studied produce a central 'cone' of maximum reinforcement with the two shallowest zones providing the vast majority of reinforcement potential

beneath a single tree of each species. This characteristic is similar to the results reported by most other root reinforcement studies, which have found that it is in the first metre or two below the soil surface where roots contribute most to soil strength (cf. Shields & Gray, 1992; Riestenberg, 1994; Abernethy & Rutherfurd, 2001). Interestingly, a comparison of increased shear strengths from this study with those of Abernethy & Rutherfurd's (2001) and Shields & Gray's (1992) data reveals S_r values of similar magnitude (Fig. 6.5). *C. glauca* values are close to that of *S. mexicana* (Elderberry) while the two Eucalypts and *A. floribunda* exhibit similar strengths to the other Australian species: *E. camaldulensis* (River Red Gum) and *M. ericifolia* (Swamp Paperbark).
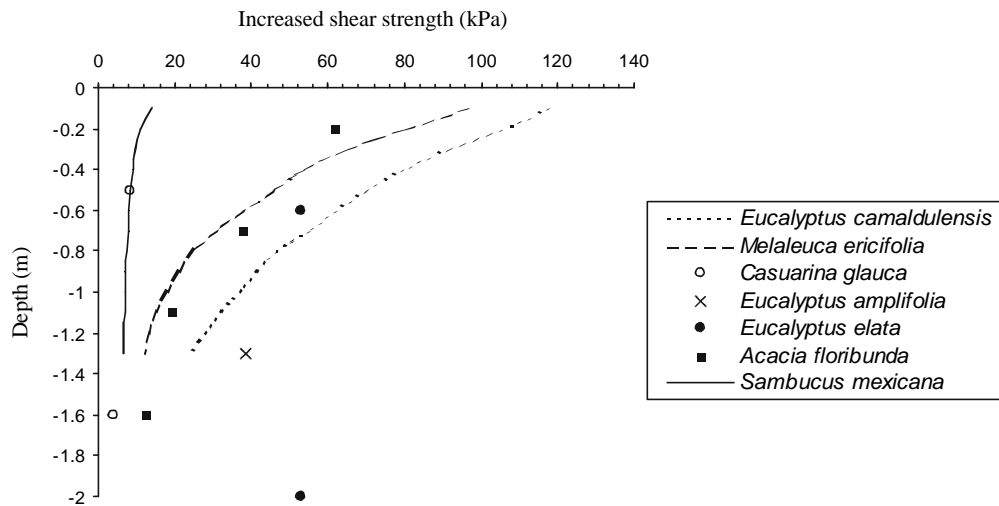
Figure 6.5: Comparison of increased shear strength values directly below the tree stem over the first 2 m of soil depth with those of Abernethy & Rutherfurd (2001)(*E. camaldulensis* and *M. ericifolia*) and Shields & Gray (1992)(*S. mexicana*). For the four species of this study the value of increased shear resistance presented is that predicted at the depth midpoint for each soil layer.

6.3   Earth reinforcement beneath multiple individuals

In order to estimate the improvement in riverbank stability below a cover of one species of tree, a model of the two dimensional distribution of root reinforcement due to individuals spaced at regular intervals is now presented. The model overlays root zone diagrams, such as those in Figs. 6.1-6.4, with others of the same species (e.g. Fig. 6.6). In this manner the boundaries of new root zones are determined. They incorporate the area-weighted average quantity of root material from the smaller overlapping zones of which they consist.

To a certain extent the determination of new root zones beneath multiple trees is limited because of the inability of the slope stability program 'XSLOPE' to model an infinite number of soil layers. Limitations on the number of soil layers and the number of nodal points that make up a bank profile meant that the new root zones were set at the first 25 % lateral distance from the tree stem, and in depth quartiles (see Fig. 6.6). Therefore the root reinforcement beneath a forest of trees of the same species consists of seven soil layers: four directly below the tree stem and three in the soil mass between the stems.
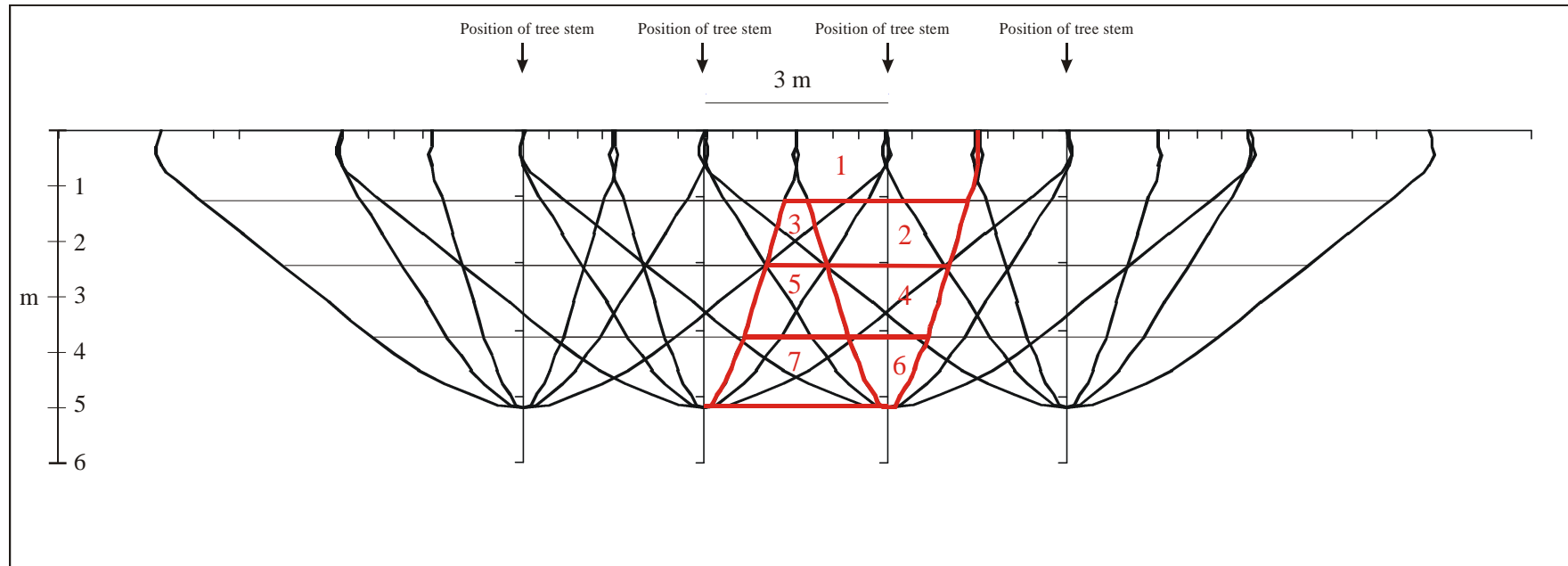
Figure 6.6: An example of the root reinforcement zone definitions for the soil beneath multiple trees of the same species. This illustration shows an *E. elata* forest with individuals spaced at 3 m intervals. Root reinforcement zone boundaries are marked in red. Made up of a number of smaller root zones where root material overlaps from different individual trees, the amount of reinforcement within is calculated using an area-weighted average RAR over each of the smaller zones that exist within its boundaries. Roots are assumed to grow uninhibited as a mass of intermingled elements despite the presence of the other trees.

Table 6.5: Values of S_r for each soil layer below a mature *E. elata* forest spaced at 3 m intervals, as represented in Figure 6.6.

	S_r (kPa)		S_r (kPa)
Layer 1	53.75	Layer 5	4.22
Layer 2	53.75	Layer 6	5.24
Layer 3	11.89	Layer 7	1.81
Layer 4	11.86		

The top soil layer (number 1) represents a continuous 'root mat' below the entire population of trees. Layers 2, 4, and 6 occur directly below the tree stems while layers 3, 5, and 7 occur in the volume of soil between individual trees. This sequence varied slightly depending on the different tree spacing. For instance when spaced closer together it was sometimes possible to use a second continuous 'root mat' layer in the second depth quartile, as volumes of soil with smaller quantities of root material between the trees were 'squeezed' out.

To determine S_r for each soil layer (marked by the red lines in Fig. 6.6), the Root Area Ratio of each individual tree within each small soil zone (marked by the black lines in Fig. 6.6) was added and then averaged across the entire new layer. S_r was calculated in the same manner as for individual trees, with the maximum RAR again capped at 1.0 %. The values of increased shear strength for the *E. elata* example presented in Figure 6.6 are given in the table below it (Table 6.5). This process was repeated for each species and for each tree size to be modelled in chapter seven. A total of nine times. The root distribution patterns and increased shear resistance values for an example of each species are presented in Appendix D-I.

This simplified model for multiple individuals assumes that roots will grow in their customary manner irrespective of the other trees located around them. It is not well known to what extent this occurs in nature although Coppin & Richards (1990) suggest that in vegetation and plant communities there is 'some degree of overlap' between the root distributions of individual trees. Watson & O'Loughlin (1985) report that they excavated many roots that were in direct contact with other roots of adjacent trees. Ashton (1975) reported the same finding directly beneath the tree stem. Observations of intermingled roots from different individuals growing within the same soil mass are common along the banks of the Nepean River although the extent to which the overall architecture of each tree's root system has been influenced by the presence of the other trees nearby is not known. Nevertheless the commonality of the phenomenon observed in the field and reported in the studies above, in combination with the conservative estimates of maximum root extent adopted for mature trees in this study suggest that the simplifying assumption, that the individual root system morphology has not been significantly altered by the presence of nearby trees, is reasonable.

6.4   Earth reinforcement beneath multiple species

Multiple species forests have been modelled using two species at a time. The distribution of reinforced earth beneath these 'species pairs' was determined in the same manner described in the previous two sections. However given the different tree sizes between species there was usually a greater number of 'root mat' soil layers close to the surface than beneath the single species forests. For example *E. amplifolia* modelled with *A. floribunda* (Fig. 6.7) consists of five continuous 'root mat' soil layers that exhibit no lateral variation in values of increased soil cohesion. Further soil layers occur both directly beneath the tree stems of the *E. amplifolia* trees (layers 6, 8, and 10) and also in between them (layers 7, 9, 11).
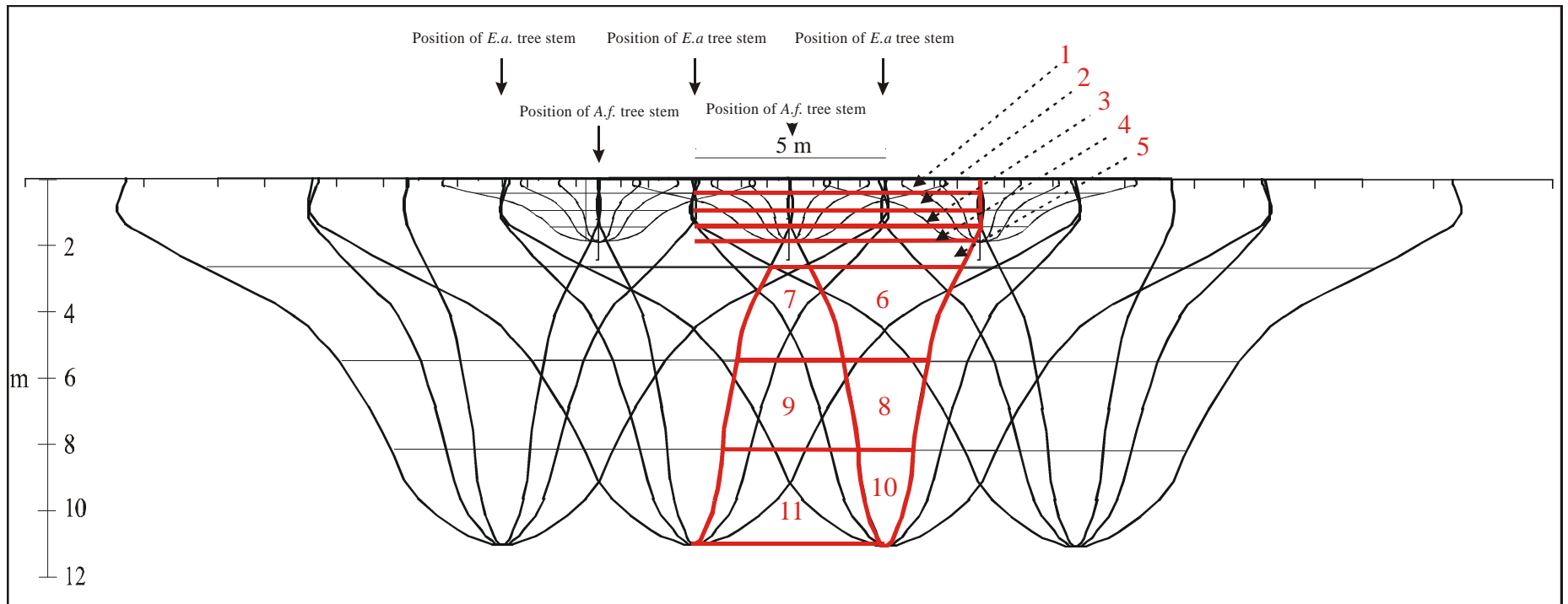
Figure 6.7: An example of the root reinforcement zone definitions for the soil beneath multiple trees of different species. This illustration shows an *E. amplifolia* and *A. floribunda* forest with individuals spaced at approximately 2.5 m intervals. Root reinforcement zone boundaries are marked in red. Made up of a number of smaller root zones where root material overlaps from different individual trees, the amount of reinforcement within is calculated using an average RAR over each of the smaller zones that exist within its boundaries. Roots are assumed to grow uninhibited as a mass of intermingled elements despite the presence of the other trees.

Table 6.6: Values of S_r for each soil layer below a mature *E. amplifolia* and *A. floribunda* forest spaced at 2.5 m intervals, as represented in Figure 6.7.

	S_r (kPa)		S_r (kPa)
Layer 1	86.09	**Layer 7**	3.21
Layer 2	62.94	**Layer 8**	13.81
Layer 3	46.90	**Layer 9**	3.02
Layer 4	43.75	**Layer 10**	7.18
Layer 5	38.09	**Layer 11**	2.60
Layer 6	25.44		

As with the single species model the soil layer boundaries are marked at the depth quartiles for both species and at the 25 % lateral root extent for the larger tree in the pair.

The increased shear resistance was calculated in the same manner as for the single species forest and with the maximum RAR again capped at a total for both species of 1.0 %. The values of increased shear strength for the *E. amplifolia* and *A. floribunda* example presented in Figure 6.7 are given in the table below it (Table 6.6). This process was repeated for each species pair that was assessed (Table 6.7) and the full results are presented in Appendix D-II.

Table 6.7: Combination of species pairs modelled in a multiple species forest.

1st species in pair	2nd species in pair
Casuarina glauca	*Acacia floribunda*
Eucalyptus amplifolia	*Casuarina glauca*
Eucalyptus amplifolia	*Acacia floribunda*
Eucalyptus elata	*Casuarina glauca*
Eucalyptus elata	*Acacia floribunda*

6.5   Concluding statement

The root distribution data presented in chapter three has been combined with the soil-root system strength data presented in chapters four and five to produce models of reinforced earth that describes the increased soil shear resistance within the soil mass beneath some native riparian trees. The models presented provide a realistic assessment of soil reinforcement and enable riverbank stability to be assessed under a range of vegetation covers. The stability analyses are presented in the following chapter.

Chapter Seven

The stability of root-reinforced riverbanks

7.1   Introduction and overview

Until recently the effect of vegetation on river channel form has been considered in the context of erosion rates and the change in parameters such as channel width and depth. These investigations tended to focus on resultant effects and empirical relationships rather then determining the causal mechanisms that govern a river channel's response to erosive events. Although the influence of channel boundary conditions on the rate of change is often acknowledged, the extent to which vegetation alters the boundary condition and therefore influences riverine morphology has been somewhat overlooked.

Recent work has begun to utilise the growing body of research into the geomechanical effects of vegetation on hill-slope stability, and apply it to the riverine setting (see Hubble & Hull, 1996; Abernethy & Rutherfurd, 2000a; Hubble, 2001; in press). Riverbanks are essentially a type of slope and so their stability is governed by the same principles as are hill-slopes and embankments. Hence the stability of an individual riverbank can be assessed in terms of slope geometry, hydrological conditions, surcharge weight, material properties, and of course vegetative reinforcement. Variations in these parameters will affect the calculated factor of safety of a slope.

A riverbank stability analysis differs from a hill-slope analysis primarily by the scale of the slide features relative to the overall geometry and by the hydrological conditions generally considered to precipitate failure. Although there are many different forms of riverbank collapse (see Hey *et al.*, 1991), the large size of the failure blocks in comparison to the size of the slope in most cases tends to reduce the utility of the infinite slope method used commonly in conventional hill-slope analysis, to that of a guide or first approximation of a bank's stability (cf. Hubble & Hull, 1996). Although Thomson (1970) provides an exception, the use of any number of solutions by slices or wedges is more appropriate in the riverine environment. The failure of a hill-slope often occurs under conditions of top-down saturation where a thin zone of saturated material is found close to the ground surface as in the case of a 'perched' water table, with flow considered parallel to the slope (e.g. Wu, 1995). Failure of riverbanks however generally occurs after the complete inundation by flooding and is triggered by the rapid draw-down of the water level in the channel with the bank material remaining saturated (Hubble & Hull, 1996; Lawler *et al.*, 1997). These conditions may lead to a build-up of pore pressure which destabilises the bank.

Despite these differences, the general principles involving a balance of forces, both restoring and destabilising, apply to both riverbanks and hill-slopes alike. The assessment of riverbank stability using geomechanical models will therefore provide an understanding of their resistance to change within environments where mass collapse is a common occurrence and a major erosive process. This resistance and the factors that influence it allow a discussion of channel boundary conditions that are more or less inhibitive to a wider morphological response.

Morphological change within the Nepean River system has been characterised over the last 50 years or so by the mass collapse of the banks, and has been more prevalent on those banks cleared of vegetation (Hubble, 1997; Docker & Hubble, 2001c). The stability of these riverbanks has been assessed in these previous studies although the quantitative mechanical influence of vegetation has been necessarily inferred from studies undertaken in exotic locations using exotic tree species. The data on enhanced soil strength and its distribution within riverbank stratum presented in chapters three, four and five, and synthesised in chapter six into a model of reinforced earth, allows a much more sophisticated and therefore accurate riverbank stability analysis to be conducted. The effect of devegetation as well as the potential stability enhancements due to the revegetation of 'present-day' profiles are assessed by modelling the changes in bank stability due to differences in tree species, density, mix, size, and position on a bank profile.

7.2   Stability modelling input parameters

7.2.1   The slope stability program 'XSLOPE'

The riverbank stability analysis was undertaken using the professionally certified and indemnified software package 'XSLOPE' developed at the Centre for Geotechnical research at the University of Sydney (Balaam, 1994). The program is based on Bishop's method of slices (Bishop, 1955) and assumes a rotational failure over a circular arc. Circular failure arcs are the failure mechanism generally associated with homogenous soil (Craig, 1992) and are the most commonly observed type affecting the banks of the Nepean River study area (Hubble, 2001).

The mathematical expression for the factor of safety (FoS) used by XSLOPE places the factor of safety term on both sides of the equation (see chapter two). Therefore an iterative method of solution is required whereby the initial FoS on the right hand side of the equation is calculated using the Swedish slice analysis of Fellenius (1936). The iterative solution for the FoS of the slope usually converges satisfactorily in less than four iterations (Balaam, 1994).

The XSLOPE analysis calculates the factor of safety for a large number of assumed circles, in the case of this study, 5000, and determines the critical circle, that is the one with the minimum factor of safety. The circle centres and radii are automatically determined for the specified number of circles but an interactive analysis also allows these values to be determined manually. Thus the factor of safety for a specified circle can be assessed under different bank material conditions such as changes in shear strength associated with different vegetated conditions. For a complete description of XSLOPE, see Balaam (1994).

7.2.2   Riverbank geometry

The riverbank stability assessments presented below focus on typical riverbank geometries present within the study area both prior-to and after failure. 'Pre-failure' bank geometries, those assumed to exist prior-to failure, were determined by a comparison of the existing profile with those immediately upstream and down and also to the general shape of the banks as they appear in the 'pre-failure' aerial photographic record. Although this method is not ideal, it is the only practical method available because prior survey data does not exist. It has been used with some success in other parts of the Hawkesbury-Nepean channel (Docker, 1997; Hubble, 1998; in press). 'Present-day' bank geometries, those as they exist today, are available for approximately forty cross-sections within the Camden Valley (Hubble, 1996) and twelve within the Wallacia Valley (Docker, 1997). Cross-sections were determined by standard surveying techniques (Uran & Price, 1985) using a theodolite and staff where sighting was possible and by tape and pole where sighting was impeded by thick vegetation. Low-flow channel cross-sections were obtained by the lead line method at a spacing of 2 metres across the channel.

Three typical 'pre-failure' riverbank profiles (Fig. 7.1) were selected for assessment on the basis that they were representative of three of the most common geometries observed within the study area.
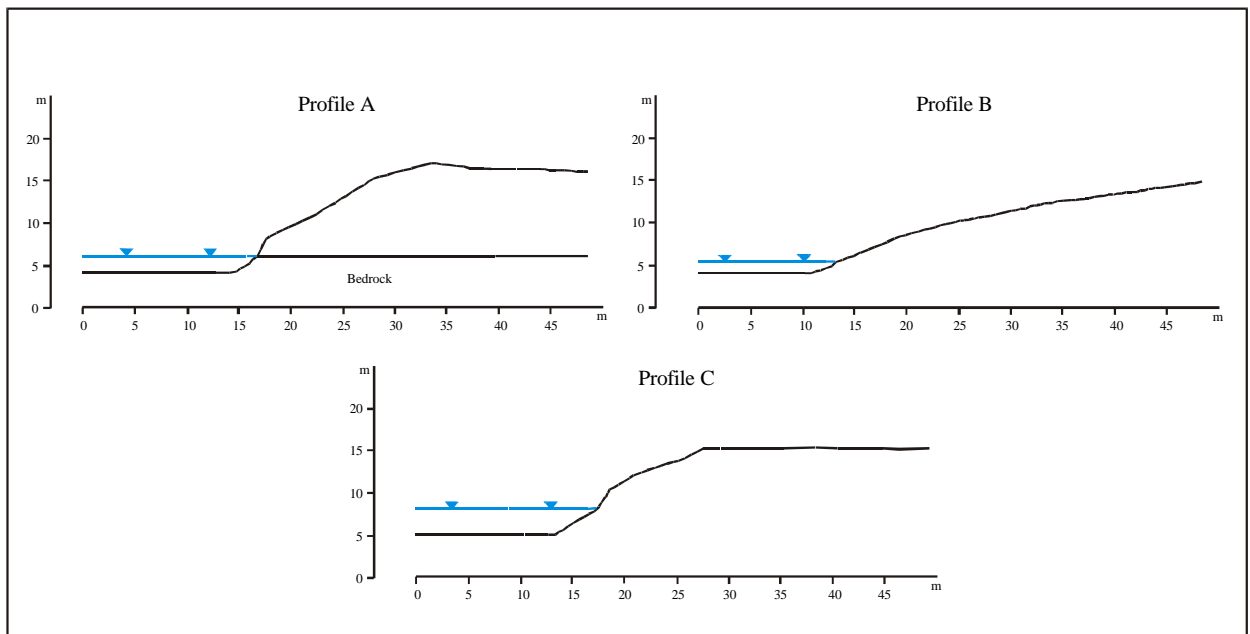
Figure 7.1: 'Pre-failure' riverbank profiles used in the stability analysis. These profiles are regarded as typical of a large number of riverbanks within the study area. Profile A exhibits a layer of bedrock at the level of the permanent waterline. Profile A and C are located within the Wallacia Valley. Profile B is located within the Camden Valley.

- Profile A exhibits a very steep bank face and a bank height of eleven metres above the waterline. It represents the 'stormwater-drain' style of the channel within the Wallacia Valley that has resulted from significant entrenchment and down-cutting into the sandstone and shale basement. The location of this profile (Fig. 7.3) is in an area where Wianamatta Group

shales are expected to outcrop within the channel (see Jones & Clark, 1991). Although bedrock has not been observed specifically at this site, given observations of its presence at the waterline in nearby locations (e.g. Fig. 3.19), this bank is assessed with a conservative estimate of a flat bedrock base located at the permanent water level of the channel.

- ▪ <u>Profile B</u> exhibits a fairly low angle slope with a reasonably smooth surface. It is located within the Camden Valley (Fig. 7.3) immediately upstream of Brownlow Hill weir and has been modelled previously using estimates of vegetative reinforcement (Hubble, 2001). There is no distinct levee crest although the height from the water level to the location of the actual failure scarp is approximately 5 metres.

- ▪ <u>Profile C</u> exhibits a steep bank face and a comparatively low bank height of 6.12 metres. It is located within the Wallacia Valley (Fig. 7.3) in a relatively thick colluvium.

The 'present-day' riverbank profiles used for stability modelling were the two 'present-day' profiles of Profile A and C, and a generalised profile based on the average dimensions of all one-hundred-and-four bank profiles from both the Camden and Wallacia Valleys (Hubble, 1996; Docker, 1997). That is, a height of eleven metres and a bank face angle of 23.7 degrees (Fig. 7.2).
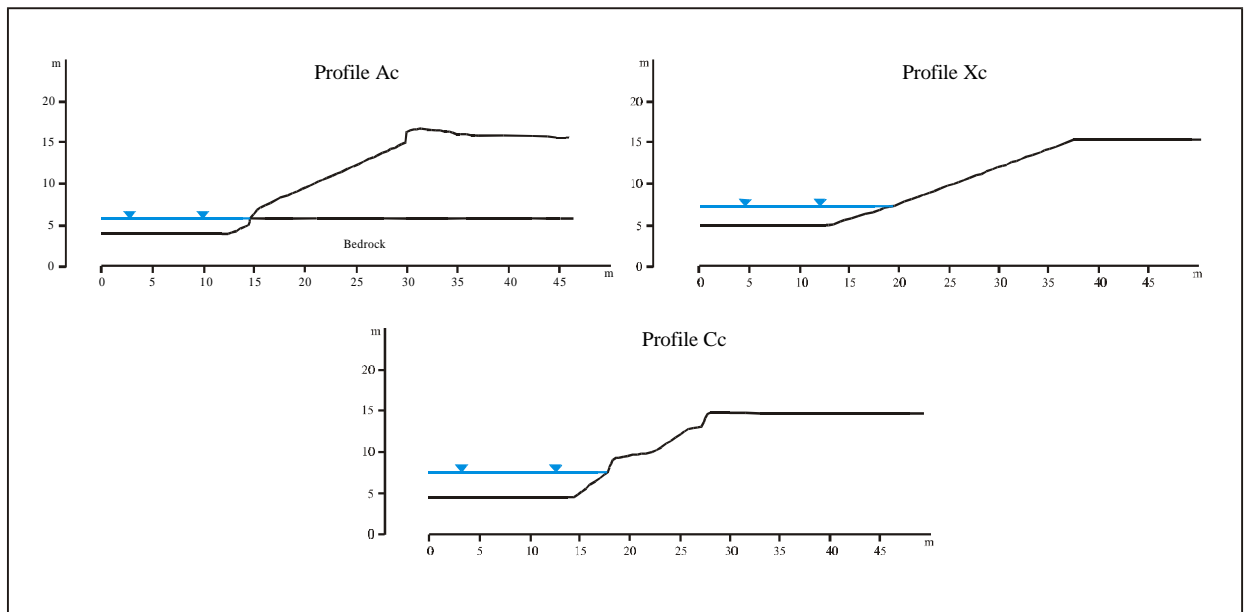
Figure 7.2: 'Present-day' riverbank profiles used in the stability analysis. Profile Ac and Cc are regarded as typical of a large number of riverbanks within the study area and are the 'present-day' geometries of Profiles A and C used in the 'pre-failure' analysis. Profile Xc is a generalised riverbank profile based on the average dimensions of 104 profile geometries from within the study area.
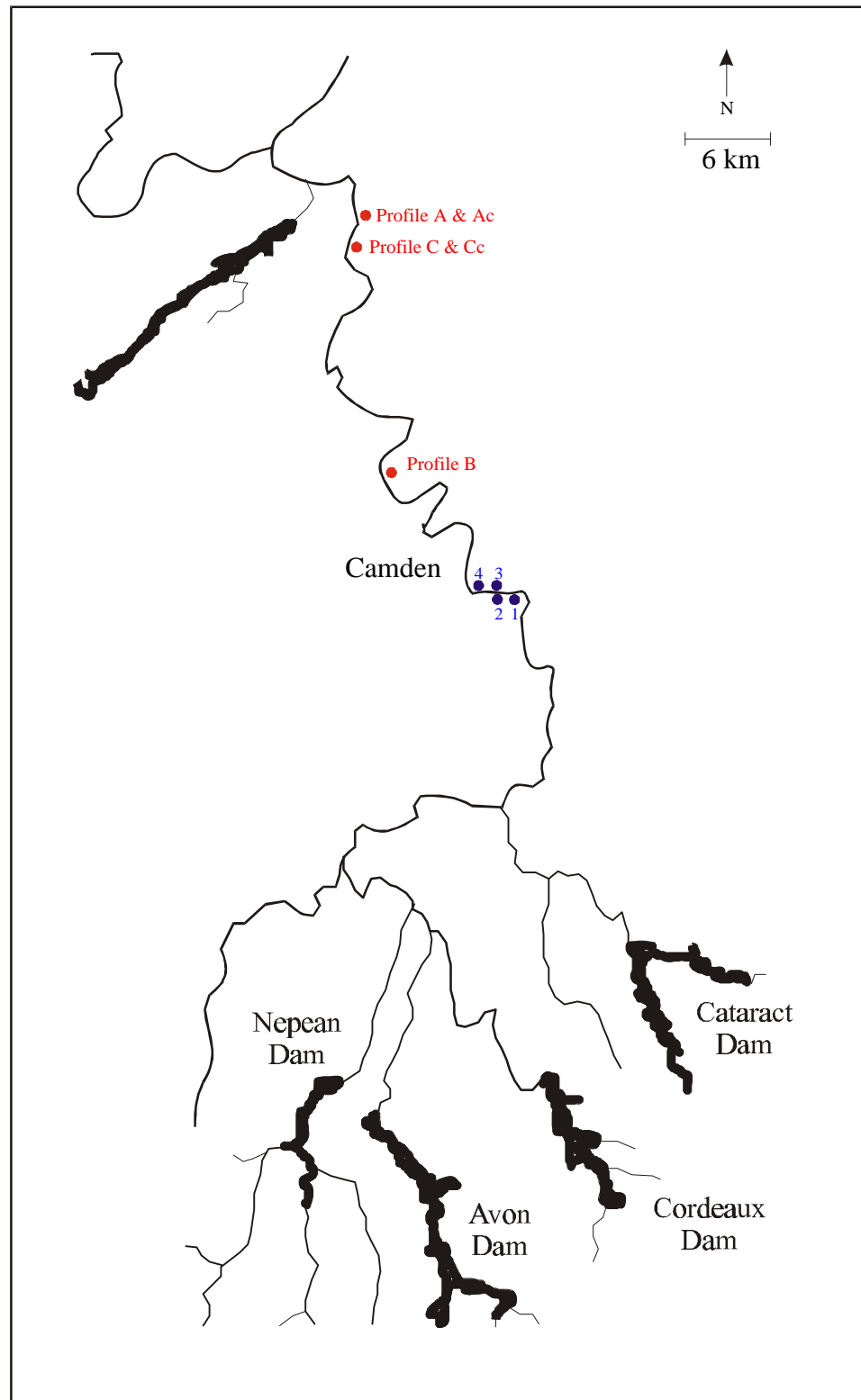
Figure 7.3: Map illustrating the location of the riverbank profiles assessed for stability in this study. Also shown are the locations of four sites where measurements of natural tree spacing and size were undertaken.

7.2.3   Soil properties and groundwater condition

For the purposes of modelling bank stability in this study it is sufficient to describe the geotechnical properties of the bank material in terms of its bulk unit weight and its effective shear strength. Saturated bulk density was measured by obtaining representative soil samples of a known standard volume (7.2 cm³) in cube samplers from each site, saturating them by immersion for 96 hours and weighing them. Soil strength parameters were determined by conducting saturated but drained, direct shear tests on both remoulded and undisturbed samples in the laboratory. Low normal confining loads were applied to represent the equivalent depths of about three, six and twelve metres as these replicate the shallow failure conditions observed in the field. The parameters obtained for each site (Table 7.1) were considered to be homogenous throughout the bank material at each specific location due to a lack of variation in the sediments observed at the site. There was however variation between sites with cohesion ranging from 0-9 kPa and friction angle from 33 to 47 degrees. This is consistent with a general fining of sediments downstream within each valley and also between valleys (Hubble & Harris, 1993) with bank sediments classified as either silty sands or clay sands. The two Wallacia Valley profiles (A and C) examined in this chapter presented more cohesive banks than average and were the same as the clay sands present in the tree plantation. Profile B and the average (Xc) were slightly less cohesive. Consequently the soil parameters used in the XSLOPE models varied slightly between locations.

Table 7.1: Soil properties used in riverbank stability models. Refer to Figure 7.3 for profile locations.

Profile	Cohesion c' (kPa)	Internal friction angle f' (degrees)	Saturated Bulk Unit Density g (kN m⁻³)	Classification
A and Ac	8.3	39.7	20.89	Clay Sand
B	2	38	18.5	Silty Sand
C and Cc	8.3	39.7	20.89	Clay Sand
Xc	2.2	41.4	19.28	Silty Sand

The most critical hydrological conditions for a riverbank are believed to occur during periods of rapid drawdown of river stage (Lawler *et al.*, 1997) following bank-full discharge or overbank flow. Full saturation ensures that there is no soil suction and that the shear strength of the bank soil is at a minimum. The uplift pressure of the pore water also reduces the overall stability. While the water is high within the channel it is able to counteract the destabilising forces by providing a lateral supporting pressure against the bank. However when the floodwater recedes and this support is removed the still-saturated bank material is vulnerable.

The Nepean River's banks, composed as they are of very fine sands, are probably at the low end of the permeability scale for sands. This suspected lower permeability has implications for saturating the banks in the first place and the history of riverbank collapse over the last half century is perhaps instructive in this matter. It has been noted that the most intensive period of bank failure occurred when there were a succession of very large floods one after the other, between 1947 and 1955, and also between 1961 and 1965 (Hubble, 2001). Large floods (> 10 m above the permanent waterline)

have occurred on a number of occasions since this time, but mostly in isolation. It is possible that one large flood event moving rapidly through the system is not sufficient to completely saturate the bank material. Thus the worst case scenario of completely saturated bank material during a period of rapid drawdown within the channel, is probably quite rare. Anecdotal evidence from landholders along the river suggests that it is the second of two closely spaced floods that cause the most damage.

The stability modelling presented here investigates two scenarios. The first is the worst case situation of complete drawdown to the permanent water level with completely saturated bank material; and the second is a more moderate situation of drawdown to the permanent waterline but with the top metre or two of bank material below the levee crest remaining unsaturated, as would occur in the numerous floods that do not completely fill the channel, and even those isolated bank-full discharges that rise and fall too rapidly for complete saturation to occur.

These situations are modelled in XSLOPE using a piezometric surface that enables the calculation of pore-water pressures at all points below it. It does this using the expression of pore-water pressure as a function of the major principal stress (Bishop, 1954) whereby the vertical head of soil and water above a given soil element is a useful approximation of the major principal stress. Above the piezometric surface pore-pressures are calculated as zero. The free weight of the water in the channel acts as a hydrostatic load against the channel bottom and the bank surface up to the level of the permanent low-flow water line.

7.2.4   The mechanical effect of vegetation on riverbank stability

The models of earth reinforcement proposed in chapter six are used to calculate the increased strength of the bank soil within distinct soil layers on the bank profile. XSLOPE only functioned properly with a maximum of 18 soil layers and 75 nodal points. These limits constrained the possible intricacy of the root reinforcement distribution, for in reality the variation in root area quantity tends to be a smooth function of depth and lateral distance from the stem (see chapter three). XSLOPE however required the specification of distinct boundaries between zones of different root area quantities. The boundaries were set by depth quartile to the maximum vertical root extent, and at 25 %, 50 % and 100 % of the maximum lateral root extent (see chapter six).

The nodal co-ordinates (X and Y for this two dimensional analysis) for the soil layers in each test were calculated according to the determined position of the tree or trees on the riverbank and the geometry of the bank. They were entered manually for each profile and vegetative condition in what is a laborious and time consuming process. Distance away from the trunk was always measured parallel to the bank surface and depth was always in a direct vertical line below the surface. Figure 7.4 illustrates an example of the nodal points and soil layers required for (a) a single tree growing at the levee crest of the average bank profile (Xc), and (b) multiple trees of the same species on the average bank profile. The soil reinforcement parameters for each layer, in accordance with the

specified vegetated condition are calculated and presented in chapter six. Below the permanent water level soil reinforcement is set to zero for all species except *C. glauca*. *C. glauca* is an exception because it is commonly observed with roots growing freely into permanently saturated bank material, and indeed directly into open water (see chapter three).

Riverbanks were assessed under both single species and multiple species forests. The factor of safety for the critical circle was obtained for each condition. The FoS for the critical circle of the same bank profile in the un-reinforced state was also assessed under different vegetated conditions, using XSLOPE's 'interactive analysis'. This analysis allows the manual specification of a circle centre, radius, and its entry and exit points on the bank profile in order to determine the factor of safety for a specific failure plane. It is instructive in demonstrating the change in stability due to the presence of vegetation for what would otherwise be the critical failure plane.
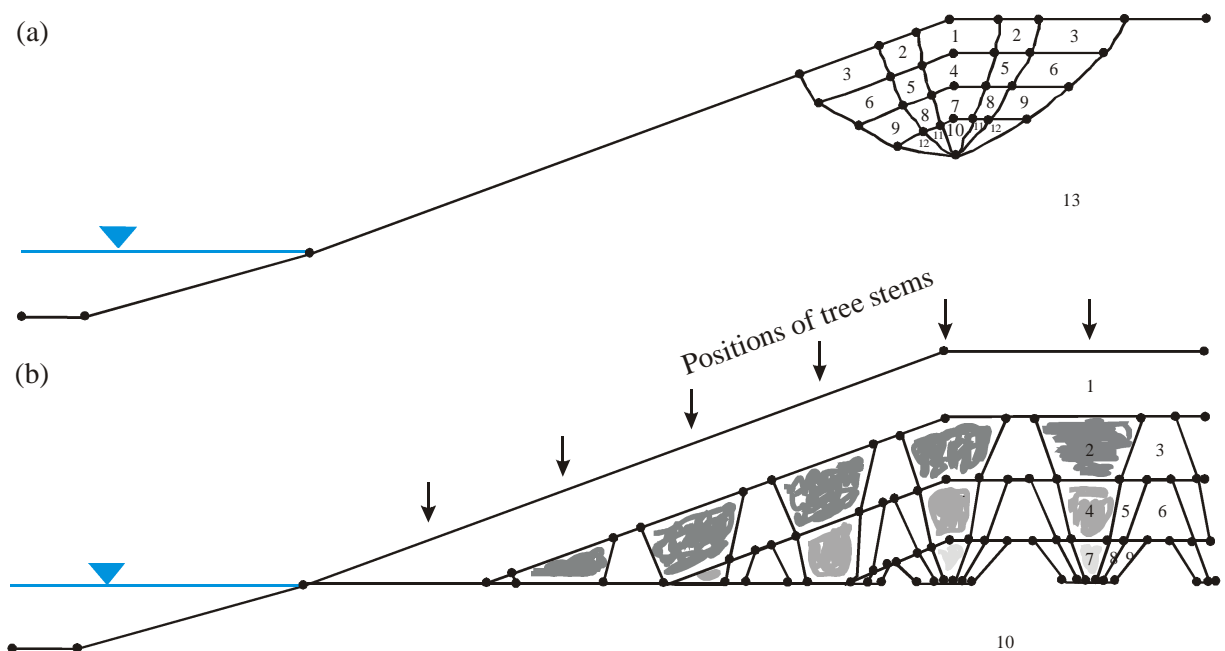
Figure 7.4: Examples of the nodal co-ordinate point structure used for input to XSLOPE. Nodes are marked by points and soil layers are numbered. Each soil layer has different soil strength parameters based on the quantity of reinforcement present. The structure shown in (a) is for a single *E. elata* tree located at the levee crest of an average bank profile. The structure shown in (b) is for a forest of *E. amplifolia* trees spaced at 5 m intervals over an average bank profile.

7.2.5   The Factor of Safety output

The utility or accuracy of the Factor of Safety value obtained from stability analyses depends very much on the validity of the assumptions on which the numerical calculation is based and the accuracy and representativeness of the soil properties obtained through laboratory and field testing. As a result there are certain imperfections in any stability analysis that affect the final value obtained. To overcome these imperfections and the difficulties with establishing the veracity of the assumptions inherent in FoS calculations it is standard engineering practice to incorporate a sensible margin for error before accepting any FoS as being safe in the design context (see Casagrande, 1964;

Hunt, 1986). The size of the margin for error generally depends on the risk to human life or the dependence of a community on the structure involved (cf. Mostyn & Small, 1987). For the riverbank analysis conducted here the concern is to produce a meaningful assessment of their stability under varying vegetative conditions and not one of design safety. Consequently it is not necessary to apply any strict margin of error in the appraisal of calculated Factors of Safety. The reader should however be aware of the errors involved in any such calculation as there are numerous examples of slopes with Factors of Safety well over 1.2 that have indeed failed (Mostyn & Small, 1987). To account for this uncertainty a set of broad definitions developed by Hubble (2001) will be used to describe the results of the Bishop's circle calculations within XSLOPE (Table 7.2). It is also important to note that in an assessment of the influence of root reinforcement on the stability of riverbanks and the relative merits of different tree species, it is the change in FoS that is important rather than the actual FoS value obtained.

Table 7.2: Terms used to describe the stability of riverbanks arising from Bishop's circle calculations in this study (From Hubble, 2001).

Bishop's Circle Factor of Safety	*Bank stability condition*
Less than 0.60	Extremely Unstable
0.60 to 0.79	Very Unstable
0.80 to 0.94	Unstable
0.95 to 0.99	Critically Unstable
1.00 to 1.05	Critically Stable
1.06 to 1.19	Marginally Stable
1.20 to 1.40	Stable
1.41 to 1.60	Very Stable
Greater than 1.60	Extremely Stable

7.3   Un-reinforced riverbank stability: the control

The stability of all six riverbank profiles was assessed for the un-vegetated case, that is with no reinforcement due to tree roots. The 'pre-failure' banks (Profiles A, B, and C) all gave factors of safety less than unity (Table 7.3) under completely saturated conditions. This is clearly expected given that they subsequently failed. With the saturated bank material reduced by around 1.5 m from the top of the levee crest only Profile C remained unstable. Of the 'present-day' profiles the typical banks (Profile Ac and Cc) present minimum factors of safety above 1.00, as indeed does the average profile (Xc). Higher factors of safety are expected for 'present-day' banks due to a general reduction in the slope that results from prior failure. Factors of safety for the critical slip circles and a selection of other representative slip circles are illustrated below (Figs. 7.4 & 7.5). For the 'pre-failure' banks the actual location of the subsequent failure scarps corresponds quite well to those predicted using XSLOPE. Profile C is an exception although given the likelihood of progressive failure, that is, first the small block described by the predicted critical surface and then a secondary failure at the location of the present-day scarp, this profile is still considered a good estimate of the 'pre-failure' geometry.

Table 7.3: Critical factors of safety for un-reinforced riverbank profiles.

Riverbank Profile	Complete bank saturation	Partly drained bank
A	0.85	1.18
B	0.95	1.08
C	0.88	0.96
Ac	1.08	1.36
Xc	1.05	1.48
Cc	1.05	1.25
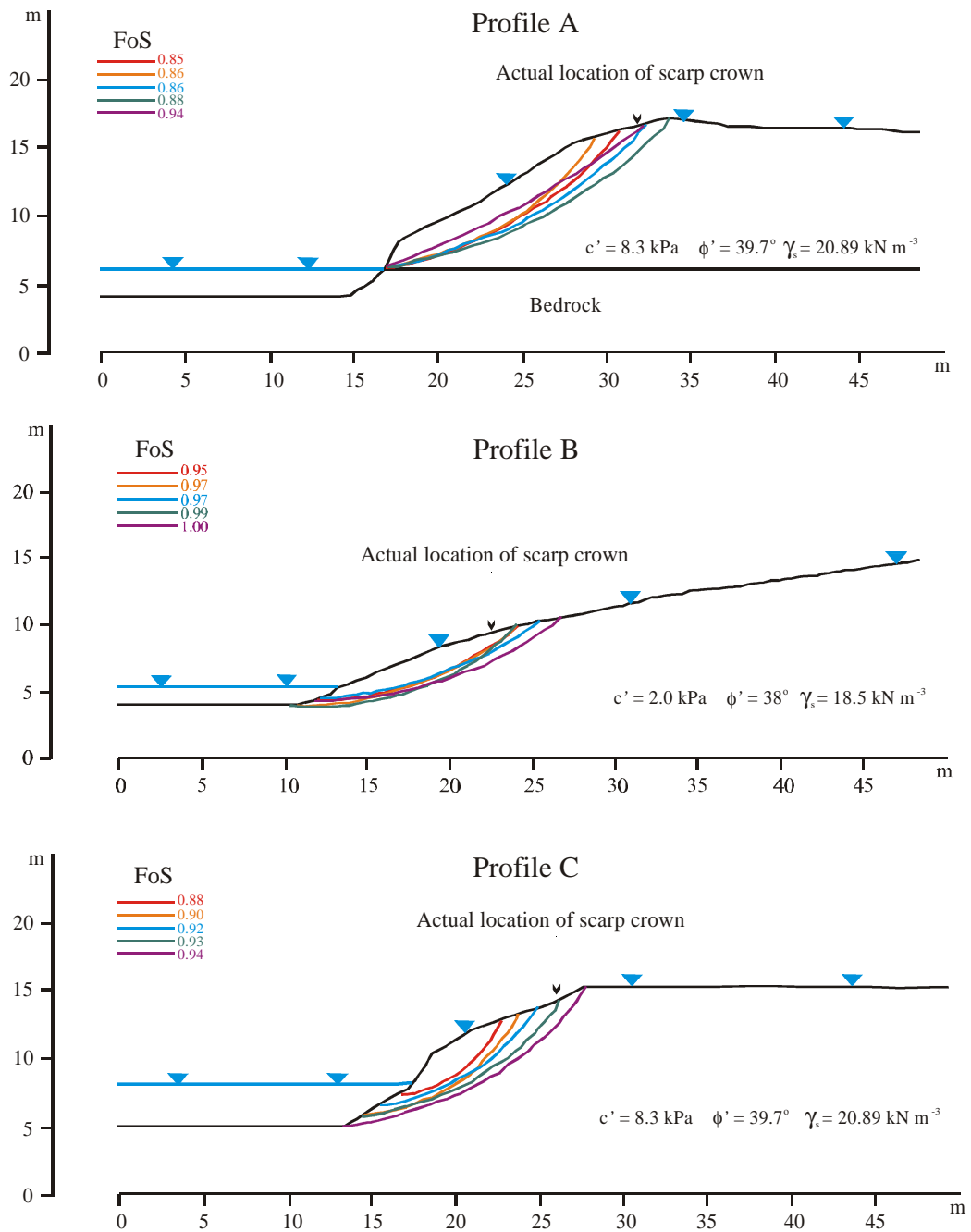
Figure 7.5: Slip circles obtained for un-reinforced 'pre-failure' profiles (A, B, and C). The critical failure surface and a selection of other representative circles are illustrated.
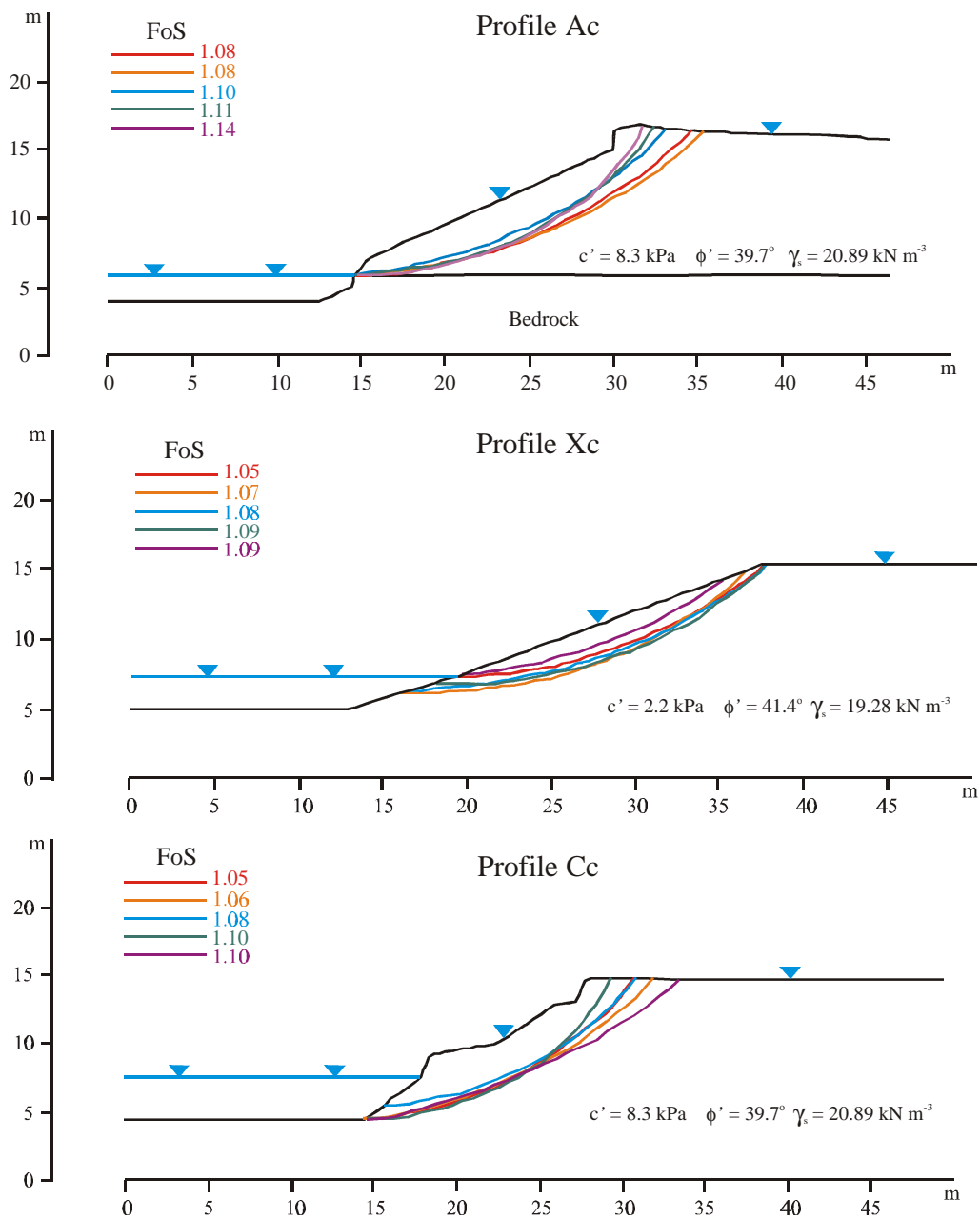
Figure 7.6: Slip circles obtained for un-reinforced 'present-day' profiles (Ac, Xc, and Cc). The critical failure surface and a selection of other representative circles are illustrated.

The results presented here indicate that 'present-day' un-reinforced riverbanks that have previously failed are less likely to do so again. Even with complete saturation of the bank material they are critically to marginally stable and so the excessive morphological change observed post-1947 is perhaps unlikely to be repeated on the same scale in the near future. This postulation of course relies heavily on the banks remaining in their present condition for some time, not altered significantly by human derived impacts such as dredging, and resistant to other erosive processes such as toe scour.

7.4   The effect of individual tree location on riverbank stability

While tree species selection for this study was done partly on the basis that they represented individuals predominantly from different zones within the riparian environment (i.e. *C. glauca* primarily at the waterline, *A. floribunda* in the low to mid-bank region, and the two Eucalypts at the levee crest and floodplain), in nature the trees do not necessarily restrict themselves exclusively to these areas. *C. glauca* and *A. floribunda* have been observed at all locations on the banks and the Eucalypts have been observed from the floodplain down to the mid-bank region.

This section presents an analysis of the effect that the location of an individual tree has on the stability of 'present-day' banks of the Nepean River. Stability assessments were undertaken for each species on each of the three 'present-day' profiles (Ac, Xc, Cc). Trees were positioned at the locations shown below (Fig. 7.7), from the toe of the bank up to a maximum of 5 m beyond the levee crest on the floodplain side. For profiles Ac and Cc five tree positions were assessed while for profile Xc, there were six, as a result of its longer bank face.
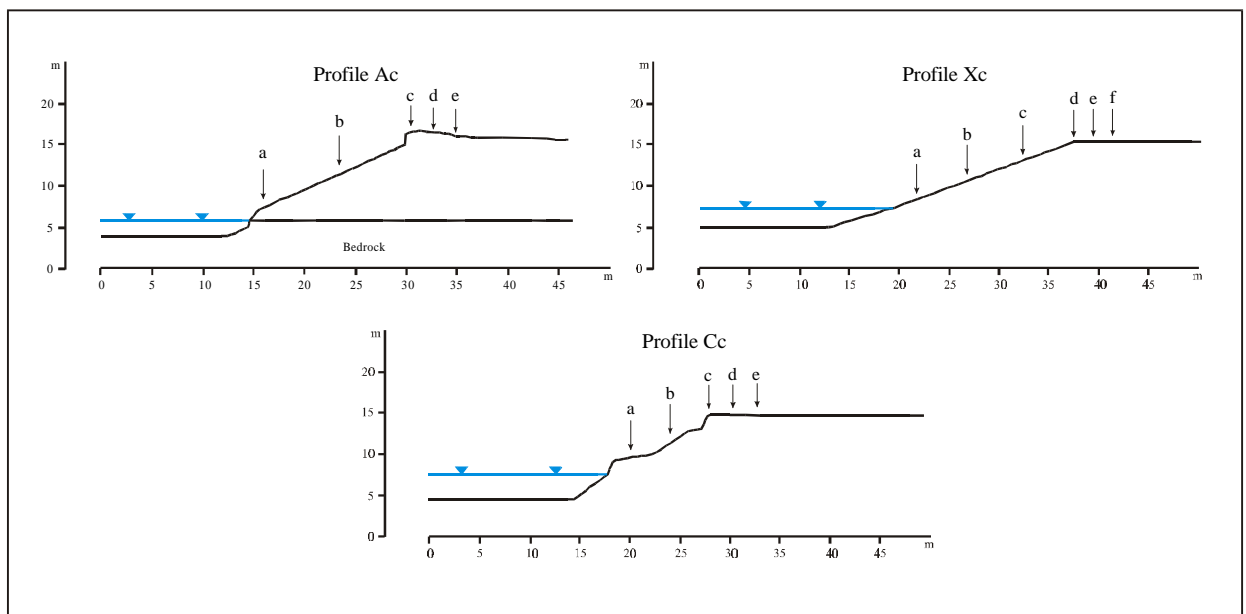
Figure 7.7: The different tree positions assessed on Profiles Ac, Xc, and Cc. Factors of safety for each location are presented in Tables 7.4 to 7.6 below.

Table 7.4: The effect of tree position on Profile Ac for a single tree of each species. The factor of safety for the critical failure surface and the percentage increase above the bare bank profile is given. The FoS for the bare profile is 1.08.

Tree position	C. glauca		E. amplifolia		E. elata		A. floribunda	
	FoS	%	FoS	%	FoS	%	FoS	%
Un-reinforced	1.08	-	1.08	-	1.08	-	1.08	-
a	1.09	1	1.30	20	1.18	9	1.13	5
b	1.08	0	1.25	16	1.13	5	1.10	2
c	1.10	2	1.24	15	1.15	6	1.09	1
d	1.12	4	1.17	8	1.16	7	1.08	0
e	1.08	0	1.10	2	1.14	6	1.10	2

Table 7.5: The effect of tree position on Profile Xc for a single tree of each species. The factor of safety for the critical failure surface and the percentage increase above the bare bank profile is given. The FoS for the bare profile is 1.05.

Tree position	C. glauca		E. amplifolia		E. elata		A. floribunda	
	FoS	%	FoS	%	FoS	%	FoS	%
Un-reinforced	**1.05**	-	**1.05**	-	**1.05**	-	**1.05**	-
a	1.10	5	1.08	3	1.08	3	1.06	1
b	1.07	2	1.12	7	1.11	6	1.05	0
c	1.07	2	1.26	20	1.15	10	1.05	0
d	1.07	2	1.12	7	1.10	5	1.08	3
e	1.05	1	1.09	4	1.08	3	1.06	1
f	1.05	1	1.07	2	1.08	3	1.06	1

Table 7.6: The effect of tree position on profile Cc for a single tree of each species. The factor of safety for the critical failure surface and the percentage increase above the bare bank profile is given. The FoS for the bare profile is 1.05.

Tree position	C. glauca		E. amplifolia		E. elata		A. floribunda	
	FoS	%	FoS	%	FoS	%	FoS	%
Un-reinforced	**1.05**	-	**1.05**	-	**1.05**	-	**1.05**	-
a	1.10	5	1.06	1	1.07	2	1.05	0
b	1.06	1	1.12	7	1.11	6	1.05	0
c	1.06	1	1.26	20	1.16	10	1.06	1
d	1.09	4	1.23	17	1.21	15	1.06	1
e	1.06	1	1.09	4	1.16	10	1.09	4

In most cases the addition of one mature tree did not make a significant difference to the overall stability of the bank profile. 43 of the 64 models tested exhibited an increase in the factor of safety of 5 % or less and both *C. glauca* and *A. floribunda* did not increase the FoS by greater than 5 % for any tree position on any bank. This is not surprising given the relatively large size of the banks in comparison to the area of reinforced material. The minimum failure surface generally moved to another location either under the root system or further down the bank face with only a relatively small increase in the calculated stability (Fig. 7.8 and Appendix E-I). The deeper rooting trees (*E. amplifolia* and *E. elata*) improved stability more by moving the minimum circle further. The average FoS increase was 10 % for *E. amplifolia*, 7 % for *E. elata*, 2 % for *C. glauca* and 1 % for *A. floribunda*.

Different species were also more or less effective in different locations. For instance on Profile Ac the maximum FoS increase for *C. glauca* was on the floodplain in position *d*, while for the other three species it was at the bottom of the slope in position *a*. Position *a* is the logical place as this is where the failure surface is forced by the bedrock (see Fig. 7.6). It cannot physically extend any deeper. The ability of a tree to increase the FoS of any failure surface passing through this zone will therefore depend on the increased shear resistance resulting from the root area ratio within this zone. *C. glauca* has by far the lowest root area ratios of all species tested (chapter three). This situation does not exist at the top of the slope where there are more possibilities for the failure surface to exit (Fig. 7.6), so that even a low root area ratio will force the failure plane to move and therefore increase its FoS, even if only slightly.

On profiles Xc and Cc where bedrock does not constrain root growth or the failure surface *C. glauca* is more effective at the bottom of the slope (position *a*). It does of course have the advantage over the other three species of being able to grow its roots into the saturated bank material with no apparent distress. For the species thought to be less water tolerant, *E. amplifolia*, *E. elata* and *A. floribunda,* the most effective tree position is at or very near the levee crest. When in the correct position a single *E. amplifolia* tree is a significantly more effective bank stabiliser than any of the other species. On the Profiles Ac and Xc the effectiveness of *E. amplifolia* is twice as great as *E. elata.*
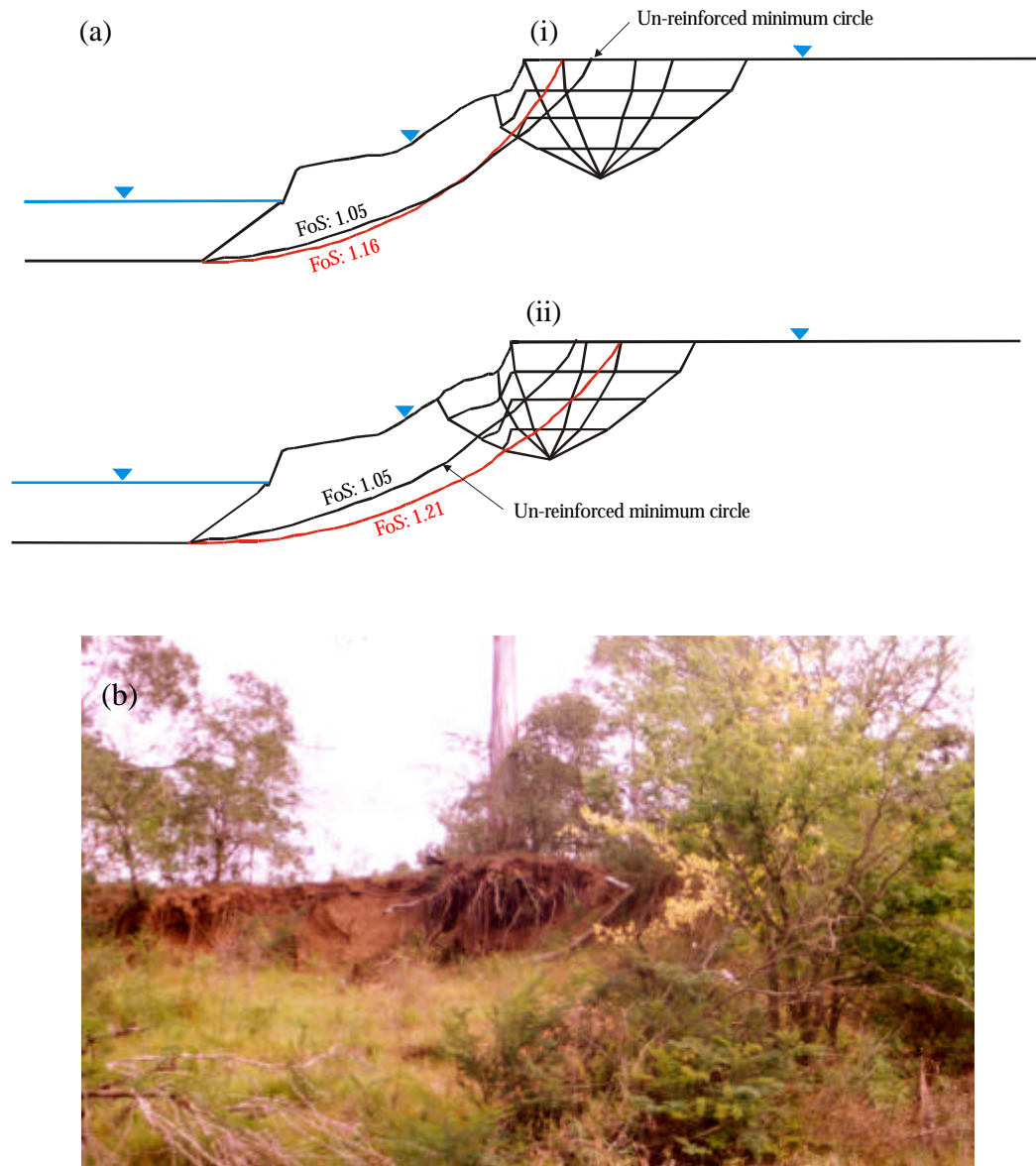
Figure 7.8: Different tree positions force the critical failure surface around the zones of greatest increased soil shear resistance. (a) Shown are the root reinforcement zones below a mature *E. elata* in positions *d* and *e* on Profile Cc. (b) Photograph of a failure scarp passing through the outer reinforced zones of a mature Eucalypt at the levee crest, similar to the modelled surface illustrated in (i) above.

7.5   Effect of a single species forest on riverbank stability

It is apparent from the previous section that the presence of a single tree on a bank will not have a large effect on its stability. The size of the banks in relation to the extent of root reinforcement beneath a single tree is too great for any substantive impact on the factor of safety of the modelled slopes. Therefore this section investigates the same riverbank profiles with multiple trees of the same species. It employs the root reinforcement distributions described in chapter six, which have been input to XSLOPE in the same manner as was employed for single trees in the previous section.

The analysis in this section examines both 'pre-failure' and 'present-day' riverbank profiles. The assessment of 'pre-failure' profiles allows consideration of the effect of devegetation while the assessment of 'present-day' profiles allows consideration of potential revegetation outcomes. Both assessments focus on the relative merits of the four riparian species in contributing to changes in the factors of safety of the modelled slopes.

7.5.1   A single species forest on 'pre-failure' riverbank profiles

7.5.1.1   Natural Vegetation Densities

There are very few examples of natural riparian vegetation remaining within the study area. The clearing of land was extensive, originally for agricultural purposes and later to enable sand mining of the bank and floodplain. According to Benson & Howell (1993) the best remaining example of native vegetation growing on alluvium along the Nepean River occurs at Camden Park near Bergins Weir. In order to gain an understanding of some typical tree spacings amongst natural stands of large, mature trees, four sites were selected in this area for measurement (for location see Fig. 7.3). As expected tree spacing was not regular and ranged from 0.5 m to 18 m. The average was between 4.2 m and 5.6 m for trees that ranged in average diameter from 0.29 m to 0.90 m (Table 7.7). The maximum recorded diameter was 1.4 m.

Table 7.7: Typical tree spacings for natural stands of mature trees growing within the study area.

Site Number	Tree types and heights	Average tree spacing	Average tree diameter	Tree diameter range
1	Mostly *E. elata* trees up to 30/40 m	5.5 m	0.90 m	0.45 – 1.21 m
2	Mostly *Angophora subvelutina* up to 40/50 m	4.2 m	0.64 m	0.30 – 1.05 m
3	Eucalypts and Casuarinas up to 20/25 m	4.7 m	0.29 m	0.18 – 0.51 m
4	Eucalypts including *E. elata* and *E. amplifolia* up to 30/40 m	5.6 m	0.51 m	0.13 – 1.4 m

To model tree spacing that was representative of the natural densities described above it was necessary to make some simplifications in order to retain as much as possible the detail of the root reinforcement models as presented in chapter six. Importantly the number of nodal points entered into XSLOPE for any one individual tree had to be kept as low as possible so that more nodes could be used in the preservation of at least the number of soil layers previously described, i.e. 12 for an individual tree. Setting the tree spacing at distances relative to the reinforcement models enabled a reduction in nodal points and therefore the retention of complexity in the reinforcement (Fig. 7.9).

(a) *E. elata* spaced at 50 % of the maximum lateral distance of the reinforcement model
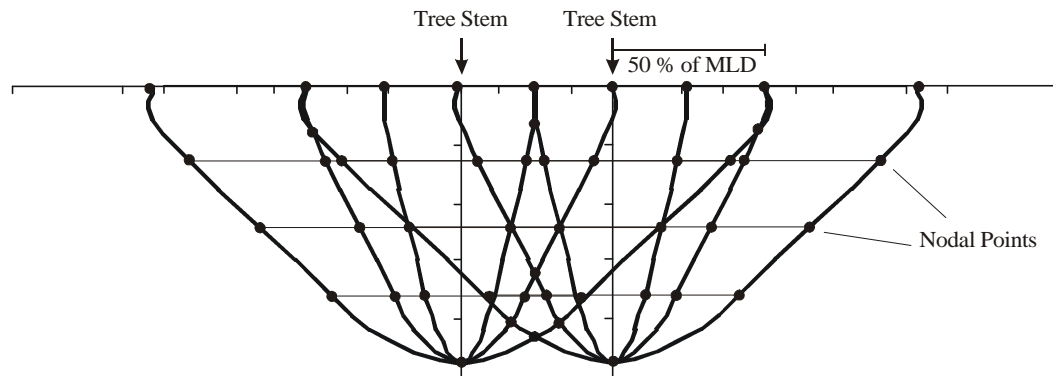
(b) *E. elata* spaced at a distance not relative to the reinforcement model
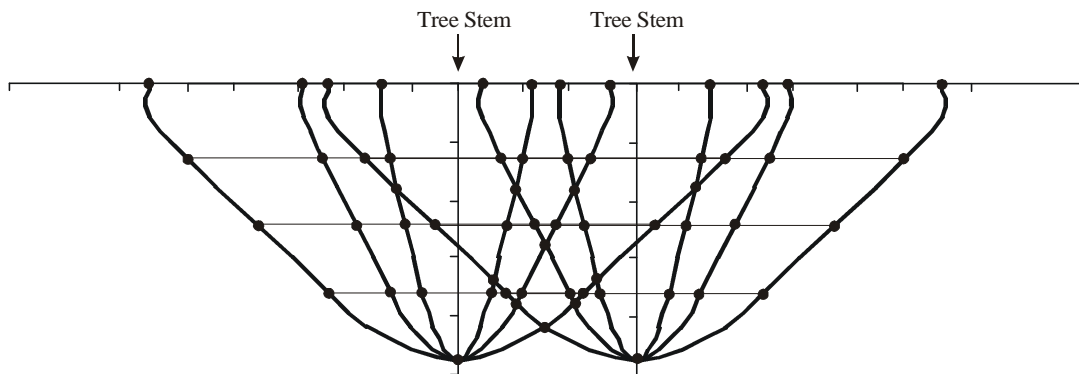
Figure 7.9: (a) Tree spacing set relative to the reinforcement model; in this case at 50 % of the maximum lateral root distance. (b) Tree spacing set at a distance not relative to the reinforcement model. In the first case the number of nodal points to enter into XSLOPE is 48 while in the second case the number of nodal points is 60. Setting the tree spacing relative to the reinforcement model enabled the retention of complexity of the reinforcement (by reducing the number of nodal points) while still allowing trees to be spaced over a range present in natural conditions.

Setting the tree spacing to distances relative to the root reinforcement models also enabled the large trees (*C. glauca*, *E. amplifolia*, and *E. elata*) to cover the range of average values measured in the field. These spacings were set at 50 % and 100 % of the maximum lateral root distance for a single tree, as well as a standard minimum value of 2 m. Under these constraints *C. glauca* was modelled at spacings of 2 m, 4 m, and 8 m; *E. amplifolia* at 2 m, 5 m, and 10 m; and *E. elata* at 2 m, 3 m, and 6 m. The standard value of 2 m may appear too close to be a realistic reflection of a fully vegetated riverbank for these three species. However mature trees of all these species have been observed this close and indeed closer, if only in groups of two or three. This standard value therefore represents

the likely upper limit of reinforced riverbank stability, with the single tree analysis in the previous section representing the lower limit for mature trees.

A. floribunda, being only a small tree (to 8 m in height) exhibits 50 % and 100 % maximum lateral root extents of 1.8 m and 3.6 m respectively. It was therefore modelled at these spacings as well as the standard 2 m. The species appears perfectly comfortable growing at these distances. The trees in the Cobbity plantation used for soil-root shear strength experiments were planted at 1.3 m apart and had grown up to 4 m within 18 months.

7.5.1.2 Stability Analysis Results

In all the cases modelled, riverbanks presenting with a forest of mature trees exhibited a factor of safety increase. Clear differences exist between species and between tree density of the same species (Tables: 7.8 to 7.10). Under a partly saturated bank, in all cases the vegetated banks increased the stability by a smaller amount than for the completely saturated condition, although the difference was small. For all species there was a general increase in stability associated with an increasing tree density (Figs. 7.11, 7.13, 7.15). *E. amplifolia* was by far the most effective species at increasing the stability of these riverbanks although the magnitude of this dominance varied between different profiles.

(i) Profile A: Steep and high bank in cohesive soils above bedrock

Even when it is spaced at 10 m intervals *E. amplifolia* increased the stability of Profile A by a larger amount than both *C. glauca* and *A. floribunda* spaced at 2 m and *E. elata* at 3 m. *E. amplifolia* spaced at 2 m increased the stability of Profile A by almost twice as much as *E. elata* at the same spacing (105 % compared to 58 %)(Table 7.8).

Table 7.8: Stability analysis results for single species forests on riverbank Profile A. The critical failure surfaces are illustrated in Figure 7.10.

Species and spacing (Tree spacing in parentheses)	Complete bank saturation		Partly drained bank		Fixed failure circle	
	FoS	% Increase	FoS	% Increase	FoS	% Increase
Bare	**0.85**	-	**1.18**	-	**0.85**	-
C. glauca **(8 m)**	0.88	4	1.21	3	0.88	4
C. glauca **(4 m)**	0.93	9	1.25	6	0.95	12
C. glauca **(2 m)**	0.99	16	1.29	9	1.03	21
E. amplifolia **(10 m)**	1.24	46	1.56	32	1.57	85
E. amplifolia **(5 m)**	1.42	67	1.76	49	2.26	166
E. amplifolia **(2 m)**	1.74	105	2.06	75	2.38	180
E. elata **(6 m)**	1.21	42	1.54	31	1.74	105
E. elata **(3 m)**	1.21	42	1.56	32	1.91	125
E. elata **(2 m)**	1.34	58	1.72	46	1.95	129
A. floribunda **(3.6 m)**	0.87	2	1.19	1	1.01	19
A. floribunda **(2 m)**	1.02	20	1.33	13	1.14	34
A. floribunda **(1.8 m)**	1.02	20	1.34	14	1.17	38
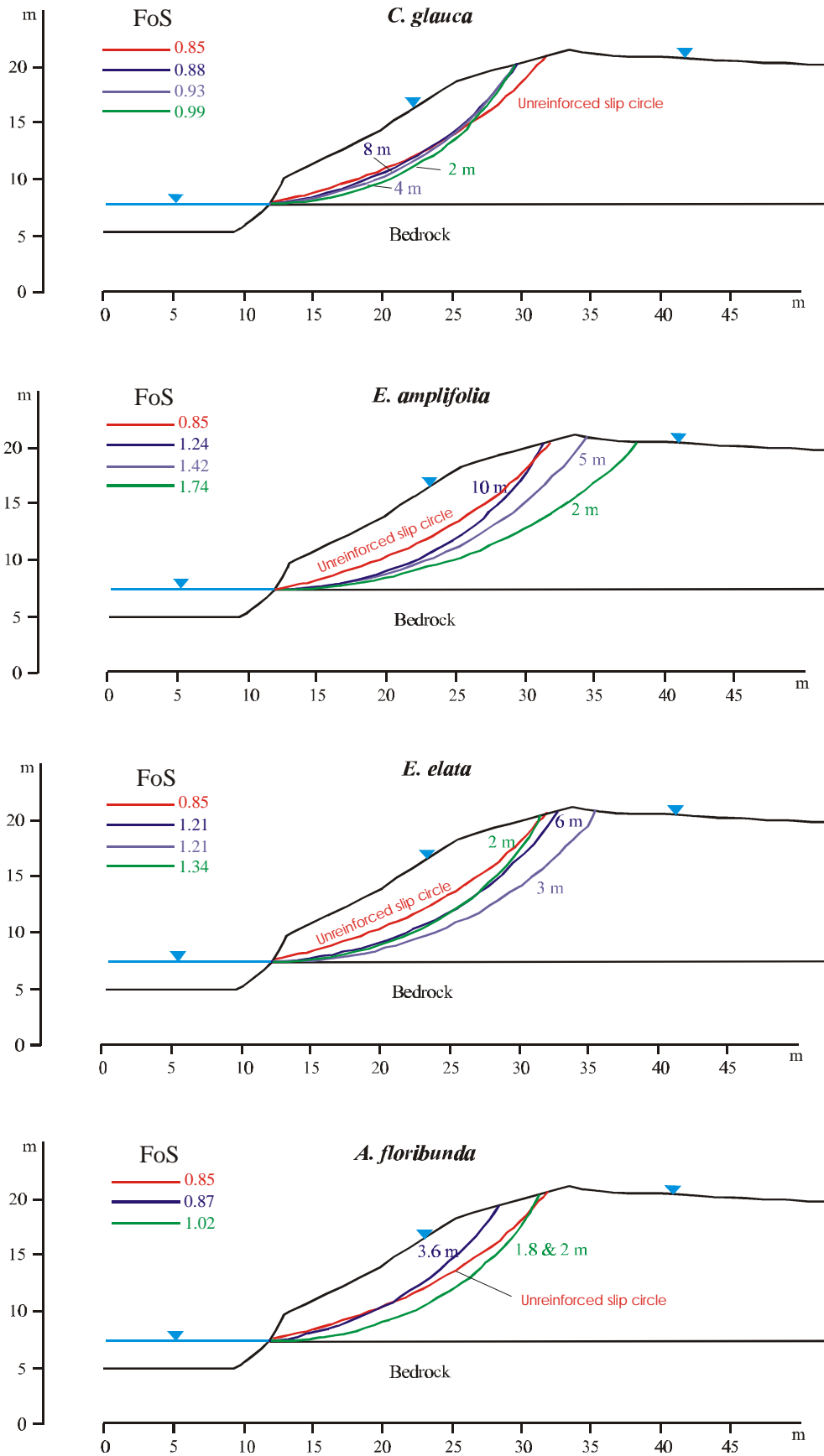
Figure 7.10: The critical failure surfaces for each species and tree spacing on Profile A.

Different amounts of reinforcement associated with different tree spacings move the critical failure surface to different positions within the bank profile (Fig. 7.10). Generally, the failure surface is forced deeper within the bank by trees which are more closely spaced. The differences between species type and tree spacing are illustrated in Figure 7.11. The greater the density of tree cover the greater the FoS of the riverbank.

Figure 7.11: Increased riverbank stability resulting from differences in tree species and density on Profile A. As tree spacing decreases the FoS increases for all species.

A forest of mature *C. glauca* trees spaced at 2 m intervals was not sufficient to increase stability of this profile above the critical FoS under completely saturated conditions. *E. amplifolia* and *E. elata* were able to increase the FoS from unstable to stable (FoS > 1.20) at their maximum assessed spacings of 10 m and 6 m respectively. *A. floribunda* was able to stabilise the bank when spaced at 2 m intervals, but increasing this to 3.6 m reduced the FoS to only marginally above that of a bare bank, and still unstable.

As a common upper bound of vegetated earth reinforcement the 2 m spacing limit allowed a comparison of the likely maximum value of increased stability between species. At this spacing *E. amplifolia* increases the FoS of the bank to extremely stable, *E. elata* increases it to stable, *A. floribunda* to critically stable, and *C. glauca* to critically unstable. For the failure surface fixed at that derived under bare conditions the factor of safety increased from between 4 % for *C. glauca* spaced at 8 m to 180 % for *E. amplifolia* spaced at 2 m.

(ii) Profile B: Gentle slope with low height, in less cohesive soils

The stability analysis results for riverbank Profile B are presented in Table 7.9 and the critical failure surfaces in Figure 7.12. It is evident that *E. amplifolia* spaced at 10 m is as effective as *C. glauca* at 4 m and more effective than *A. floribunda* at 3.6 m. Its maximum FoS increase was 80 % compared to 77 % for *E. elata*. *E. elata* spaced at 6 m was also more effective than *C. glauca* at 2 m and *A. floribunda* at 3.6 m. The differences between species type and tree spacing are illustrated in Figure 7.13.

Ph.D. Thesis: Benjamin Docker

Table 7.9: Stability analysis results for single species forests on riverbank Profile B. The critical failure surfaces are illustrated in Figure 7.12.

Species and spacing (Tree spacing in parentheses)	Complete bank saturation		Partly drained bank		Fixed failure circle	
	FoS	% Increase	FoS	% Increase	FoS	% Increase
Bare	**0.95**	-	**1.08**	-	**0.95**	-
C. glauca (8 m)	1.05	11	1.17	8	1.28	35
C. glauca (4 m)	1.13	19	1.28	19	1.33	40
C. glauca (2 m)	1.25	32	1.39	29	1.47	55
E. amplifolia (10 m)	1.14	20	1.23	14	1.90	100
E. amplifolia (5 m)	1.61	69	1.79	66	3.56	275
E. amplifolia (2 m)	1.71	80	1.89	75	4.02	323
E. elata (6 m)	1.29	36	1.42	31	3.09	225
E. elata (3 m)	1.65	74	1.85	71	4.51	375
E. elata (2 m)	1.68	77	1.88	74	5.14	441
A. floribunda (3.6 m)	1.07	13	1.21	12	1.53	61
A. floribunda (2 m)	1.31	38	1.47	36	2.34	146
A. floribunda (1.8 m)	1.33	40	1.50	39	2.87	202
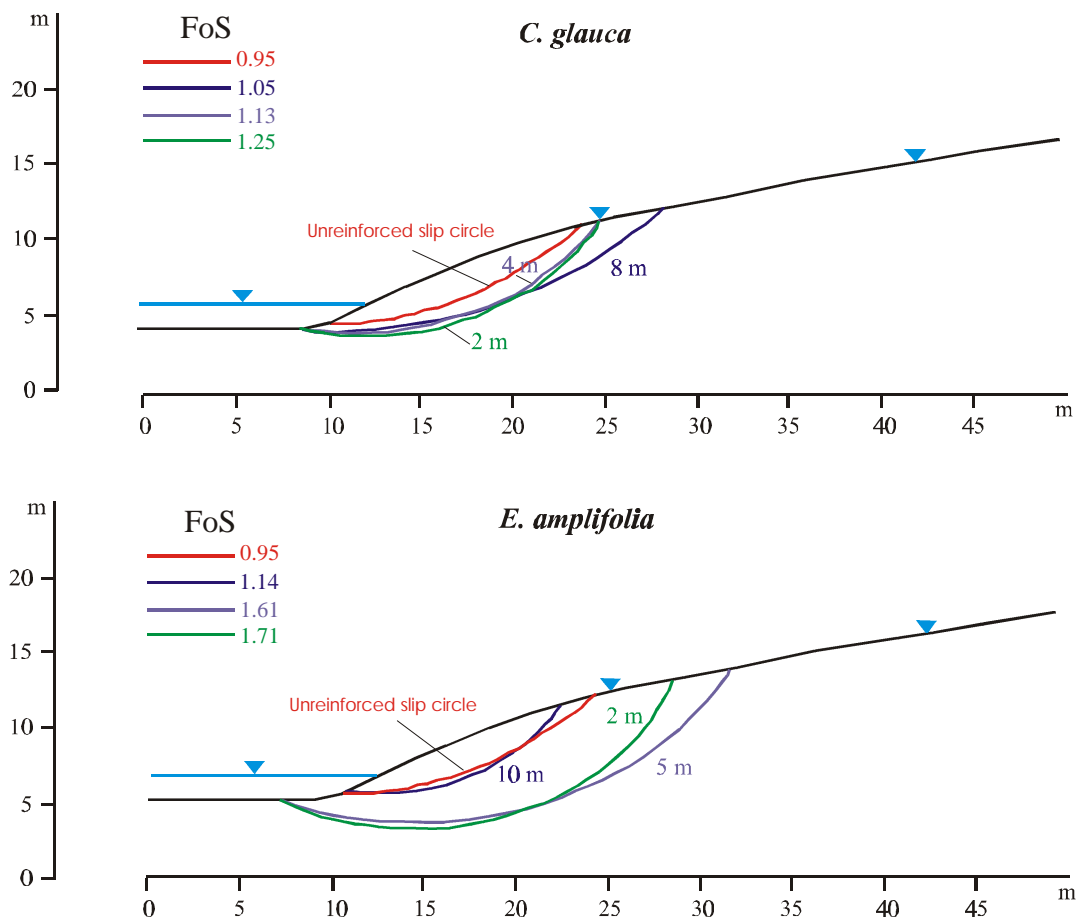
Figure 7.12 (i): The critical failure surfaces for *C. glauca* and *E. amplifolia* at each tree spacing on Profile B.
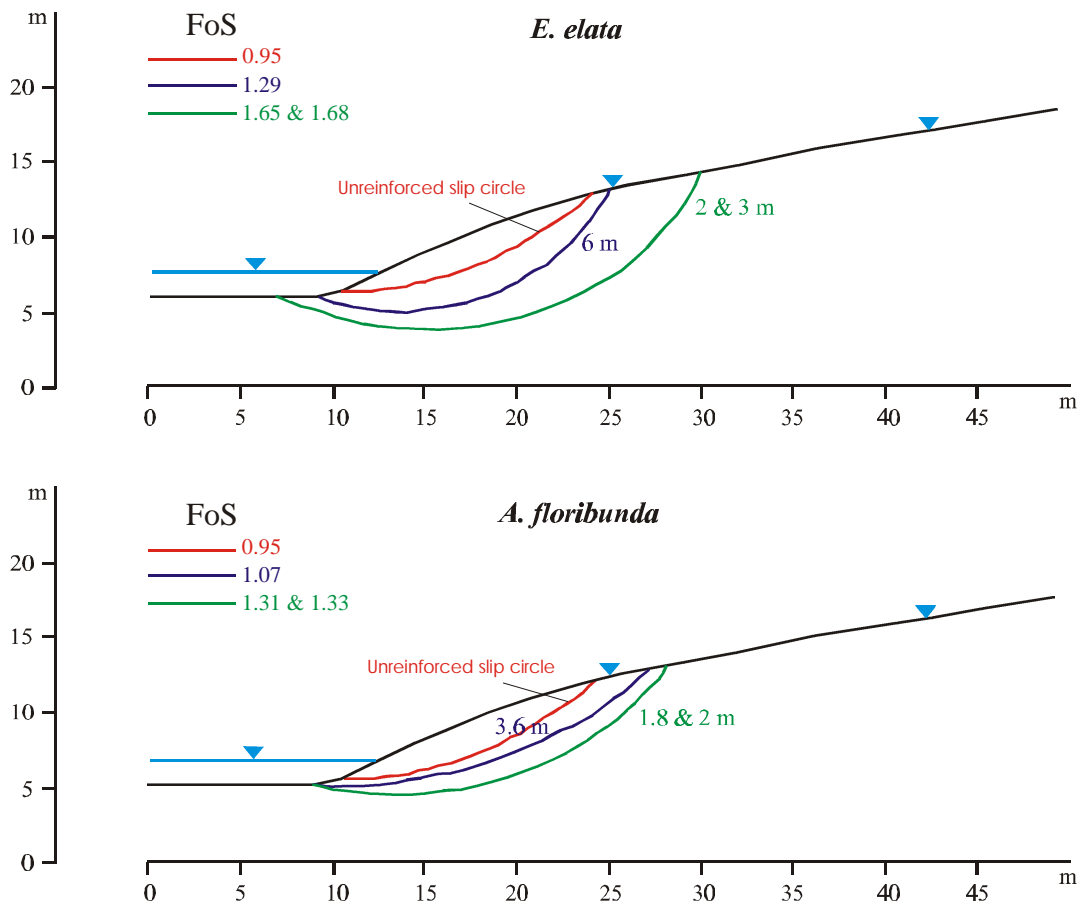
Figure 7.12 (ii): The critical failure surfaces for *E. elata* and *A. floribunda* at each tree spacing on Profile B.

In contrast to profile A, all species were able to increase the factor of safety under completely saturated conditions to greater then 1.00 even at the lowest density of tree cover modelled. Similar to Profile A, different amounts of reinforcement associated with different tree spacings moved the critical failure surface to different positions within the bank profile (Fig. 7.12). Generally, the failure surface is forced deeper within the bank by trees which are more closely spaced. The greater the density of tree cover the greater the FoS of the riverbank (Fig. 7.13).
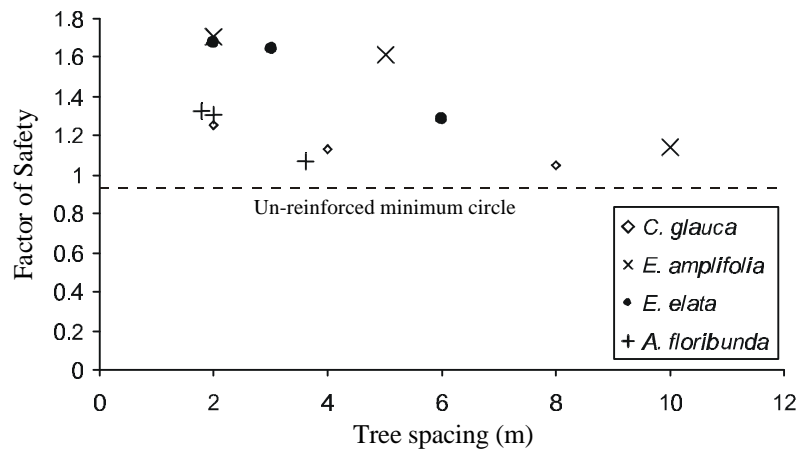
Figure 7.13: Increased riverbank stability resulting from differences in tree species and density on Profile B. As tree spacing decreases the FoS increases for all species.

Ph.D. Thesis: Benjamin Docker

Of the four species only *E. amplifolia* was less effective on Profile B relative to Profile A. Spaced at 2 m intervals both *E. amplifolia* and *E. elata* increased the FoS of the profile to extremely stable. *A. floribunda* and *C. glauca* increased it to stable. The difference between the Eucalypts and the other two species is expected due to their large relative size and therefore greater root quantity throughout a greater volume of soil. Factors of safety for the failure surface fixed at that derived under bare conditions increased from 35 % for *C. glauca* spaced at 8 m to 441 % for *E. elata* spaced at 2 m.

(iii) Profile C: Steep but relatively low height in cohesive soils

The stability analysis results for riverbank Profile C are presented in Table 7.10 and the critical failure surfaces in Figure 7.14. *E. amplifolia* spaced at 10 m was as effective as *C. glauca* at 4 m and more effective than *A. floribunda* at 3.6 m. Its maximum FoS increase was 57 % compared to 50 % for *E. elata*. *E. elata* spaced at 6 m was more effective than both *C. glauca* and *A. floribunda* at 2 m. The differences between species type and tree spacing are illustrated in Figure 7.15. Overall the vegetated conditions modelled on this profile were less effective than for the other two. This probably results from Profile C's comparatively small height (6.12 m above the permanent water level) and therefore smaller volume of soil that could be enhanced by root reinforcement.

Table 7.10: Stability analysis results for single species forests on riverbank Profile C. The critical failure surfaces are illustrated in Figure 7.14.

Species and spacing (Tree spacing in parentheses)	Complete bank saturation		Partly drained bank		Fixed failure circle	
	FoS	% Increase	FoS	% Increase	FoS	% Increase
Bare	**0.88**	-	**0.96**	-	**0.88**	-
C. glauca (8 m)	0.94	7	1.01	5	0.94	7
C. glauca (4 m)	1.01	15	1.09	14	1.28	45
C. glauca (2 m)	1.04	18	1.13	18	1.47	67
E. amplifolia (10 m)	1.01	15	1.09	14	2.23	153
E. amplifolia (5 m)	1.28	45	1.37	43	2.33	165
E. amplifolia (2 m)	1.38	57	1.44	50	2.34	166
E. elata (6 m)	1.07	22	1.13	18	1.98	125
E. elata (3 m)	1.29	47	1.38	44	3.06	148
E. elata (2 m)	1.32	50	1.40	46	3.08	250
A. floribunda (3.6 m)	0.93	6	0.99	3	1.12	27
A. floribunda (2 m)	1.06	20	1.17	22	1.44	64
A. floribunda (1.8 m)	1.07	22	1.17	22	1.70	93
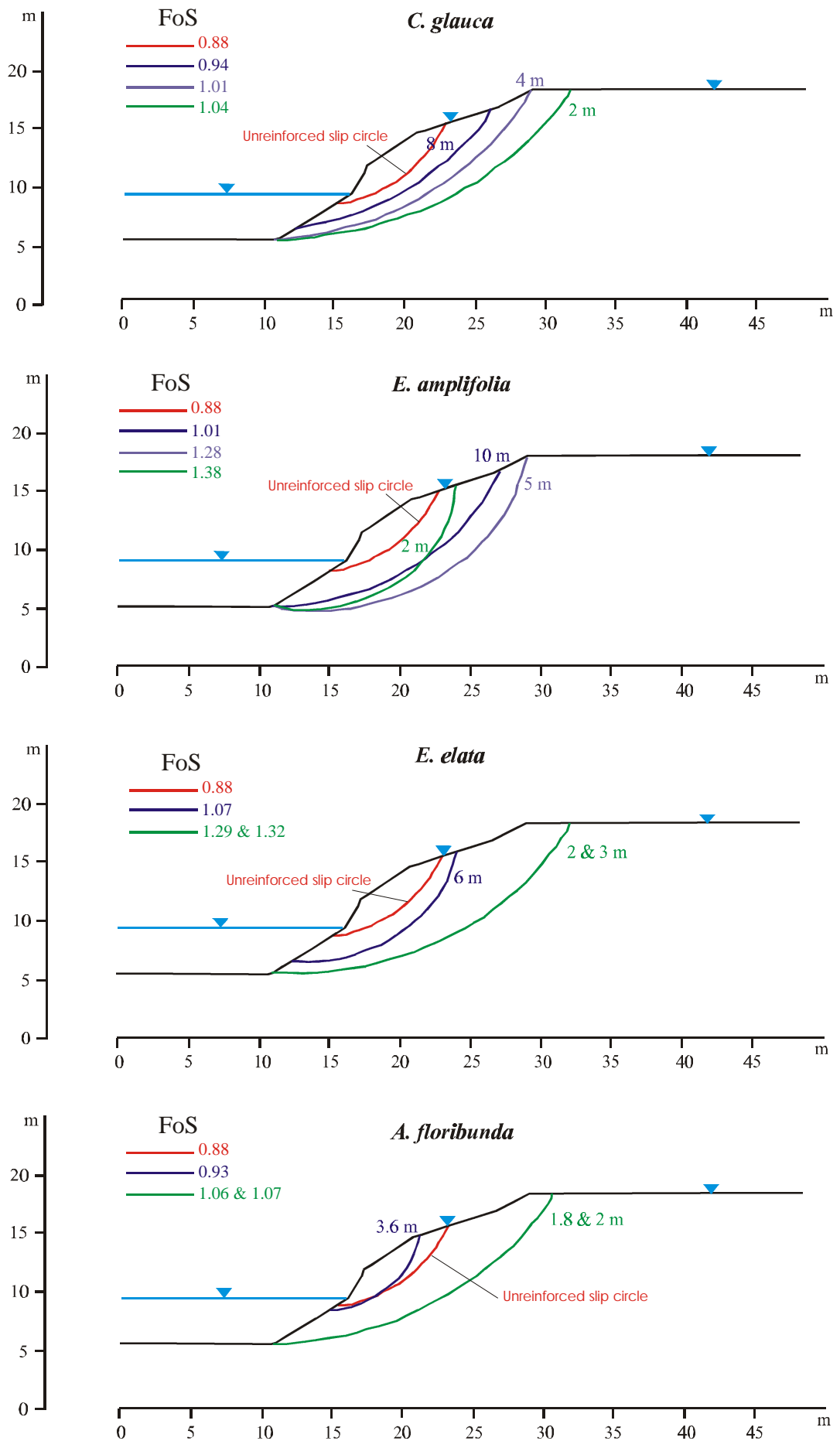
Figure 7.14: The critical failure surfaces for each species and tree spacing on Profile C.

The presence of any of the species on Profile C increased the factor of safety to above 1.00 under completely saturated bank conditions. *E. amplifolia* and *E. elata* recorded a FoS above unity at the maximum spacing modelled but for *C. glauca* the distance between trees needed to be reduced to 4 m and for *A. floribunda* to 2 m. At a spacing of 2 m both *E. amplifolia* and *E. elata* increased the FoS of the profile to the stable condition. *A. floribunda* increased it to marginally stable and *C. glauca* increased it to critically stable. Factors of safety for the failure surface fixed at that derived under bare conditions increased from 7 % for *C. glauca* spaced at 8 m to 250 % for *E. elata* spaced at 2 m.

Similar to Profiles A and B, different amounts of reinforcement associated with different tree spacings moved the critical failure surface to different positions within the bank profile (Fig. 7.14). Generally, the failure surface is forced deeper within the bank by trees which are more closely spaced. The greater the density of tree cover the greater the FoS of the riverbank (Fig. 7.15).
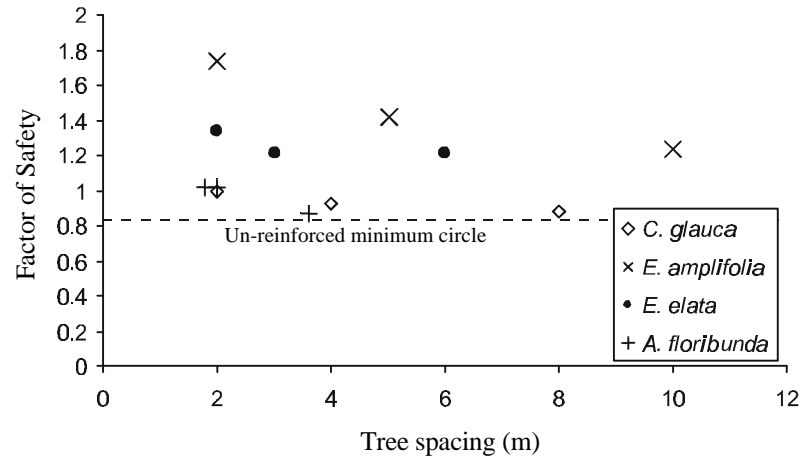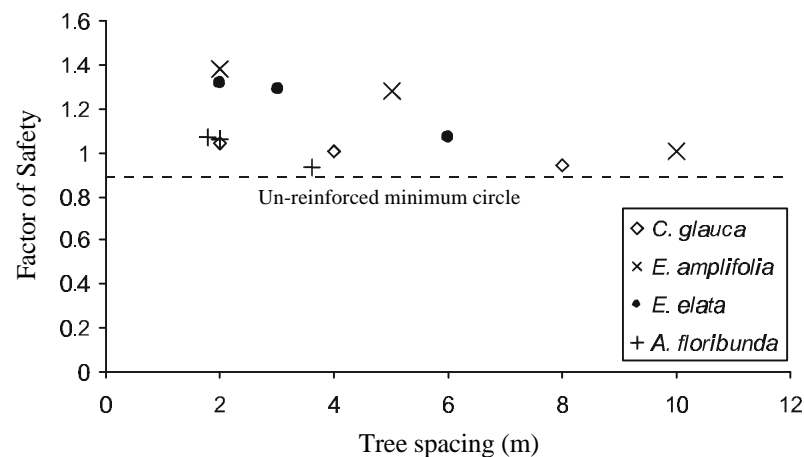

Figure 7.15: Increased riverbank stability resulting from differences in tree species and density on Profile C. As tree spacing decreases the FoS increases for all species.

7.5.1.3 Summary

The results presented in this section demonstrate the stabilising effects of riparian vegetation on fully saturated and partly drained riverbanks subjected to rapid draw-down. Only six of the thirty-six vegetated stability analyses conducted under completely saturated bank conditions failed to increase the FoS of an unstable, un-reinforced riverbank, above the critical value of 1.00. The issue however is not determined simply by the presence or lack of vegetation. Differences in the species and the spacing between trees has a marked effect on the amount of increase in stability. Riverbanks vegetated with *E. amplifolia* present with the highest Factors of Safety, followed by *E. elata*, *A. floribunda*, and *C. glauca*. The differences between species vary depending on the geometry of the bank profile and subsurface conditions. For instance the larger trees are particularly effective on Profile A where the critical failure surface is forced through the same volume of soil by the presence of bedrock.

Increasing the density of mature trees on a riverbank increases its stability. For *C. glauca* over the three profiles this effect was an average increase in FoS of 0.02 per metre, that is for every metre closer together that the trees were spaced, there was an average increase of 0.02 in the FoS of the slope. For *E. amplifolia* the average increase was 0.06 per metre, for *E. elata* it was 0.07 per metre, and for *A. floribunda* it was 0.10 per metre.

Vegetation provides a greater benefit to completely saturated riverbanks than to banks that have partly drained. This is because the effect of the root reinforcement is less significant in terms of stabilising the bank than is the reduction in bank material weight that results from a reduced volume of saturated soil. However the presence of vegetation still increased the bank stability of the partly drained profiles by up to 75 %.

7.5.2   A single species forest on 'present-day' riverbank profiles

This section presents the results of riverbank stability modelling conducted on 'present-day' riverbank profiles vegetated with a single species forest. The profiles were modelled with forests of different tree sizes. These sizes were: a Mature Tree as previously described, half of the mature size, one quarter of the mature size, and one eighth of the mature size. Profiles were modelled with trees of decreasing size until the increase in FoS above the un-reinforced bank was 5 % or less. This process provides an indicative result of the length of time after planting that different tree species take to provide a significant effect on riverbank stability.

7.5.2.1 Typical Planting Densities

Profiles were modelled with tree spacings set relative to the maximum lateral root extent (as in the previous section). The spacings used were 50 % of the maximum lateral root extent for mature trees (i.e. 4 m for *C. glauca*, 5 m for *E. amplifolia*, 3 m for *E. elata*, and around 2 m for *A. floribunda*), reducing to 2 m for trees half and a quarter of this size, and to 0.75 m and 1 m for trees that are one eighth of the mature size. These spacings are generally consistent with and representative of planting recommendations outlined in Benson & Howell (1993). Benson & Howell's (1993) strategy for the rehabilitation of riparian vegetation along the Hawkesbury-Nepean River suggests that trees should be planted at spacings of between 2 m and 5 m so that accounting for some losses, large mature trees will be spaced at around 10 m apart with shrubs and understorey forest in between. Coppin & Richards (1990) suggest planting trees of between 2 m and 2.5 m apart, while Burston & Brown (1996) indicate that 3 m is standard practice. The simplifications imposed by XSLOPE and described in section 7.5.1.1 meant that it was not possible to model all suggested planting densities.

7.5.2.2 Stability Analysis Results

(i) Profile Ac: Steep and high bank in cohesive soils above bedrock

The stability analysis results for riverbank Profile Ac are presented in Table 7.11 and the critical failure surfaces in Figure 7.16. As with the 'pre-failure' bank profiles, *E. amplifolia* is clearly the most effective species in terms of increasing the stability of the bank. Spaced at 5 m it is significantly more effective than the other three species are at greater densities, and produces an increase in FoS of greater than 5 % at a height of 7.5 m (quarter size). *E. elata* produces an equivalent increase in FoS at a height of 15 m (half size) while *A. floribunda* and *C. glauca* are mature (8 m and 20 m respectively) before they exhibit similar results. The partly drained state of the bank material, as with 'pre-failure' profiles, reduces the influence of vegetation on bank stability.

Table 7.11: Stability analysis results for single species forests on riverbank Profile Ac. The critical failure surfaces are illustrated in Figure 7.16.

Species, size and spacing (Tree spacing in parentheses)	Complete bank saturation		Partly drained bank		Fixed failure circle	
	FoS	% Increase	FoS	% Increase	FoS	% Increase
Bare	**1.08**	-	**1.36**	-	**1.08**	-
C. glauca (4 m)	1.14	6	1.43	5	1.18	9
C. glauca half size (2 m)	1.09	1	1.38	1	1.11	3
E. amplifolia (5 m)	1.68	56	1.94	43	2.37	119
E. amplifolia half size (2 m)	1.50	39	1.78	31	1.85	71
E. amplifolia quarter size (2 m)	1.19	10	1.46	7	1.27	18
E. amplifolia one eighth size (1 m)	1.10	2	1.38	1	1.12	4
E. elata (3 m)	1.45	34	1.75	29	1.93	79
E. elata half size (2 m)	1.20	11	1.48	9	1.31	21
E. elata quarter size (1.35 m)	1.09	1	1.38	1	1.09	1
A. floribunda (2 m)	1.27	18	1.55	14	1.34	24
A. floribunda half size (1.5 m)	1.12	4	1.40	3	1.13	5
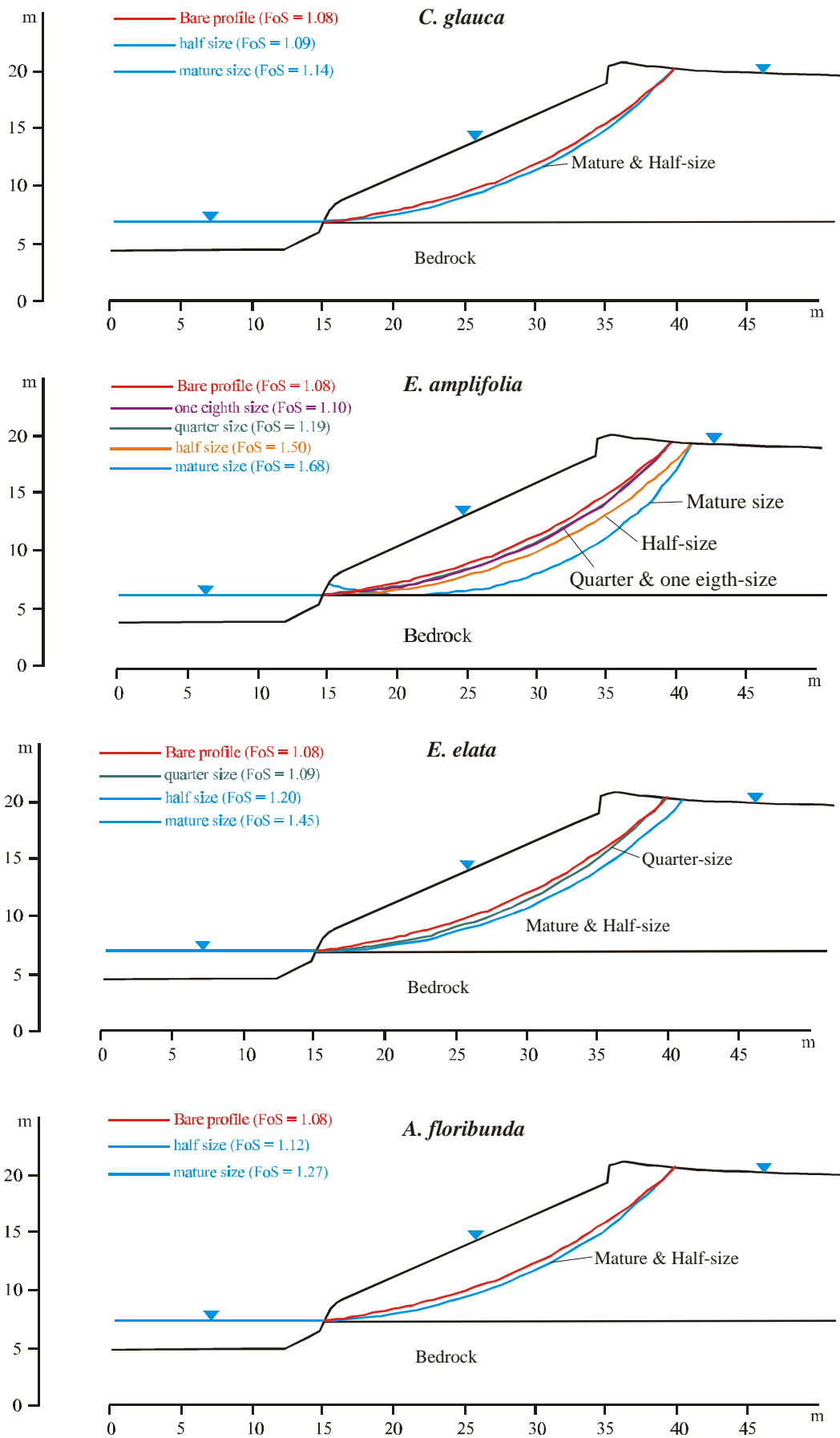
Figure 7.16: The critical failure surfaces for each species at different tree sizes on Profile Ac.

A standard comparison between three of the species that are half-size and spaced at 2 m intervals presents large differences between the relative increase in FoS of the bank. *E. amplifolia* increases the FoS to very stable and *E. elata* increases it to stable, but with *C. glauca* it remains marginally stable. Reinforcing the critical failure plane of the un-reinforced profile gave a maximum increase in FoS of 71 % for *E. amplifolia* and a minimum of 3 % for *C. glauca*.

As the size of the trees increased the critical failure surface was generally forced deeper within the bank material (Fig. 7.16). This was apparent for all species but was more obvious for the deeper rooting trees: *E. amplifolia* and *E. elata*.

(ii) Profile Xc: Average dimensions of surveyed banks within the study area

The stability analysis results for riverbank Profile Xc are presented in Table 7.12 and the critical failure surfaces in Figure 7.17. *E. amplifolia* is again the most effective species at increasing the stability of the profile. It produces a greater increase in FoS at 5 m spacing than *E. elata* at 3 m (Table 7.12). On this profile both the Eucalypts are capable of increasing the FoS by more than 5 % when they are a quarter of the size of a mature tree (7.5 m for *E. amplifolia* and *E. elata*). For both *C. glauca* and *A. floribunda* to achieve a similar result, a mature forest is required.

Table 7.12: Stability analysis results for single species forests on riverbank Profile Xc. The critical failure surfaces are illustrated in Figure 7.17.

Species, size and spacing (Tree spacing in parentheses)	Complete bank saturation		Partly drained bank		Fixed failure circle	
	FoS	% Increase	FoS	% Increase	FoS	% Increase
Bare	**1.05**	-	**1.48**	-	**1.05**	-
C. glauca (4 m)	1.17	11	1.54	4	1.26	20
C. glauca half size (2 m)	1.09	4	1.50	1	1.14	9
E. amplifolia (5 m)	1.44	37	1.73	17	3.69	251
E. amplifolia half size (2 m)	1.37	30	1.67	13	2.69	156
E. amplifolia quarter size (2 m)	1.20	14	1.55	5	1.43	36
E. amplifolia one eighth size (1 m)	1.09	4	1.50	1	1.12	7
E. elata (3 m)	1.41	34	1.70	15	4.94	370
E. elata half size (2 m)	1.28	22	1.61	9	2.44	132
E. elata quarter size (1.35 m)	1.13	8	1.52	3	1.22	16
E. elata one eight size (0.75 m)	1.08	3	1.50	1	1.09	4
A. floribunda (2 m)	1.26	20	1.60	8	1.89	80
A. floribunda half size (1.5 m)	1.10	5	1.52	3	1.21	15
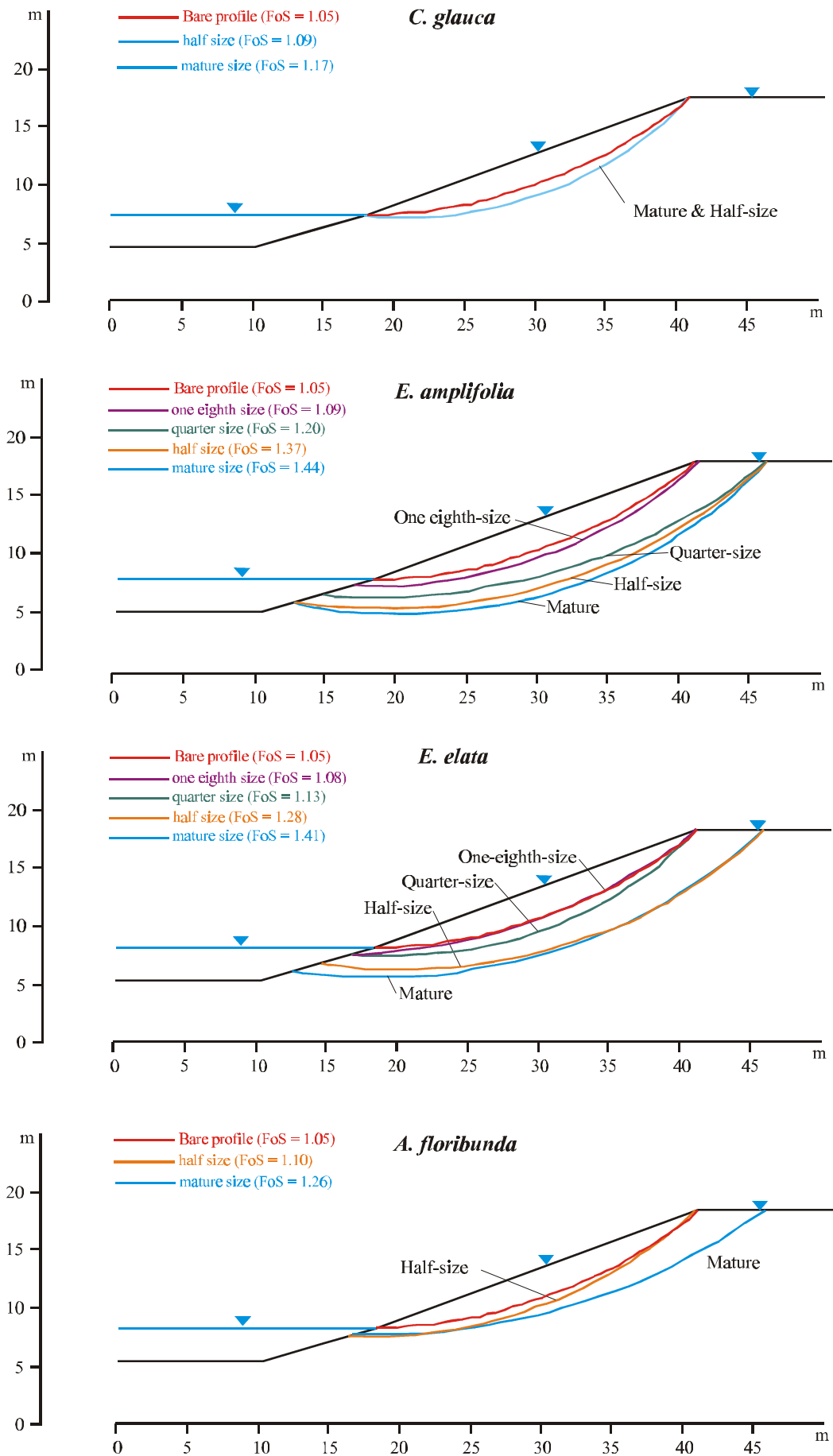
Figure 7.17: The critical failure surfaces for each species at different tree sizes on Profile Xc.

For trees that are half size and spaced at 2 m intervals *E. amplifolia* and *E. elata* increase the FoS of the bank to stable. *C. glauca* increases the FoS from critically stable to marginally. These differences between species are significantly less than for Profile Ac. Reinforcing the critical failure plane of the un-reinforced profile gave a maximum increase in FoS of 156 % for *E. amplifolia* and a minimum of 9 % for *C. glauca*. As with Profile Ac an increase in tree size and therefore the extent of root reinforcement caused the critical failure surface to be forced deeper within the bank material (Fig. 7.17).

(iii) Profile Cc: Steep but relatively low height in cohesive soils

The stability analysis results for riverbank Profile Cc are presented in Table 7.13 and the critical failure surfaces in Figure 7.18. As with every other profile modelled *E. amplifolia* is the most effective species at increasing the FoS of the bank (Table 7.13). In this case mature *E. amplifolia* spaced at 5 m are just as effective as *E. elata* at 3 m and more effective than both *C. glauca* and *A. floribunda* at their designated spacings (4 m and 2 m respectively). To achieve a FoS increase of greater then 5 % on this profile an *E. amplifolia* forest at a quarter of the mature size is sufficient. For *E. elata* a forest at half the mature size is required, while for *C. glauca* and *A. floribunda* a mature forest is required.

Table 7.13: Stability analysis results for single species forests on riverbank Profile Cc. The critical failure surfaces are illustrated in Figure 7.18.

Species, size and spacing (Tree spacing in parentheses)	Complete bank saturation		Partly drained bank		Fixed failure circle	
	FoS	% Increase	FoS	% Increase	FoS	% Increase
Bare	**1.05**	-	**1.25**	-	**1.05**	-
C. glauca **(4 m)**	1.13	8	1.32	6	1.13	8
C. glauca **half size (2 m)**	1.09	4	1.32	6	1.09	4
E. amplifolia **(5 m)**	1.41	34	1.62	30	1.58	50
E. amplifolia **half size (2 m)**	1.30	24	1.51	21	1.48	41
E. amplifolia **quarter size (2 m)**	1.13	8	1.34	7	1.16	10
E. amplifolia **one eighth size (1 m)**	1.07	2	1.27	2	1.08	3
E. elata **(3 m)**	1.41	34	1.60	28	1.58	50
E. elata **half size (2 m)**	1.23	17	1.42	14	1.26	20
E. elata **quarter size (1.35 m)**	1.09	4	1.29	3	1.09	4
A. floribunda **(2 m)**	1.18	12	1.38	10	1.18	12
A. floribunda **half size (1.5 m)**	1.09	4	1.29	3	1.09	4
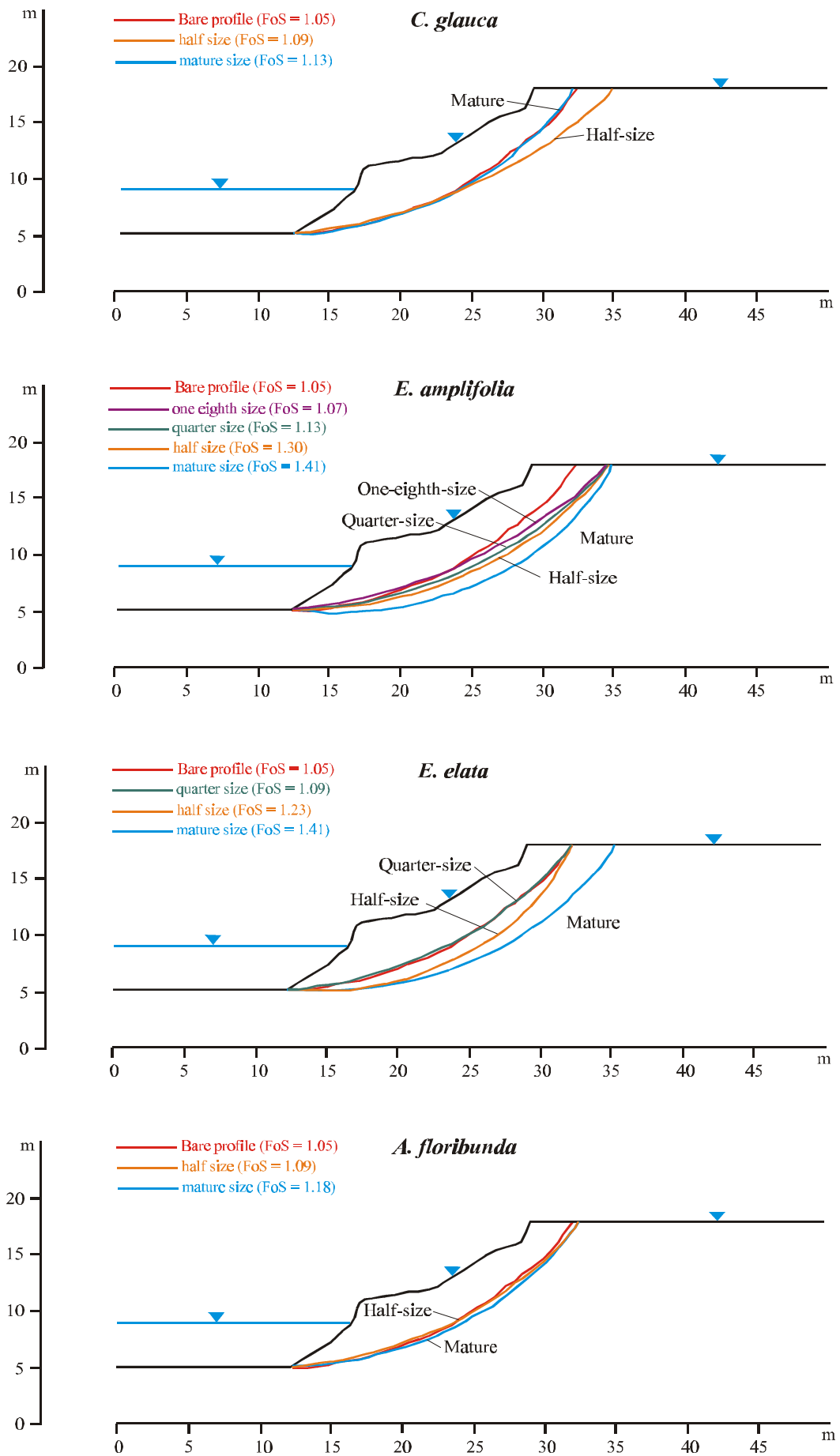
Figure 7.18: The critical failure surfaces for each species at different tree sizes on Profile Cc.

For trees that are half size and spaced at 2 m intervals *E. amplifolia* and *E. elata* increased the FoS of the bank to stable. *C. glauca* increased the FoS from critically stable to marginally stable. The differences between species are significantly less than for Profile Ac and similar to Profile Xc. Reinforcing the critical failure plane of the un-reinforced profile gave a maximum increase in FoS of 50 % for *E. amplifolia* and *E. elata*, and a minimum of 4 % for *C. glauca*. As with Profiles Ac and Xc an increase in tree size and therefore the spatial extent of root reinforcement generally caused the critical failure surface to be forced deeper within the bank material (Fig. 7.18).

7.5.2.3 Summary

'Present-day' riverbanks are considerably more stable when vegetated rather than bare. However as with 'pre-failure' banks, different species provide a greater or lesser stabilising effect. *E. amplifolia* is consistently the most effective species at increasing a bank's stability, followed by *E. elata*, *A. floribunda*, and finally *C. glauca*. The dominance of the two Eucalypts in this regard illustrates the potential of large trees to reinforce the bank material. *A. floribunda* has stronger roots than either of the Eucalypts (chapters four and five) but its more restricted root system (chapter three) reduces the volume of soil through which these roots can act. *E. amplifolia* roots recorded the smallest increased shear resistance of all four species (chapter five) however its extensive root system in both the vertical and lateral directions more than makes up for this lower strength. It is apparent from the results presented here that the species selected for revegetation will have a large bearing on the effectiveness of the bank stabilisation objectives.

The modelling presented in this section provides an understanding of the relative stabilising effects of four tree species common to the study area. It does not take account of the ecological advantages of multiple species growing over the bank profile. This is addressed in the following section.

7.6   The effect of a multiple species forest on riverbank stability

A single species riparian forest is a highly unlikely natural situation and has not been observed on the banks of the Nepean River (Benson & Howell, 1993). Realistic assessment of a natural forested bank should focus on a multiple species analysis which replicates as closely as possible the natural situation. This section presents the stability modelling results for both 'pre-failure' and 'present-day' bank profiles reinforced with the roots of multiple tree species.

'Pre-failure' riverbank profiles were modelled by placing the four species in bank locations where they are most commonly found. That is *C. glauca* at the waterline, *A. floribunda* in the mid-bank region, *E. elata* at the levee crest, and *E. amplifolia* on the floodplain. The modelling of four species on the one profile presented some difficulties for XSLOPE because of its maximum limit of 18 soil layers. Therefore each species was limited to four layers each and had to be modelled using only the first 25 % lateral distance boundary. Given the substantial reduction in root area ratio beyond this

boundary the loss of accuracy is expected to be minimal. For instance, the single species analysis in section 7.4 demonstrates that only a small increase in FoS is observed when the critical failure surface extends through the reinforced area beyond 25 % of the maximum lateral root extent (e.g. 6 % for *E. elata* in position *e* on Profile Ac, 10% for *E. elata* in position *e* on Profile Cc (Appendix E-I)).

The limit on the number of soil layers presents discontinuities of reinforcement in the areas of overlap between different species. In order to model the reinforcement in these zones a minimum background value of S_r was used. The value was based on the minimum outer zone reinforcement for each of the species concerned.

Tree spacings were chosen according to the spatial root distribution models for each species (chapter six), in order that the upper layer of soil represented a continuous 'root mat' below each group of trees. Hence the tree spacing was 4 m for *C. glauca*, 5 m for *E. amplifolia*, 3 m for *E. elata*, and 1.8 m for *A. floribunda*. An additional model was generated for half-size forests at a spacing of 2 m. Critical factors of safety were determined for each 'pre-failure' profile under the different vegetated conditions modelled.

'Present-day' bank profiles were modelled using two species on each profile. This enabled each profile to be assessed under a continuous root reinforcement. Profiles were modelled with large trees alternating with smaller trees over the entire bank profile. *E. amplifolia* was paired with *C. glauca* or *A. floribunda*; *E. elata* was paired with *C. glauca* or *A. floribunda*; and *C. glauca* was paired with *A. floribunda*. The larger tree of the pairing was spaced at 50 % of its maximum lateral root extent with the smaller tree at the midpoint between two large ones. Critical factors of safety were determined for each 'present-day' profile under the different vegetated conditions modelled.

7.6.1   Stability analysis results for 'pre-failure' riverbank profiles

The stability analysis results for 'pre-failure' riverbank profiles are presented in Table 7.14 and the critical failure surfaces are presented in Figures 7.19 to 7.21 and Appendix E-II.

Table 7.14: Results of multiple species analysis on 'pre-failure' riverbanks. Given below are the critical FoS, the percentage increase in stability over the bare profile, and the FoS of the failure surface fixed at the critical location from the un-reinforced analysis.

Vegetated condition	Profile A			Profile B			Profile C		
	FoS	% Increase	Fixed	FoS	% Increase	Fixed	FoS	% Increase	Fixed
Bare Profile	**0.85**	-	-	**0.95**	-	-	**0.88**	-	-
Mature Forest	1.20	41	1.86	1.29	36	2.19	1.19	35	1.59
Half-size Forest	1.02	20	1.14	1.10	16	1.36	0.99	13	1.10

Figure 7.19: The critical failure surface and a selection of other representative circles under riverbank Profile A vegetated with multiple species. *C. glauca* growing at the waterline, *A. floribunda* on the mid-bank region, *E. elata* from mid-bank to the levee crest, and *E. amplifolia* on the floodplain. The different reinforced soil layers representing different soil reinforcement values beneath each species are illustrated: visually describing a series of cones with decreasing soil shear resistance towards their points. The range in soil cohesion beneath each tree species is 16.79 to 12.04 kPa for *C. glauca*, 70.05 to 20.4 kPa for *A. floribunda*, 61.05 to 13.54 kPa for *E. elata*, and 46.85 to 15.48 kPa for *E. amplifolia*.

Figure 7.20: The critical failure surface and a selection of representative circles under riverbank Profile B vegetated with multiple species. *C. glauca* growing at the waterline, *A. floribunda* on the mid-bank region, *E. elata* from mid-bank to the levee crest, and *E. amplifolia* on the floodplain. The different reinforced soil layers representing different soil reinforcement values beneath each species are illustrated. The range in soil cohesion beneath each tree species is 10.49 to 3.72 kPa for *C. glauca*, 63.75 to 14.10 kPa for *A. floribunda*, 54.75 to 7.24 kPa for *E. elata*, and 40.55 to 9.18 kPa for *E. amplifolia*.
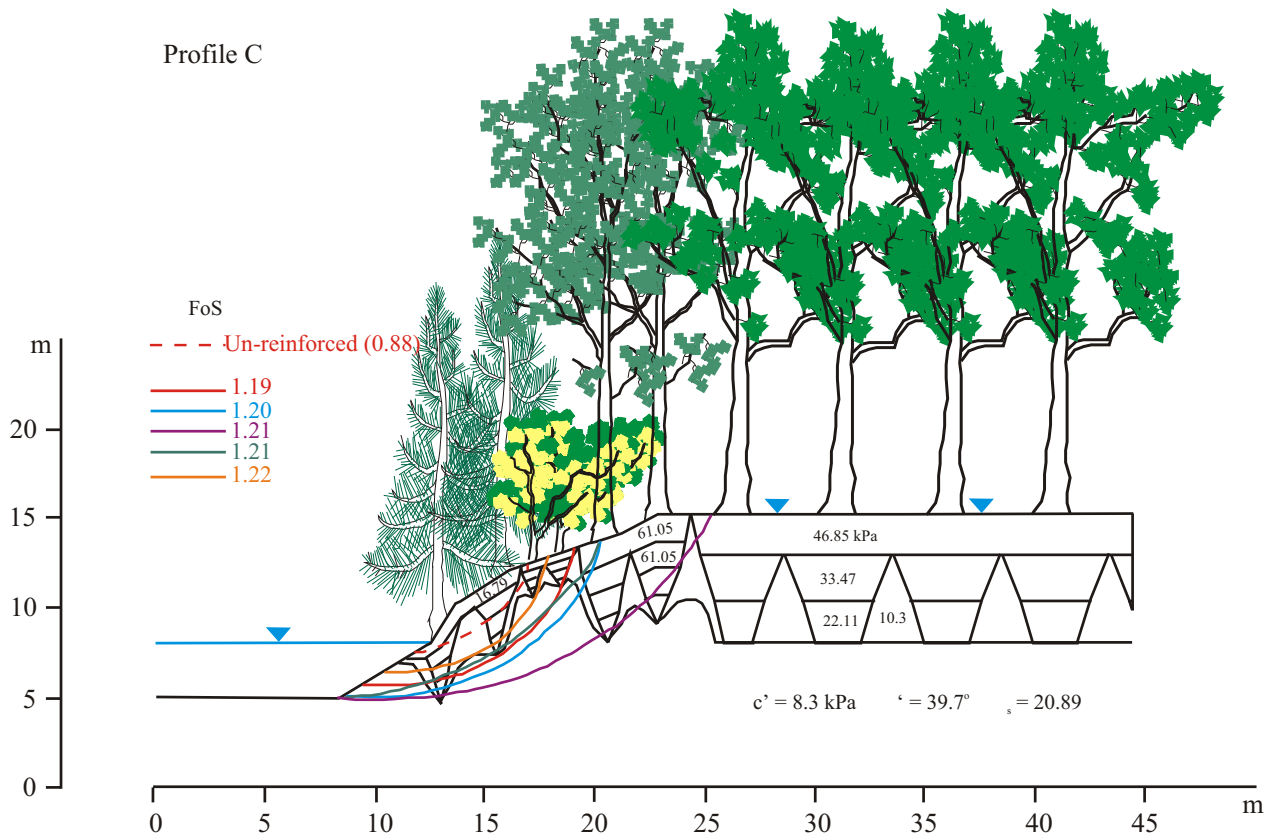
Figure 7.21: The critical failure surface and a selection of representative circles under riverbank Profile C vegetated with multiple species. *C. glauca* growing at the waterline, *A. floribunda* on the mid-bank region, *E. elata* from mid-bank to the levee crest, and *E. amplifolia* on the floodplain. The different reinforced soil layers representing different soil reinforcement values beneath each species are illustrated. The range in soil cohesion beneath each tree species is 16.79 to 12.04 kPa for *C. glauca*, 70.05 to 20.4 kPa for *A. floribunda*, 61.05 to 13.54 kPa for *E. elata*, and 46.85 to 22.11 kPa for *E. amplifolia*.

Figures 7.19 to 7.21 illustrate the zones of root-reinforced soil modelled beneath each tree species for the three 'pre-failure' riverbank profiles. Visually the appearance is of a continuous 'root mat' for the first 25 % of root depth, which is underlain by a series of cones beneath each individual tree. The cones decrease in root reinforcement towards their points.

The 'pre-failure' profiles vegetated with multiple species presented significant increases in the stability of the banks compared to the bare profile (Table 7.14). On all profiles the mature forest increased the FoS above 1.00, and even a half-size forest on Profiles A and B increased the bank stability from unstable to critically stable. A half-size forest on Profile C was critically unstable. The most effective increase in stability occurred on Profile A (41 % for a mature forest) although the difference between profiles was small (36 % for Profile B and 35 % for Profile C). The factor of safety for the failure plane fixed to the critical location from the un-reinforced analysis increased by 119 % for Profile A, 131 % for Profile B, and 81 % for Profile C.

There is a tendency for the failure surfaces to exit the mid- to upper-bank region between different species, where the amount of reinforcement is lower (Figs. 7.19 to 7.21). The presence of reinforced soil beneath the trees also pushes the critical failure surface deeper within the bank to avoid the areas of highest additional shear resistance. The magnitude of this effect is enough to suggest that these banks would not have failed if they had not been cleared of vegetation prior to flooding.

7.6.2   Stability analysis results for 'present-day' riverbank profiles

The stability analysis results for 'present-day' riverbank profiles are presented in Table 7.15 and the critical failure surfaces are presented in Figures 7.22 and 7.23 and Appendix E-III.

Table 7.15: Results of multiple species analysis on 'present-day' riverbanks. Given below are the critical FoS, the percentage increase in stability over the bare profile, and the FoS of the failure surface fixed at the critical location from the un-reinforced analysis.

Species pairs	Profile Ac			Profile Xc			Profile Cc		
	FoS	% Increase	Fixed	FoS	% Increase	Fixed	FoS	% Increase	Fixed
Bare Profile	**1.08**	-	-	**1.05**	-	-	**1.05**	-	-
C. glauca & *A. floribunda*	1.30	20	1.30	1.25	19	1.59	1.18	12	1.18
E. amplifolia & *C. glauca*	2.06	91	2.51	1.46	39	4.10	1.40	33	1.55
E. amplifolia & *A. floribunda*	2.09	94	2.75	1.50	43	4.59	1.42	35	1.59
E. elata & *C. glauca*	1.62	50	1.82	1.36	30	3.15	1.28	22	1.50
E. elata & *A. floribunda*	1.71	58	1.90	1.39	32	3.87	1.27	21	1.59
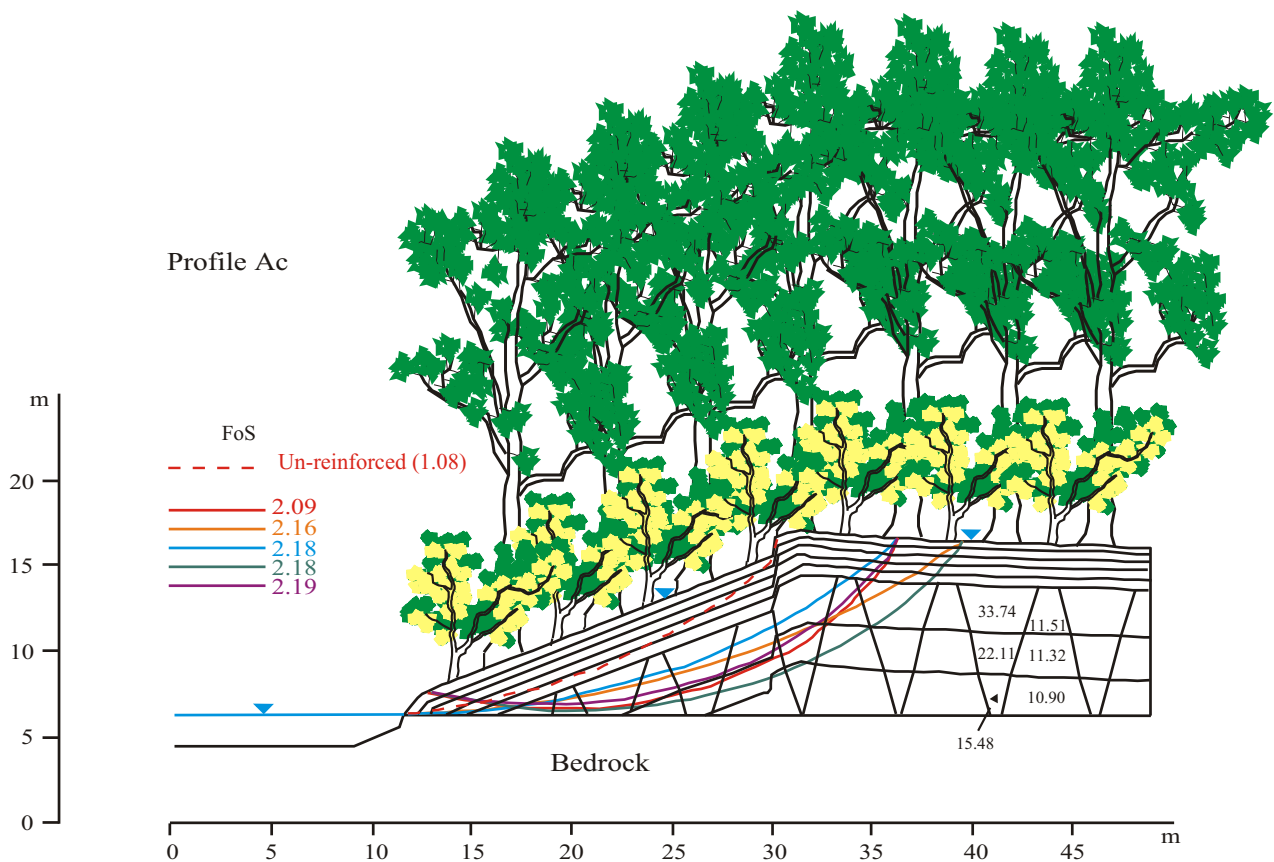
Figure 7.22: The critical failure surface and a selection of other representative circles under riverbank Profile Ac vegetated with mature *E. amplifolia* and *A. floribunda* trees. Such a condition allows a series of high reinforcement upper soil layers consisting of the roots of both species and varying only with depth to overlie the cones of the deeper rooting *E. amplifolia*. The range in soil cohesion over the high reinforcement upper layers is from 94.39 to 46.39 kPa. Values for other soil layers are shown (in kPa).
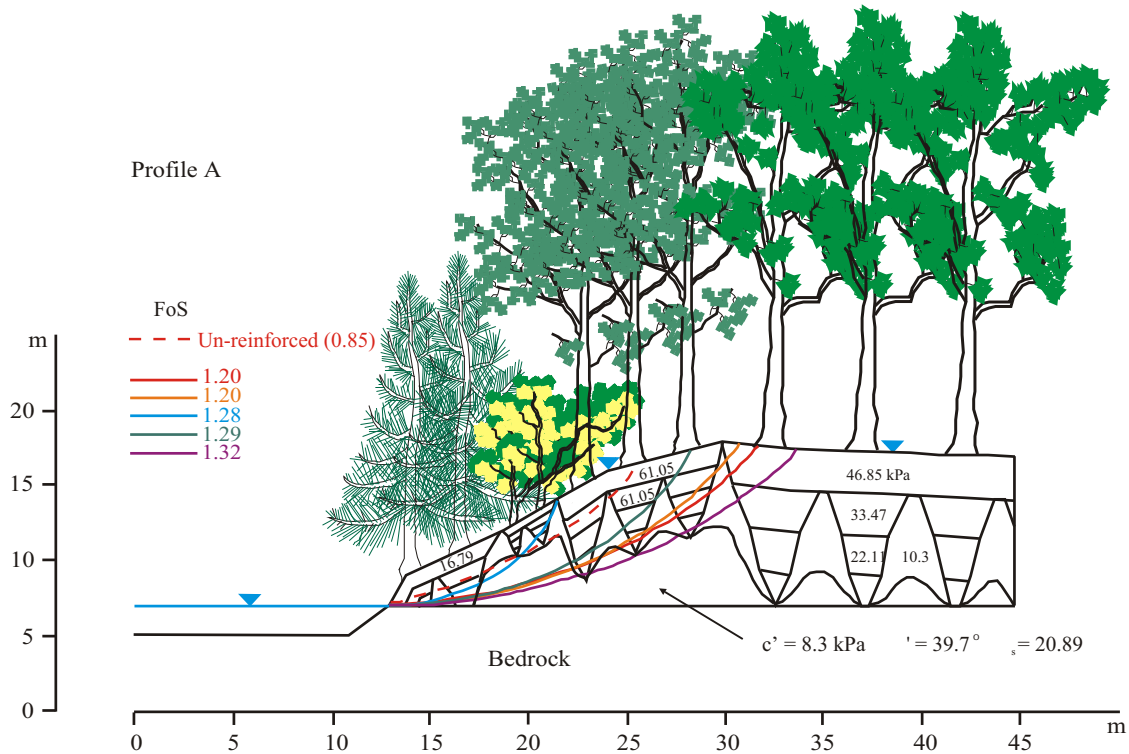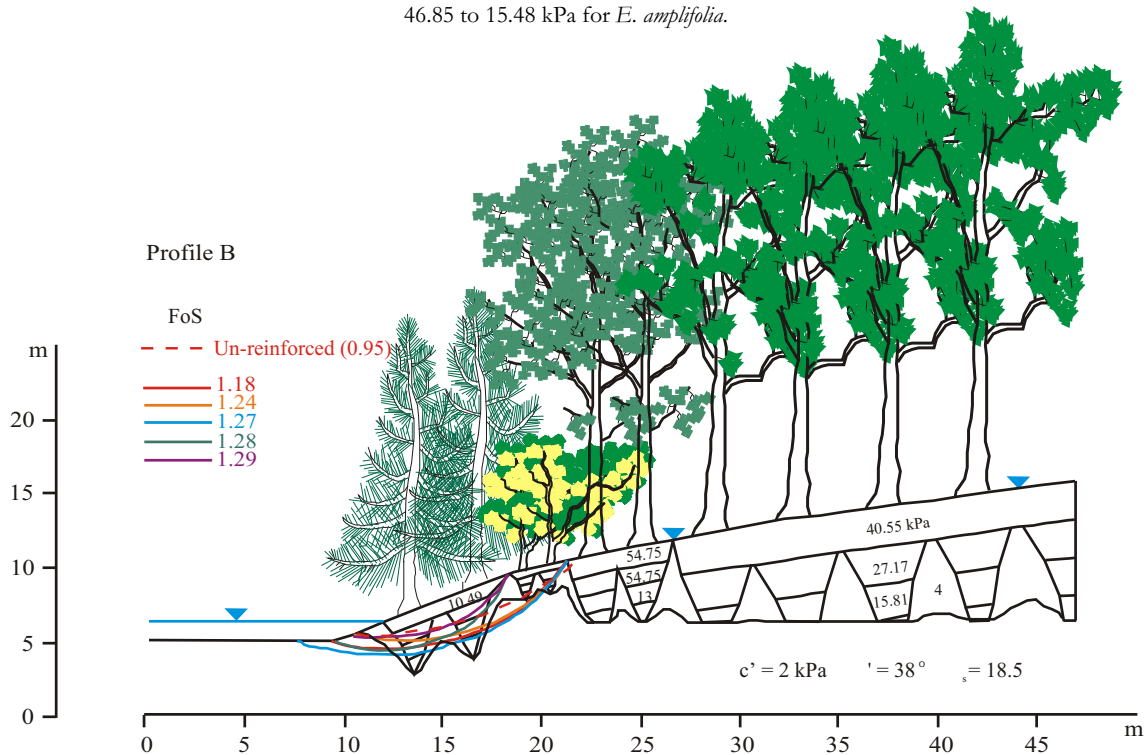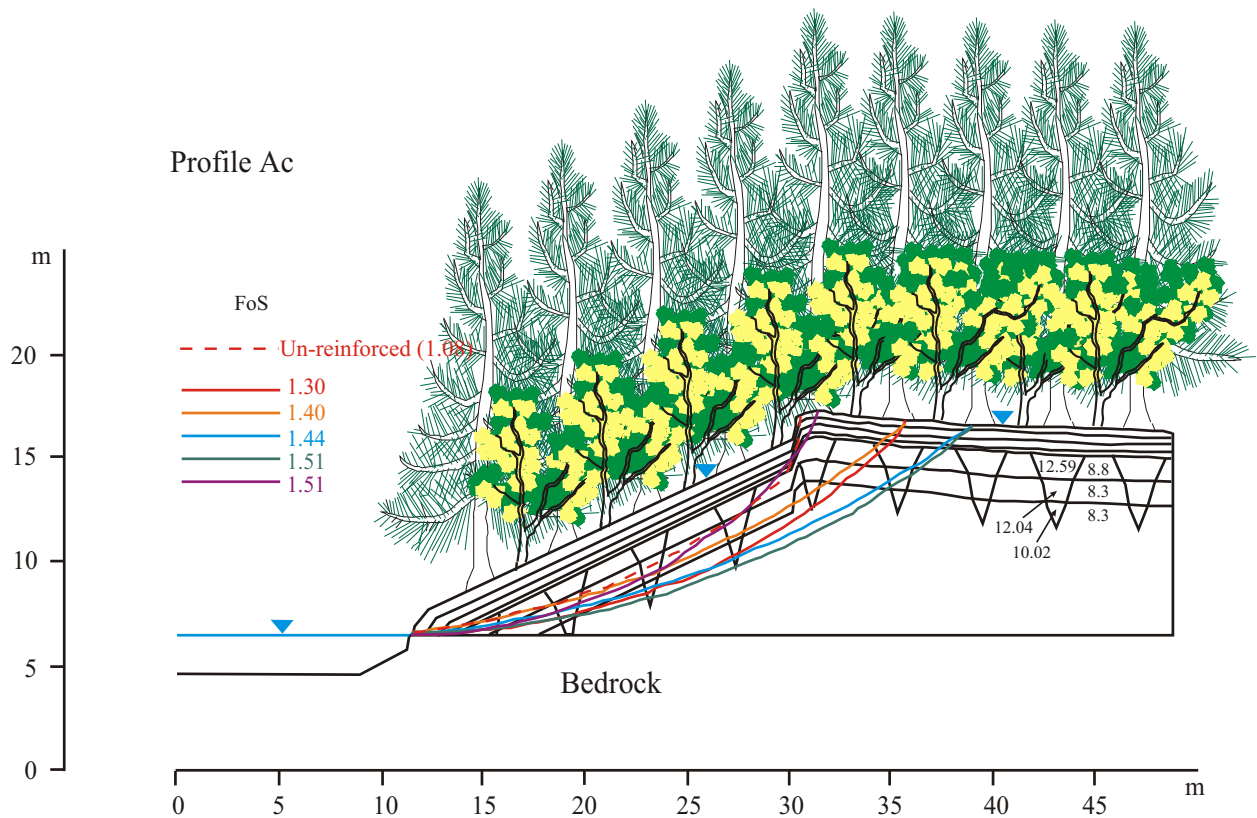
Figure 7.23: The critical failure surface and a selection of other representative circles under riverbank Profile Ac vegetated with mature *C. glauca* and *A. floribunda* trees. The range in soil cohesion over the high reinforcement upper layers is from 71.49 to 16.75 kPa. Values for other soil layers are shown (in kPa).

In all cases modelled the vegetated condition increased the FoS significantly above that of an un-reinforced bank profile (Table 7.15). The effect was more pronounced on Profile Ac (Av. 63 % increase) compared to Profile Xc (Av. 33 % increase) and Profile Cc (Av. 25 % increase). As with the vegetated conditions in the previous sections this is due to the reduced ability of the failure surface to avoid the root-reinforced soil as a result of the bedrock in Profile Ac.

Differences between species pairs are significant in terms of the relative increase in riverbank stability. On all three profiles the most effective pair is that of *E. amplifolia* and *A. floribunda*, followed closely by *E. amplifolia* and *C. glauca*. The least effective pair is that of *C. glauca* and *A. floribunda* (Table 7.15). It is also apparent that the selection of the larger tree in the pairing is more important than the selection of the smaller one. For instance the average difference in increased riverbank stability over the three profiles between a large Eucalypt paired with *A. floribunda* and a large Eucalypt paired with *C. glauca*, is 3 % for *E. amplifolia* and 4 % for *E. elata*. However the difference between either *C. glauca* or *A. floribunda* paired with *E. amplifolia* as opposed to *E. elata* is on average 21 % over the three profiles.

Modelling species in pairs enabled the delineation of continuous root reinforcement layers close to the ground surface (Figs. 7.22 & 7.23). Here the intermingled roots are able to bind the soil tightly

into a reinforced mass with little variation in the lateral direction. This lack of lateral variation prevents the failure surface from exploiting zones of relative weakness. The critical failure surface is therefore often that which exhibits the shortest possible route through the high reinforcement upper layers. This is observable with both the most effective pair (*E. amplifolia* & *A. floribunda*) and the least effective pair (*C. glauca* & *A. floribunda*) on Profile Ac. In both cases the critical failure plane is forced below the zones of highest reinforcement until a point where a high exit angle can be realised (on the floodplain side of the levee crest).

7.7   Sensitivity analysis of the modelling

The model of earth reinforcement under riparian vegetation requires two specific inputs in its determination of the extent and amount of reinforcement. These are tree height and stem diameter at the ground surface. The values chosen for a mature tree of each species were based on observations and measurements within the field as well as data provided by Benson & Howell (1993). The dimensions represent typical specimens from within the study area, however natural biological variation means that there is a considerable range about the chosen values. To test the sensitivity of the final riverbank stability output to different input values of both tree height and stem diameter a forested riverbank profile of each species was examined over a range of what could be considered 'mature' dimensions. The profile chosen was the 'present-day' average profile (Xc), with tree heights and stem diameters based on field measurements taken from sites 1 and 4 (see section 7.5.1). The results are presented below (Table 7.16 to 7.19).

Table 7.16: Factors of safety for *C. glauca* forest on Profile Xc with different tree dimensions.

	Tree Height		
Stem Diameter	**15 metres**	**20 metres**	**25 metres**
0.16 m	1.14	1.08	1.10
0.32 m	1.26	1.17	1.24
0.48 m	1.33	1.26	1.32

Table 7.17: Factors of safety for *E. amplifolia* forest on Profile Xc with different tree dimensions.

	Tree Height		
Stem Diameter	**25 metres**	**30 metres**	**40 metres**
0.35 m	1.31	1.28	1.27
0.70 m	1.45	1.44	1.44
1.20 m	1.52	1.54	1.57

Table 7.18: Factors of safety for *E. elata* forest on Profile Xc with different tree dimensions.

	Tree Height		
Stem Diameter	**25 metres**	**30 metres**	**40 metres**
0.45 m	1.36	1.34	1.31
0.90 m	1.36	1.41	1.42
1.40 m	1.39	1.43	1.50

Table 7.19: Factors of safety for *A. floribunda* forest on Profile Xc with different tree dimensions.

	Tree Height		
Stem Diameter	**6 metres**	**8 metres**	**10 metres**
0.12 m	1.20	1.20	1.21
0.24 m	1.26	1.26	1.26
0.36 m	1.29	1.31	1.32

Over a large range in tree sizes the calculated FoS varies by a maximum of ± 13 % for *C. glauca*, ± 13 % for *E. amplifolia*, ± 8 % for *E. elata*, and ± 5 % for *A. floribunda*, from the typical values chosen to represent a mature forest in this study (the middle tree height and stem diameters given in Tables 7.16 to 7.19). These values therefore allow a representative assessment of riverbank stability under a mature forest that contains a range of actual tree sizes. Using this approximately median value should balance out the variance that exists due to a range of actual tree sizes. A more comprehensive analysis of forested slope stability would require the determination of the FoS under all potential tree sizes or perhaps under the random distribution of different sized trees on a bank. Both of these options are beyond the capacity of XSLOPE without significant reductions in the complexity of the root reinforcement models presented in chapter six.

7.8   Summary and discussion

The stability analyses presented in sections 7.4 to 7.6 clearly demonstrate that the presence of vegetation on alluvial riverbanks usually results in a considerable increase in their stability. However the specific vegetated conditions present have a determining influence on the actual amount of increased stability. Differences in species, tree density, location and size all impact upon the Factor of Safety of a given riverbank. It is also apparent that the differences in profile geometry, location of bedrock and position of the watertable between distinct profiles will influence the extent to which vegetation can increase their stability. Between the two vegetated extremes examined, that is from a single mature tree to a very dense mature forest spaced at 2 m intervals, there is a range of increased stability across all profiles from 0 % to 105 %. This range encompasses the possibility of having no effect to the possibility of increasing a bank's stability from unstable to extremely stable.

This finding is in disagreement with Amarasinghe (1993) and Masterman (1994), who found through studies in the UK that root reinforcement failed to produce any significant effect on operational bank material strength. In these two cases the positive effect of root reinforcement was offset by the negative influences of surcharge weight and wind-throw and because most mass-collapse failures occurred at depths below the rooting depths of the plants. It has been demonstrated by Abernethy & Rutherfurd (2000b) and Hubble (2001) that surcharge weight generally has only a minor impact on overall bank stability, and it has been demonstrated in this study that even relatively shallow rooting plants (e.g. *A. floribunda*) are able to push the failure

surface to deeper soil thus increasing calculated factors of safety. Furthermore, the location of trees at positions on the bank where potential failure surfaces exit the slope can be sufficient to improve bank stability above the critical value of 1.00 even if the majority of the failure surface is located at a depth below the maximum root depth of the trees (see also Abernethy & Rutherfurd, 2000a).

A single mature tree is capable of increasing bank stability from between 0 % and 20 % depending on its species and location on the bank profile. This is less than the 10 % to 100 % increase calculated for a single River Red Gum on bank profiles of the Latrobe River in Victoria (Abernethy & Rutherfurd, 2000a), although it is not unexpected given the much smaller bank heights on that river (max. 5.5 m) and the high level of the water in the channel (2.6 m below the bank crest). It is difficult to compare different environments and species, however the stabilising effects of vegetation on steep and high riverbanks such as those observed in the Nepean River system, are similar to those described by Abernethy & Rutherfurd (2000a). The issue of scale is clearly an important one as the relative proportion of reinforced bank material is much greater on smaller riverbanks. Other factors however, may affect the relative importance of scale. For instance the Nepean River is incised for much of its length within bedrock (hence the large height of its banks) and the profile modelled on a bedrock basement in this study is influenced to a greater extent by vegetation than those characterised by thick alluvium, even when the possible effect of roots anchoring the alluvium to the bedrock is discounted. The maximum increase in stability for Profile A (with bedrock) is 105 % compared to 80 % for Profile B, and 57 % for Profile C. This is despite the smaller heights of both profiles B and C.

The Factor of Safety values obtained through the stability modelling of both 'pre-failure' and 'present-day' riverbanks indicate that fully vegetated bank profiles are much more likely to resist failure than un-reinforced profiles. Where channel change is primarily by widening through mass collapse, this finding has significant implications for the determination of factors responsible for prior morphological change, and for predicting and possibly preventing future channel change.

Vegetation and prior morphological change

It has been suggested from investigations along the Nepean River (e.g. Erskine & Warner, 1988) and elsewhere (Thorne, 1982), that channel boundary properties play a secondary role to fluvial actions in determining a channel's morphology. That influences such as riparian vegetation may aid in slowing bank retreat in the short-term, but over the long-term they are overwhelmed by hydrological processes that lead to bed and bank scour and ultimately bank collapse through over-steepening of the bank face. On the Nepean River this effect is compounded by undercutting of the banks due to wind waves attacking the banks at the permanent water level on the weir-induced 'lakes'. The ability of riparian trees to resist fluvial entrainment of soil particles and therefore scour of the bank toe is untested and although vegetated banks are more able to resist the mass collapse that results from over-steepening due to toe removal (Hubble, 2001) it is unclear at this point whether or not they have any role in prevention of this removal in the first place. The photograph

of a mature Casuarina in chapter three (Fig. 3.15) that stands on fractured bedrock with the bank material almost completely removed from around its roots to a depth of 1.7 metres, suggests that such a role may be minimal.

Despite the uncertainty over the role of vegetation in preventing toe scour, Hubble (2001) demonstrated that the removal of riparian vegetation from the banks of the upper Nepean River played a critical role in their subsequent collapse during the prevailing wetter climatic conditions of the 1950s and 1960s. The stability analysis presented in section 7.5.1 supports this finding by demonstrating that even with completely saturated bank material and rapid draw-down in the channel, a typical well vegetated 'pre-failure' riverbank remains stable. Clearly the magnitude of the riparian vegetative influence is sufficient to prevent bank collapse over a range of bank geometries under worst-case hydrological conditions. However the vegetation must be of a sufficient density, size and species that a particular riverbank requires. Consequently, rates of channel widening through bank collapse will vary according to the amount and type of vegetation present. These findings confirm those of Kirkup *et al.* (1998), Brooks & Brierley (2000), and Hubble (2001): that the importance of anthropogenic activities (in this case devegetation) in accelerating channel change on NSW rivers since European settlement is greater than has been previously allowed for by investigators that have focused almost exclusively on climatic factors (e.g. Erskine & Warner, 1988).

Revegetation of 'present-day' riverbank profiles

The results presented in this study indicate that future channel widening on the Nepean River should be concentrated, as it has been in the past, on banks with lower vegetation densities; the effects of undercutting and localised scour notwithstanding. Therefore revegetation of the banks should result in reduced mass collapse and a slower rate of channel widening.

This study demonstrates that it is the larger tree species that contribute most to bank stability, even when smaller ones have significantly greater root strengths. Shields & Gray (1992) recommend woody shrubs and small trees to enhance the structural integrity of levees however in this study the deeper rooting trees, *E. amplifolia* and *E. elata*, have been found to provide much greater reinforcement potential than the smaller *A. floribunda* by reinforcing a much larger volume of bank material. *C. glauca* also reinforces a large volume of soil, but the quantity of root material within this zone is significantly less than the other species and as a result its contribution to increased shear strength is smaller.

The large differences between species in terms of their ability to increase riverbank stability, means that revegetation strategies with this objective in mind should consider carefully the species to be planted. From the analysis in this study the species selected would be, in order of greatest stabilisation potential: *E. amplifolia*, *E. elata*, *A. floribunda*, and *C. glauca*. Sound ecological practice however suggests a mix of native species is preferable (Benson & Howell, 1993), not only for the benefit of other organisms that may inhabit the environment but also for the health of the trees

themselves; single species forest being more prone to attack by pest and disease. Employing the use of a single species forest therefore based simply on the fact that it may have greater earth reinforcement potential may in fact undermine the perceived benefits by compromising the overall health of the plantation. Combining two species together in an assessment of stability, as in section 7.6.2, suggests that the selection of the dominant or large tree in a combination of two is much more significant than the selection of the smaller trees. Therefore when selecting species for revegetation, once a suitable large growing tree has been decided upon and placed at a suitable density, any number of different smaller understorey trees and shrubs could be used to satisfy the ecological requirements. For the banks of the Nepean River both large Eucalypts assessed in this study should provide a large reinforcement once mature. Even trees of 7.5 m in height have been shown to improve riverbank stability by up to 14 % in some instances, providing benefits within a few years of planting.

7.9   Conclusions

Riverbank stability was determined for representative 'pre-failure' and 'present-day' profiles within the study area. The spatial distribution of increased shear resistance provided by the tree roots of four native riparian species was incorporated into slope stability models thereby enabling an assessment of various vegetated conditions. Single species and multiple species analyses were undertaken with completely saturated banks under rapid draw-down and also partly drained banks under rapid draw-down. The results have enabled a rigorous assessment of the vegetative influence on bank collapse within the study area, using well constrained root reinforcement values obtained for species extant within this environment, rather than the conservatively estimated parameters of previous studies. The following conclusions are drawn from this chapter:

1. The presence of vegetation on riverbanks improves their stability, although the amount varies significantly over a range of geometries and vegetated conditions. The primary mechanism is to force the critical failure surface deeper within the soil layer, below the root-reinforced material, thus increasing its factor of safety and the overall stability of the bank.

2. The incised nature of the stream within sandstone and shale bedrock allows for a greater effectiveness of vegetation in improving bank stability on those profiles where this condition is present. In these cases the failure plane must pass through the root reinforced bank material due to the presence of the bedrock. This finding does not account for the additional stabilisation that probably results from tree roots anchoring the alluvium to the bedrock.

3. There are clear differences between the ability of different tree species to improve the stability of alluvial riverbanks. Of the four species assessed in this study *E. amplifolia* is the most effective, followed by *E. elata*, *A. floribunda*, and then *C. glauca*.

4. The stabilising effect of a single tree will vary with its position on the riverbank, with different species more effective in different locations and on different geometries. As a general rule trees positioned at either the levee crest or the toe of the bank will be more effective than trees

located elsewhere, as this is where the failure surface is most likely to exit the slope. On banks of the size present on the Nepean River more than one tree is usually necessary to provide a significant improvement to stability.

5. A lower density of tree cover results in lower bank stability for all the species studied. No critical spacing was determined although when spaced at similar intervals as observed under natural conditions the trees were able to provide a substantial improvement in riverbank stability. In some cases from unstable (0.80 < FoS < 0.94) to extremely stable (FoS > 1.60).

Chapter Eight

Conclusions and implications of the research

8.1 Summary and implications of the research

Summary

Some aspects of riverine morphological change have traditionally been examined in terms of broad cause and effect relationships with temporal coincidence offered as sufficient proof. This has been particularly so in studies that have examined the effect of riparian vegetation or the consequence of its removal, on bank stability. Previous investigators have noted the correlation between vegetation removal and increased incidence of bank collapse, but with a few exceptions (e.g. Hubble & Hull, 1996; Abernethy & Rutherfurd, 2000; Hubble, 2001), have steered away from examining the underlying geomechanical principles. These principles are essentially the same as those affecting hill-slope stability where it is found that mechanical root reinforcement is probably the greatest vegetative influence on the overall stability of a slope. Applying this knowledge to the riparian environment in order to extend the knowledge base concerning vegetative effects on riverine morphology has been the major focus of this thesis.

A series of field and laboratory investigations were undertaken on four Australian riparian tree species in order to assess the effects of tree root reinforcement on the stability of typical riverbank profiles within the study area. The entire root systems of juvenile trees grown in a plantation were excavated and measured leading to the development of relationships describing the spatial distribution of root material both with depth and with lateral distance from the tree stem. Field observations of the partially exposed root systems of mature trees enabled a conservative prediction of the root area ratio as it varies beneath these larger trees.

Direct in-situ shear tests were conducted to ascertain the relationships between increased soil shear strength and root area ratio at the shear surface. These relationships were combined with the spatial distribution data to describe the amount and distribution of reinforced earth beneath each of the four species examined. Direct in-situ shear tests simulate the development of a failure plane in the soil. It was therefore possible to observe the effect of tree roots growing across this surface and to propose a likely root failure process within this environment. Tensile strength and field pull-out tests were also conducted in order to shed light on this process and to evaluate the utility of the simple root reinforcement model of Waldron (1977) and Wu *et al.* (1979).

Incorporating the distribution of root reinforced earth into the slope stability programme XSLOPE enabled an assessment of the potential influence of tree roots on bank stability along the Nepean River. The effect of devegetation was assessed on 'pre-failure' bank profiles by determining whether or not vegetation would have had the capacity through the process of root reinforcement, to increase the stability of these very unstable profiles to a condition of theoretical stability. The effect of revegetation was assessed on 'present-day' bank profiles by determining the influence of various vegetated conditions on improvements to the stability of marginally stable banks.

Implications of the research

Riverbank instability is one of the primary mechanisms of change to the hydraulic geometry of a channel. This is particularly so on the dam and weir impounded upper Nepean River, where flow is virtually non-existent except during periods of intense rainfall and subsequent flooding. The ability of riparian vegetation to improve bank stability is therefore an important mechanism of control for overall channel morphology. It is important that the underlying mechanisms of this control are understood if its influence is to be suitably grasped. The research presented in this thesis therefore has implications for improved understanding of historical channel change and for future riverine management.

First and foremost the addition of root reinforcement values for four species to the Australian 'database', now consisting of six Australian riparian tree species provides a basis for future investigation. It is now possible to make reasonable estimates of the mechanical effect of trees on bank stability within Australia based on Australian species, rather than using values derived from exotic species, as was previously necessary.

This research has highlighted the importance of understanding the root failure process during an assessment of root reinforcement. Although previous researchers have noted the progressive failure of root systems during shear (e.g. see Greenway, 1987), it has generally been overlooked in favour of the utility of the simple root model of Waldron (1977) and Wu *et al.* (1979) even though this model assumes simultaneous tensile failure of all roots. While this may occur in many environments, particularly where the shear zone is confined to a thin zone, it is not the case within alluvial soils of the Nepean River. Overlooking this fact would result in a substantial overestimate of the increased shear resistance provided by tree roots.

The stability analysis conducted in this study has validated the belief of some investigators that the amount of root reinforcement could have been significant enough to prevent much of the mass bank collapse that has occurred within the study area. Previously this assertion was based on conservative estimates of root reinforcement values. Now this assertion is based on measured root reinforcement values for species common to the study area and throughout southeastern Australia. As a result future stability analysis on banks of the Nepean River can be undertaken with a degree of accuracy and with a confidence that was not previously possible.

This research also has implications for future riverine management. In particular the importance of tree selection for revegetation. Not all trees provide the same amount of reinforcement and the differences between species can be substantial. The effects of tree location and planting density are also shown to be important.

8.2   Specific findings

This research into the root reinforcement of alluvial riverbanks has yielded the specific findings listed below. While the values obtained are only directly applicable to the upper Nepean River study area they have more general significance throughout southeastern Australia. The general principles are relevant for universal consideration.

1. Riparian vegetation has been recognised by many geomorphologists as a control on channel morphological change however a quantified understanding of this control has in effect been non-existent. The earth reinforcing effects of tree roots on slope stability have been recognised in work undertaken on hill-slopes yet the transfer of this knowledge to the riverine setting has been slow. Indeed the assessment of riverbank stability by geomechanical means was only first attempted in an Australian fluvial setting by Hubble & Hull in 1996. It is apparent that the potential for a tree to reinforce riverbank soil is limited by the spatial distribution of its root system and the strength of the soil-root system.

2. (i) The spatial root distribution beneath trees varies markedly between species, and with depth and lateral distance from the tree stem. With depth there are generally two distinct zones. The first occurs from between 0 and approximately 15 % of the maximum root depth and consists of approximately 80 % of the total root material quantity. In this zone the root system consists of both vertical and lateral roots, the size and density of which will vary between species. The second zone occurs below approximately 15 % of the maximum root depth and consists primarily of vertical roots. The quantity of root material in this zone decreases exponentially with depth due to the taper of individual vertical roots. In the lateral direction the maximum extent of the root system decreases with depth and the quantity of root material within this maximum extent decreases exponentially with distance away from the tree stem. It does so at all depths.

    (ii) The root systems of three of the species: *C. glauca*, *E. elata*, and *A. floribunda* were quite similar in that they exhibited a 'heart-shaped' system. *E. amplifolia* was markedly different, demonstrating an extensive 'tap-root' system with large vertical roots directly below the tree stem and with minimal fine roots. By a measure of root extent and quantity at a young age *E. amplifolia* exhibits by far the greatest earth–reinforcement potential, followed by *E. elata*, *A. floribunda*, and finally *C. glauca*.

    (iii) Mature trees growing within the study area exhibit similar overall root system morphologies to the small trees examined. The distribution of root material beneath them can therefore be estimated and modelled as soil zones that contain decreasing values of root area ratio with depth and distance from the tree stem. Mature trees have been observed to have large roots extending to depths not previously reported in slope stability studies. This

may be a consequence of the large height of riverbanks within the study area and the sandy bank material of which they consist. *E. elata* exhibits the greatest RAR values in the soil beneath it although *E. amplifolia* potentially reinforces a larger volume of soil.

3. (i) The pull-out strength of individual tree roots varies substantially between species. It is directly related to the diameter of the root at the ground surface. Roots tend to break at a distance within the soil where their diameter has reduced due to taper, and therefore their pull-out strength is considerably lower than their tensile strength as calculated by the diameter at the ground surface. Pull-out strengths describe a negative power relationship with increasing diameter and are within the range of values obtained in previous studies. In order of greatest individual root pull-out resistance are *A. floribunda*, *E. amplifolia*, *E. elata*, and *C. glauca*.

(ii) Inter-species differences in the depth at which root failure occurs are due to differences in root strength and the soil-root bond. For the depths measured in this study, the soil-root bond was negligible for all species except *A. floribunda*. This is most likely due to its more highly branched structure and tendency to break at greater depths within the soil due to a higher tensile strength.

4. (i) The shear resistance of the soil increases with increasing root area ratio at the shear plane. It is a linear relationship for three of the species (*C. glauca*, *E. amplifolia*, and *E. elata*) and a positive power relationship for one (*A. floribunda*). The range of values measured are larger but of the same order of magnitude as previous studies that used similar methods in different environments and using different species. In order of greatest soil strength enhancement for equivalent RAR are *A. floribunda*, *E. elata*, *C. glauca*, and *E. amplifolia*.

(ii) The riparian tree roots studied, fail progressively at different shear displacements by breaking in tension at a distance below the shear zone and then pulling out of the soil in a similar manner as would a series of ground anchors. The total shear resistance measured at any instant is therefore made up of varying proportions of the full tensile strengths of each of the individual roots involved. The rate of strength mobilisation and therefore the displacement at which full tensile strength is reached is different for every root. It is likely that it varies with root morphology and location on the shear surface. It is not necessary for all roots to have failed in tension for the peak shear resistance to have passed. The peak shear resistance of a soil block containing roots is reached at a point where the soil on its own would be at or close to residual strength values.

(iii) Calculating the increased shear resistance from pull-out or tension tests on individual roots and using the simple root model of Waldron (1977) and Wu *et al.* (1979) will lead to substantial overestimates of the contribution of roots to soil shear strength in this

environment. Overestimates of this type average 265 % for the four species investigated in this study.

5. The actual shear resistance measured from direct in-situ tests gives the most appropriate values of root reinforcement for use in this environment. Integrating these with the spatial distribution data, enables the development of a model of the potential earth reinforcement beneath riparian trees. It involves soil zones of different reinforcement strength relative to their position with depth and lateral distance from the tree stem. *A. floribunda* provides the greatest reinforcement values, while *E. amplifolia* provides reinforcement through a much larger volume of soil than any of the other species.

6. (i) The presence of vegetation on riverbanks improves their stability, although the amount varies significantly over a range of geometries and vegetated conditions. The primary mechanism is to force the critical failure surface deeper within the soil layer, below the root-reinforced material, such that the minimum factor of safety of the bank is higher than it would be with no reinforcement present. The magnitude of increased stability on vegetated 'pre-failure' riverbanks could have been significant enough to prevent much of the mass collapse observed in the study area between 1947 and 1992, had the vegetation not been cleared prior to the onset of wetter climatic conditions.

(ii) There are clear differences in the potential ability of different species to improve riverbank stability. Of the four species assessed in this chapter *E. amplifolia* is the most effective, followed by *E. elata*, *A. floribunda*, and then *C. glauca*.

(iii) The effect of a single tree will vary with its position on the riverbank, with different species more effective in different locations and on different geometries. As a general rule trees positioned at either the levee crest or the toe of the bank will be more effective, as this is where the failure surface is likely to exit the slope. On banks of the size present on the Nepean River more than one tree is usually necessary to provide a significant improvement to stability.

(iv) A lower density of tree cover results in lower bank stability for all the species studied. No critical spacing was determined although when spaced at similar intervals as observed under natural conditions the trees were able to provide a substantial improvement in riverbank stability. In some cases from unstable ($0.80 < FoS < 0.94$) to extremely stable ($FoS > 1.60$).

(vi) There is great potential for revegetation of 'present-day' riverbank profiles to greatly enhance their resistance to failure. The presence of vegetation has the capacity to increase the FoS of banks from marginally stable to very stable. Revegetation schemes should however consider very carefully the species selected for use. The stability modelling

undertaken in this study suggests that if a suitable large species can be used and planted at a sufficient density, the selection of the smaller (filler) trees to achieve ecological diversity is less important.

8.3   Limitations of this research and future work

Any research project of this nature possesses limitations as to the utility of its findings given the constraints forced upon it by the practicalities of addressing the problem. This is particularly so when funding and time constraints impact upon overall research design and methodology development. The research presented in this thesis is limited primarily through the issue of scale, in particular concerning the root system architecture measurements. Experimental work was undertaken on small trees up to 4.5 m tall even though it is expected mature trees will provide the greatest earth reinforcement potential. Practically and experimentally is was not possible to examine larger trees, however as a result it was necessary to make some assumptions concerning the likely maximum root depths and the spatial distribution of root material within these depths. Field observations of the partially exposed root systems of mature trees growing within the study area suggest that these scaling assumptions are valid, and conservatively so. Essentially, given the range of measurements expected for mature trees that over the course of a lifetime have been subject to slightly different soil conditions, light availability, competition, and infestation of pest and disease, the values and relationships assumed, based on measurements of juveniles and observation of mature trees are expected to be typical and are in any consideration the only ones available. At any rate the sensitivity analysis on tree size inputs presented in chapter seven suggests that even with large differences of tree height (10 m) and stem diameter (0.45 m), and therefore differences in the estimated maximum root extent and total root quantity, the resultant effect on the FoS within a species is quite small and certainly within the expected natural variation inherent in such calculations. Nevertheless, without definitive measurements taken from a range of mature samples the question of spatial distribution of root material beneath mature trees remains an assumption. Definitive measurement of mature root systems is an area that needs considerable further investigation. Traditional excavation techniques are cumbersome, dangerous and labour intensive, therefore future investigation may do well to focus on developments in Ground Penetrating Radar and imaging technologies (e.g. see Wielopolski *et al.*, 2000).

It is clear from this study that there are large differences in the relative ability of different tree species to contribute to increased soil shear strength. It follows therefore that the greater number of species that can be tested and added to the database, the better the understanding will be of the total mechanical effect of vegetation on both hill-slope and riverbank stability. Currently only six species have been assessed in Australia, the four measured in this study, and the two of Abernethy (1999). It is also likely that the same species growing in different environments will have a greater or lesser effect on soil strength as a result of the effects of different site conditions on root system morphology. Further work needs to be done to measure this effect because at present the values

obtained at one location have somewhat limited applicability to other environments. Thus a limitation of this research and indeed the whole field: the actual values measured are perhaps only directly applicable to the study area from which they were obtained.

It is apparent from this study that the presence of trees on the bank causes the critical failure surface to be forced deeper within the bank material. It follows that if vegetation type and density is not sufficient to prevent failure then the size of the block that fails will be larger than it would be without vegetation. If, as many geomorphologists assert, riparian vegetation is not significant in the long-term morphologic development of a channel when compared to climatic factors, could it be then that under certain vegetated conditions, the quantity of eroded material supplied to the channel is greater than when banks are un-vegetated? A study into the effect of vegetation on the scale of mass failure features would be instructive.

The basis of this research has been the fundamental interaction of tree roots with the surrounding soil. There are many unanswered and indeed unasked questions concerning the processes of interaction at this basic level. The widespread use of the simple root model is something that needs further investigation. This study indicates that the assumptions inherent in the simple root model are not valid for any of the species examined here and yield substantial overestimates of the value of increased shear resistance. A more complete understanding of the progressive failure of root systems and the accuracy of the limit equilibrium method for modelling this would be of particular benefit. It would also be useful to determine the specific root characteristics that influence the shear displacement at which peak shear resistance is reached, both resulting from the individual root and the overall root enhanced soil.

This research has focused only on the mechanical vegetative effects on slope stability. As discussed in chapter two the other direct effect, that of soil moisture modification is also likely to be a significant factor in the influence of trees on slope stability. A complete understanding of vegetative effects on riverbank stability would need to consider this. In particular, what effect do riparian trees have on both the rate of saturation of a bank and the rate of drainage? Such a question may be critical concerning the development of excess pore pressures and the effect of the rapid drawdown condition assumed to precipitate failure in this study and others. Similarly, a complete understanding of the influence of vegetation in the riparian zone requires a better understanding of its effects on other forms of riverine erosion, such as toe retreat from sediment scour and wind-wave attack. Such processes are often cited as precursors to bank stability problems in the first place.

These suggestions for future work represent only some of many potential paths of inquiry. The quantified effect of riparian vegetation on riverbank stability is very much in its infancy, not only within this country but throughout the world.

8.4   Reference list

Abam, T.K.S. 1997. Aspects of alluvial riverbank recession: some examples from the Niger delta. *Environmental Geology*, 31(3/4): 211-220.

Abe, K. and Ziemer, R.R. 1991. Effect of tree roots on a shear zone: modelling reinforced shear stress. *Canadian Journal of Forestry Research*, 21: 1012-1019.

Abernethy, B. 1999. *On the role of woody vegetation in riverbank stability*. Ph.D. Thesis, Monash University, Melbourne.

Abernethy, B. and Rutherfurd, I.D. 1998. Where along a river's length will vegetation most effectively stabilise stream banks? *Geomorphology*, 23(1): 55-75.

Abernethy, B. and Rutherfurd, I.D. 2000a. The effect of riparian tree roots on the mass-stability of riverbanks. *Earth Surface Processes and Landforms*, 25: 921-937.

Abernethy, B. and Rutherfurd, I.D. 2000b. Does the weight of riparian trees destabilize riverbanks? *Regulated Rivers*, 16: 565-576.

Abernethy, B. and Rutherfurd, I.D. 2001. The distribution and strength of riparian tree roots in relation to riverbank reinforcement. *Hydrological Processes*, 15(1): 63-79.

Amarasinghe, I.V. 1993. *Effects of bank vegetation in waterways with special reference to bank erosion, shear strength, root density and hydraulics*. Ph.D. Thesis, The Open University, Milton Keynes, UK.

Ashton, D.H. 1975. The root and shoot development of *Eucalyptus regnans* F. Meull. *Australian Journal of Botany*. 23: 867-887.

Bache, D.H. and MacAskill, I.A. 1984. *Vegetation in civil and landscape engineering*. Granada Publishing, London. 317 pp.

Balaam, N.P. 1994. *XSLOPE Users Manual*. Centre for Geotechnical Research, University of Sydney. 88 pp.

Bell, F.C. and Erskine, W.D. 1981. Effects of recent increases in rainfall on floods and runoff in the upper Hunter Valley. *Search*. 12: 82-83.

Benson, D. H. and Howell, J. 1993. *A strategy for the rehabilitation of the riparian vegetation of the Hawkesbury-Nepean River*. Royal Botanic Gardens, Sydney. 166 pp.

Berthouex, P.M. and Brown, L.C. 1994. *Statistics for environmental engineers*. Lewis Publishers, Boca Raton. 335 pp.

Bishop, A.W. 1954. The use of pore-pressure coefficients in practice. *Gèotechnique*. 4: 148-152.

Bishop, A.W. 1955. The use of the slip circle in the stability analysis of slopes. *Gèotechnique*. 5: 7-17.

Bishop, P.M. 1982. Stability or change: a review of ideas on ancient drainage in eastern New South Wales. *Australian Geographer*. 15: 219-230.

Bishop, P.M. 1986. Horizontal stability of the Australian continental drainage divide in south central New South Wales during the Cainozoic. *Australian Journal of Earth Sciences*. 33: 295-308.

Bishop, D.M. and Stevens, M.E. 1964. *Landslides on logged areas in southeast Alaska*. Research Paper NOR-1. 18 pp. Forest Service. U.S. Dept. of Agriculture, Juneau, Alaska.

Böhm, W. 1979. *Methods of studying root systems*. Springer-Verlag. Berlin. 188 pp.

Burroughs, E.R. and Thomas, B.R. 1977. *Declining root strengths in Douglas-fir after falling as a factor in slope stability.* Research Paper INT-190. 27 pp. Forest Service. U.S. Dept. of Agriculture, Ogden, Utah.

Burston, J. and Brown, W. 1996. Watercourse revegetation – just a walk in the park! In: *Proceedings of the First National Conference on Stream Management in Australia.* Eds: I. Rutherfurd and M. Walker. Merrijig, 19-23 February, 1996. pp. 247-252.

Broms, B.B. 1977. Triaxial tests with fabric reinforced soil. *Proceedings of an International Conference on Fabrics in Geotechnics., Paris*, Volume 3: 129-134.

Brooks, A.P. and Brierley, G.J. 1997. Geomorphic responses of the lower Bega River to catchment disturbance, 1851-1926. *Geomorphology*, 18: 291-304.

Brooks, A.P. and Brierley, G.J. 2000. The role of European disturbance in the metamorphosis of the lower Bega River. In: *River Management: The Australasian Experience.* Eds: S. Brizga and B. Finlayson. John Wiley & Sons Ltd. Chichester. pp 221-246.

Brown, C.B and Sheu, M.S. 1975. Effects of deforestation on slopes. *Journal of Geotechnical Engineering Division.* ASCE, 101(GT1): 147-165.

Casagrande, A. 1964. The role of calculated risk in earthwork and foundation engineering. In: *Terzaghi Lectures 1963-1972.* Ed: J. Hilf. American Society of Civil Engineers, New York. pp. 72-138.

Clarke, M.N. and Geary, M.G. 1987. *Channel Geometry, Morphological Changes and Bank Erosion.* New South Wales Public Works Department Report No. 87067.

Clausnitzer, V. and Hopmans, J.W. 1994. Simultaneous modelling of transient three-dimensional root growth and soil water flow. *Plant and Soil.* 164: 299-314.

Coatsworth, A. and Evans, J. 1984. Discussion on Influence of vegetation on shrinking and swelling of clays. *Gèotechnique.* 34: 154-155.

Collios, A., Delmas, P., Gourc, J.P. and Giroud, J.P. 1980. *Experiments on soil reinforcement with geotextiles.* Presented at the April 14, 1980, ASCE Session on the use of geotextiles for soil improvement, Portland, Oregon. pp. 53-73.

Collison, A.J.C., Anderson, M.G. and Lloyd, D.M. 1995. Impact of vegetation on slope stability in a humid tropical environment: a modelling approach. *Proceedings of the Institution of Civil Engineers for Water, Maritime, and Energy*, 112: 168-175.

Collison, A.J.C. and Anderson, M.G. 1996. Using a combined slope hydrology/stability model to identify suitable conditions for landslide prevention by vegetation in the humid tropics. *Earth Surface Processes and Landforms*, 21: 737-747.

Coppin, N.J. and Richards, I.G. 1990. *Use of vegetation in Civil Engineering.* Butterworths. London. 292 pp.

Cornish, P.M. 1977. Changes in seasonal and annual rainfall in New South Wales. *Search.* 8: 38-40.

Craig, R.F. 1992. *Soil Mechanics.* 5th Edition. Chapman and Hall. 427 pp.

Dabral, B.G., Pant, S.P. and Pharasi, S.C. 1987. Root habits of Eucalyptus - some observations. *Indian Forester.* 113 (1): 11-32.

De Mello, V.F.B. 1977. Reflections on design decisions of practical significance to embankment dams. *Geotechnique*, 27: 279-355.

Diggle, A.J. 1988. ROOTMAP - a model in three-dimensional coordinates of the growth and structure of fibrous root systems. *Plant and Soil.* 105: 169-178.

Docker, B.B. 1997. *Morphological Change on the Nepean River: Causes and extent of bank failure and erosion within the Wallacia Valley.* Unpublished B.Sc. Honours Thesis, University of Sydney. 84 pp.

Docker, B.B. and Hubble, T.C.T. 2001a. Earth reinforcement potential of four tree species as determined by root system architecture. *Proceedings of the 14th Southeast Asian Geotechnical Conference*, Hong Kong 10th-14th December, Balkema, Lisse. pp: 741-744.

Docker, B.B. and Hubble, T.C.T. 2001b. Strength and distribution of *Casuarina glauca* roots in relation to slope stability. *Proceedings of the 14th Southeast Asian Geotechnical Conference*, Hong Kong 10th-14th December, Balkema, Lisse. pp: 745-749.

Docker, B.B. and Hubble, T.C.T. 2001c. Riverbank collapse on the Nepean River in the Wallacia Valley: Assessing possible causes by historical and geomechanical methods. *Journal of the Royal Society of New South Wales*, 134: 65-78.

Ekanyake, J.C. and Phillips, C.J. 1999. A method for stability analysis of vegetated hillslopes: an energy approach. *Canadian Geotechnical Journal*, 36: 1172-1184.

Ellison, L. and Coaldrake, J.E. 1954. Soil mantle movement in relation to forest clearing in Southeastern Queensland. *Ecology*, 35: 380-388.

Endo, T. and Tsurata, T. 1969. Effect of tree's roots upon the shearing strength of soils. *Annual Report No. 18 of the Hokkaido Branch Government Forest Experiment Station*, Tokyo, 1968. pp. 167-182.

Erskine, W.D. 1986. River metamorphosis and environmental change in the MacDonald Valley, New South Wales, since 1949. *Australian Geographical Studies*, 24: 88-107.

Erskine, W.D. and Bell, F.C. 1982. Rainfall, floods and river channel changes in the upper Hunter. *Australian Geographical Studies.* 20: 183-196.

Erskine, W.D. and Warner, R.F. 1988. Geomorphic effects of alternating flood- and drought-dominated regimes on New South Wales coastal rivers. In: *Fluvial Geomorphology of Australia.* Ed: R.F. Warner. Academic Press, Australia. pp. 223-244.

Erskine, W.D. and White, L.J. 1996. Historical river metamorphosis of the Cann River, East Gippsland, Victoria. In: *Proceedings of the First National Conference on Stream Management in Australia.* Eds: I. Rutherfurd and M. Walker. Merrijig, 19-23 February, 1996. pp. 277-282.

Erskine, W.D. and Green, D. 2000. Geomorphic effects of extractive industries and their implications for river management: the case of the Nepean River, NSW. In: *River Management: the Australasian Experience.* Eds: S. Brizga and B. Finlayson. John Wiley & Sons, Chichester. pp. 123-149.

Fellenius, W. 1936. Calculation of the stability of earthdams. *Trans. 2nd Congress on Large Dams.* 4: 445-460.

Gentilli, J. 1971. Climatic fluctuations. In: *Climates of Australia and New Zealand, World Survey of Climatology*, Vol. 13, Elsevier, Amsterdam. pp. 189-211

Gray, D.H. 1978. Role of woody vegetation in reinforcing soils and stabilizing slopes. *Proceedings of a Symposium on Soil Reinforcing and Stabilizing Techniques in Engineering Practice*, New South Wales Institute of Technology, 16th-19th October, Sydney, Australia. pp. 253-306.

Gray, D.H. and Leiser, A.T. 1982. *Biotechnical slope protection and erosion control.* Van Nostrand Reinhold Co., New York.

Gray, D.H. and Megahan, W.F. 1981. *Forest vegetation removal and slope stability in the Idaho Batholith.* Research Paper, INT-271, 23 pp. Forest Service. U.S. Dept. of Agriculture, Ogden, Utah.

Gray, D.H. and Ohashi, H. 1983. Mechanics of fiber reinforcement in sand. *Journal of Geotechnical Engineering. ASCE.* 109 (3): 335-353.

Gray, D.H. and Sotir, R.B. 1996. *Biotechnical and Soil Bioengineering Slope Stabilisation: A Practical Guide for Erosion Control.* John Wiley & Sons, New York, 378 pp.

Greenway, D.R. 1987. Vegetation and slope stability. In: *Slope Stability.* Eds: M.G. Anderson and K.S. Richards. John Wiley & Sons Ltd, Chichester. pp: 187-230.

Hahn, G.J. 1973. The coefficient of determination exposed!. *Chemtech,* October: 609-611.

Hall, L.D. 1927. The physiographic and climatic factors controlling the flooding of the Hawkesbury River at Windsor. *Proceedings of the Linnean Society of New South Wales.* 52: 133-152.

Hanna, T.H. 1982. *Foundations in Tension: Ground Anchors.* Trans Tech Publications. Clausthal. 573 pp.

Harvey, M.D. and Watson, C.C. 1986. Fluvial processes and morphological thresholds in incised channel restoration. *Water Resources Bulletin,* 22(3): 359-368.

Hausmann, M.R. 1976. Strength of reinforced soil. *Proceedings of the 8th Australian Road Research Conference* Volume 8(13): 1-8.

Helliwell, D.R. 1986. The extent of tree roots. *Arboricultural Journal.* 10: 341-347.

Henderson, R., Ford, E.D. and Renshaw, E. 1983. Morphology of the structural root system of Sitka Spruce. 2. Computer simulation of rooting patterns. *Forestry.* 56: 121-135.

Hewitt, J.S. and Dexter, A.R. 1979. An improved model of root growth in structured soil. *Plant and Soil.* 52: 325-343.

Hewitt, J.S. and Dexter, A.R. 1984. The behaviour of roots encountering cracks in soil. II. Development of a predictive model. *Plant and Soil.* 79: 11-28.

Hey, R.D. and Thorne, C.R. 1986. Stable channels with mobile gravel beds. *Journal of Hydraulic Engineering,* 112(8): 671-689.

Hey, R.D., Heritage, G.L., Tovey, N.K., Boar, R.R., Grant, N. and Turner, R.K. 1991. *Streambank Protection in England and Wales* R&D Note 22, National Rivers Authority, London, 75 pp.

Hicken, E.J. 1967. Channel morphology, bankfull stage, and bankfull discharge of streams near Sydney. *Australian Journal of Science.* 30 (7): 274-275.

Hicken, E.J. 1984. Vegetation and river channel dynamics. *Canadian Geographer.* 28: 111-126.

Howell, J., McDougall, L. and Benson, D. 1995. *Riverside plants of the Hawkesbury-Nepean.* Royal Botanic Gardens, Sydney. 62 pp.

Huang, H.Q. and Nanson, G.C. 1997. Vegetation and channel variation; a case study of four small streams in southeastern Australia. *Geomorphology.* 18: 237-249.

Hubble, T.C.T. 1996. *The History of River Bank Erosion in the Camden Valley of the Nepean River: An attempt to resolve and evaluate the relative contributions of long-term geomorphic change and recent human influence using the aerial photographic record.* O.S.I. Report 72, University of Sydney. 49 pp.

Hubble, T.C.T. 1997. River bank erosion on the Nepean River, New South Wales: The relative contributions of long-term geomorphic change and recent human influence. In: *Collected case*

studies in Engineering Geology, Hydrogeology and Environmental Geology. Third Series. Ed: G. McNally. EEHSG of Geological Society of Australia. 361 pp.

Hubble, T.C.T. 1998. Maintaining riverbank stability: a geomechanical perspective. In: *Proceedings of the Eighth International Congress of the International Association for Engineering Geology and the Environment.* Eds: D. Moore and O. Hungr. Vancouver Canada. pp. 1827-1834.

Hubble, T.C.T. 2001. *The history and causes of riverbank failure on the upper Nepean River between 1947 and 1992.* Ph.D. Thesis, University of Sydney.

Hubble, T.C.T. IN PRESS. Slope stability analysis of potential bank failure due to toe erosion on weir-impounded lakes: an example from the Nepean River, New South Wales, Australia. *Regulated Rivers Research.*

Hubble, T.C.T. and Harris, P.T. 1993. *Hawkesbury-Nepean River Sediment Dynamics Mapping Study.* Ocean Sciences Institute Report No. 53, University of Sydney. October, 1993.

Hubble, T.C.T. and Hull, T. 1996. A model for bank collapse on the Nepean River, Camden Valley, New South Wales, Australia. *Australian Geomechanics.* 29: 80-98.

Hunt, R.E. 1986. *Geotechnical Engineering, analysis and evaluation.* McGraw-Hill Inc. 729 pp.

Ingold, T.S. 1982. *Reinforced earth.* Thomas Telford Ltd, London. pp. 141.

Janbu, N. 1954. *Stability analysis of slopes with dimensionless parameters.* Harvard Soil Mechanics Serial No. 46. Harvard University Press, Cambridge, Massachusetts.

Jennings, J.N. 1971. *Karst.* MIT Press, Cambridge, Massachusetts. 252 pp.

Jewell, R.A. and Wroth, C.P. 1987. Direct shear tests on reinforced sand. *Geotechnique,* 37: 53-68.

Jones, D.C. and Clarke, N.R. 1991. *Geology of the Penrith 1:100 000 Sheet 9030.* New South Wales Geological Survey, Sydney. 201 pp.

Kassif, G. and Kopelovitz, A. 1968. *Strength properties of soil root systems. Technion Institute of Technology,* Haifa, Israel.

Kawaguchi, T., Namba, S., Takiguchi, K., Kono, T. and Kishioka, T. 1959. Landslides and soil losses at the mountain districts of Izu Peninsula in the flood of 1958 and their control. *Japanese Forest Experimentation Station Bulletin.* 117: 83-120.

Kirkup, H., Brierley, G., Brooks, A. and Pitman, A. 1998. Temporal variability of climate in south-eastern Australia: a reassessment of flood- and drought-dominated regimes. *Australian Geographer.* 29 (2): 241-255.

Kitamura, Y. and Namba, S. 1976. A field experiment on the uprooting resistance of tree roots. In: *Proceedings of 77th Meeting of the Japanese Forest Society.* translated from Japanese by J.M. Arata and R.R. Ziemer. pp. 568-570. U.S. Dept. of Agriculture, Forest Service, Arcata, California.

Kozlowski, T.T. 1971. *Growth and development of trees. Volume II: Cambial growth, root growth, and reproductive growth.* Academic Press. New York. 514 pp.

Kraus, E.B. 1955. Secular changes of east-coast rainfall regimes. *Quarterly Journal of the Royal Meteorological Society.* 91: 430-439.

Lambe, T.W. and Whitman, R.V. 1979. *Soil Mechanics,* S.I. Version. John Wiley and Sons. 553 pp.

Lawler, D.M., Thorne, C.R., and Hooke, J.M. 1997. Bank erosion and instability. In: *Applied Fluvial Geomorphology for River Engineering and Management,* Eds: C.R. Thorne, R.D. Hey, and M.D. Newson. John Wiley & Sons Ltd. Chichester. pp. 137-172.

Long, N.T., Guegan, Y. and Legeay, G. 1972. *Étude de la terre armée a l'appareil triaxial.* Rapp. de Recherche. No. 17, LCPC.

Lowe, J. 1967. Stability analysis of embankments. *Journal of the Soil Mechanics and Foundations Division,* Proceedings of the American Society of Civil Engineers. 93 (SM4): 1-33.

Luckman, P.G., Hathaway, R.L. and Edwards, W.R.N. 1982. *Root systems, root strength and slope stability.* Internal Report 34. National Water and Soil Conservation Organisation. Ministry of Works and Development, Wellington, New Zealand.

Lungley, D.R. 1973. The growth of root systems - A numerical computer simulation model. *Plant and Soil.* 38: 145-159.

Masterman, R.J.W. 1994. *Vegetation effects on riverbank stability.* Ph.D. Thesis. University of Nottingham.

Midgley, S.J., Turnbull, J.W., and Johnston, R.D. 1983. *Casuarina ecology management and utilisation.* Proceedings of an International Workshop, Canberra, Australia, 17-21 August, 1981. CSIRO, Melbourne.

Millar, R.G. and Quick, M.C. 1993. Effect of bank stability on geometry of gravel rivers. *Journal of Hydraulic Engineering,* 119(12): 1343-1363.

Montgomery, D.R. 1997. What's best on the banks? *Nature,* 388: 328-329.

Morgenstern, N.R. and Price, V.E. 1965. Analysis of the stability of general slip surfaces. *Geotechnique.* 15: 79-83.

Mosley, M.P. 1981. Semi-determinate hydraulic geometry of river channels, South Island, New Zealand. *Earth Surface Processes and Landforms.* 6: 127-137.

Mostyn, G. and Small, J.C. 1987. Methods of Stability Analysis. In: *Soil slope instability and stabilisation.* Eds: B. Walker and R. Fell. Balkema. pp 71-120.

Nakano, H. 1971. *Soil and water conservation functions of forest on mountainous land.* report. Government Forest Experiment Station (Japan). Forest Influences Division. 66 pp.

Nanson, G.C. 1986. Episodes of vertical accretion and catastrophic stripping: A model of disequilibrium flood-plain development. *Geological Society of America Bulletin.* 97: 1467-1475.

Nanson, G.C. and Erskine, W.D. 1988. Episodic changes of channels and floodplains on coastal rivers in NSW. In: *Fluvial Geomorphology of Australia.* Ed: R.F. Warner. Academic Press, Sydney. pp. 201-221.

Nash, D. 1987. A comparative review of limit equilibrium methods of slope stability. In: *Slope Stability.* Eds: M.G. Anderson and K.S. Richards. John Wiley & Sons Ltd, Chichester. pp: 11-76.

Nilaweera, N.S. and Nutalaya, P. 1999. Role of tree roots in slope stabilisation. *Bulletin of Engineering Geology and the Environment,* 57: 337-342.

O'Loughlin, C.L. 1974a. The effects of timber removal on stability of forest soils. *Journal of Hydrology, New Zealand.* 13: 121-134.

O'Loughlin, C.L. 1974b. A study of tree root strength deterioration following clear-felling. *Canadian Journal of Forest Research.* 4 (1): 107-113.

O'Loughlin, C.L. and Pearce, A.J. 1976. Influence of Cenozoic geology on mass movement and sediment yield response to forest removal, North Westland, New Zealand. *Bulletin of the International Association of Engineering Geologists.* 14: 41-46.

O'Loughlin, C.L. and Watson, A. 1979. Root-wood strength deterioration in radiata pine after clear-felling. *New Zealand Journal of Forest Science*, 9(3): 284-293.

O'Loughlin, C.L. and Ziemer, R.L. 1982. The importance of root strength and deterioration rates upon edaphic stability in steepland forests. In: *Ecology of Subalpine Zones, Oregon State University.* Corvallis. Proceedings of the International Union of Forestry Research Organisations Workshop. Ed: R.H. Waring. pp. 70-78.

O'Loughlin, C.L., Rowe, L.K. and Pearce, A.J. 1982. *Exceptional storm influences on slope erosion and sediment yields in small forest catchments, North Westland, New Zealand.* National Conference Publication 82/6. pp. 84-91. Institute of Engineering, Barton, ACT, Australia.

Page, K. 1988. Bankfull discharge frequency for the Murrumbidgee River, New South Wales. In: *Fluvial Geomorphology of Australia.* Ed: R.F. Warner. Academic Press Australia. pp. 267-281.

Pages, L., Jordan, M.O. and Picard, D. 1989. A simulation model of the three-dimensional architecture of the maize root system. *Plant and Soil.* 119: 147-154.

Pickup, G. 1976. Geomorphic effects of changes in river runoff, Cumberland Basin, N.S.W. *Australian Geographer.* 13: 188-193.

Pittock, A.B. 1975. Climate change and the patterns of variation in Australian rainfall. *Search.* 6: 498-504.

Poulos, H.G. and Davis, E.H. 1980. *Pile foundation and analysis.* John Wiley & Sons, New York.

Riestenberg, M.M. 1987. *Anchoring of thin colluvium on hillslopes by roots of sugar maple and white ash.* Ph.D. Thesis, University of Cincinnati, Ohio.

Riestenberg, M.M. 1994. Anchoring of thin colluvium by roots of sugar maple and white ash on hillslopes in Cincinnati. *U.S. Geological Survey Bulletin 2059-E.*

Riestenberg, M.M. and Sovonick-Dunford, S. 1983. The role of woody vegetation in stabilizing slopes in the Cincinnati area, Ohio. *Geological Society of America Bulletin.* 94: 506-518.

Riley, S.J. 1988. Secular change in the annual flows of streams in the NSW Section of the Murray-Darling Basin. In: *Fluvial Geomorphology of Australia.* Ed: R.F. Warner. Academic Press Australia. pp. 245-266.

Robinson, L. 1991. *Field Guide to the Native Pants of Sydney.* Kangaroo Press, Kenthurst. 448 pp.

Roesen, S. 1995. *Losing ground, an environmental history of the Hawkesbury-Nepean catchment area.* Hale and Ironmonger, Sydney.

Rose, D.A. 1983. The description of the growth of root systems. *Plant and Soil.* 75: 405-415.

Schiechtl, H.M. 1980. *Bioengineering for land reclamation and conservation.* University of Alberta Press, Edmonton, Canada.

Schlosser, F. and Long, N. 1973. *Étude du compartement du materiau terre armée.* Annles de l'Inst. Techq. du Batmend et des Tran. Publ. Suppl. No. 304. Sér. Matér. No. 45.

Schlosser, F. and Long, N. 1974. Recent results in French research on reinforced earth. *Journal of the Construction Division. ASCE.* 100: 223-237.

Schmidt, K.M., Roering, J.J., Stock, J.D., Dietrich, W.E., Montgomery, D.R. and Schaub, T. 2001. The variability of root cohesion as an influence on shallow landslide susceptibility in the Oregon Coast Range. *Canadian Geotechnical Journal*, 38: 995-1024.

Schumm, S.A. 1960. The effect of sediment type and on the shape and stratification of some modern fluvial deposits. *American Journal of Science*, 258: 177-184.

Schumm, S.A. 1971. Fluvial geomorphology: channel adjustment and river metamorphosis. In: *River Mechanics*. Vol. 1. Ed: H.W. Shen. Fort Collins, Colorado, U.S.S.

Selby, M.J. 1981. Landslides and deforestation. Paper presented in the *1981 Conference of the New Zealand Geographical Society*, Victoria University, Wellington, New Zealand.

Shewbridge, S.E. and Sitar, N. 1989. Deformation characteristics of reinforced sand in direct shear. *Journal of Geotechnical Engineering. ASCE*. 115 (8): 1134-1147.

Shields, F.D. and Gray, D.H. 1992. Effects of woody vegetation on sandy levee integrity. *Water Resources Bulletin*, 28(5): 917-931.

Simon, A. 1989. A model of channel response in disturbed alluvial channels. *Earth Surface Processes and Landforms*. 14: 11-26.

Simon, A. and Hupp, C.R. 1986. Channel widening characteristics and bank-slope development along a reach of Cane Creek, West Tennessee. In: *Selected Papers in the Hydrological Sciences*. Ed: S. Subitzky. U.S. Geological Survey Water-Supply Paper 2290: 113-126.

Simon, A. and Hupp, C.R. 1990. The recovery of alluvial systems in response to imposed channel modifications, West Tennessee, USA. In: *Vegetation and Erosion*. Ed: J.B. Thornes. John Wiley & Sons Ltd. pp. 145-160.

Simon, A. and Hupp, C.R. 1992. *Geomorphic and Vegetative Recovery Processes along Modified Stream Channels of West Tennessee*. U.S. Geological Survey Open-File Report. pp. 91-502.

Simon, A. and Downs, P.W. 1995. An interdisciplinary approach to evaluation of potential instability in alluvial channels. *Geomorphology*. 12: 215-232.

Simpson, H.J. and Cane, M.A. 1993. Annual river discharge in southeastern Australia related to El-Niño-Southern Oscillation forecasts of surface temperatures. *Water Resources Research*. 29: 3671-3680.

Simpson, H.J., Cane, M.A., Lin, S.K., and Zebiak, S.E. 1997. Forecasting annual discharge of the River Murray, Australia, from a geophysical model of ENSO. *Journal of Climate*. 6: 386-390.

Smith, D.G. 1976. The effect of vegetation on lateral migration of anastomosed channels of a glacial meltwater river. *Geological Society of America Bulletin*. 79: 1573-1588.

Somerville, A. 1979. Root anchorage and root morphology of *Pinus radiata* on a range of ripping treatments. *New Zealand Journal of Forest Science*. 9(3): 294-315.

Spencer, E. 1967. A method of analysis fro stability of embankments using parallel inter-slice forces. *Gèotechnique*. 17: 11-26.

Stace, H.C.T., Hubble, G.D., Brewer, R., Nothcote, K.H., Sleeman, J.R., Mulcahy, M.J. and Hallsworth, E.G. 1968. *A handbook of Australian soils*. Rellim Technical Publications, Adelaide.

Stone, E.L. and Kalisz, P.J. 1991. On the maximum extent of tree roots. *Forest Ecology and Management*. 46: 59-102.

Styczen, M.E. and Morgan, R.P.C. 1995. Engineering properties of vegetation. In: *Slope Stabilization and Erosion Control: A Bioengineering Approach.* Eds: R.P.C. Morgan and R.J. Rickson. E & FN Spon, London. pp. 5-58.

Sutton, R.F. 1969. *Form development of conifer root systems.* Technical Communication No. 7. Commonwealth Agricultural Bureaux. Farnham Royal, Bucks., England.

Swanston, D.N. 1970. *Mechanics of debris avalanching in shallow till soils of southeast Alaska.* Research Paper PNW-103. 17 pp. Forest Service. U.S. Dept. of Agriculture, Portland, Oregon.

Swanston, D.N. 1974. *Slope stability problems associated with timber harvesting in mountainous regions of the western United States.* General Technical Report PNW-21. 14 pp. Forest Service. U.S. Dept. of Agriculture, Portland, Oregon.

Swanston, D.N. and Dyrness, C.T. 1973. Stability of steepland. *Journal of Forestry.* 71 (5): 264-269.

Tengbeh, G.T. 1989. *The effect of grass cover on bank erosion.* Ph.D. Thesis. Silsoe College, Cranfield Institute of Technology.

Tardieu, F. 1988. Analysis of the spatial variability of maize root density. I. Effect of wheel compaction on the spatial arrangement of roots. *Plant and Soil.* 107: 259-266.

Terwilliger, V.J. and Waldron, L.J. 1990. Assessing the contribution of roots to the strength of undisturbed, slip prone soils. *Catena.* 17: 151-162.

Terwilliger, V.J. and Waldron, L.J. 1991. Effects of root reinforcement on soil-slip patterns in the Transverse Ranges of Southern California. *Geological Society of America Bulletin.* 103: 775-785.

Terzaghi, K. 1943. *Theoretical Soil Mechanics.* John Wiley & Sons Ltd, New York. 510 pp.

Thomson, S. 1970. Riverbank stability study at the University of Alberta, Edmonton. *Canadian Geotechnical Journal.* 7: 157-168.

Thorne, C.R. 1982. Processes and mechanisms of river bank erosion. In: *Gravel-bed Rivers.* Eds: R.D. Hey, J.C. Bathurst, and C.R. Thorne. John Wiley & Sons Ltd. Chichester. pp. 227-259.

Thorne, C.R. 1990. Effects of vegetation on riverbank erosion and stability. In: *Vegetation and Erosion.* Ed: J.B. Thornes. John Wiley & Sons, Chichester. pp. 125-43.

Thorne, C.R. 1991. Analysis of channel instability due to catchment land-use change. In: *Symposium Proceedings: Sediment and stream water quality in a changing environment, Vienna.* Eds: N.E. Peters and D.E. Wallings. International Association of Hydrological Sciences, Publication 203: 111-122.

Thorne, C.R. and Osman, A.M. 1988a. Riverbank stability analysis. I: theory. *Journal of Hydraulic Engineering,* ASCE, 114(2): 134-150.

Thorne, C.R. and Osman, A.M. 1988b. Riverbank stability analysis. II: application. *Journal of Hydraulic Engineering,* ASCE, 114(4): 151-172.

Trimble, S.W. 1997. Stream channel erosion and change resulting from riparian forests. *Geology,* 25(5): 467-469.

Tsukamoto, Y. and Kusakabe, O. 1984. Vegetation influences on debris slide occurrence on steep slopes in Japan. In: *Proceedings of a Symposium on the effects of forest land use on erosion and slope stability,* Environment & Policy Institute, Honolulu, Hawaii.

Tumay, M.T., Antonini, M. and Arman, A. 1979. Metal versus nonwoven fiber fabric earth reinforcement in dry sands: A comparative statistical analysis of model tests. *Geotechnical Testing Journal.* 2 (1): 44-56.

Uran, J, and Price, W.F. 1985. *Surveying for engineers.* 2nd Edition. Macmillan, London.

Vidal, H. 1969. The principle of reinforced earth. *Highway Research Record No. 282.* pp. 1-16.

Waldron, L.J. 1977. The shear resistance of root-permeated homogenous and stratified soil. *Journal of the Soil Science Society of America.* 41: 843-849.

Waldron, L.J. and Dakessian, S. 1981. Soil reinforcement by roots: Calculation of increased soil shear resistance from root properties. *Soil Science.* 132 (6): 427-435.

Waldron, L.J., Dakessian, S. and Nemson, J.A. 1983. Shear resistance enhancement of 1.22 meter diameter soil cross-sections by pine and alfalfa roots. *Soil Science Society of America Journal.* 47: 9-14.

Walker, P.H. 1960. *A soil survey of the county of Cumberland, Sydney Region, New South Wales.* NSW Department of Agriculture Soil Survey Unit - Bulletin 2.

Wang, W.L. and Yen, B.C. 1974. Soil arching in slopes. *Journal of the Geotechnical Engineering Division, ASCE,* 100(GT1): 61-78.

Warner, R.F. 1983. Channel changes in sandstone and shale reaches of the Nepean River, NSW. In: *Aspects of Australian Sandstone Landscapes.* Eds: R.W. Young and G.C. Nanson. Australian and New Zealand Geomorphology Group Special Publication No. 1. pp. 106-119.

Warner, R.F. 1987a. The impacts of alternating flood- and drought-dominated regimes on channel morphology at Penrith, New South Wales, Australia. In: *The influence of climate change and climatic variability on the hydrologic regime and water resources (Proceedings of the Vancouver Symposium, August, 1987).* IAHS Publication No. 168. pp. 327-338.

Warner, R.F. 1987b. Spatial adjustments to temporal variations in flood regime in some Australian Rivers. In: *River Channels: Environment and Process.* Ed: K. Richards. Blackwell, Oxford. pp. 14-40.

Warner, R.F. 1991. Impacts of environmental degradation on rivers, with some examples from the Hawkesbury-Nepean system. *Australian Geographer.* 22 (1): 1-13.

Warner, R.F. 1997. Floodplain stripping: another form of adjustment to secular hydrologic regime change in Southeast Australia. *Catena.* 30: 263-282.

Watson, A. and O'Loughlin, C.L. 1985. Morphology, strength, and biomass of Manuka roots and their influence on slope stability. *New Zealand Journal of Forestry Science.* 15 (3): 337-348.

Watson, A. and O'Loughlin, C.L. 1990. Structural root morphology and biomass of three age classes of Pinus radiata. *New Zealand Journal of Forestry Science.* 20(1): 97-110.

Wielopolski, L., Daniels, J., Hendrey, G., McGuigan, M. 2000. Imaging tree roots in situ. In: *Proceedings of the Eighth International Conference on Ground Penetrating Radar.* Eds: D.A. Noon, G.F. Stickley, D. Longstaff. SFEI 4084. Gold Coast, Australia 23-26 May 2000.

Williams, A.A.B. and Pidgeon, J.T. 1983. Evapotranspiration and heaving clays in South Africa. *Gèotechnique.* 33: 141-150.

Wolman, M.G. and Gerson, R. 1978. Relative scales of time and effectiveness of climate in watershed geomorphology. *Earth Surface Processes and Landforms.* 3: 189-208.

Wu, T.H. 1976. *Investigation of landslides on Prince of Wales Island, Alaska.* Geotechnical Engineering Report, No. 5. Department of Civil Engineering, Ohio State University, Columbus.

Wu, T.H. 1984. Effect of vegetation on slope stability. In: *Soil Reinforcement and Moisture Effects on Stability*. Transportation Research Record 965. Transportation Research Board, Washington, DC. pp. 37-46.

Wu, T.H. 1995. Slope Stabilization. In: *Slope stabilization and erosion control: a bioengineering approach*. Eds: R.P.C. Morgan and R.J. Rickson. E & FN Spon. London.

Wu, T.H., McKinnell, W.P. and Swanston, D.N. 1979. Strength of tree roots and landslides on Prince of Wales Island, Alaska. *Canadian Geotechnical Journal*. 16: 19-33.

Wu, T.H., Beal, P.E., and Lan, C. 1988a. In-situ shear test of soil-root systems. *Journal of Geotechnical Engineering*. 114(12): 1376-1394.

Wu, T.H., Bettandapura, D.P., and Beal, P.E. 1988b. A statistical model of root geometry. *Forest Science*. 34(4): 980-997.

Wu, T.H., Riestenberg, M.M. and Flege, A. 1995. Root properties for design of slope stabilization. In: *Vegetation and Slopes*. Ed: D.H. Barker. Thomas Telford, London.

Wu, T.H. and Swanston, D.N. 1980. Risk of landslides in shallow soils and its relation to clear-cutting in southeastern Alaska. *Forest Science*. 26 (3): 495-510.

Wu, T.H. and Watson, A. 1998. *In-situ* shear tests of soil blocks with roots. *Canadian Geotechnical Journal*. 35: 579-590.

Yadav, J.S.P. 1983. Soil limitations for successful establishment and growth of Casuarina plantations. In: *Casuarina ecology management and utilization*. Eds: S.J. Midgley, J.W. Turnbull and R.D. Johnston. Proceedings of an International Workshop, 17-21 August 1981, Canberra, Australia. CSIRO, Melbourne. pp. 138-150.

Yen, C.P. 1984. Tree root patterns and erosion control. *Proceedings of the International Workshop on Soil Erosion and its Counter-measures*, 11th-19th November, Chiangmai, Thailand. pp. 92-111.

Zhou, Y., Watts, D., Cheng, X., Li, Y., Luo, H. and Xiu, Q. 1997. The traction effect of lateral roots of *Pinus yunnanensis* on soil reinforcement: a direct in situ test. *Plant and Soil*. 190: 77-86.

Ziemer, R.R. 1981. *Roots and the stability of forested slopes*. Publication No. 132. International Association of Hydrologic Sciences. pp. 343-361.

Ziemer, R.R. and Swanston, D.N. 1977. *Root strength changes after logging in southeast Alaska*. Research Note PNW-306. 10 pp. Forest Service. U.S. Dept. of Agriculture, Portland, Oregon.

Zimmer, W.J. and Grose, R.J. 1958. Root systems and root/shoot ratios of seedlings of some Victorian Eucalypts. *Australian Forestry*. 22 (1): 13-18.

Appendix A

Data supporting Chapter 3
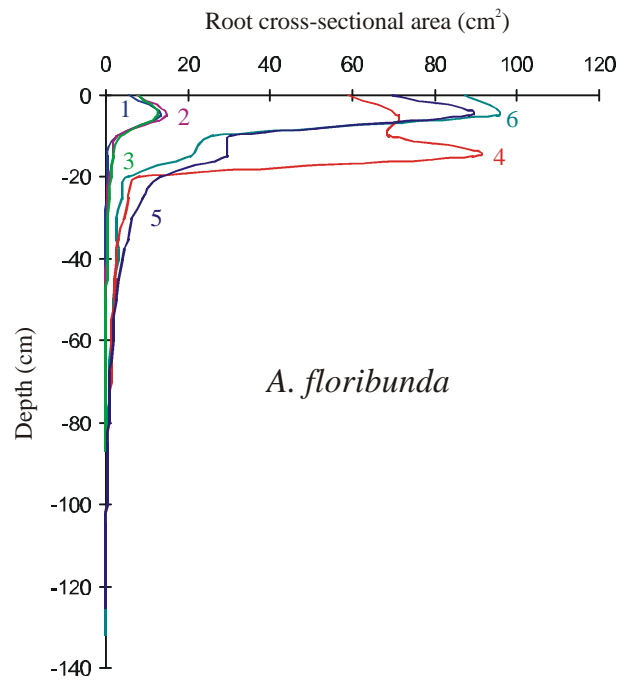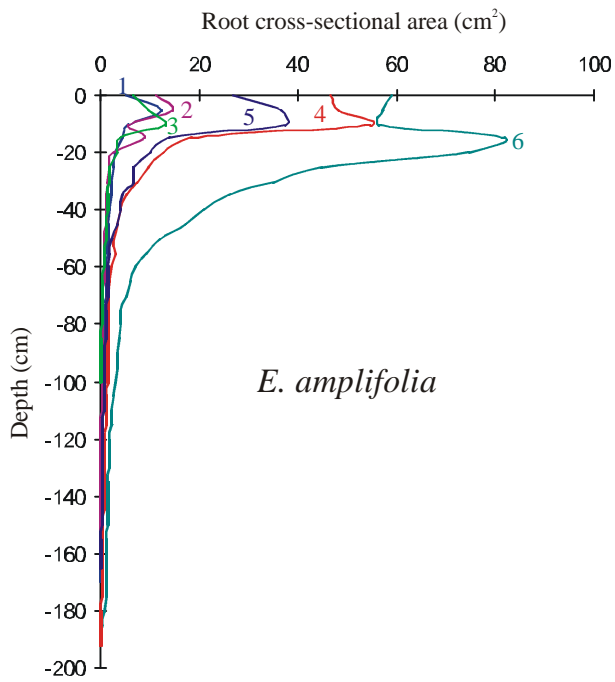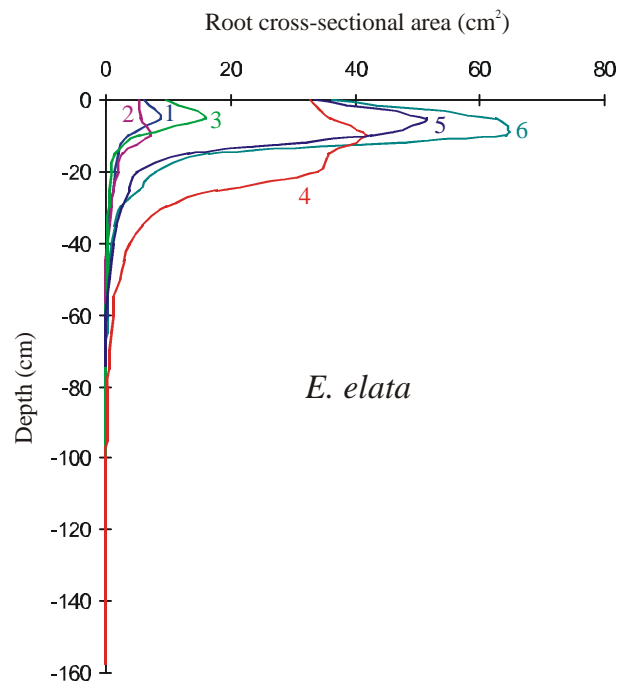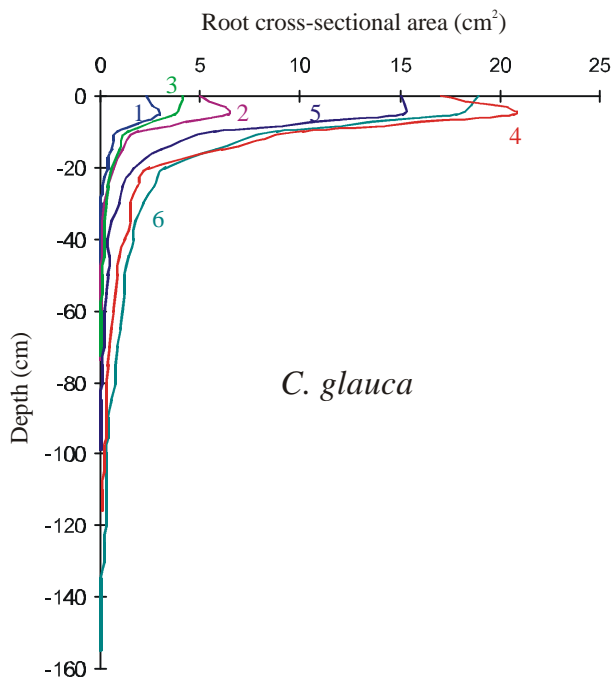
A-I: Plots of root cross-sectional area with depth for each species.

A-II: Maximum lateral root extent in cm by depth quartile

	Sample No.	C. glauca	E. amplifolia	E. elata	A. floribunda
0-25 % of MVD	1	68	95	85	85
	2	100	95	28	120
	3	110	100	103	150
	4	219	201	140	379
	5	231	153	120	139
	6	291	213	202	347
	Average	**170**	**141**	**120**	**203**
25-50 % of MVD	1	63	30	42	70
	2	40	49	70	88
	3	80	60	86	145
	4	124	141	140	110
	5	166	70	89	126
	6	124	82	125	107
	Average	**100**	**72**	**92**	**108**
50-75 % of MVD	1	30	24	45	29
	2	22	49	45	66
	3	48	52	27	27
	4	65	60	75	90
	5	45	70	88	84
	6	48	34	73	87
	Average	**43**	**48**	**59**	**64**
75-100 % of MVD	1	10	18	38	39
	2	20	23	23	72
	3	6	48	27	23
	4	40	28	23	75
	5	41	70	28	82
	6	38	28	57	82
	Average	**26**	**36**	**33**	**62**

A-III: Spatial root distribution with lateral distance from the tree stem. Qp is the quantity of roots passing a given vertical plane at a distance b from the tree stem.

	Depth Quartile	Equation	Regression Coefficient
C. glauca	0-25%	$Qp = 2.2414e^{-0.049.b}$	$R^2 = 0.98$
	25-50%	$Qp = 0.1746e^{-0.033.b}$	$R^2 = 0.99$
	50-75%	$Qp = 0.0747e^{-0.136.b}$	$R^2 = 1.00$
	75-100%	$Qp = 0.008e^{-0.064.b}$	$R^2 = 0.79$
E. amplifolia	0-25%	$Qp = 2.6917e^{-0.045.b}$	$R^2 = 0.96$
	25-50%	$Qp = 0.7910e^{-0.088.b}$	$R^2 = 0.98$
	50-75%	$Qp = 0.1779e^{-0.060.b}$	$R^2 = 0.87$
	75-100%	$Qp = 77760e^{-1.167.b}$	$R^2 = 1.00$
E. elata	0-25%	$Qp = 3.147.e^{-0.057.b}$	$R^2 = 0.98$
	25-50%	$Qp = 2.2626.e^{-0.069.b}$	$R^2 = 1.00$
	50-75%	$Qp = 0.1241.e^{-0.026.b}$	$R^2 = 0.99$
	75-100%	$Qp = 0.0153.e^{-0.020.b}$	$R^2 = 1.00$
A. floribunda	0-25%	$Qp = 6.7705.e^{-0.068.b}$	$R^2 = 0.97$
	25-50%	$Qp = 1.2594.e^{-0.077.b}$	$R^2 = 0.96$
	50-75%	$Qp = 0.2327.e^{-0.088.b}$	$R^2 = 0.98$
	75-100%	$Qp = 0.0833.e^{-0.111.b}$	$R^2 = 1.00$

Appendix B

Data supporting Chapter 4
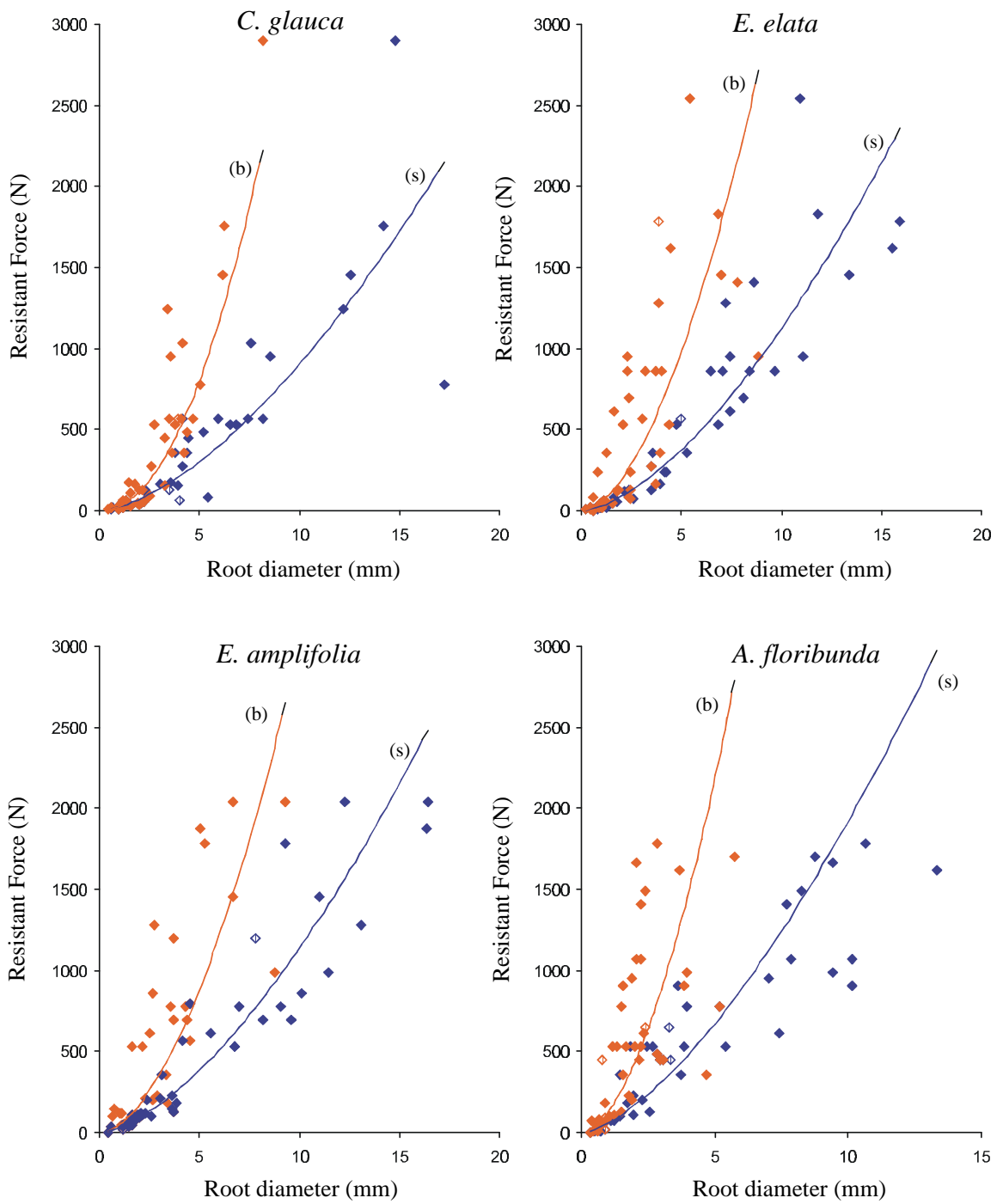
B-I: Root pull-out resistance versus stem diameter at the broken end (b) and at the surface (s); with individual data points for each test.
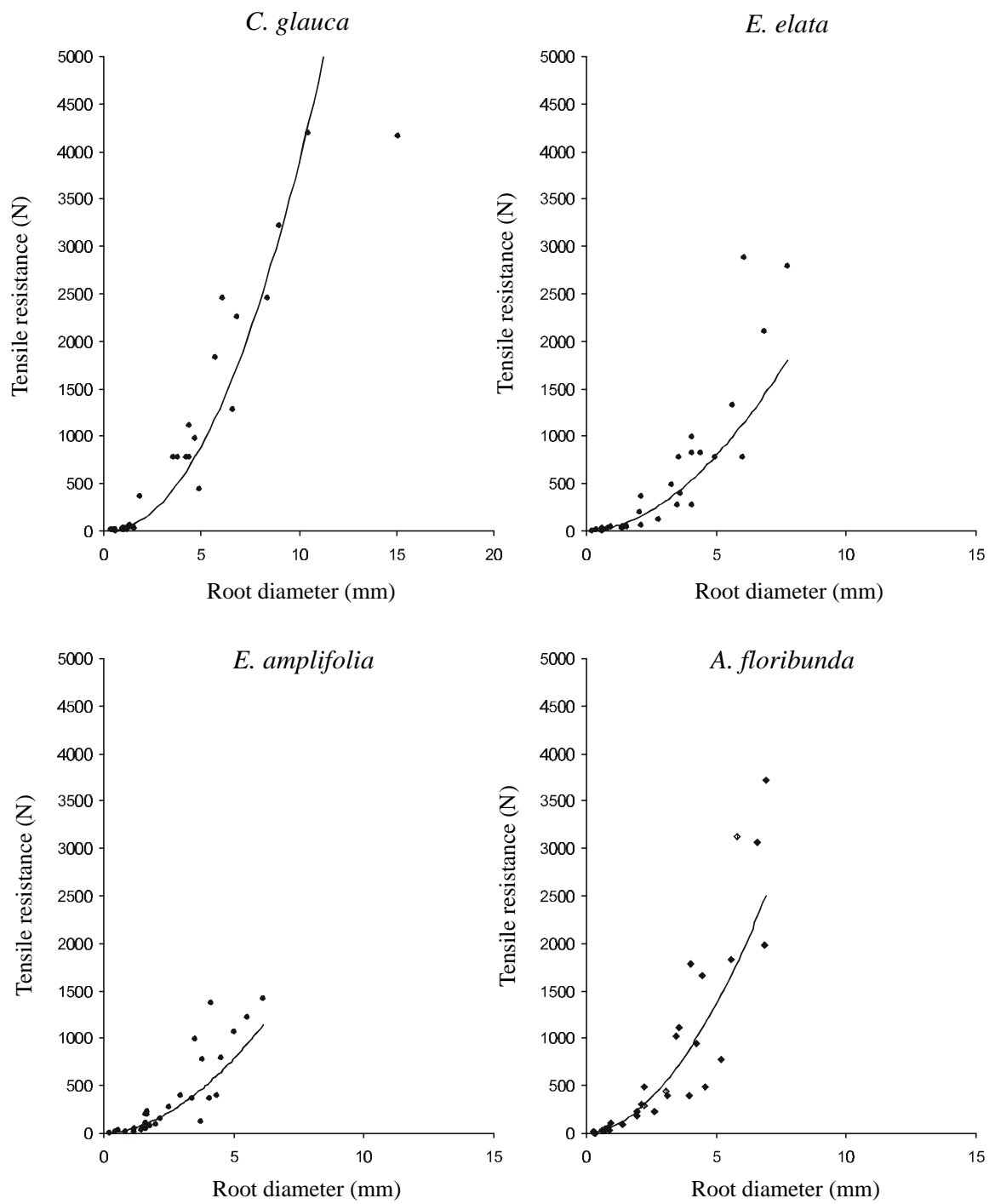
B-II: Tensile resistance versus diameter plots with individual data points for each test.
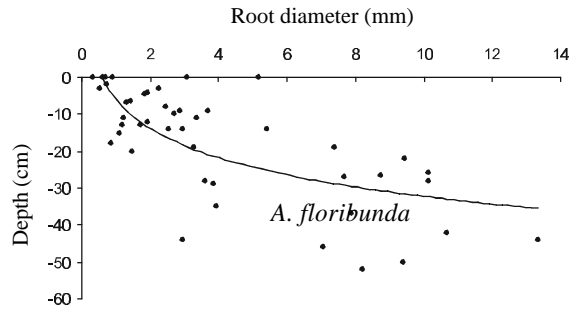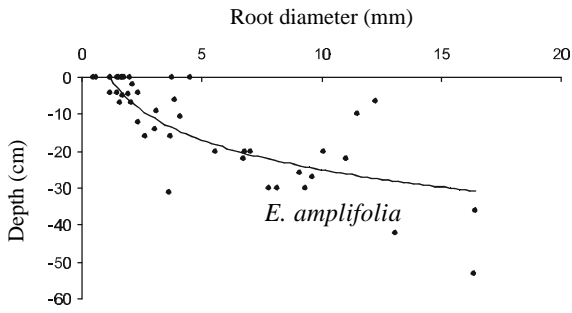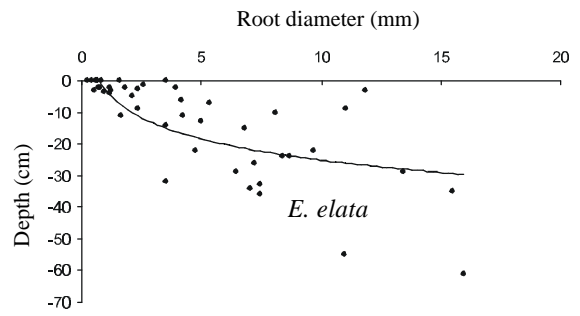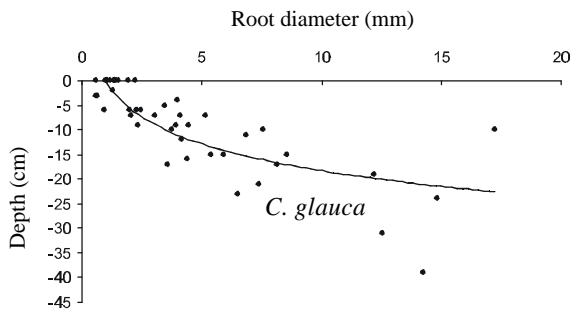
B-III: Relationship between root diameter at the surface and the depth of likely tensile failure of the root.

B-IV: Experimental data from root pull-out tests on roots of *C. glauca*.

Sample No. (Prefix CGPT)	Diameter at Surface (mm)	Diameter at broken end (mm)	Depth of root failure (cm)	Max. Pull-out resistance (N)	'Effective' tensile strength (MPa)
1	1.38	1.38	0	36.29	24.26
2	0.65	0.61	-3	16.69	47.28
3	1.28	1.18	-2	23.54	18.29
4	3.56	1.51	-17	174.56	17.54
5	4.18	2.57	-12	275.80	20.10
6	8.17	4.69	-17	569.80	10.87
7	5.93	3.93	-15	569.80	20.63
8	0.56	0.41	-3	8.83	35.85
9	1.33	1.33	0	47.07	33.88
10	4.41	4.24	-16	359.80	23.57
11	0.96	0.93	-6	28.44	39.29
12	4.47	3.29	-9	443.80	28.28
13	6.87	2.73	-11	527.80	14.24
14	3.48	2.01	-5	125.53	13.20
15	2.23	2.23	0	51.00	13.06
16	0.58	0.58	0	21.58	81.68
17	1.95	1.95	0	45.11	15.10
18	4.01	1.17	-4	60.80	4.81
19	7.58	4.17	-10	1031.80	22.86
20	1.37	1.37	0	62.76	42.57
21	1.33	1.33	0	46.09	33.18
22	2.35	1.55	-9	109.84	25.32
23	3.77	3.65	-10	359.80	32.23
24	12.18	3.40	-19	1241.80	10.66
25	2.45	2.51	-6	95.13	20.18
26	8.56	3.56	-15	947.80	16.47
27	0.98	0.98	0	12.75	16.90
28	3.05	1.81	-7	165.74	22.68
29	1.53	1.53	0	31.38	17.07
30	4.13	3.48	-7	569.80	42.53
31	12.56	6.20	-31	1451.80	11.72
32	1.17	1.17	0	19.61	18.24
33	3.93	3.25	-9	152.99	12.61
34	14.81	8.15	-24	2901.30	16.84
35	2.31	2.16	-6	125.53	29.95
36	1.98	2.01	-6	33.25	12.42
37	7.41	4.09	-21	569.80	13.21
38	0.97	0.97	0	29.42	39.81
39	5.18	4.37	-7	485.30	23.05
40	2.06	1.92	-7	43.15	12.95
41	14.23	6.28	-39	1751.80	11.02
42	5.42	2.47	-15	85.32	3.70
43	1.03	1.03	0	16.67	20.01
44	17.23	5.02	-10	779.80	3.34
45	6.52	3.8	-23	527.80	15.81
Average	**4.49**	**2.64**	**-9**	**378.64**	**22.43**

B-V: Experimental data from root pull-out tests on roots of *E. amplifolia.*

Sample No. (Prefix EAPT)	Diameter at Surface (mm)	Diameter at broken end (mm)	Depth of root failure (cm)	Max. Pull-out resistance (N)	'Effective' tensile strength (MPa)
1	1.46	1.24	-4	50.02	29.88
2	3.73	3.71	0	127.49	11.67
3	0.57	0.58	0	33.34	130.65
4	1.71	1.71	0	68.65	29.89
5	1.77	1.77	0	76.50	31.09
6	1.17	1.17	0	14.71	13.68
7	2.33	1.13	-4	122.59	28.75
8	1.63	1.63	0	49.04	23.50
9	1.45	1.45	0	37.27	22.57
10	0.45	0.45	0	2.94	18.49
11	2.08	1.01	-7	114.74	33.77
12	1.99	1.99	0	92.19	29.64
13	1.56	1.28	-7	58.84	30.78
14	1.62	1.62	0	105.92	51.39
15	1.95	1.95	-4.5	113.76	38.09
16	1.18	1.18	0	39.23	35.87
17	2.13	1.85	-2	112.78	31.65
18	1.71	1.53	-5	88.26	38.43
19	1.5	1.5	0	65.71	37.18
20	1.19	1.15	-4	43.15	38.80
21	7.81	3.69	-30	1199.80	25.04
22	12.25	9.32	-6.5	2039.80	17.31
23	9.31	5.27	-30	1787.80	26.26
24	4.53	4.53	0	800.00	49.64
25	5.55	2.51	-20	611.80	25.29
26	8.15	3.73	-30	695.80	13.34
27	6.75	2.19	-22	527.80	14.75
28	9.59	4.35	-27	695.80	9.63
29	3.9	3.45	-6	183.39	115.35
30	3.05	2.27	-14	207.91	28.46
31	6.79	1.63	-20	527.80	14.58
32	3.63	0.77	-31	144.16	13.93
33	16.38	5.07	-53	1871.80	8.88
34	13.07	2.76	-42	1283.80	9.57
35	11.48	8.75	-10	989.80	9.56
36	2.61	0.67	-16	100.03	18.70
37	3.68	2.93	-16	226.54	21.30
38	4.13	4.50	-10.5	569.80	42.53
39	16.43	6.66	-36	2039.80	9.62
40	10.11	2.65	-20	863.80	10.76
41	11.03	6.73	-22	1451.80	15.19
42	3.13	3.35	-9	359.80	46.76
43	7.02	3.56	-20	779.80	20.15
44	2.37	2.71	-12	201.04	45.57
45	9.07	4.30	-26	779.80	12.07
Average	**5.00**	**2.85**	**-13**	**496.81**	**27.33**

B-VI: Experimental data from root pull-out tests on roots of *E. elata.*

Sample No. (Prefix EEPT)	Diameter at Surface (mm)	Diameter at broken end (mm)	Depth of root failure (cm)	Max. Pull-out resistance (N)	'Effective' tensile strength (MPa)
1	0.72	0.91	-2	21.58	53.00
2	0.50	0.47	-3	12.75	64.94
3	3.54	1.27	-32	359.80	36.56
4	13.42	7.00	-29	1451.80	10.26
5	7.21	3.87	-26	1283.80	31.44
6	7.47	2.30	-33	947.80	21.63
7	11.05	8.87	-9	947.80	9.88
8	15.51	4.45	-35	1619.80	8.57
9	1.25	1.03	-3	22.56	18.38
10	2.37	2.39	-2.5	79.44	18.01
11	1.81	1.25	-2	51.98	20.20
12	0.62	0.62	0	2.94	9.74
13	8.38	3.68	-24	863.80	15.66
14	10.96	5.46	-55	2543.80	26.96
15	11.85	6.86	-3	1829.80	16.59
16	0.81	0.81	0	30.40	58.99
17	0.79	0.55	-2	10.79	22.01
18	0.95	0.43	-3.5	22.56	31.83
19	2.13	1.79	-5	119.65	33.58
20	2.35	1.83	-9	129.45	29.85
21	3.53	2.47	-14	130.43	13.33
22	7.04	3.21	-34	863.80	22.19
23	7.47	1.65	-36	611.80	13.96
24	0.41	0.41	0	20.59	155.95
25	3.93	3.70	-2	160.83	13.26
26	0.21	0.21	0	6.86	198.06
27	4.15	2.45	-6	235.37	17.40
28	0.65	0.65	0	9.81	29.56
29	6.45	2.83	-29	963.80	26.44
30	6.82	4.36	-15	527.80	17.45
31	1.67	0.61	-11	80.42	36.71
32	8.09	2.36	-10	695.80	13.54
33	1.17	0.98	-2	41.19	38.31
34	4.21	0.80	-11	233.80	16.80
35	0.60	0.60	0	6.37	22.53
36	9.68	3.98	-22	863.80	11.74
37	2.59	2.47	-1.5	75.51	14.33
38	4.98	3.05	-13	569.80	29.25
39	3.50	3.50	0	275.80	28.67
40	5.31	3.94	-7	359.80	16.25
41	1.15	1.15	-4	62.76	60.42
42	15.93	3.90	-61	1878.80	8.97
43	8.66	7.77	-24	1409.80	23.93
44	1.58	1.58	0	45.11	23.01
45	4.73	2.11	-22	527.80	30.04
Average	**4.85**	**2.58**	**-13**	**507.09**	**31.49**

B-VII: Experimental data from root pull-out tests on roots of *A. floribunda*.

Sample No. (Prefix AFPT)	Diameter at Surface (mm)	Diameter at broken end (mm)	Depth of root failure (cm)	Max. Pull-out resistance (N)	'Effective' tensile strength (MPa)
1	0.52	0.45	-3	8.83	41.58
2	1.11	0.40	-15	74.53	77.02
3	1.19	0.67	-13	85.32	76.71
4	2.55	1.48	-14	123.57	24.20
5	1.73	0.89	-13	185.35	78.85
6	0.31	0.31	0	3.92	51.94
7	7.39	2.33	-19	611.80	14.26
8	3.85	1.20	-29	527.80	45.34
9	10.15	2.05	-26	1073.80	13.27
10	0.75	0.59	-2	8.83	19.99
11	8.23	2.39	-52	1493.80	28.08
12	0.88	0.45	-18	67.67	111.26
13	1.95	1.21	-12	113.76	38.09
14	10.66	2.87	-42	1787.80	20.03
15	7.69	2.21	-27	1409.80	30.35
16	2.26	1.92	-3	203.99	50.85
17	9.40	2.06	-50	1661.80	23.95
18	1.95	1.78	-4	227.52	76.18
19	3.61	1.53	-28	905.80	88.50
20	2.87	2.86	-9	485.80	75.09
21	13.33	3.68	-44	1619.80	11.61
22	5.18	5.18	0	779.80	37.00
23	0.63	0.63	0	26.48	84.95
24	3.09	3.09	0	443.80	59.18
25	1.24	0.95	-11	76.49	63.34
26	1.85	1.68	-4.5	527.80	196.35
27	2.45	2.25	-8	527.80	111.96
28	3.37	2.93	-11	443.80	49.76
29	2.95	2.18	-14	443.80	64.93
30	2.69	2.02	-10	527.80	92.87
31	1.45	1.57	-6.5	359.80	217.89
32	3.29	2.38	-19	653.80	76.91
33	2.97	0.80	-44	443.80	64.06
34	1.47	1.07	-20	101.99	60.09
35	3.94	1.52	-35	779.80	63.96
36	3.71	4.68	-9	359.80	33.28
37	7.88	2.22	-37	1073.80	22.02
38	10.15	3.87	-28	905.80	11.19
39	0.90	0.90	0	19.61	30.82
40	8.76	5.75	-26.5	1703.80	28.27
41	5.43	1.36	-14	527.80	22.79
42	7.05	1.88	-46	947.80	24.28
43	0.70	0.70	0	46.09	119.76
44	1.31	0.87	-7	90.22	66.94
45	9.43	3.98	-22	989.80	14.17
Average	**4.09**	**1.95**	**-18**	**566.28**	**58.09**

B-VIII: Experimental data from root tensile tests on roots of *C. glauca* and *A. floribunda.*

Sample No. (Prefix CG/AFPT)	*C. glauca*			*A. floribunda*		
	Diameter at broken end (mm)	Max. Tensile resistance (N)	Tensile strength (MPa)	Diameter at broken end (mm)	Max. Tensile resistance (N)	'Tensile strength (MPa)
1	0.61	4.90	16.78	0.31	3.92	51.94
2	0.58	21.58	81.68	5.18	779.80	37.00
3	1.37	62.76	42.57	0.63	26.48	84.95
4	1.33	46.09	33.18	3.09	443.80	59.18
5	0.98	12.75	16.90	0.90	29.61	46.54
6	1.53	31.38	17.07	0.70	46.09	119.76
7	1.17	19.61	18.24	5.56	1829.80	75.36
8	0.97	29.42	39.81	3.58	1115.80	110.85
9	1.03	16.67	20.01	0.71	35.31	89.18
10	4.41	1115.80	73.05	0.81	55.90	108.48
11	6.63	1283.80	37.19	0.93	104.93	154.47
12	4.37	779.80	51.99	4.55	485.80	29.88
13	3.55	779.80	78.78	5.81	3131.80	118.13
14	6.82	2249.80	61.59	1.37	92.16	62.52
15	13.10	4157.80	30.85	1.93	226.36	77.37
16	4.92	443.80	23.34	6.93	3719.80	98.62
17	1.83	359.80	136.79	1.93	186.33	63.69
18	1.03	29.42	35.31	0.29	12.56	190.15
19	6.07	2459.80	85.00	2.25	492.80	123.94
20	1.57	35.31	18.24	3.12	402.50	52.65
21	4.67	982.80	57.38	3.96	392.80	31.89
22	3.82	779.80	68.04	6.87	1986.80	53.60
23	5.69	1829.80	71.96	3.48	1026.80	107.95
24	8.41	2459.80	44.28	6.58	3068.80	90.25
25	0.49	10.79	57.21	2.63	224.80	41.38
26	4.24	779.80	55.23	4.02	1786.80	140.78
27	10.52	4198.80	48.31	2.12	304.56	86.28
28	0.36	7.85	77.07	2.25	295.64	74.35
29	8.98	3210.80	50.70	4.46	1658.80	106.18
30	1.29	51.30	39.25	4.25	946.80	66.74
Average	**3.74**	**941.72**	**49.59**	**3.04**	**830.47**	**85.14**

B-IX: Experimental data from root tensile tests on roots of *E. amplifolia* and *E. elata.*

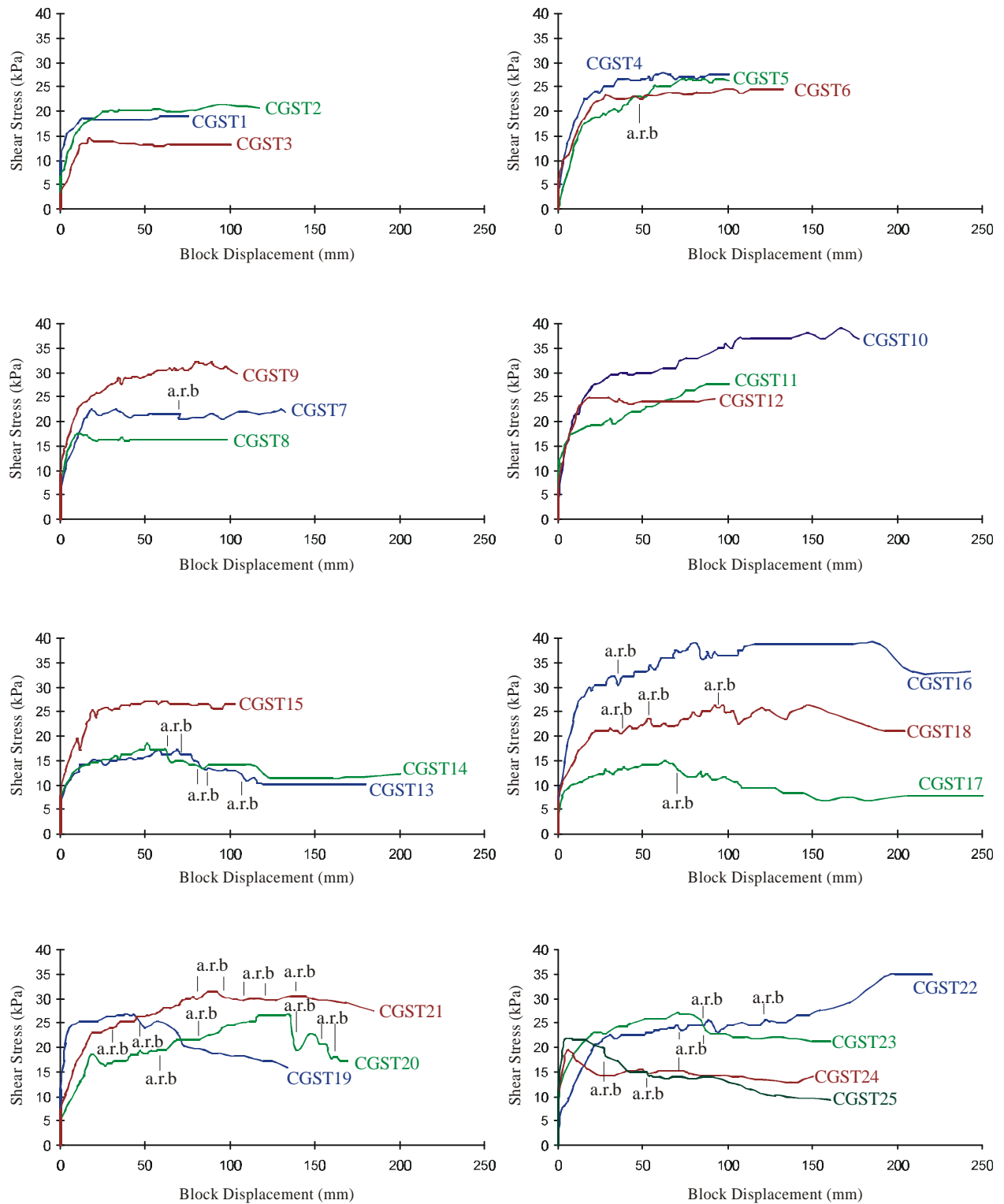| Sample No. (Prefix EA/EEPT)	E. amplifolia			E. elata		
	Diameter at broken end (mm)	Max. Tensile resistance (N)	Tensile strength (MPa)	Diameter at broken end (mm)	Max. Tensile resistance (N)	'Tensile strength (MPa)
1	3.77	779.80	69.86	0.62	29.40	97.38
2	3.71	127.49	11.79	0.81	30.40	58.99
3	0.58	33.34	126.19	0.41	20.59	155.95
4	1.71	68.65	29.89	0.21	6.86	198.06
5	1.77	76.50	31.09	0.65	9.81	29.56
6	1.17	14.71	13.68	0.60	6.37	22.53
7	1.63	49.04	23.50	3.50	275.80	28.67
8	1.45	37.27	22.57	1.58	45.11	23.01
9	0.45	12.94	81.36	4.43	821.80	53.32
10	1.99	92.19	29.64	0.93	49.03	72.18
11	1.62	105.92	51.39	1.41	32.25	20.65
12	1.18	39.23	35.87	2.13	55.90	15.69
13	1.50	65.71	37.18	4.05	821.80	63.79
14	4.53	800.00	49.64	6.09	2879.80	98.86
15	4.11	1367.80	103.10	4.07	275.80	21.20
16	0.83	19.61	36.25	6.05	779.80	27.13
17	0.23	4.90	118.03	3.61	401.80	39.26
18	3.52	989.80	101.71	1.38	41.26	27.59
19	4.35	401.80	27.04	3.55	779.80	78.78
20	5.03	1073.80	54.04	2.79	129.45	21.17
21	3.41	359.80	39.40	7.73	2795.80	59.57
22	4.05	359.80	27.93	4.95	779.80	40.52
23	2.50	275.80	56.19	4.05	989.80	76.83
24	1.65	233.80	109.34	3.31	485.80	56.46
25	2.95	401.80	58.79	2.13	359.80	100.97
26	2.15	149.80	41.26	1.56	41.87	21.91
27	1.64	191.80	90.80	1.37	36.78	24.95
28	1.69	191.80	85.50	2.07	191.80	56.99
29	5.52	1213.80	50.72	5.62	1321.80	53.28
30	6.15	1423.80	47.93	6.85	2096.80	56.90
Average	**2.56**	**365.42**	**55.39**	**2.95**	**553.10**	**56.74**

Appendix C

Data supporting Chapter 5

C-I: Additional experimental data for direct shear tests on soil-only blocks.

| Sample No.	Applied Normal Load (kg)	Weight of Soil above the shear plane (kg)	Peak Shear Resistance (kg)	Moisture Content (%)
1	205	160	431	15
2	67	187	371	16
3	142	199	405	17
4	452	115	551	17
5	420	95	636	18
6	470	113	508	18
7	0	125	294	25

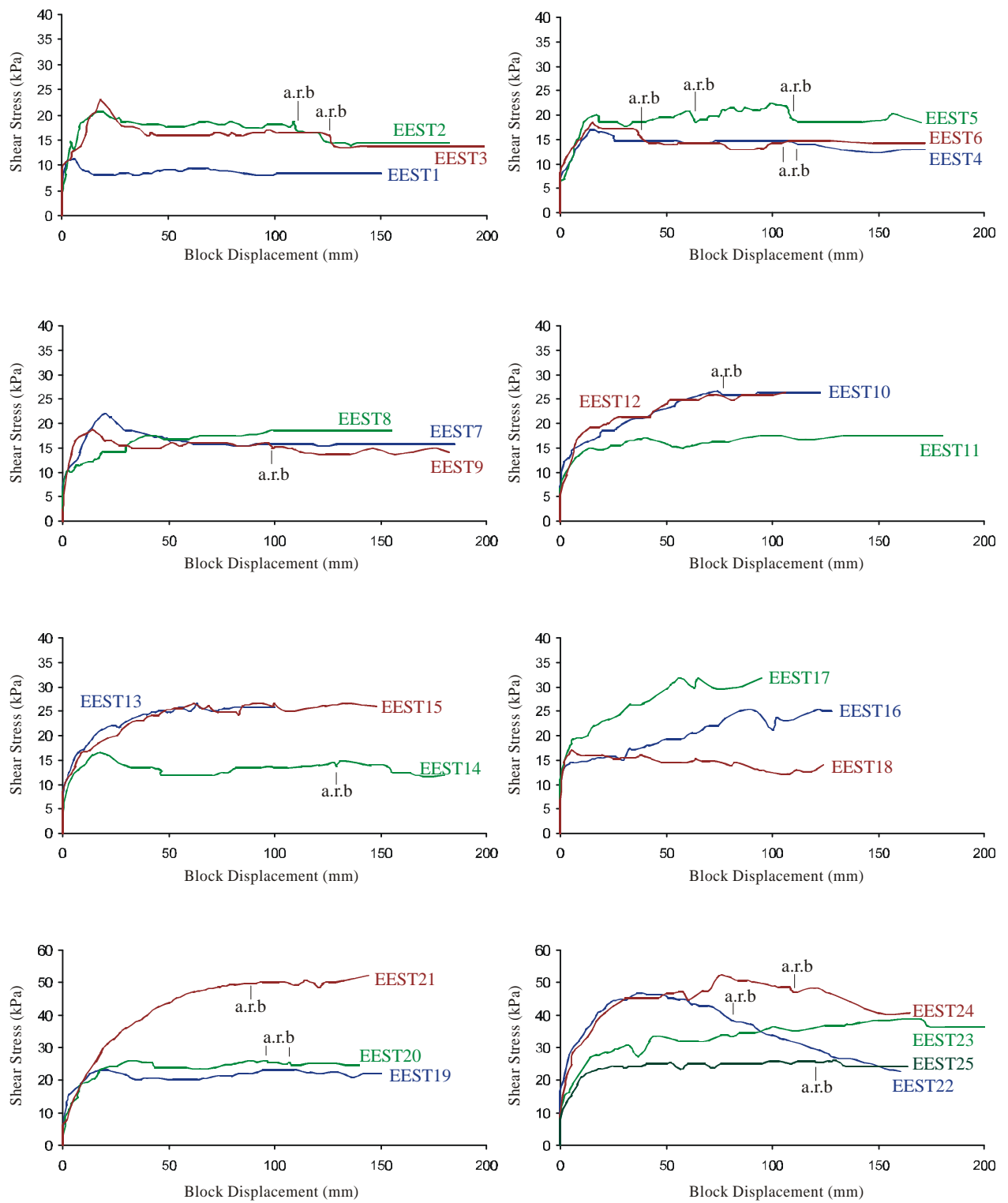| Sample No.	Applied Normal Load (kg)	Weight of Soil above the shear plane (kg)	Peak Shear Resistance (kg)	Moisture Content (%)
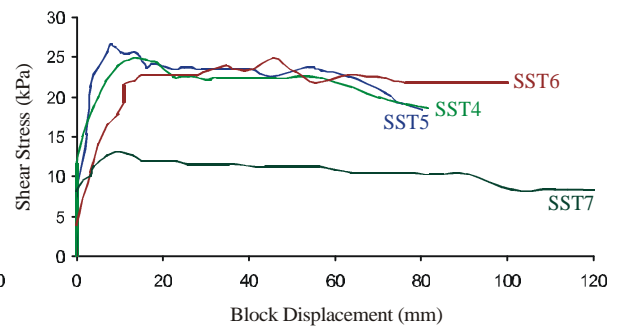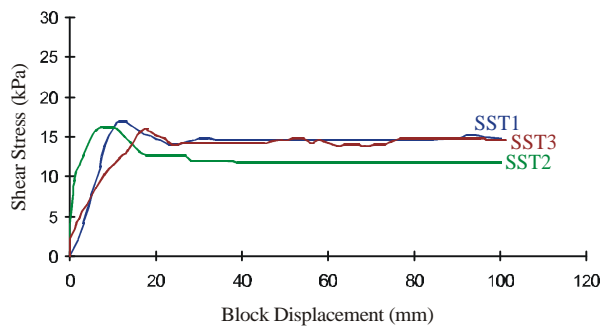
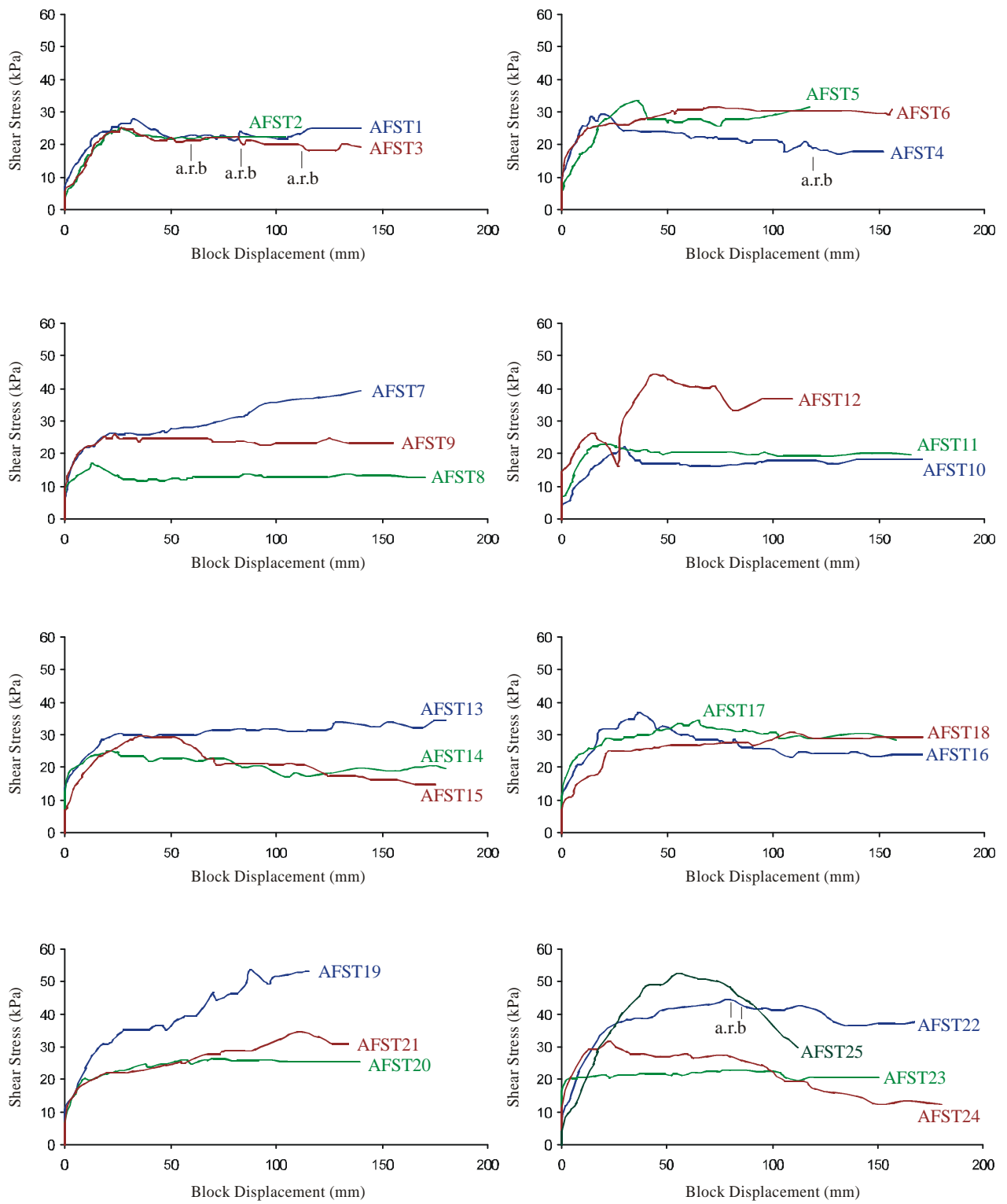**C-II:** Shear stress versus displacement plots for blocks containing no roots.

C-III: Shear stress versus displacement plots for blocks containing *C. glauca* roots (a.r.b = audible root breakage).
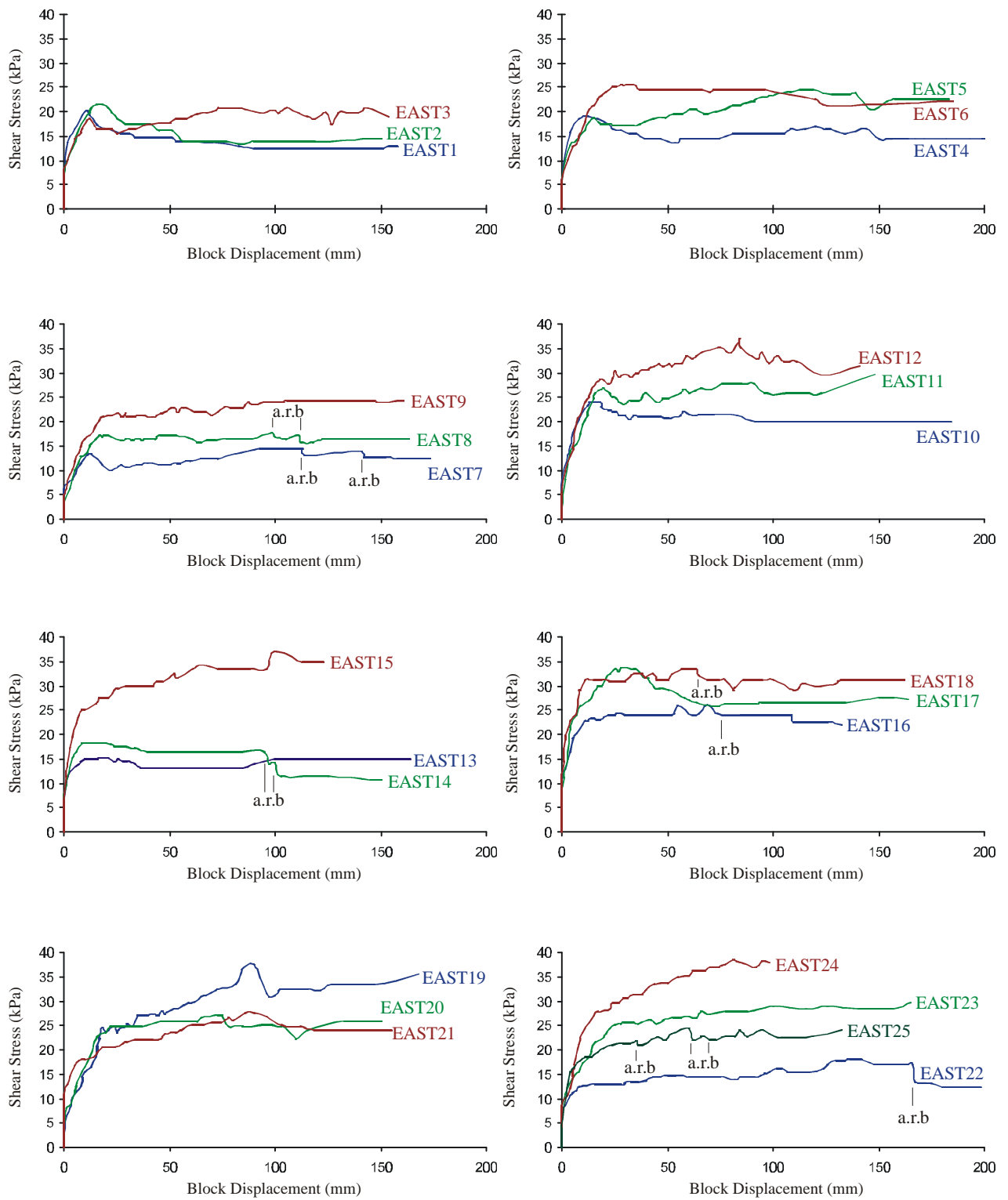
C-IV: Shear stress versus displacement plots for blocks containing *E. amplifolia* roots (a.r.b = audible root breakage).

C-V: Shear stress versus displacement plots for blocks containing *E. elata* roots (a.r.b = audible root breakage).

C-VI: Shear stress versus displacement plots for blocks containing *A. floribunda* roots (a.r.b = audible root breakage).

C-VII: Additional experimental data for direct shear tests on blocks containing roots of *C. glauca*.

Sample No. (Prefix CGST)	Above ground Biomass (kg)	Cross-sectional area of roots (cm²)	Applied Normal Load (kg)	Weight of Soil above the shear plane (kg)	Peak Shear Resistance (kg)	Moisture Content (%)
1	3.60	0.62	284	141	486	14
2	4.30	1.66	360	164	542	18
3	4.10	1.00	205	164	371	19
4	5.57	2.74	351	95	572	17
5	5.18	2.96	205	95	551	18
6	7.05	2.38	220	107	551	17
7	4.75	2.22	220	107	465	17
8	6.55	1.15	73	114	362	21
9	4.20	3.63	418	87	662	19
10	3.70	6.19	433	114	808	16
11	6.50	4.41	265	114	572	17
12	0.90	0.37	463	132	508	17
13	4.15	2.60	0	107	354	18
14	5.05	2.30	0	114	380	18
15	4.80	2.24	440	114	559	10
16	5.25	4.15	230	85	593	17
17	4.65	0.96	0	99	268	17
18	7.65	2.85	110	74	423	18
19	6.65	5.62	0	95	491	18
20	11.20	4.08	0	114	551	18
21	2.20	4.55	136	101	576	17
22	6.35	4.41	275	114	722	17
23	15.75	3.67	59	118	619	18
24	9.60	1.32	0	97	336	17
25	5.30	1.49	66	146	406	18

C-VIII: Additional experimental data for direct shear tests on blocks containing roots of *E. amplifolia.*

Sample No. (Prefix EAST)	Above ground Biomass (kg)	Cross-sectional area of roots (cm²)	Applied Normal Load (kg)	Weight of Soil above the shear plane (kg)	Peak Shear Resistance (kg)	Moisture Content (%)
1	0.50	1.55	55	127	465	16
2	0.90	2.06	110	113	439	16
3	1.80	1.00	165	150	422	17
4	1.40	1.99	0	132	388	16
5	1.50	1.70	114	133	508	15
6	1.20	1.46	235	126	529	17
7	2.50	2.44	0	101	294	20
8	3.45	2.35	110	106	405	19
9	3.25	4.42	165	118	559	17
10	4.15	4.72	209	132	615	15
11	4.30	7.03	198	139	679	16
12	5.60	7.58	249	127	850	17
13	3.30	3.34	0	155	388	15
14	4.80	6.43	0	127	465	18
15	5.30	6.11	407	127	936	18
16	3.65	4.97	180	127	593	16
17	4.55	7.52	359	141	859	19
18	3.80	4.45	304	132	679	15
19	4.20	6.54	227	132	765	22
20	3.55	5.68	77	113	551	19
21	5.00	6.01	183	99	593	17
22	4.15	4.75	0	121	422	19
23	6.40	6.86	260	117	765	22
24	5.10	8.58	348	118	885	18
25	6.10	8.79	0	114	559	15

**C-IX:** Additional experimental data for direct shear tests on blocks containing roots of *E. elata.*

Sample No. (Prefix EEST)	Above ground Biomass (kg)	Cross-sectional area of roots (cm²)	Applied Normal Load (kg)	Weight of Soil above the shear plane (kg)	Peak Shear Resistance (kg)	Moisture Content (%)
1	1.70	0.34	0	110	234	20
2	3.70	3.47	0	122	475	21
3	3.30	1.53	55	87	422	20
4	4.20	2.55	55	109	388	17
5	5.50	1.55	110	97	456	20
6	4.65	1.08	110	110	379	18
7	2.05	0.46	165	122	508	19
8	6.00	4.66	0	98	379	25
9	1.55	0.43	55	66	285	22
10	10.70	9.39	180	117	611	22
11	3.80	3.30	77	92	371	21
12	7.70	5.10	337	122	602	22
13	3.70	1.72	180	130	611	22
14	9.45	1.81	0	146	439	22
15	9.95	6.37	169	127	637	21
16	4.15	4.03	0	108	551	21
17	7.15	4.87	315	145	808	26
18	3.35	1.02	77	123	422	30
19	4.70	5.12	337	118	559	17
20	12.60	8.79	110	100	619	19
21	18.80	14.05	205	139	1270	17
22	7.20	8.79	99	109	957	20
23	16.40	9.83	55	125	850	21
24	9.85	13.40	99	82	979	17
25	6.95	5.93	77	85	533	19

C-X: Additional experimental data for direct shear tests on blocks containing roots of *A. floribunda..*

Sample No. (Prefix AFST)	Above ground Biomass (kg)	Cross-sectional area of roots (cm²)	Applied Normal Load (kg)	Weight of Soil above the shear plane (kg)	Peak Shear Resistance (kg)	Moisture Content (%)
1	1.75	1.31	0	105	705	20
2	1.85	0.92	0	120	615	17
3	4.45	0.80	55	129	572	16
4	3.70	0.53	110	154	688	15
5	3.00	0.92	110	151	765	15
6	3.10	0.77	110	129	722	19
7	3.20	2.95	132	129	893	18
8	1.60	0.10	77	102	354	19
9	2.85	1.44	55	97	533	34
10	2.35	1.36	55	103	486	23
11	2.40	1.21	110	109	474	21
12	5.95	1.41	77	93	808	22
13	3.85	2.53	33	103	636	20
14	2.95	1.78	0	97	431	22
15	1.90	0.77	55	106	722	23
16	3.00	1.85	165	105	936	19
17	6.10	1.84	44	103	765	19
18	3.90	2.80	22	70	551	23
19	3.10	4.32	99	72	1030	21
20	4.40	2.28	0	105	559	20
21	1.10	1.21	176	87	730	19
22	4.00	2.73	110	127	1000	17
23	3.75	2.22	0	97	474	19
24	3.00	0.93	0	100	619	18
25	7.70	3.66	33	147	1364	17

C-XI: Increase in peak shear resistance (kPa) for soil blocks containing roots over soil blocks without roots.

Sample	C. glauca	E. amplifolia	E. elata	A. floribunda
1	-0.38	6.14	-1.21	15.83
2	-0.57	5.58	8.17	12.85
3	-3.60	1.97	8.99	10.74
4	5.21	5.79	3.26	13.11
5	8.49	8.01	6.90	17.10
6	7.73	5.70	2.59	15.81
7	3.58	2.07	5.21	22.69
8	2.73	2.62	6.18	2.47
9	7.84	7.54	4.66	12.05
10	13.66	6.67	9.42	8.40
11	7.17	11.33	3.31	7.18
12	-2.21	17.78	4.75	29.05
13	4.68	2.21	9.08	20.83
14	5.70	5.91	3.92	12.41
15	1.41	14.66	9.77	16.20
16	16.96	8.43	12.81	20.95
17	2.35	12.44	11.38	21.34
18	10.01	10.98	3.24	18.16
19	14.29	17.48	2.46	38.74
20	14.00	12.03	11.20	13.65
21	14.23	10.27	34.03	17.79
22	14.18	5.52	31.11	28.69
23	12.99	12.55	24.32	10.77
24	6.52	16.86	36.87	18.99
25	5.41	12.04	12.02	38.96
Average:	**6.90**	**8.90**	**10.58**	**17.79**
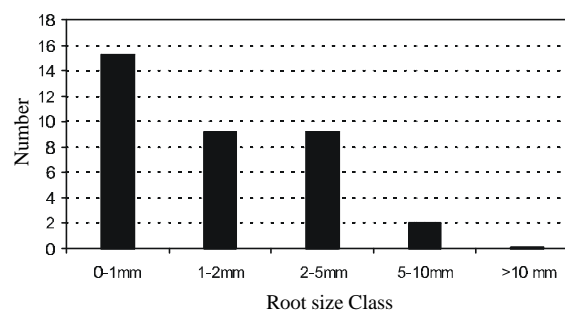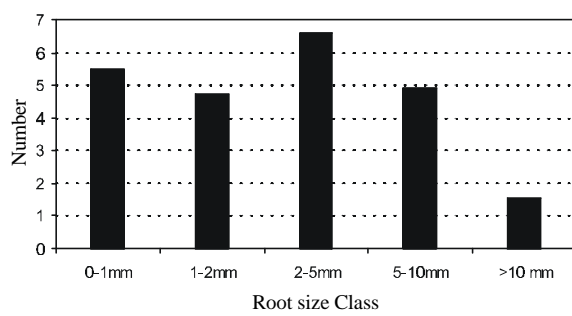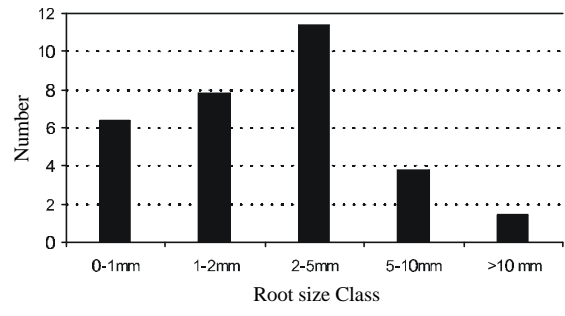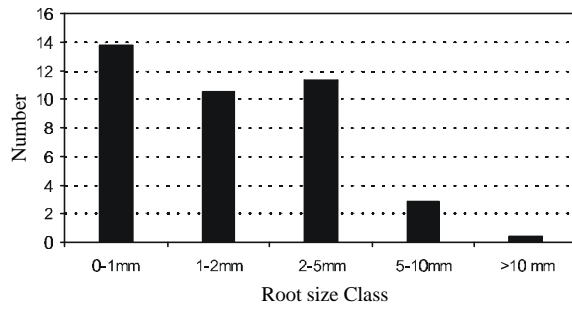
C-XII: Average root numbers on the shear plane at the conclusion of in-situ shear tests, and broken up by size class for the four tree species. (a) *C. glauca*, (b) *E. amplifolia*, (c) *E. elata*, (d) *A. floribunda*.

C-XIII: *C. glauca* root quantity data by size class determined from direct in-situ shear tests and the increased shear resistance calculated assuming simultaneous tensile root failure.

Sample No. (Prefix CGST)	Total Root Number	0-1 mm	1-2 mm	2-5 mm	5-10 mm	> 10 mm	Increased Shear Resistance (kPa)
1	15	5	5	4	1	0	4.51
2	32	16	8	7	0	1	9.78
3	59	39	11	9	0	0	6.05
4	62	22	23	14	3	0	19.85
5	38	9	6	20	3	0	20.84
6	45	10	17	14	4	0	23.10
7	50	18	9	21	2	0	16.96
8	44	22	11	11	0	0	7.93
9	43	10	15	12	6	0	24.72
10	36	8	13	10	3	2	31.17
11	38	6	14	10	7	0	25.31
12	13	8	2	3	0	0	2.16
13	41	8	11	19	3	0	20.16
14	46	20	7	17	2	0	16.18
15	29	6	10	9	4	0	15.43
16	29	5	8	12	2	2	33.01
17	17	7	5	4	1	0	6.63
18	43	14	9	15	5	0	30.75
19	32	4	7	15	5	1	27.62
20	37	9	10	14	2	2	29.45
21	51	4	28	15	2	2	34.03
22	43	24	5	7	6	1	30.85
23	73	39	14	13	7	0	24.35
24	30	15	9	5	1	0	7.02
25	28	16	7	3	2	0	7.02
Average	**39**	**13.8**	**10.6**	**11.3**	**2.8**	**0.4**	**18.99**

C-XIV: *E. amplifolia* root quantity data by size class determined from direct in-situ shear tests and the increased shear resistance calculated assuming simultaneous tensile root failure.

Sample No. (Prefix EAST)	Total Root Number	0-1 mm	1-2 mm	2-5 mm	5-10 mm	> 10 mm	Increased Shear Resistance (kPa)
1	20	3	5	11	1	0	9.75
2	13	2	4	4	2	1	13.94
3	13	6	1	4	2	0	9.43
4	14	5	2	1	6	0	15.10
5	16	6	1	7	2	0	13.16
6	13	4	4	2	3	0	9.84
7	23	7	4	7	5	0	23.16
8	31	9	6	12	4	0	21.76
9	21	4	5	6	5	1	25.87
10	27	5	5	9	7	1	23.68
11	18	2	6	3	3	4	40.28
12	11	1	1	4	1	4	29.85
13	35	14	2	12	7	0	20.68
14	18	2	2	6	6	2	23.20
15	35	10	4	12	9	0	31.56
16	18	4	3	4	5	2	27.60
17	30	5	7	6	10	2	33.50
18	19	3	3	4	8	1	32.30
19	19	1	3	7	5	3	42.03
20	32	6	5	11	8	2	46.37
21	38	16	8	5	6	3	43.19
22	35	9	11	10	4	1	29.28
23	21	5	7	2	4	3	34.55
24	31	3	9	9	6	4	47.84
25	31	5	10	7	4	5	44.87
Average	**23.3**	**5.5**	**4.7**	**6.6**	**4.9**	**1.6**	**27.71**

C-XV: *E. elata* root quantity data by size class determined from direct in-situ shear tests and the increased shear resistance calculated assuming simultaneous tensile root failure.

Sample No. (Prefix EEST)	Total Root Number	0-1 mm	1-2 mm	2-5 mm	5-10 mm	> 10 mm	Increased Shear Resistance (kPa)
1	16	9	2	5	0	0	3.64
2	19	3	4	7	3	2	23.11
3	19	7	5	3	4	0	11.57
4	18	2	4	7	4	1	19.35
5	28	9	8	8	3	0	16.75
6	20	2	8	9	1	0	9.22
7	11	3	8	5	0	0	3.82
8	43	5	8	26	2	2	42.73
9	19	10	8	4	0	0	3.64
10	33	4	7	14	3	5	53.47
11	20	2	5	12	0	1	17.82
12	37	2	10	20	3	2	41.45
13	25	3	13	7	2	0	12.73
14	37	9	15	11	2	0	14.12
15	48	13	11	10	10	2	51.37
16	35	1	8	19	7	0	34.92
17	62	14	13	30	4	1	41.81
18	18	5	5	7	1	0	7.26
19	20	5	5	3	6	1	21.48
20	50	9	14	17	8	2	51.82
21	45	9	7	14	10	5	83.25
22	40	13	5	15	3	4	43.13
23	40	9	9	12	7	3	59.87
24	48	10	15	13	5	5	59.76
25	22	2	6	7	6	1	32.48
Average	**30.8**	**6.4**	**7.8**	**11.4**	**3.8**	**1.5**	**30.42**

C-XVI: *A. floribunda* root quantity data by size class determined from direct in-situ shear tests and the increased shear resistance calculated assuming simultaneous tensile root failure.

Sample No. (Prefix AFST)	Total Root Number	0-1 mm	1-2 mm	2-5 mm	5-10 mm	> 10 mm	Increased Shear Resistance (kPa)
1	40	11	17	11	1	0	24.45
2	42	13	18	11	0	0	20.46
3	25	10	6	8	1	0	16.46
4	20	7	7	6	0	0	9.95
5	37	12	15	10	0	0	18.75
6	31	17	7	7	0	0	13.89
7	25	3	5	11	6	0	51.79
8	1	0	0	1	0	0	1.17
9	21	8	5	6	2	0	17.26
10	17	7	4	3	3	0	17.43
11	29	4	14	11	0	0	18.20
12	37	12	8	17	0	0	25.67
13	28	10	5	8	5	0	44.76
14	33	12	9	9	3	0	26.04
15	24	9	6	9	0	0	14.08
16	23	11	2	7	3	0	22.42
17	42	24	5	10	3	0	30.68
18	36	8	12	12	4	0	43.94
19	61	36	8	11	5	1	54.67
20	91	48	28	13	2	0	41.64
21	42	29	4	8	1	0	21.31
22	44	21	8	11	4	0	38.91
23	44	25	7	7	5	0	37.62
24	36	16	10	9	1	0	19.11
25	70	29	22	16	2	1	48.97
Average	**36**	**15.3**	**9.3**	**9.3**	**2**	**0.1**	**27.19**

Appendix D

Data supporting Chapter 6
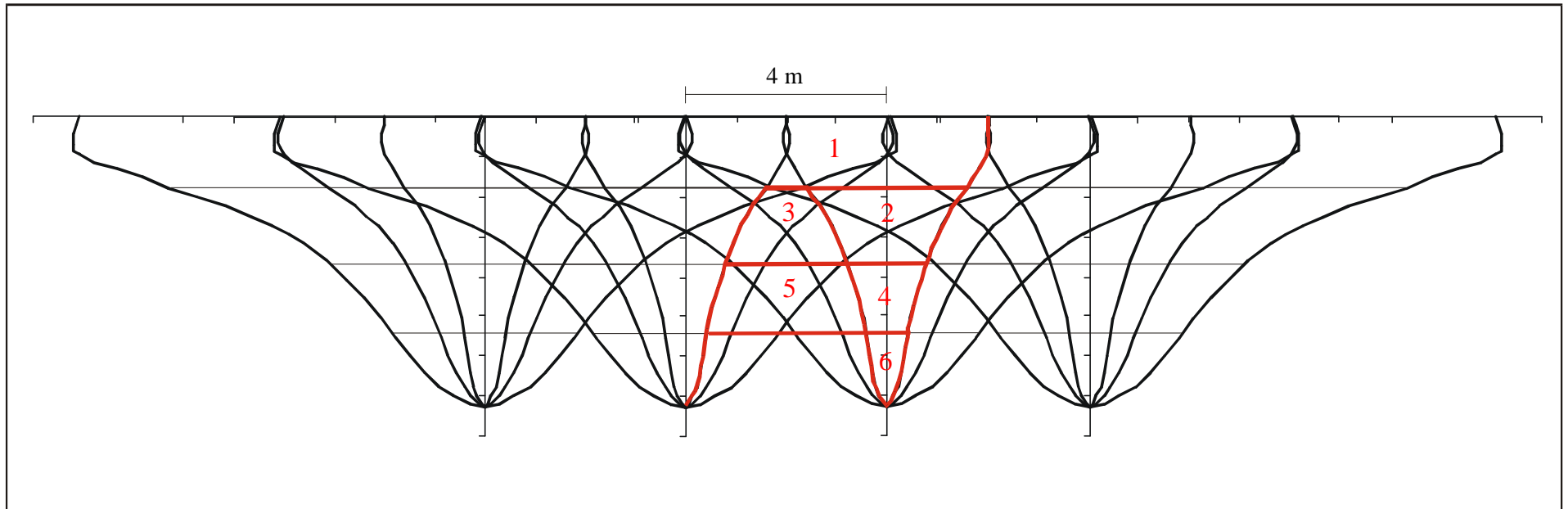
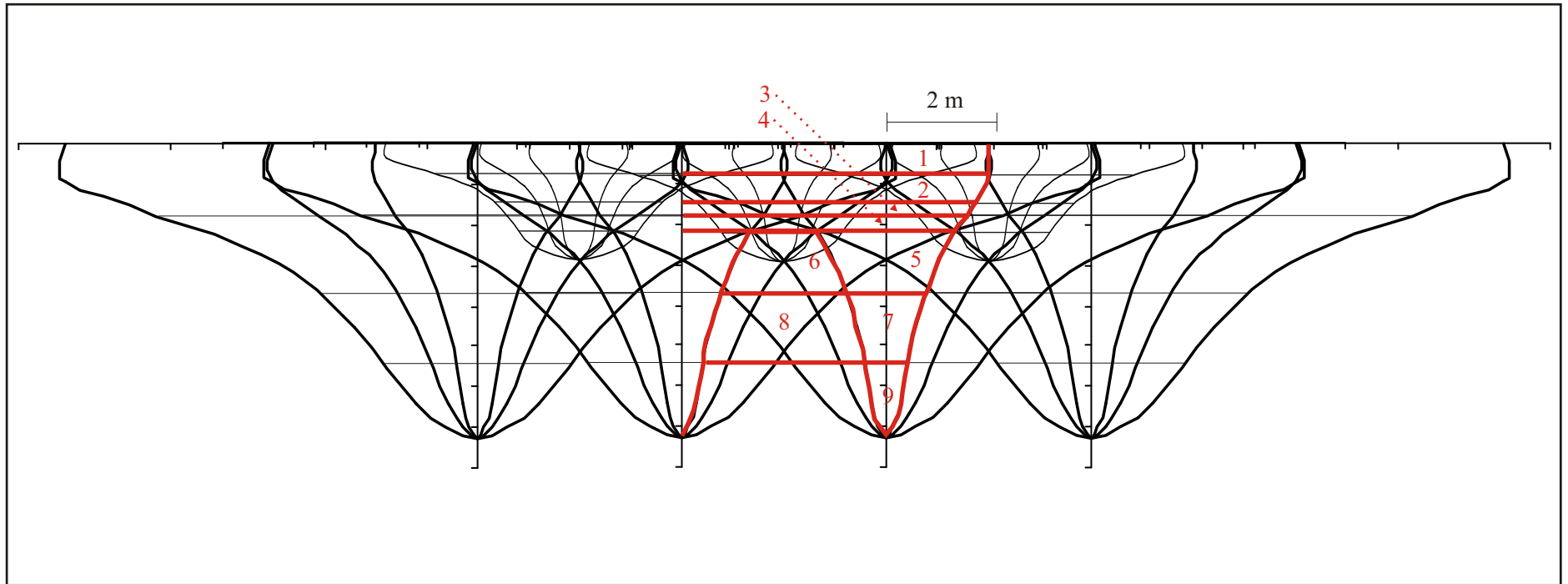**D-I(a):** Soil zones representing increased soil shear strengths beneath a *C. glauca* forest. Values of Sr are given in the table below.

Reinforced soil layer	S_r (kPa)	Reinforced soil layer	S_r (kPa)
1	9.43	4	3.74
2	3.92	5	0.00
3	0.16	6	1.72
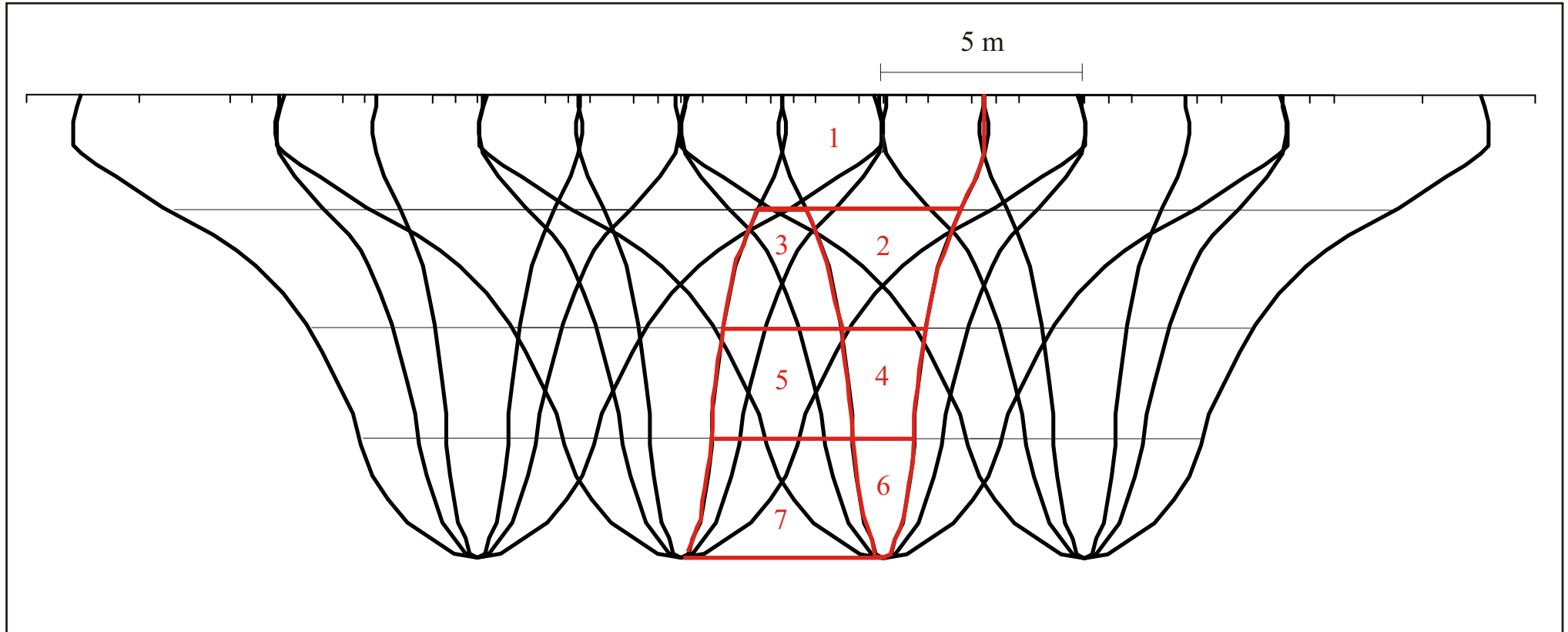
D-I(b): Soil zones representing increased soil shear strengths beneath an *E. amplifolia* forest. Values of S_r are given in the table below.

| Reinforced soil layer	S_r (kPa)	Reinforced soil layer	S_r (kPa)
1	38.97	5	3.56
2	25.36	6	7.18
3	4.09	7	2.95
4	13.81		
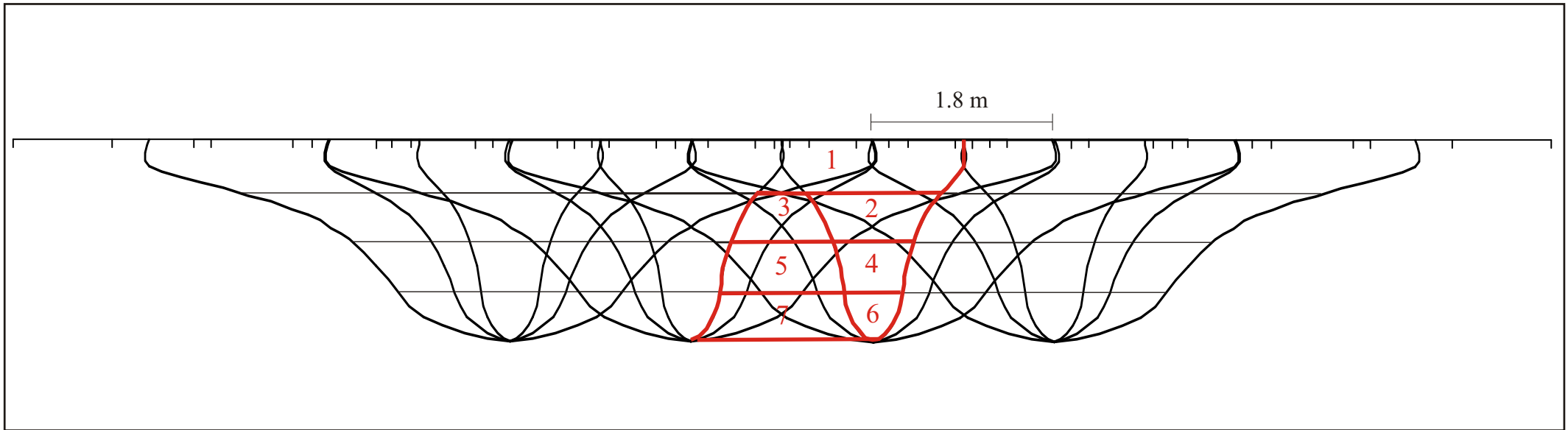
D-I(c): Soil zones representing increased soil shear strengths beneath an *A. floribunda* forest. Values of S_r are given in the table below.

| Reinforced soil layer	S_r (kPa)	Reinforced soil layer	S_r (kPa)
1	61.87	5	5.47
2	34.87	6	12.1
3	11.35	7	1.96
4	19.24		
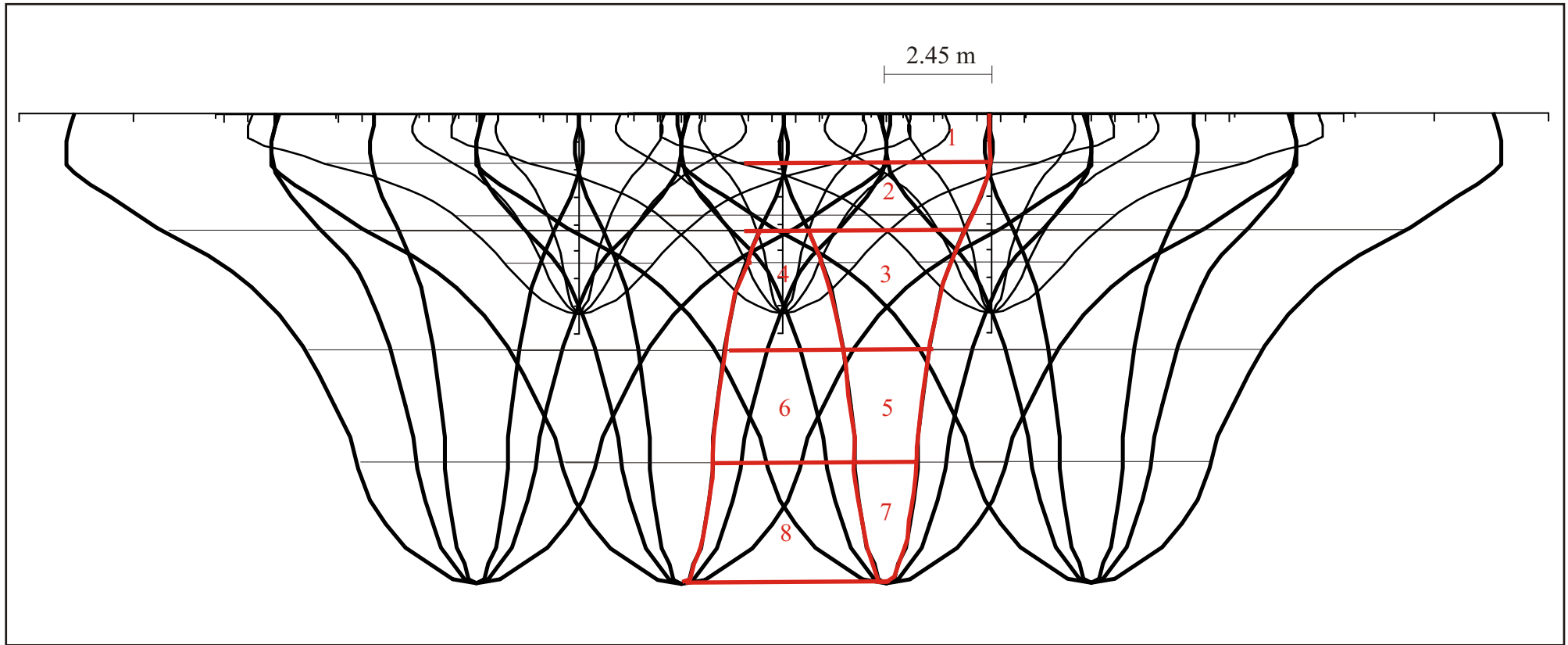
D-II(a): Soil zones representing increased soil shear strengths beneath an *E. amplifolia* and *C. glauca* forest. Values of S_r are given in the table below.

Reinforced soil layer	S_r (kPa)	Reinforced soil layer	S_r (kPa)
1	47.17	5	13.81
2	40.45	6	2.98
3	25.44	7	7.18
4	4.74	8	2.26
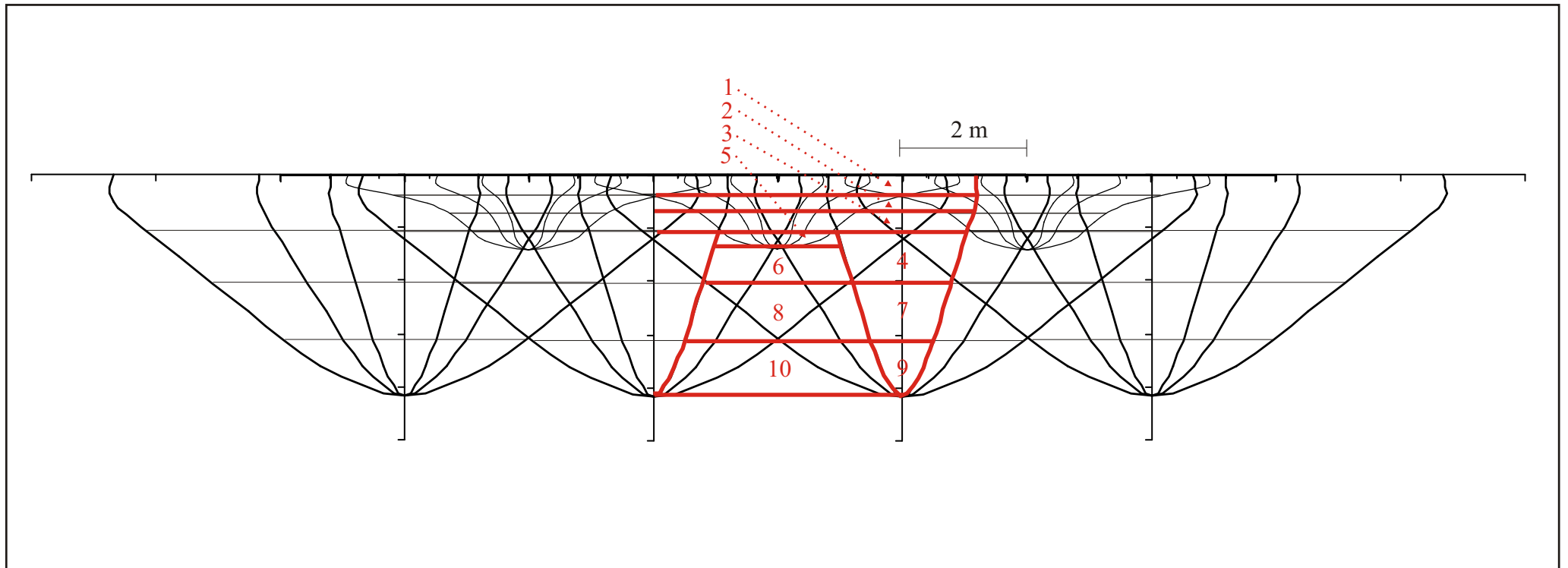
D-II(b): Soil zones representing increased soil shear strengths beneath an *E. elata* and *A. floribunda* forest. Values of S_r are given in the table below.

Reinforced soil layer	S_r (kPa)	Reinforced soil layer	S_r (kPa)
1	83.66	6	5.35
2	66.08	7	11.23
3	56.79	8	2.64
4	52.75	9	5.24
5	12.66	10	1.49
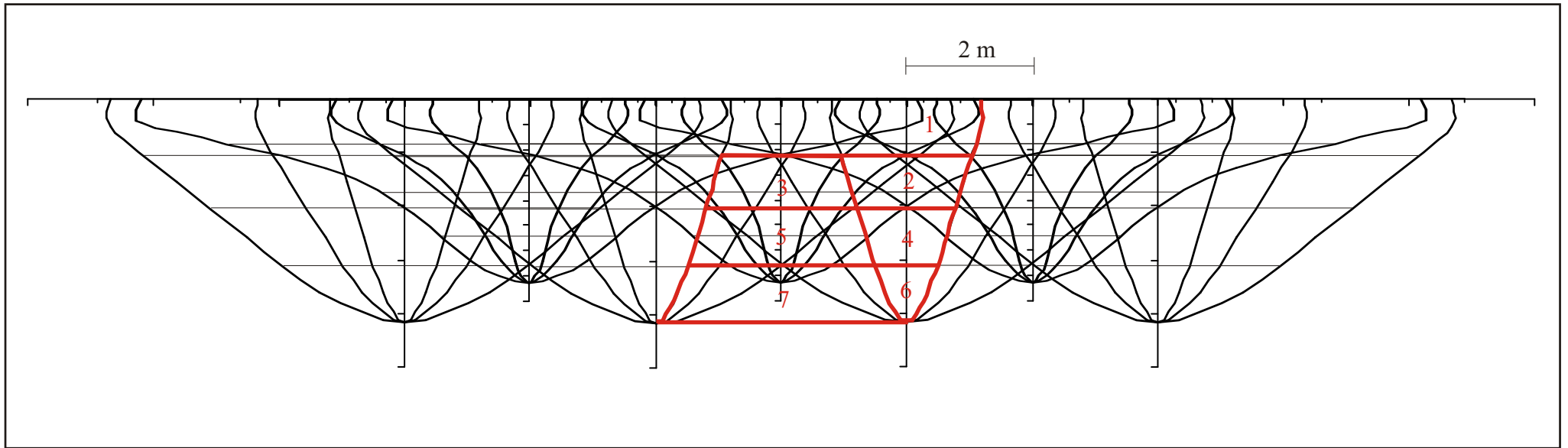
D-II(c): Soil zones representing increased soil shear strengths beneath an *E. elata* and *C. glauca* forest. Values of S_r are given in the table below.

Reinforced soil layer	S_r (kPa)	Reinforced soil layer	S_r (kPa)
1	55.57	5	3.09
2	52.75	6	5.24
3	7.69	7	1.56
4	11.23		

D-II(d): Soil zones representing increased soil shear strengths beneath a *C. glauca* and *A. floribunda* forest. Values of S_r are given in the table below.

Reinforced soil layer	S_r (kPa)	Reinforced soil layer	S_r (kPa)
1	63.19	6	0.50
2	28.92	7	3.74
3	15.24	8	0.00
4	8.45	9	1.72
5	4.29	10	0.00

Appendix E

Data supporting Chapter 7
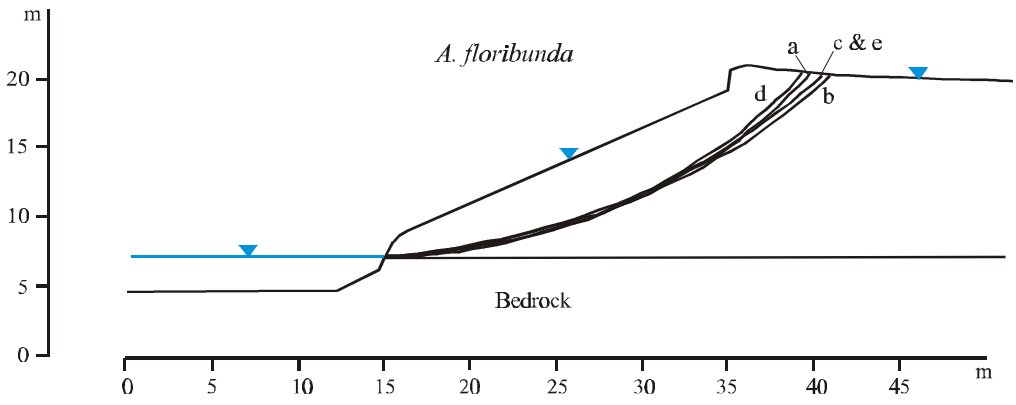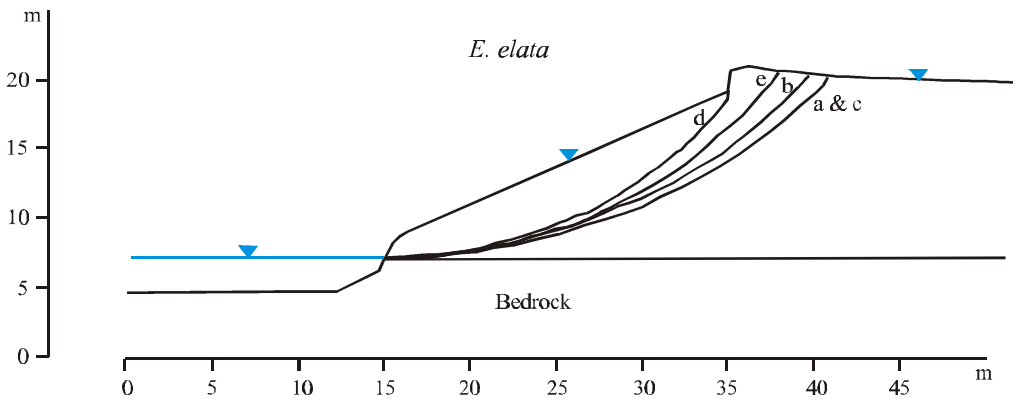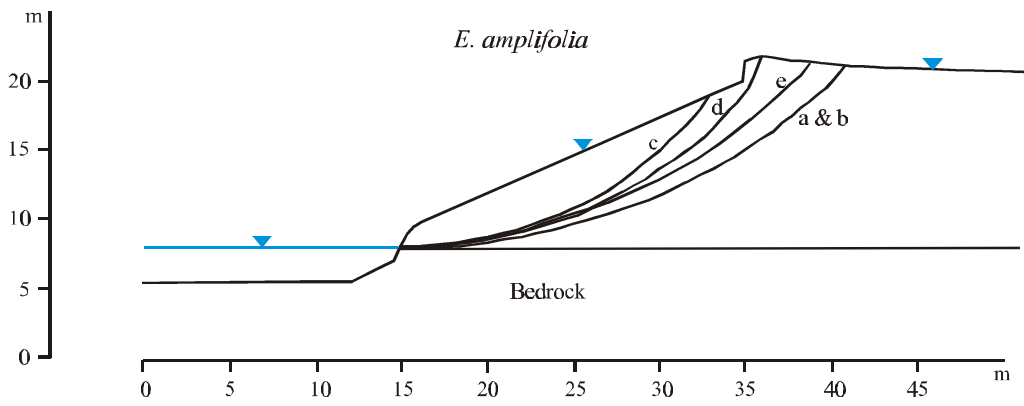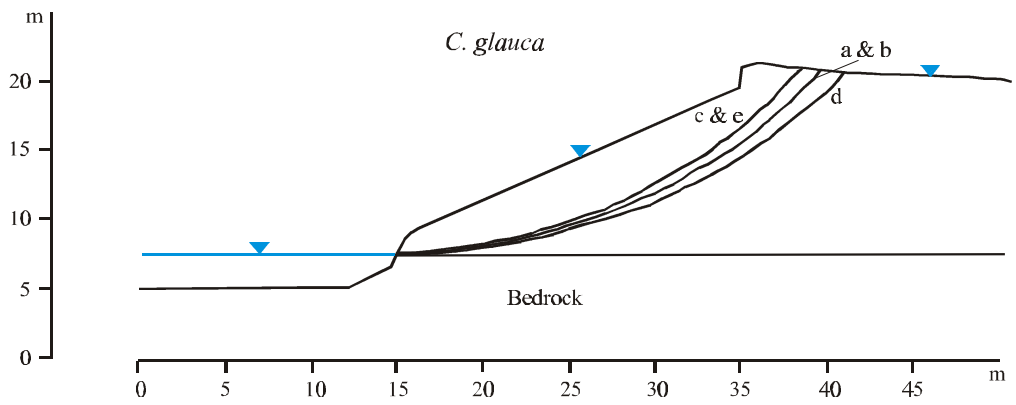
E-I(a): Critical failure surfaces for different tree locations on Profile Ac. Tree locations are shown in Figure 7.7.
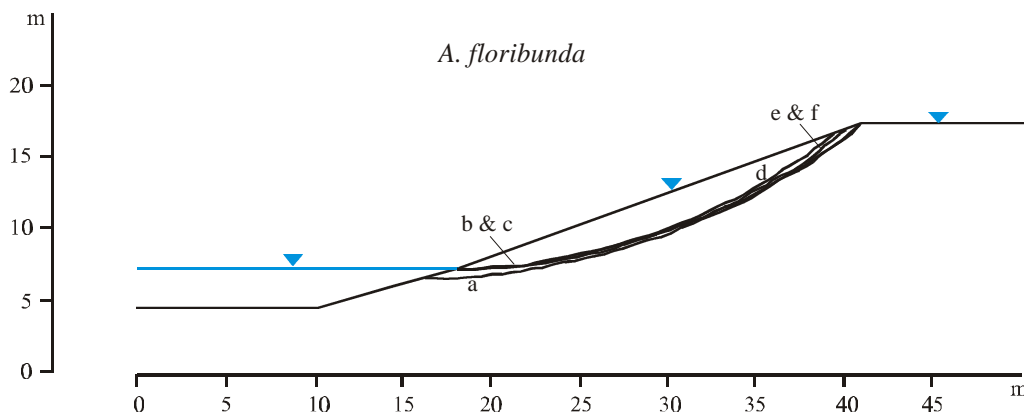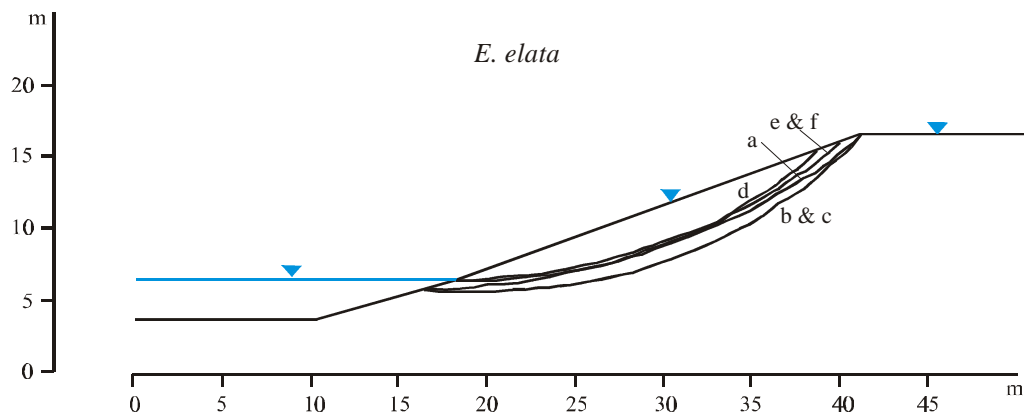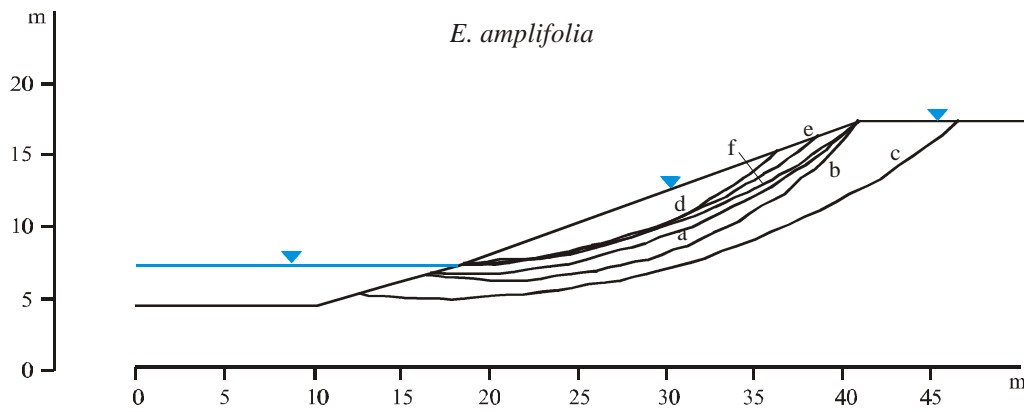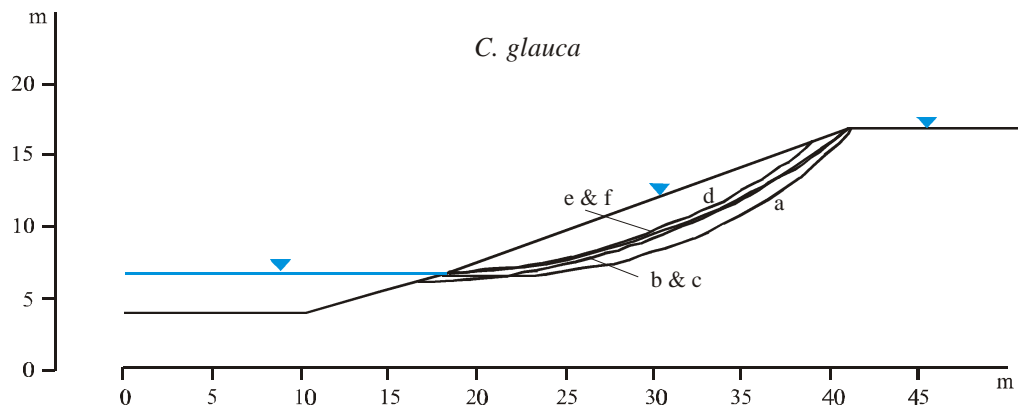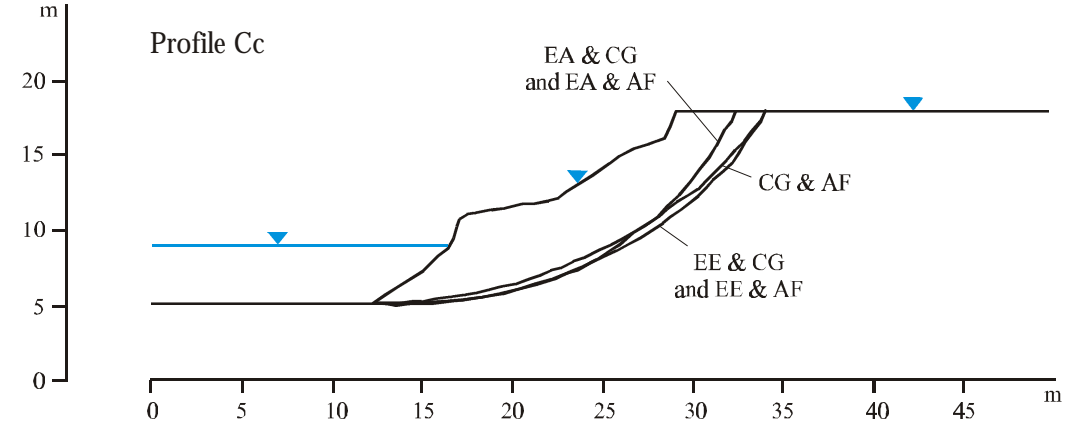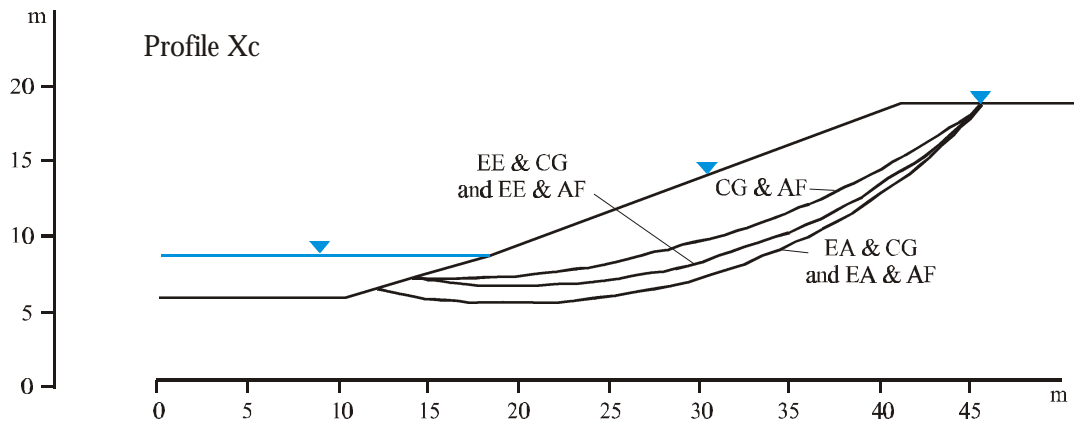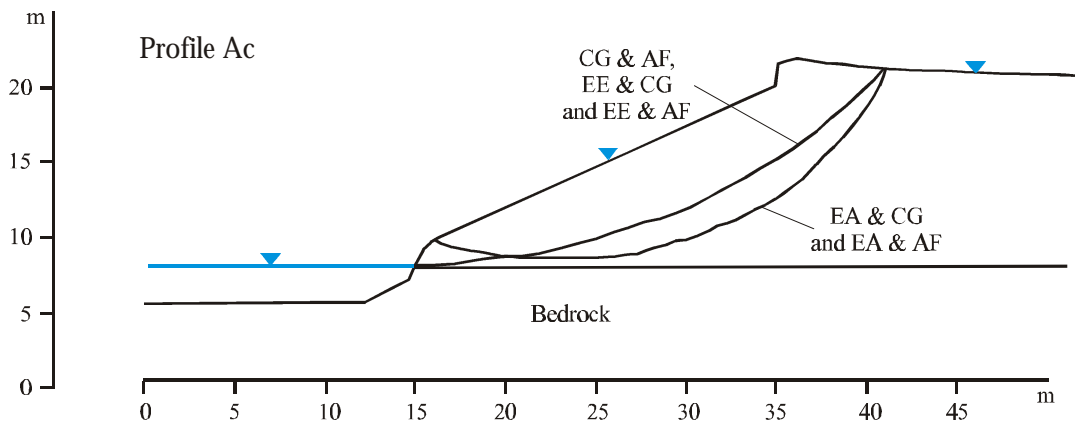
E-I(b): Critical failure surfaces for different tree locations on Profile Xc. Tree locations are shown in Figure 7.7.
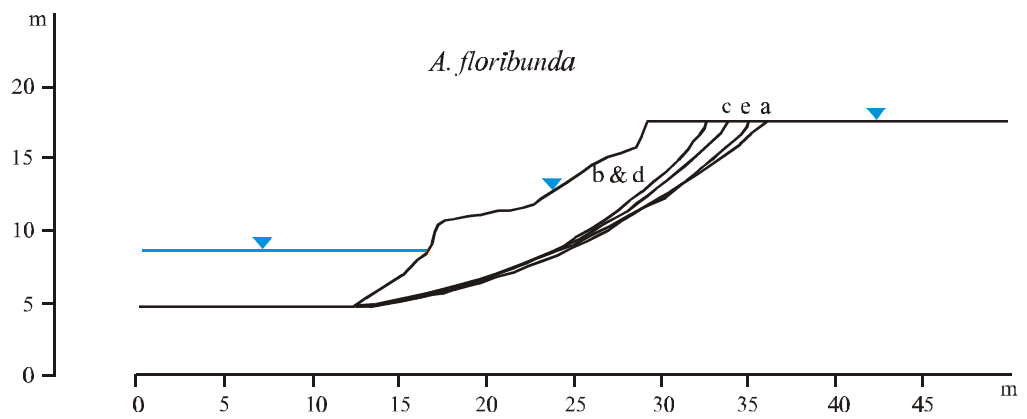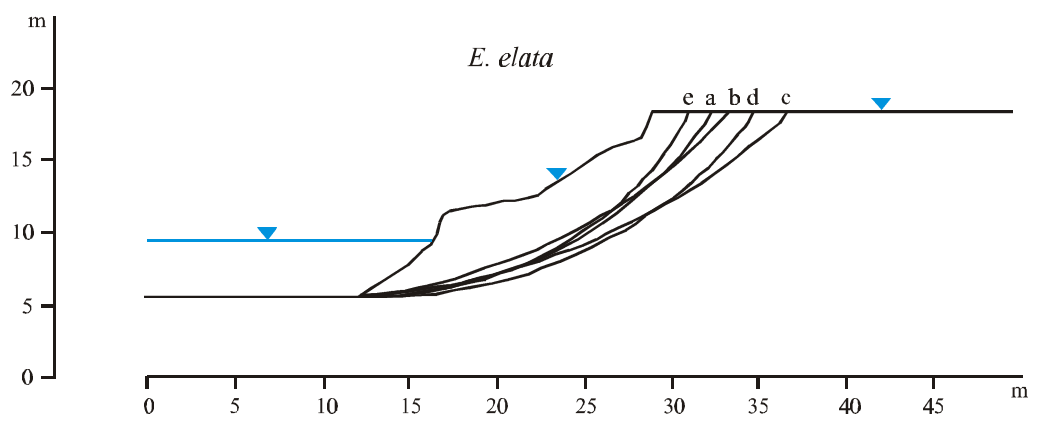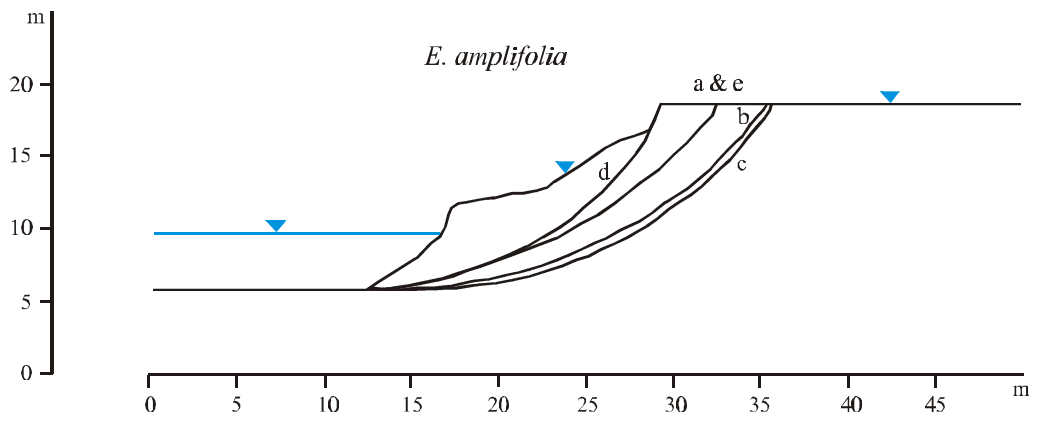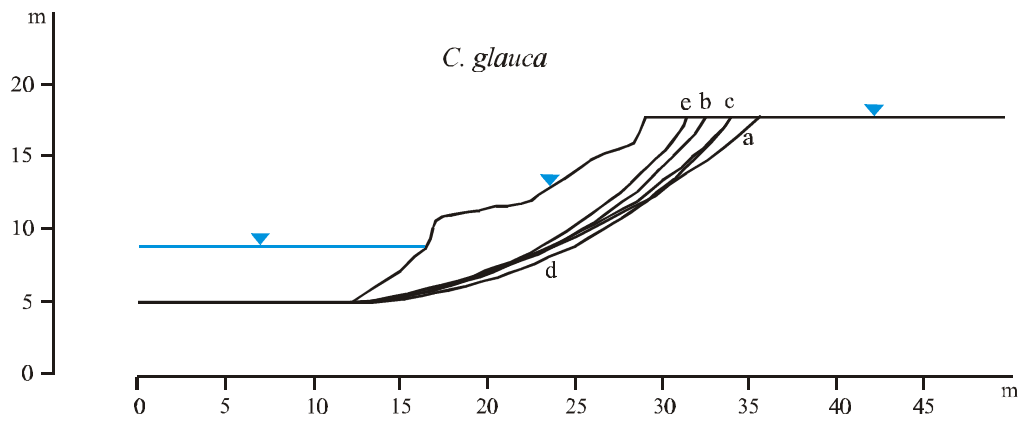
E-I(c): Critical failure surfaces for different tree locations on Profile Cc. Tree locations are shown in Figure 7.7.
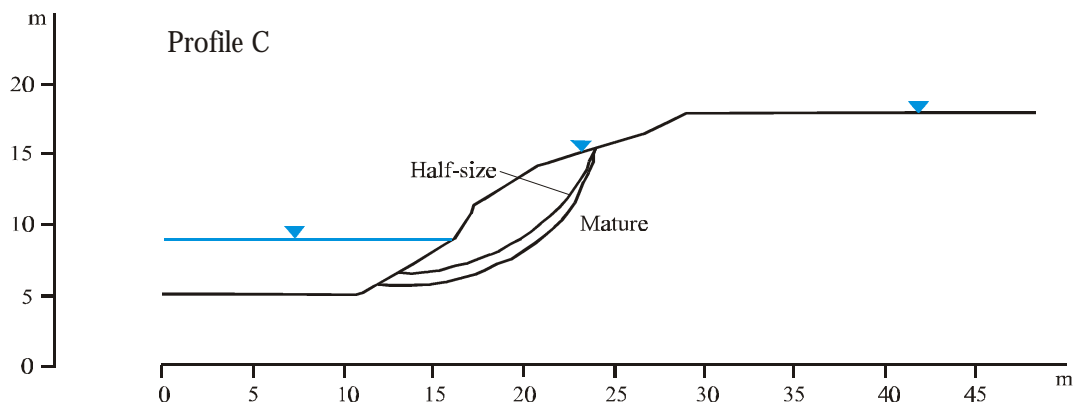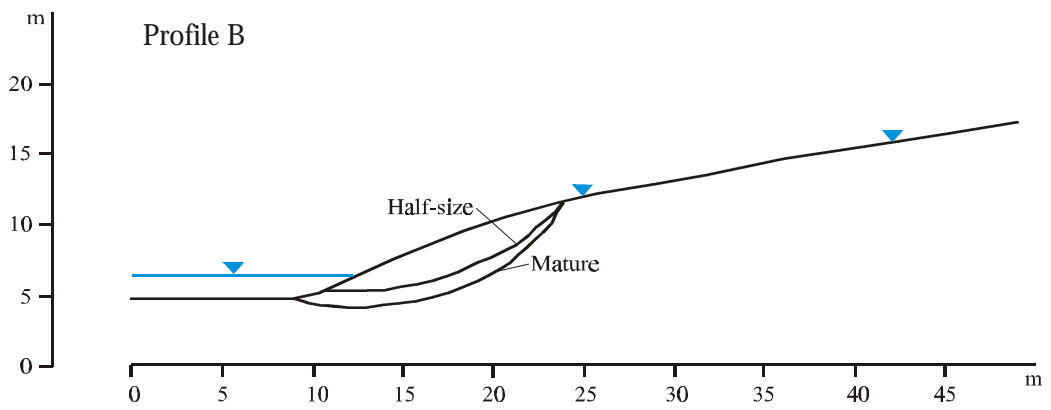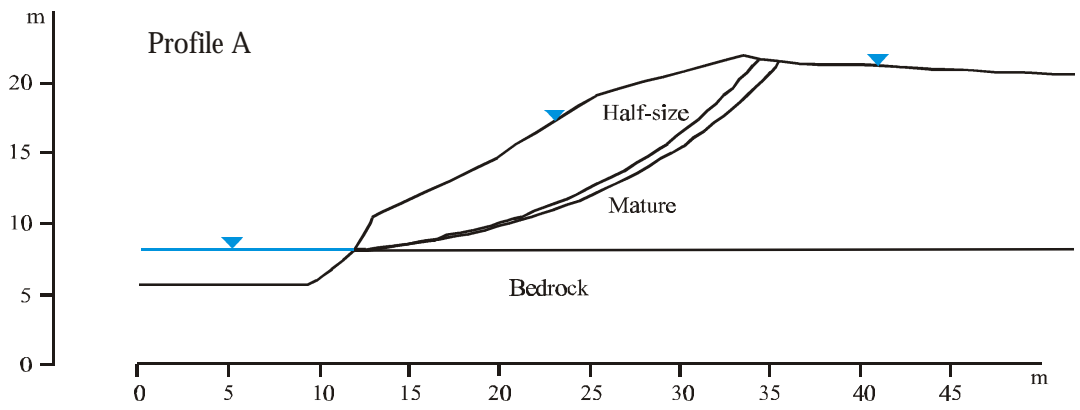
E-II: Critical failure surfaces on 'pre-failure' bank profiles typically vegetated with multiple species.

E-III: Critical failure surfaces on 'present-day' bank profiles vegetated with species pairs.